

Mycotoxin degradation in food and feed grains by atmospheric cold plasma technology

by

Ehsan Feizollahi

A thesis submitted in partial fulfillment of the requirements for the degree of

Doctor of Philosophy
in
Food Science and Technology

Department of Agricultural, Food and Nutritional Science
University of Alberta

© Ehsan Feizollahi, 2023

Abstract

Contamination of grains with mycotoxins causes quality loss and hence considerable financial loss to the grain industry. Also, mycotoxins negatively affect human and animals' health. Several mycotoxins are resistant to high temperatures and the elimination of them from grains is a challenging task. Atmospheric cold plasma (ACP) is an emerging non-thermal technology, that has attracted attention due to its mycotoxin degradation potential. The overall objective of this research was to assess the efficacy of different ACP systems including dielectric barrier discharge (DBD), plasma jet, and bubble spark discharge (BSD) to degrade selected mycotoxins, i.e., deoxynivalenol (DON) and zearalenone (ZEA) in their pure form and on grains. Specifically, the influence of important process and product factors on the mycotoxin degradation efficacy of ACP as well as the degradation mechanism of DON during ACP treatment were studied. Furthermore, the efficacy of ACP treatment on *Fusarium graminearum* inactivation was determined in order to assess the potential use of this technology in the barley malting industry.

In the first study, the degradation of DON mycotoxin by DBD-ACP and sequential treatment with heat and light emitting diode (LED) was tested. The ACP treatment was more effective when DON was in solution form compared to dry state. There were major changes in DON functional groups after ACP treatment. The LED treatment using light pulses with 395 nm wavelength reduced DON content, however this treatment was not as effective as ACP treatment. There was no synergistic DON degradation effect when ACP was used in sequential combination with thermal or LED treatment. In the second study, DON was spiked on barley (*Hordeum vulgare*) grains and the efficacy of ACP on the degradation of DON and selected barley quality parameters was investigated. The results from optical emission spectroscopy (OES) proved the presence of reactive oxygen and nitrogen species (RONS) and N₂ spectra were dominant. Ozone was the most prevalent

reactive species present followed by nitrous oxides and hydrogen peroxide. The ACP was able to significantly reduce DON content in a short period of time. Elevating the relative humidity (RH) of the surrounding air, post-treatment storage of barley grains, and increasing the moisture content of barley did not impact the DON degradation efficacy of ACP. Steeping of barley grains prior to ACP treatment significantly increased the DON degradation rate by ACP treatment. No significant differences were observed for the tested quality parameters of barley i.e., protein, beta-glucan, and moisture content, in comparison with control samples.

The third study focused on the impact of selected product and process factors on ZEA degradation using two technologies i.e., jet ACP and DBD-ACP. In comparison to DON, ZEA was more sensitive to ACP treatment. Type of product (barley grains, canola grains, and canola meal) affected the ACP efficacy and the presence of oxygen in the carrier gas to produce ACP significantly increased the ZEA degradation by ACP treatment. Type of gas mixtures (100% N₂, 90% N₂+ 10% O₂, 80% N₂+ 20% O₂, air) did not influence ZEA degradation by 3 min DBD-ACP treatment. Direct jet-ACP with higher UV intensity had better ZEA degradation efficacy compared to indirect jet-ACP with zero UV intensity. Jet-ACP treatment with 85% Ar+15%O₂ resulted in the highest degradation of ZEA compared to 75% Ar+25% N₂ and 100% Ar. The results suggested the contribution of factors other than the assessed RONS, such as high energy electrons and free radicals in ZEA degradation.

Degradation mechanisms of DON by plasma activated water (PAW) treatment of naturally contaminated barley (NIB) grains during steeping was investigated in the fourth study. High-performance liquid chromatography ultraviolet mass spectrometry results indicated twelve major degradation products of DON after ACP treatment and their chemical formulae were determined. Oxidation was probably the main degradation mechanism of DON by ACP treatment. PAW

treatment significantly reduced DON content and using PAW in indirect mode increased β -amylase activity and germinated acrospire's percentage compared to control. In the last study, the potential of using PAW bubbles produced from selected ACP generation methods on *F. graminearum* inactivation during barley steeping was investigated. BSD-ACP produced more potent PAW with high concentrations of RONS compared to continuous jet-ACP. The results from plating and qPCR technique showed that the PAW bubble treatment did not have a significant impact on natural pathogens and *F. graminearum* inactivation on NIB grains.

This research demonstrated the efficacy of ACP treatment on ZEA and DON degradation. The fundamental information gained from this research has set the stage for further research and development and implementation of the ACP systems in commercial applications, specifically in the barley malting industry for mycotoxin degradation and germination improvement.

Preface

This thesis is an original work done by Ehsan Feizollahi at the Food Safety and Sustainability Engineering Lab at the University of Alberta under supervision of Dr. Roopesh Mohandas Syamaladevi. Thesis is written according to the guideline provided by the Faculty of Graduate Studies and Research, University of Alberta.

Chapter 2 is composed of two of my articles published as: 1) Feizollahi, E., Misra, N. N., & Roopesh, M. S. (2021). Factors influencing the antimicrobial efficacy of Dielectric Barrier Discharge (DBD) Atmospheric Cold Plasma (ACP) in food processing applications. *Critical Reviews in Food Science and Nutrition*, 61(4), 666-689. doi:10.1080/10408398.2020.1743967.

E. Feizollahi drafted the manuscript. M. S. Roopesh, and N. N. Misra, reviewed and edited the manuscript.

2) Feizollahi, E., & Roopesh, M. S. (2021). Mechanisms of deoxynivalenol (DON) degradation during different treatments: a review. *Critical Reviews in Food Science and Nutrition*, 1-22. doi:10.1080/10408398.2021.1895056

E. Feizollahi drafted the manuscript. M. S. Roopesh reviewed and edited the manuscript.

Some sections of the second article is not presented in chapter 2, as they were not relevant to the subject of this thesis.

Chapter 3 of this thesis has been published as Feizollahi, E., Arshad, M., Yadav, B., Ullah, A., & Roopesh, M. S. (2021). Degradation of deoxynivalenol by atmospheric-pressure cold plasma and sequential treatments with heat and UV light. *Food Engineering Reviews*, 13(3), 696-705.

E. Feizollahi, and M. S. Roopesh conceptualized and designed the study and interpreted the results. E. Feizollahi conducted the experiments, collected data, and did data analysis. M. Arshad, and A. Ullah, helped in doing TLC and FTIR experiments and interpreting the results. B. Yadav helped in doing the optical emission spectroscopy and results interpretation. E. Feizollahi drafted the manuscript. M. S. Roopesh, and M. Arshad reviewed and edited the manuscript. M. S. Roopesh acquired funding for the study. An abstract related to the results of chapter 3 was peer-reviewed and oral presentation was delivered at 2019 IFT/EFoST International Nonthermal processing Workshop and Short Courses, Monterrey, Mexico.

Chapter 4 of this thesis has been published as Feizollahi, E., Iqdam, B., Vasanthan, T., Thilakarathna, M. S., & Roopesh, M. S. (2020). Effects of atmospheric-pressure cold plasma treatment on deoxynivalenol degradation, quality parameters, and germination of barley grains. *Applied Sciences*, 10(10), 3530.

E. Feizollahi, and M. S. Roopesh conceptualized and designed the study and interpreted the results. E. Feizollahi and B. Iqdam conducted the experiments, collected data, and did data analysis. M. Thilakarathna helped in doing the germination experiments. E. Feizollahi drafted the manuscript. M. S. Roopesh, and T. Vasanthan reviewed and edited the manuscript. M. S. Roopesh acquired funding for the study. A technical abstract related to the results of the chapter 4 was peer-reviewed and virtual oral presentation was delivered at Cereals & Grains 2020 conference.

Chapter 5 of this thesis has been published as Feizollahi, E., & Roopesh, M. S. (2021). Degradation of Zearalenone by Atmospheric Cold Plasma: Effect of Selected Process and Product Factors. *Food and Bioprocess Technology*. doi:10.1007/s11947-021-02692-1

E. Feizollahi, and M. S. Roopesh conceptualized and designed the study and interpreted the results. E. Feizollahi conducted the experiments, collected data, did data analysis, and drafted the manuscript. M. S. Roopesh, reviewed and edited the manuscript and acquired funding for the study. A technical abstract related to the results of the chapter 5 was peer-reviewed and e-poster presentation was delivered at Institute of Food Technologists annual meeting in 2020. Another technical abstract related to the results of chapter 5 was peer-reviewed and virtual oral presentation was delivered at 8th International Conference on Plasma Medicine in 2021.

Chapter 6 of this thesis has been submitted as Feizollahi, E., Jeganathan, B., Reiz.B., Vasanthan, T., & Roopesh, M.S. Reduction of deoxynivalenol during barley steeping in malting using plasma activated water bubbles and the determination of major degradation products. *Journal of Food Engineering*.

E. Feizollahi, and M. S. Roopesh conceptualized and designed the study and interpreted the results. E. Feizollahi conducted the experiments, collected data, did data analysis, and drafted the manuscript. B. Jeganathan helped in doing the enzymatic experiments. B. Reiz helped in doing the HPLC/MS experiment. T. Vasanthan and M. S. Roopesh, reviewed and edited the manuscript. M. S. Roopesh acquired funding for the study.

Chapter 7 of this thesis has been published as Feizollahi, E., Basu, U., Fredua-Agyeman, R., Jeganathan, B., Tonoyan, L., Strelkov, S., Vasanthan, T., Siraki, A., & Roopesh, M.S. (2023). Effect of plasma activated water bubbles on *Fusarium graminearum*, deoxynivalenol, and germination of naturally infected barley during steeping. *Toxins*, 15(2), 124. Doi: 10.3390/toxins15020124

E. Feizollahi, and M. S. Roopesh conceptualized and designed the study and interpreted the results. E. Feizollahi conducted the experiments, collected data, did data analysis, and drafted the manuscript. U. Basu helped in doing the qPCR experiments and editing the qPCR section of the manuscript. R. Fredua-Agyeman, and S. Strelkov helped in doing the PDA and WA plating and providing material and lab space for fungi work. B. Jeganathan and T. Vasanthan helped in doing the enzymatic experiments. A. Siraki, and L. Tonoyan helped in doing the ESR experiments. M. S. Roopesh, reviewed and edited the manuscript and acquired funding for the study.

To my parents,

For their inspiration and support in my life and being my first teachers who taught me to believe in hard work and encouraged me to go on every adventure, especially this one!

To my brother and sister,

For being my best friends forever.

To my wife,

For her patience, and unwavering devotion.

Acknowledgements

I would like to thank my esteemed supervisor, Dr. Roopesh Mohandas Syamaladevi for his invaluable supervision, continuous support, and advice during my PhD degree. I will never forget his kind and friendly manner. He was perfect in getting me out of stress whenever I encountered a problem in the experiments. I appreciate all his support for writing reference letters for my scholarships whenever I needed. Without his valuable guidance and suggestions, it would have been impossible to complete my study. It was an enjoyable journey spending 4 years of research with him.

I would also like to thank Dr. Stephen Strelkov and Dr. Thava Vasanthan, my supervisory committee members, for their valuable suggestions and providing me with their lab for conducting the experiments and for their critical help in preparation for my candidacy examination and thesis defense. I appreciate them for investing their time in writing reference letters for my scholarships and reviewing my manuscripts and providing me with their expertise advice. My sincere thanks to Dr. Feral Temelli and Dr. Marleny D. Aranda Saldana to be in my candidacy examination committee and help in my preparation for my candidacy examination. I am grateful to Dr. Boyd Mori to be a part of my final defense examination committee and investing his time in evaluating my thesis. Also, I would like to thank Dr. Girish Ganjyal for agreeing to be a part of my final defense examination committee and providing me with his valuable feedback on my thesis. I would also like to express my appreciation to Dr. Aman Ullah to let me do FTIR and TLC experiments in his lab. My sincere thanks to Dr. Arno G. Siraki, and Lusine Tonoyan for helping in ESR experiments and Dr. Urmila Basu for helping me with qPCR experiments.

My gratitude extends to my lab mates, Abdullahi Adam, Alvita Mathias, Dr. Amritha J Prasad, Dr. Barun Yadav, Dr. Basheer Iqdam, Dr. Lihui Du, Harleen Kaur Dhaliwal, Julia Bersukova, Muhammad Faisal Arif, Pauline Chan, Samir Subedi, Sitian Zhang, and Sreelakshmi Menon for a cherished time spent together in the lab, and in social settings.

Sincere thanks to Alberta Agriculture and Forestry, Alberta Canola Producers Commission, and Natural Sciences and Engineering Research Council for funding my research.

Finally, I would like to express my gratitude to my parents, siblings, and my wife. Without their tremendous mental support, understanding and inspiration in the past few years, it would be impossible for me to complete my study.

Table of Contents

Abstract.....	ii
Preface.....	v
Dedication.....	ix
Acknowledgments.....	x
List of tables.....	xx
List of figures.....	xxii
List of abbreviations.....	xxvi
Chapter 1: General introduction and objectives.....	1
1.1 Introduction.....	1
1.2 Hypotheses.....	3
1.3 Objectives.....	4
Chapter 2: Factors influencing the food decontamination efficacy of Atmospheric Cold Plasma (ACP) in food processing applications.....	6
2.1 Introduction.....	6
2.2 Atmospheric cold plasma sources.....	8
2.2.1 Corona discharges.....	8
2.2.2 Glow discharge.....	8
2.2.3 Plasma jet.....	9
2.2.4 Dielectric barrier discharge (DBD) ACP.....	10
2.3 Application of Plasma Activated Solution in Food Preservation.....	13
2.4 Factors influencing the efficacy of DBD ACP treatment.....	14

2.4.1	Process factors	15
o	Type of gas.....	16
o	Relative Humidity (RH).....	17
o	Temperature and flow rate	18
o	Material, thickness, and spacing of electrodes and barrier	19
o	Treatment time and storage time.....	20
o	Headspace and volume ratio of product inside package and product rolling	21
o	Direct and remote exposure	22
2.4.2	Product factors	23
□	Product type and composition.....	23
□	Water content	25
2.4.3	Microbiological factors.....	26
□	Pathogen type.....	26
□	Initial count	28
□	Growth phase	29
2.5	Antimicrobial mechanisms of DBD-ACP	29
2.6	Challenges.....	30
2.7	Scale-up of atmospheric pressure DBD plasma technology.....	32
2.8	Deoxynivalenol (DON).....	33
2.9	Potential of atmospheric cold plasma for DON degradation	34
2.10	Concluding remarks	37

Chapter 3: Degradation of deoxynivalenol by atmospheric-pressure cold plasma and sequential treatments with heat and UV light	39
3.1 Introduction.....	39
3.2 Materials and methods	41
3.2.1 Mycotoxin standards.....	41
3.2.2 Sample preparation	42
3.2.3 Atmospheric-pressure cold plasma treatment of DON.....	42
3.2.4 HPLC analysis	43
3.2.5 TLC analysis.....	43
3.2.6 ATR-FTIR analysis.....	44
3.2.7 Effects of initial DON concentration and ACN/water content on DON degradation by ACP	45
3.2.8 Optical emission Spectroscopy of ACP discharge.....	45
3.2.9 Pulsed light treatment using LEDs in combination with ACP	46
3.2.10 Heat treatments in combination with ACP	46
3.2.11 Statistical analysis.....	47
3.3 Results and Discussion	47
3.3.1 DON degradation and efficacy of ACP treatment	47
3.3.2 TLC analysis.....	49
3.3.3 ATR FTIR analysis.....	50
3.3.4 Effect of initial concentration on DON degradation by ACP.....	52
3.3.5 Effect of initial ACN/water content on DON degradation with ACP	53
3.3.6 Optical emission spectroscopy of ACP discharge	55

3.3.7	DON degradation with LED pulsed light treatment in combination with ACP ...	56
3.3.8	DON degradation with heat treatment in combination with ACP	57
3.4	Conclusions.....	58
Chapter 4: Effects of atmospheric-pressure cold plasma treatment on deoxynivalenol		
degradation, quality parameters, and germination of barley grains.....		
4.1	Introduction.....	60
4.2	Material and Methods	62
4.2.1	Barley grains	62
4.2.2	Mycotoxin standards.....	63
4.2.3	Sample preparation	63
4.2.4	ACP treatment.....	63
4.2.5	Extraction and quantification of DON.....	64
4.2.6	Cold plasma diagnostics	65
4.2.7	Measurements of ozone, nitrous gas, and hydrogen peroxide concentration	65
4.2.8	Effect of moisture content of barley grains and environmental RH	66
4.2.9	Post-treatment storage of barley grains on DON degradation by ACP	66
4.2.10	Effect of steeping of barley grains on DON degradation by ACP.....	66
4.2.11	Quality parameters of barley grains after ACP.....	67
4.2.12	Germination of barley grains after ACP	67
4.2.13	Statistical analysis.....	68
4.3	Results and discussion	68
4.3.1	Effect of ACP treatment on deoxynivalenol degradation on barley grains	68

4.3.2	Cold plasma diagnostics	71
4.3.3	Ozone, nitrous gas, and hydrogen peroxide concentration in DBD-ACP	72
4.3.4	Effect of MC of barley grains and environmental RH on DON degradation by ACP	74
4.3.5	Effect of post-treatment storage of barley grains on DON degradation by ACP .	76
4.3.6	Effect of steeping the barley grains on DON degradation by ACP	77
4.3.7	Effect of ACP treatment on quality parameters of barley grains.....	79
4.3.8	Effect of ACP treatment on the germination of barley grains	80
4.4	Conclusions.....	83
Chapter 5: Degradation of zearalenone by atmospheric cold plasma: effect of selected process and product factors.....		85
5.1	Introduction.....	85
5.2	Material and Methods	87
5.2.1	Mycotoxin standards.....	87
5.2.2	Sample preparation	87
5.2.3	Atmospheric cold plasma treatment.....	87
5.2.4	HPLC analysis	88
5.2.5	Effect of product substrate on ZEA degradation	88
5.2.6	ZEA degradation by thermal and UV treatments in sequence with DBD-ACP...	90
5.2.7	Effect of different gas mixtures on ZEA degradation by DBD-ACP.....	91
5.2.8	Cold plasma diagnostics	94
5.2.9	Measurements of ozone, nitrous gas, hydrogen peroxide, and humidity.....	94

5.2.10	Temperature measurement and plasma intensity	95
5.2.11	Statistical analysis	95
5.3	Results and Discussion	96
5.3.1	ZEA degradation by DBD-ACP	96
5.3.2	Effect of gas mixtures on ZEA degradation by DBD-ACP	99
5.3.3	Effect of ACP jet treatment on ZEA degradation	106
5.4	Conclusions	108
Chapter 6: Reduction of deoxynivalenol during barley steeping in malting using plasma activated water and the determination of major degradation products		109
6.1	Introduction	109
6.2	Material and methods	111
6.2.1	Barley grains and chemicals	111
6.2.2	PAW production and characterization	112
6.2.3	Determination of DON after PAW treatments	113
6.2.4	Water uptake of barley treated by PAW	115
6.2.5	Effect of PAW on selected quality features of green malt	115
6.2.6	Degradation products of DON after ACP treatment	116
6.2.7	Statistical analysis	117
6.3	Results and Discussion	118
6.3.1	PAW characteristics	118
6.3.2	Effect of PAW on DON reduction	120

6.3.3	Effect of PAW on water uptake, germination, enzymatic activity, and protein content of barley	122
6.3.4	Degradation products of ACP treated DON	126
	133	
6.4	Conclusions.....	134
Chapter 7: Effect of plasma activated water bubbles on <i>Fusarium graminearum</i> , deoxynivalenol, and germination of naturally infected barley during steeping		
		135
7.1	Introduction.....	135
7.2	Material and methods.....	137
7.2.1	Barley grains	137
7.2.2	PAW bubble production	137
7.2.3	PAW bubble characterization	140
7.2.4	EPR spectroscopy	141
7.2.5	DON quantification after PAW bubble treatments.....	142
7.2.6	Grain germination and enzymatic activity after PAW bubble treatments	143
7.3	Analysis of microbial contamination and in vitro germination	143
7.3.1	DNA extraction.....	144
7.3.2	Quantitative PCR	144
7.3.3	Statistical analysis.....	145
7.4	Results and Discussion	145
7.4.1	Characteristics of PAW bubbles	145
7.4.2	EPR spectroscopy	149

7.4.3	DON reduction after PAW bubble treatments	152
7.4.4	Germination of NIB grains after PAW bubble treatments.....	154
7.4.5	Effect of PAW bubble treatments on microflora and <i>F. graminearum</i> in NIB grains	157
7.5	Effect of bubble ACP treatment on fungal biomass of <i>F. graminearum</i>	162
7.6	Conclusions.....	164
Chapter 8: Conclusions and recommendations.....		165
8.1	Overall conclusions.....	165
8.2	Recommendations.....	169
Bibliography		171

List of Tables

Table 2.1: Impact of ACP on bacterial cell structure.....	30
Table 3.1: Effect of the initial ACN/water content on the reduction of DON concentration by ACP	54
Table 3.2: Effect of sequential treatments with atmospheric cold plasma (ACP) and light emitting diode (LED) on DON concentration and reduction	57
Table 3.3: Effect of sequential treatments with ACP and heat on DON concentration and reduction	58
Table 4.1: Physical specifications of barley grains.....	62
Table 4.2: Ozone, nitrous oxides and hydrogen peroxide concentration during ACP treatment .	73
Table 4.3: Effect of moisture content (MC) of barley and relative humidity (RH) of the surrounding air on deoxynivalenol (DON) degradation by ACP	75
Table 4.4: Effect of post-treatment storage on DON degradation on barley by ACP	76
Table 4.5: Effect of solvent type and treatment conditions (drying time and ACP treatment time) on degradation of DON on steeped barley grains by ACP	78
Table 4.6: Effect of ACP treatment on quality parameters of barley grains.....	80
Table 4.7: Comparison of germination parameters of barley grains as a function of ACP treatment time	82
Table 5.1: Physicochemical specifications of substrates	89
Table 5.2: Effect of product substrate on degradation of ZEA and production of reactive species by dielectric barrier discharge- atmospheric cold plasma.....	98

Table 5.3: Effect of sequential dielectric barrier discharge- atmospheric cold plasma + thermal, and dielectric barrier discharge- atmospheric cold plasma + LED treatments on ZEA degradation	99
Table 5.4: Degradation of ZEA, and reactive species concentration by dielectric barrier discharge- atmospheric cold plasma treatment using selected gas mixtures.....	101
Table 5.5: Effect of atmospheric cold plasma jet in direct and indirect mode using different gas mixtures at 1 SLPM on degradation of ZEA	106
Table 5.6: Effect of atmospheric cold plasma jet using 75 % Ar+ 25 % N2 at 5 SLPM in direct and indirect modes on degradation of ZEA.....	107
Table 6.1: Physical specifications of naturally infected barley grains.....	112
Table 6.2: Characteristics of plasma activated water.....	118
Table 6.3: Reduction of deoxynivalenol after steeping of naturally contaminated barley	121
Table 6.4: Effect of plasma-activated-water on the selected malting qualities	123
Table 6.5: Major degradation compounds of deoxynivalenol after ACP treatment.....	130
Table 7.1: Nomenclature of different treatments included in this study.....	139
Table 7.2: The primers for <i>F. graminearum</i> genes.....	144
Table 7.3: Characteristics of PAW bubbles produced by different treatments used in this study. The characteristics of PAW were measured indirectly after ACP treatments, i.e., the generated PAW after plasma treatments was used for measuring the physicochemical properties of PAW	149
Table 7.4: Effect of different PAW bubble treatments on DON reduction in NIB	153
Table 7.5: Effect of different PAW bubble treatments on germination of NIB	157
Table 7.6: Effect of PAW bubble treatment on <i>F. graminearum</i> and grain germination ¹	160

List of Figures

Figure 2.1: Basic configurations of DBD-ACP systems; A: planar DBD, B: annular DBD. Adapted from (Tang et al., 2015)	11
Figure 2.2: A pictorial summary of the factors influencing the efficacy of DBD ACP treatment (A: Open atmospheric treatment, B: In-package treatment)	14
Figure 3.1: Chemical structure of DON.....	40
Figure 3.2: Schematic diagram of dielectric barrier discharge atmospheric cold plasma system used in this study.....	43
Figure 3.3: Effect of ACP treatment times at 30 kV and 2 mm gap on DON degradation (%) determined by HPLC. A) with 0 % water, 0 % ACN B) in ACN/water (20/80, v/v). Data are shown as least square means \pm standard deviations. Values with different letters are significantly different ($p < 0.05$, $n = 3$)	49
Figure 3.4: ATR-Fourier transform infrared spectrum of DON in solution (0.8 mg DON/ml ACN/water (20/80, v/v)) and dry mode (0 % water, 0 % ACN) after ACP treatment.....	52
Figure 3.5: Effect of initial concentration of DON on degradation efficiency of 15 min ACP. Data are shown as least square means \pm standard deviations. Values with different letters are significantly different ($p < 0.05$, $n = 3$).....	53
Figure 3.6: Optical emission spectra of atmospheric air DBD plasma generated at 34 kV	56
Figure 4.1: A: Schematic diagram of the experimental setup used for dielectric barrier discharge (DBD) atmospheric cold plasma (ACP) treatment. B: Close-up diagram presenting the treatment of barley grains inside the ACP chamber	64
Figure 4.2: Effect of ACP treatment on (A) relative deoxynivalenol reduction % and (B) deoxynivalenol concentration ($\mu\text{g/ml}$) on barley. Data are shown as least square means \pm standard	

deviations. Values with different letters in each figure are significantly different ($p < 0.05$, $n = 3$)

..... 69

Figure 4.3: Optical emission spectra of DBD-ACP operating in air at 34 kV, 3.5 kHz, 5 mm gap
..... 72

Figure 4.4: Effect of ACP treatment on seedling growth of barley after 7 days of germination. A:
photo images. B: scanned root images using WinRHIZO software 83

Figure 5.1: Schematic diagrams of the atmospheric cold plasma jet system..... 93

Figure 5.2: Effect of dielectric barrier discharge- atmospheric cold plasma treatment in A: solution
B: dry condition on ZEA degradation. The error bars were determined based on the standard
deviation of the replicates ($n=3$) 97

Figure 5.3: Chemical structure of zearalenone 99

Figure 5.4: Surface temperature and intensity of plasma at different gas ratios after 3 min dielectric
barrier discharge- atmospheric cold plasma treatment (A: 80 % N₂+ 20 % O₂- B: 90 % N₂+ 10 %
O₂- C: 100 % N₂- D: Air) 100

Figure 5.5: Optical emission spectra of dielectric barrier discharge- atmospheric cold plasma
operating in different gas ratios (100 N₂, 90 % N₂+ 10 % O₂, 80 % N₂+ 20 % O₂, air) and different
treatment times (10 s, 1 min, 3 min). Wavelength 285 nm is ascribed to NO; and 306-310 nm to
OH radicals. The graphs on the right are the zoomed in versions of the graphs on the left. 105

Figure 6.1: Schematic diagram and flow chart of PAW generation and treatment of NIB grains in
ACP..... 113

Figure 6.2: Total Ion Chromatogram (TIC) of DON degradation products via PAW in negative
ESI mode and the associated DON degradation products from table 5; B: DON structure and the
Key toxicity functional groups of DON. Red ellipses are the key toxic 128

Figure 6.3: Proposed Criegee mechanism for degradation of DON. Adapted from (Ren et al., 2020). B: Proposed oxidation of DON to 3-keto-DON (Wang et al., 2019); C: Proposed structure of the DON ozonolysis products from the literature. Adapted from (Li et al., 2019; Ren et al., 2020; Sun et al., 2020). 130

Figure 6.4: Extracted ion chromatograms of the possible DON degradation products. Retention times (RTs) of the compounds are presented in the figure 133

Figure 7.1: Schematic diagram of plasma activated water (PAW) bubble treatment of naturally infected barley (NIB) grains using: A, bubble spark discharge atmospheric cold plasma (ACP); and B, continuous jet ACP 140

Figure 7.2: Electron paramagnetic resonance spectra of 5 ml deionized water+50 mM DMPO treated with BSD ACP at different times and power, and the chemical structure of DMPO, DMPO-OH, and DMPOX (adapted from Chen et al. (2017)). The simulated spectrum had hyperfine splitting constants of $a^N = 7.26$ G, $a^{H(2)} = 4.02$ G, and a correlation parameter of $r = 0.98$. The EPR spectrum was simulated using WinSim2002 (NIEHS/NIH). 151

Figure 7.3: Effect of PAW bubble treatments on natural microflora, *F. graminearum* and germination of naturally infected barley grains. Treatment A: Direct 20 min BSD (ice surrounding); Treatment C: Indirect 30 min BSD; Treatment F: Direct 30 min BJ. Seeds were plated on potato dextrose agar medium (PDA) and water agar (WA)..... 161

Figure 7.4: Effect of PAW bubble treatments on the relative abundance of three target genes (Tri5, Tri6 and EF1-A) of *F. graminearum* with β -Actin as an endogenous reference gene, based on quantitative PCR analysis. Values are reported based on fold-change values. The fold-change was calculated using $\text{Fold-change} = 2^{-\Delta\Delta C_t}$ where, $\Delta C_t = C_t(\text{target gene}) - C_t(\text{reference gene})$, and $\Delta\Delta C_t = \Delta C_t(\text{treatment}) - \Delta C_t(\text{control})$. Treatment A: Direct 20 min BSD (ice surrounding);

Treatment C: Indirect 30 min BSD; Treatment F: Direct 30 min BJ. Control and treatments A, C, and F were followed by steeping and air rest step before qPCR test..... 163

List of abbreviations

AACC	American Association for Clinical Chemistry
AC	Alternating Current
ACP	Atmospheric Cold Plasma
ACN	Acetonitrile
ANOVA	Analysis of Variance
ATR-FTIR	Attenuated Total Reflectance Fourier Transform Infrared
a_w	Water Activity
CDBD	Cascaded Dielectric Barrier Discharge
CFU	Colony Forming Unit
DBD	Dielectric Barrier Discharge
DBE	Double-Bond Equivalent
DC	Direct current
DNA	Deoxyribonucleic Acid
DON	Deoxynivalenol
DW	Distilled Water
FDA	Food and Drug Administration

FTIR	Fourier Transform Infrared
HPLC	High-Performance Liquid Chromatography
Hz	Hertz
kV	Kilovolt
LC-MS	Liquid chromatography–mass spectrometry
LED	Light Emitting Diode
mA	Milliampere
MC	Moisture Content
Min	Minute
ml	Milliliter
NIB	Naturally Infected Barley
ND	Not Detected
NMR	Nuclear Magnetic Resonance
OES	Optical Emission Spectroscopy
ORP	Oxidation-Reduction Potential
PAS	Plasma Activated Solution
PAW	Plasma Activated Water

PDA	Photo Diode Array
pH	Potential of Hydrogen
RH	Relative Humidity
RNA	Ribonucleic Acid
RNS	Reactive Nitrogen Species
RONS	Reactive Oxygen and Nitrogen Species
ROS	Reactive Oxygen Species
SD	Standard Deviation
SLPM	Standard Liter Per Minute
TLC	Thin-Layer Chromatography
UV	Ultraviolet
UV/VIS	Ultraviolet–Visible
VUV	Vacuum Ultraviolet
WHO	World Health Organization
ZEA	Zearalenone

Chapter 1: General introduction and objectives

1.1 Introduction

The occurrence of foodborne pathogens in food products is one of the biggest concerns for the food industry. Pathogenic fungi (mold) are one of the major microorganisms related to foodborne outbreaks (Hygreeva et al., 2014; Olaimat & Holley, 2012; Raybaudi-Massilia et al., 2009). Mycotoxins are carcinogenic secondary metabolites produced by certain fungal species (N. Misra et al., 2019). The Canadian Food Inspection Agency reported that more than 25% of the grains produced worldwide are contaminated with mycotoxins (Canadian Food Inspection Agency, 2022). Mycotoxins pose serious threats to human and animal health such as nephrotoxicity, neurotoxicity, cancer, lung disease and in some cases, death (Akocak, 2016; Sartori et al., 2017; Wang et al., 2015). In temperate climates like in Canada, mycotoxins of major concern are deoxynivalenol (DON), nivalenol, T-2 toxin and HT-2 toxin, zearalenone (ZEA), the fumonisins, ochratoxins, and ergot alkaloids (Canadian Food Inspection Agency, 2022). DON and ZEA are the two major mycotoxins, prevalently found in barley, wheat, and canola grains, grown in western Canada.

Conventional and advanced decontamination techniques such as chemical preservation, mild heat treatments, microwave processing, ionizing irradiation, and high hydrostatic-pressure technology have limitations, including hazardous chemical residues, thermal damages to flavor and nutrition, low efficacy (Baier et al., 2014; Olaimat & Holley, 2012; Warning & Datta, 2013; Ziuzina & Misra, 2016), detrimental effects to human health and environment, and low feasibility (Akocak, 2016). Mycotoxins are resistant to high temperatures. Food processing operations like roasting, extrusion, baking, and frying can possibly only partially degrade them (Bullerman & Bianchini, 2007). Hence, more effective and practical methods are required by the food industry. With the

increased demand for a product with high quality, fresh appearance, and extended shelf life, potential for alternative “green” technologies such as Atmospheric Cold Plasma (ACP) has been investigated in recent years.

ACP is a novel non-thermal technology, which has the potential to reduce foodborne microorganisms and degrade mycotoxins without affecting the food quality (Baier et al., 2014). Plasma consists of neutral gases, ions, free electrons, atoms, and photons. The reactive chemical species, in particular reactive oxygen species (ROS) and reactive nitrogen species (RNS), have a major role in mycotoxin degradation (Akocak, 2016). DON, a major mycotoxin on barley and prevalent in Canada, could be degraded by ACP treatment; however, there is a lack of information on the factors influencing the degradation of DON by ACP and also the structural changes in DON after the treatment. Knowing the structural changes in DON could be beneficial in optimizing the ACP treatment for DON degradation.

Barley (*Hordeum vulgare*) is often associated with contamination by DON, which is mainly produced by *Fusarium graminearum* (Vidal et al., 2013). Currently there is no effective method for DON reduction in barley at the industry scale. The ACP technology could be used for reducing the concentration of DON and *F. graminearum* in barley. As one of the important aspects for consumers is the quality of the product, the effects of ACP on quality features of the treated grain has considerable importance.

The malting industry uses barley as the main grain for malt and beer production (Rani & Bhardwaj, 2021). The presence of DON in barley could be detrimental as it may withstand the beer production process and hence affects the final product quality and health of consumers. Water is being heavily used during the steeping and germination process of barley for malt production. Plasma activated water (PAW), which is produced by ACP discharge in water, could be a suitable option for steeping

and germination of barley in malting process. PAW contains reactive species such as free radicals and RONS such as ozone, hydrogen peroxide, and nitrogen oxides (Machala et al., 2018), which could react with DON and lead to its degradation. In addition, the reactive species and low pH (Rathore et al., 2021) of PAW may affect the quality parameters of the barley grains, specifically the germination capacity, which is one of the most important factors for malt production. Also, the presence of nitrate in water can increase plant growth (Chen et al., 2004); as PAW contains nitrates hence it can affect the grain germination and plant growth.

Different gas media can be used for ACP generation. The type of the gas has a substantial effect on the composition and the concentration of the reactive species that are generated in ACP (Klockow & Keener, 2009; Xu, Garner, Tao, & Keener, 2017). As reactive species are the major constituents of ACP, which induce the unique features, the change in the composition of reactive species could affect the decontamination efficacy of the ACP treatment. There is a lack of information on the effect of different gas mediums on the reactive species concentrations and the degradation of mycotoxins, which need to be investigated. Furthermore, as ACP treatment is complex and several parameters are involved in its efficacy, knowing the degradation mechanisms of DON by ACP treatment would enable the grain industry to optimize it for DON degradation.

1.2 Hypotheses

ACP can reduce the concentration of mycotoxins i.e., DON and ZEA possibly by changing their chemical structure. In grains including barley, the ACP technology has the potential to reduce DON concentration without having a negative effect on the quality parameters. The presence of water can increase the concentration of RONS during ACP treatment, which in turn will improve its mycotoxin degradation efficacy. Process and product parameters such as type of ACP system, treatment time, type of substrate/matrix, type of mycotoxin, post-treatment storage, relative

humidity of the air, and type of gas medium used to generate ACP have substantial effect on mycotoxin degradation efficacy of ACP. PAW can substitute the water used in steeping process of barley malting, which can then degrade DON and inactivate *F. graminearum*. The use of PAW can possibly improve the germination of the barley, which is beneficial during barley malting. ACP consists of various reactive species which can lead to the production of several DON degradation products due to the interaction of these species with DON structure.

1.3 Objectives

The overall objective of this research was to assess impact of ACP treatment on mycotoxin degradation and fungal inactivation and study the influence of important product and process parameters on the mycotoxin inactivation efficacy of ACP.

The specific objectives of this research were:

1. To investigate the effects of ACP, sequential treatments, and selected process/product parameters on the degradation of pure DON, and the structural changes of the treated DON.
2. To investigate the effects of ACP treatment and selected process/product parameters on the degradation of DON and the quality attributes of barley.
3. To understand the effect of different gas media used to generate ACP reactive species on ZEA degradation.
4. To assess the potential of using PAW during malting of naturally infected barley grains on DON degradation and germination properties and determine the major degradation products of DON.
5. To investigate the potential of using PAW bubbles on *F. graminearum* inactivation in naturally infected barley by using different types of ACP systems.

6. To develop a continuous PAW bubble treatment for DON degradation and germination improvement of barley during steeping.

This research focuses on the degradation of the two of the important mycotoxins in Canada, namely DON and ZEA and inactivation of *F. graminearum* fungi that produce these mycotoxins. Pure forms of DON and ZEA, grains spiked by these mycotoxins, and naturally contaminated barley grains were used to assess the potential of ACP treatment. In this research, different types of ACP treatment systems, including dielectric barrier discharge (DBD) (Chapters 3, 4, 5, 6), plasma jet (Chapters 5, 6, 7), and bubble spark discharge (BSD) (Chapter 7) were used to generate plasma in gaseous or liquid state (plasma activated water). In addition, a continuous plasma activated water generation and treatment unit was built for barley steeping experiments (Chapter 7).

Chapter 2: Factors influencing the food decontamination efficacy of Atmospheric Cold Plasma (ACP) in food processing applications

2.1 Introduction

The occurrence of foodborne pathogens in food products is one of the biggest concerns for the food industry. Harmful bacteria, fungi, and viruses are the major pathogenic microorganisms related to foodborne outbreaks (Raybaudi-Massilia et al., 2009). Conventional methods, such as heat treatments, use of ethylene or propylene oxides, fumigation, irradiation, application of disinfectants (e.g., chlorination, hydrogen peroxide), and advanced decontamination methods, such as high-pressure processing, high-intensity pulsed electric field, pulsed light, and ozone technology have the potential to reduce pathogenic microorganisms in food products (Baier et al., 2014; Olaimat & Holley, 2012; Warning & Datta, 2013; Ziuzina & Misra, 2016); apart from the benefits that the new technologies present, they have certain limitations. High capital cost, hazardous chemical residues, thermal damages to flavor and nutrition, and low antimicrobial efficacy are the most prominent issues associated with current decontamination methods. With the increased demand for products with high quality, fresh appearance, and extended shelf life, potential of alternative technologies such as atmospheric cold plasma (ACP) are currently being explored.

To describe the plasma state, it is to be recalled that upon increasing the (internal) energy of a solid, it turns into a liquid, then subsequently into gas, and ultimately into an ionized state. This ionized state of a gas is described as “plasma”. Any source of energy capable of ionizing a gas can be used for producing plasma (Mandal et al., 2018; N. N. Misra et al., 2016). Ionization of a process gas leads to the concomitant formation of various reactive chemical species, such as ions and radicals, and UV light in plasma. Plasma can be classified into thermal or nonthermal. Nonthermal

plasma, also referred to as cold plasma with a temperature of < 60 °C, is characterized by a nonequilibrium temperature between the electrons and ions (Mandal et al., 2018). Plasma can be created at atmospheric pressure with the temperature of charged and neutral heavy particles being relatively low, close to room temperature, in comparison to very high electron temperatures in plasma.

ACP is a novel, non-thermal technology to treat food products to reduce foodborne microorganisms without affecting their quality. The reactive chemical species in ACP can inactivate microorganisms on food surfaces owing to their antimicrobial properties (Baier et al., 2014). The two main effective species in the air plasma process are reactive oxygen species (ROS) and reactive nitrogen species (RNS). Excited molecules of N_2 and nitric oxide radical ($\cdot NO$) are the main RNS species (Tappi et al., 2014). Ozone (O_3), singlet oxygen (O or O^{\cdot}), superoxide ($O_2^{\cdot-}$), peroxide (O_2^{-2} or H_2O_2), and hydroxyl radicals ($\cdot OH$) are the reactive oxygen species that can effectively inactivate microorganisms. The antimicrobial property of these oxidative species can be attributed to the lipid peroxidation in cell membranes and oxidation of proteins and DNA in microbial cells (Muranyi et al., 2008).

Dielectric-barrier discharge (DBD) is one of the most commonly employed non-thermal atmospheric gas discharge sources. DBD-ACP exhibits surface decontamination effectiveness and has a huge potential to treat a variety of food products. A DBD-ACP source contains a dielectric (insulator) material in the discharge path between the electrodes. While DBDs have been extensively employed for the study of food decontamination, the factors influencing their decontamination efficacy remain to be carefully analyzed.

2.2 Atmospheric cold plasma sources

2.2.1 Corona discharges

Corona discharge occurs when a strong electric field is applied across two surfaces with drastically different radii of curvature, such as a sharp point or a thin wire electrode. The electrode with the smaller radius of curvature is referred to as the emitter electrode, while the other is known as the collector electrode. Coronas can be operated under positive or negative polarity, depending on the potential of the emitter relative to the collector electrode. In the positive corona, the high voltage electrode is the anode, whereas in the negative corona, the high voltage electrode is the cathode (Bogaerts et al., 2002; Lu et al., 2016). This type of plasma could be operated at atmospheric pressure with low gas temperatures and with relatively low power electrical discharges (Chang et al., 1991). Applications of corona plasma span across the areas of electrostatic precipitation, electrophotography, use as ionization sources for mass spectrometry at atmospheric pressure, ozone synthesis, destruction of toxic compounds, gas and liquid cleaning, etc. (Bogaerts et al., 2002; Chang et al., 1991). Coronas have remained the method of choice for ozone generation to treat vegetables and fruits (Guzel-Seydim et al., 2004).

2.2.2 Glow discharge

Glow discharge plasma is a non-thermal equilibrium discharge which generally operates at low pressure. In this type of plasma, the light emission pattern of the glow is divided into several layers between cathode and anode electrodes (Bogaerts et al., 2002; Conrads & Schmidt, 2000). Different gap distances and gas pressure affect the pattern of glow. At elevated pressures, the glow is unstable and could be changed to a spark; hence, design considerations are important at atmospheric or high pressures (Bogaerts et al., 2002). Moreover, at elevated pressures, the temperature of the used gas could rise to a few thousand Kelvins, while at low-pressure glows, the

temperature is close to room temperature. This type of plasma is used in glow discharge lasers, as a molecular optical emission detector for gas chromatography, sterilization of microorganisms on surfaces in the healthcare industry, production of ozone, plasma polymerization, and material treatment (Bogaerts et al., 2002). The different types of glow discharge are low-pressure glow discharge, atmospheric pressure glow discharge, micro-discharges, hollow cathode discharge, and glow discharge with liquid electrodes (Lu et al., 2016).

2.2.3 Plasma jet

In the case of atmospheric pressure plasma jets, the projection of the discharge plasma species is in an open environment and is operated in a non-sealed electrode arrangement (Winter et al., 2015). The plasma jets can be used for direct treatment of various objects without the limitation of the treatment size. They have been used for the inactivation of bacteria, wound healing, and cancer treatment (Kong et al., 2009; Morfill et al., 2009). Plasma jets can operate with a kHz AC power supply, microwave, RF, and pulsed DC supply. By using noble gases such as helium, the plasma jet can be generated more easily. Nevertheless, due to lower reactive species in noble gases, they are mixed with a small percentage of reactive gases, such as O₂ or air. They can be used for the treatment of bulk material or treatment in small sizes (Lu et al., 2016).

In high voltage pulsed discharge plasma, pulse rising time and pulse duration (width) are the most important factors. Implementing advanced pulsed power generators has facilitated the production of a high repetition rate of nanosecond pulsed discharges. The parameters of a typical pulsed voltage discharge are 100–500 ns pulse duration, 10–100 pulse rising time, and repetition rates up to tens of kHz. In addition, high voltage amplitudes could be applied to achieve a highly non-equilibrium state in a nanosecond pulsed discharge. DBD-ACP, corona discharge, and glow discharge plasma could be driven by nanosecond pulsed voltages and exhibit distinctive discharge

characteristics (Lu et al., 2016). They could be operated at much higher peak voltages and peak currents for the same average power and better efficiencies (Bogaerts et al., 2002). In pulsed DBDs, the discharge uniformity is higher and the operating temperature is lower than the AC power supply DBDs (Miao et al., 2018; Q. Wang et al., 2018).

2.2.4 Dielectric barrier discharge (DBD) ACP

One of the widespread methods for the generation of ACP is the use of DBD. Here, the plasma discharge is produced between two parallel electrodes, where both or at least one electrode is wrapped by a dielectric (Becker et al., 2004; Klockow & Keener, 2009). DBD presents numerous advantages in terms of flexibility of geometrical configurations and miniaturization, operating parameters, simple design, cost, safety, and characteristics of the power supply (Li et al., 2016; Tang et al., 2015; Tappi et al., 2014).

Typical planar (plate-to-plate), and annular DBD configurations are presented in Figure 2.1. This reactor is simple and could be easily scaled up for high production volume (Di et al., 2018). In DBD-ACP, the discharge is blocked by a dielectric barrier layer, such as alumina, glass, silica glass, ceramic materials, and thin enamel or polymer layers (Kogelschatz, 2003; Ragni et al., 2010), which covers one or both electrodes, or it can be suspended between two electrodes (Figure 2.1); hence, a spark or arc discharge can be avoided. The efficacy of this system strongly depends on the process parameters employed (gas pressure, gas type, gas flow, frequency and power of plasma excitation, time), device set-up (reactor geometry), type of the substrate, packaging material, and the exposure of the substrate (Misra et al., 2011; N. N. Misra et al., 2019; Suwal et al., 2019). At very high frequencies, the ability of the dielectric to limit current may be compromised and it may lose its dielectric properties. The operating conditions for DBD treatments typically fall in the range of the following: gas pressures of $\sim 10^4$ – 10^6 Pa; frequency

band 50 Hz–10 MHz; AC or pulsed DC current; voltage amplitude $\sim 1\text{--}100\text{ kV}_{\text{rms}}$; electrode gap ~ 0.1 millimeter to several centimeters; and different dielectric material layers like glass, quartz, ceramics, and polymer layers. The DBD device is simple, stable, reliable, and economical (Kogelschatz, 2003; Rybkin & Shutov, 2017). In most high-power applications, liquid cooling of at least one of the electrodes is applied (Kogelschatz, 2003). It is important to distinguish between volumetric DBD and surface DBD. In surface DBD, the electrodes are asymmetrically placed and separated by the dielectric, with no additional volumetric air gap. Consequently, the discharge occurs at the surface of the barrier. More details about surface DBD are provided by N. N. Misra et al. (2019).

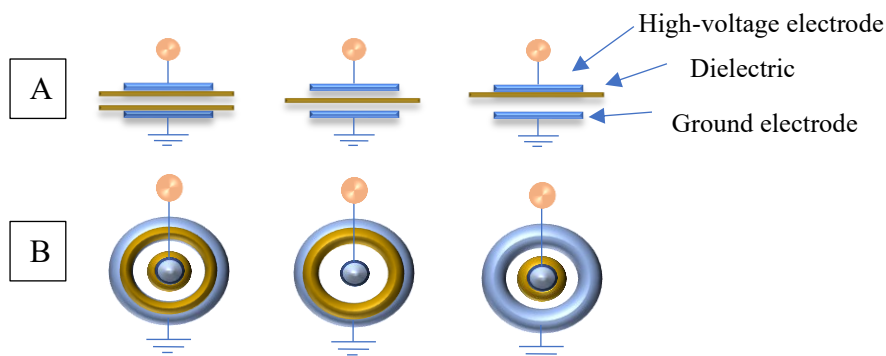


Figure 2.1: Basic configurations of DBD-ACP systems; A: planar DBD, B: annular DBD. Adapted from (Tang et al., 2015)

Besides the planar DBDs, there are also annular (co-axial) ones in which discharge gaps between cylindrical electrodes and dielectrics are annular (Figure 2.1). Similar to planar DBDs, coaxial DBDs are simple, suitable for the treatment of large quantities, and could easily be scaled-up (Di et al., 2018). The shape of the coaxial DBDs allows for larger gas volume to be treated, resulting in the higher production of reactive species (Q. Wang et al., 2018). For chemical engineering applications, co-axial DBD reactors are preferred for decomposition of gaseous

pollutants (Gadkari & Gu, 2017; Miao et al., 2018), while planar DBDs are preferred for material processing (Kostov et al., 2009). The gas in DBDs' gap can either flow through the gap (ozone generation, surface treatment, pollution control), be fully encapsulated (excimer lamps, excimer-based fluorescent lamps and light panels, plasma display panels), or be recirculated (CO₂ lasers) (Kogelschatz, 2003). The discharge produced in annular DBDs has been reported to be less homogenous and stable than planar DBDs (Subedi, 2010). Planar and annular DBD are the most common DBD configurations. Advances with respect to other DBD configurations and understanding of the discharge characteristics were also reviewed (Brandenburg, 2017).

Dielectric barrier discharge (DBD) offers desirable efficiencies at short-term treatments of less than 1 min (Baier et al., 2014). Using ambient air in DBDs instead of noble gases (e.g., argon or helium) enables the application of ACP in large scales and reduces the operating costs (Baier et al., 2014). DBD-ACP sources have been used for surface treatments including textile and polymer treatment, ozone synthesis, destruction of pollutants (e.g., volatile organic compounds, nerve gases, odors, NH₃, H₂S, NO_x, SO₂, etc.), plasma display panels, high-power CO₂ lasers, excimer UV/VUV lamps, hydrogen production from natural gas, and yeast and bacterial inactivation (Kogelschatz, 2003; Morgan, 2009). The electrical energy coupled into this system is transferred to electrons, and the surrounding gas remains close to ambient temperature (Mandal et al., 2018). Besides, the non-equilibrium plasma DBDs can be operated at elevated pressures. These features make them unique for many industrial applications. More details about the principle and applications of DBD-ACP can be found elsewhere (Becker et al., 2004; Brandenburg, 2017; Fridman, 2008; Samoilovich et al., 1997).

2.3 Application of Plasma Activated Solution in Food Preservation

A plasma-treated or -activated solution (PAS) produced by the treatment of aqueous solutions such as water, phosphate buffered saline, NaCl, and N-Acetylcysteine (NAC) by ACP can generate hydrogen peroxide (H_2O_2), nitrite (NO_2^-), and nitrate (NO_3^-) in the liquid phase (Ercan et al., 2016; Ma et al., 2015; Oehmigen et al., 2011). PAS contains reactive species such as ROS and RNS and it can be used to inactivate microorganisms and degrade mycotoxins. Furthermore, the short inactivation times, lack of toxic chemicals, and low thermal loads make this an effective biological disinfectant (Shintani et al., 2010). The possibility of producing PAS by DBD-ACP has been demonstrated in recent research (Brisset & Pawlat, 2016; Zhang et al., 2017). PAS can be used in the treatment of cancer (Chauvin et al., 2018), the inactivation of bacteria (Shen et al., 2016), or the increasing of plant growth (Judée et al., 2018) and seed germination (Than et al., 2022). Characterization of tap and deionized water activated by the low-temperature plasma demonstrated that the treated tap water exhibited a larger conductivity, acidity, and concentration of reactive nitrogen and oxygen species in comparison with the deionized water (Bafail et al., 2018).

The bactericidal activity of plasma-activated water (PAW) results from the synergistic effects of a high positive oxidation-reduction potential (ORP) and low pH ($\text{pH} \approx 2-3$) (Kaushik et al., 2018; Oehmigen et al., 2010). H_2O_2 , OH, O, O_3 and RNS contribute to the high ORP (Lukes et al., 2012; Traylor et al., 2011; Van Gils et al., 2013). RNS also plays a dominant role in the acidification of PAW (Kaushik et al., 2018). Studies reported the antimicrobial efficacy of PASs by DBD against *Candida albicans*, *Escherichia coli*, *Staphylococcus aureus*, *Staphylococcus epidermitis*, and *Enterococcus faecalis* (Ercan et al., 2013; Laurita et al., 2015). The ROS and RNS produced in PAW were dependent on many factors, such as the discharge type, the plasma working

gas, the treatment time, the storage time, and the chemical composition of the surrounding environment (Kaushik et al., 2018).

2.4 Factors influencing the efficacy of DBD ACP treatment

Figure 2.2 presents a summary of the important process, product, and microbiological factors influencing the efficacy of DBD-ACP treatment in open and in-package environments. The following sections provide a detailed description of these important factors.

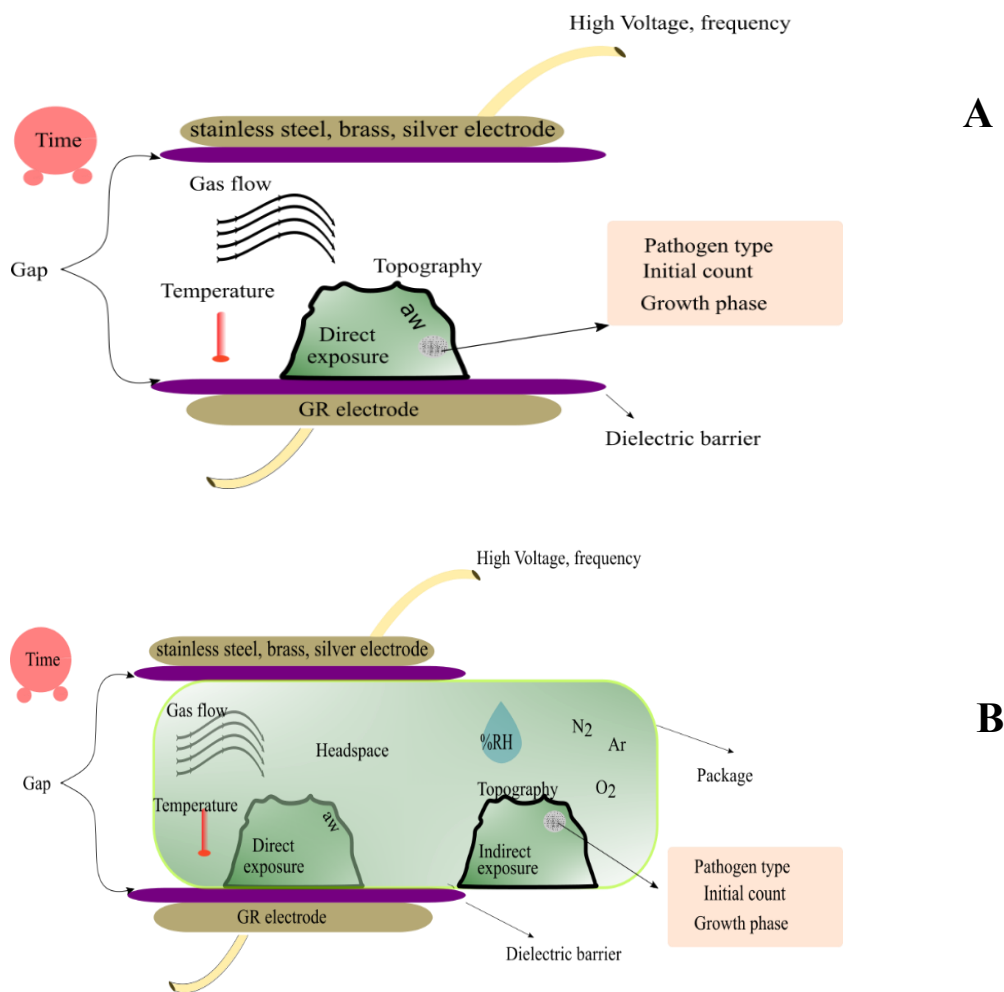


Figure 2.2: A pictorial summary of the factors influencing the efficacy of DBD ACP treatment (A: Open atmospheric treatment, B: In-package treatment)

2.4.1 Process factors

- *Voltage, frequency, and current*

Plasma process factors such as voltage, frequency, current, and electric field strength can influence microbial inactivation during ACP treatment. Higher microbial inactivation rates with an increase in power, voltage, and frequency during ACP have been reported (Albertos et al., 2017; Liao et al., 2018; Sarangapani et al., 2016; J. Wang et al., 2018).

One of the main chemical species produced in ACP systems is ozone (O_3), a strong oxidizing agent which is used as a disinfectant in drinking water plants. At high voltages, dissociation of oxygen molecules occurs and ozone is produced; hence, the concentration of ozone is directly linked with applied voltage and frequency (Morgan, 2009). Large amounts of ozone production at high voltages may be related to the improved antimicrobial efficiency. In order to generate ozone, a diatomic oxygen molecule must first be split by ultraviolet radiation, corona discharge, or DBD methods. Then the resulting oxygen free radical reacts with another diatomic oxygen to form the triatomic ozone molecule. Morgan (2009) reported that no ozone was detected at applied voltages below 2 kV due to the voltage not reaching the threshold value for the breakdown of the O–O bond, which requires high energy. The generated ozone concentrations were 1600, 2200, and 2800 ppm for the applied voltages of 60, 70, and 80 kV, respectively, after 8 min of ACP treatment (Sarangapani et al., 2016). However, J. Wang et al. (2018) reported that an increase in voltage from 55 to 80 kV increased ozone concentration from 200 to 950 ppm, but the effectiveness of in-package ACP treatment against the growth of natural microflora on raw chicken fillets that were packed in the air and stored at refrigerated temperature did not change. They assumed that the ACP treatment had injured the microbes instead of killing them and, during the enumeration on ideal media, the injured microbes were recovered and masked the treatment differences. Technological

challenges, for instance high power consumption, need for better insulation, higher cost, and negative impacts on quality, must be prioritized in practice when increasing the voltage and frequency. Current also may have a significant impact on the antimicrobial efficacy of DBD-ACP treatment. In a study on the inactivation of yeast by DBD-ACP with different current amplitudes (0.4, 0.8 and 1 mA), the lowest D-value was achieved with a 1 mA current. With a 0.4 mA current, complete inactivation of *S. cerevisiae* and *M. frigidus* could not be achieved within an exposure time of 30 min (Morgan, 2009; Morgan et al., 2009). In DBD-ACP, using oxygen as the working gas, the concentration of the ozone was increased with an increase in the current (Garamoon et al., 2002).

- **Type of gas**

The type of gas used is critical, especially in the case of in-package ACP treatment and DBD plasma jet systems, as the plasma chemistry is dependent on the properties of the gas medium. Any gas can technically be used to create ACP, and the inactivation rate of microorganisms will be different based on the type of gas used (Xu et al., 2017). The presence of oxygen is suggested to be critically important during ACP treatments for achieving required inactivation, in comparison with nitrogen alone, to significantly reduce microorganisms (Kim et al., 2014). In gas mixtures containing oxygen, ozone, and other effective antimicrobial reactive species such as singlet oxygen, superoxide anions and hydroxyl radicals can be produced during the ACP treatment. Ozone has a long life, is very oxidative in nature, and can react with water to produce peroxide. Hence, the presence of oxygen results in the generation of reactive oxygen species (e.g., ozone, peroxides) (H. Shi et al., 2017), which is one of the main reasons for the microbial inactivation. ACP reactive species can cause cellular protein degradation, fragmentation and release of DNA, and loss of permeability and cell leakage due to oxidative damage of the cell membrane.

Intracellular oxidative stress leads to cell apoptosis and deformation of mycelial tips (in fungi) (Liao, Liu, et al., 2017; N.N. Misra et al., 2019). In one study, ACP treatment in the presence of modified atmosphere using 65% O₂ + 16% N₂ + 19% CO₂ resulted in reductions of 3.1 and 3.4 log for total mesophiles and yeasts/molds counts, respectively, in packaged strawberries, while using 90% N₂ + 10% O₂ resulted in 3.7 and 3.3 log reductions, respectively (Misra et al., 2014). Morgan et al. (2009) used ACP generated by argon and oxygen for yeast inactivation and the results suggested that the inactivation rate after ACP treatment using oxygen was more effective than when using argon. They reported that the D-values of *S. cerevisiae* and *M. frigida* were 3.2 and 3.4 min when oxygen was used as the gas during ACP treatment, while the D-values were 7.3 and 4.7 min, respectively, when argon was used. The proposed two inactivation mechanisms in oxygen DBD discharge were (1) oxidation of DNA and proteins by ozone, (2) etching and erosion by oxygen radicals (O₂⁺, O⁺) and atomic oxygen (O) (Morgan et al., 2009). Using pure argon for in-package ACP treatment has shown less antimicrobial effect in comparison to 93% Ar + 7% CO₂ (Chiper et al., 2011). This shows the importance of O₂ as an antimicrobial agent in the system.

The concentration of the gas used in plasma is also important in achieving required inactivation of target microorganisms. Morgan et al. (2009) reported that the D-values of *S. cerevisiae* and *M. frigida* were decreased with increasing oxygen concentration. This may be due to a higher generation of ions and reactive species such as ozone, O, O⁺ when elevated oxygen concentrations were used.

- **Relative Humidity (RH)**

Environmental relative humidity (RH) is an important factor influencing plasma physics and chemistry. An increase in RH has been reported to increase the microbial inactivation during ACP treatment. This may be attributed to the increase in the concentration of OH radicals at high RH

due to the presence of water molecules, which is one of the most effective reactive oxygen species, leading to high oxidation (Berardinelli et al., 2012). However, water vapor reduces the number of micro-discharges due to the reduction in the surface resistance of the dielectric material by the adsorption of water molecules (Falkenstein, 1997; Falkenstein & Coogan, 1997). In the presence of high humidity in the discharge, electron energy can be lost in electron-molecule collisions, and so, this quenching effect can weaken the plasma (Bruggeman et al., 2009; Butscher, Van Loon, et al., 2016).

Muranyi et al. (2008) reported an optimum RH in the range of 70% for the inactivation of *A. niger* conidiospores. Interestingly, the inactivation efficacy decreased at a higher RH than 70%. In contrast to *A. niger*, the inactivation of *B. subtilis* endospores decreased with increasing humidity of the dry air with 0% RH. In their study, the negative effect of humidity was most apparent for a treatment time of 1 s at 80% relative humidity (Muranyi et al., 2008). It was assumed that the reduced discharge homogeneity at high humidity, poorer transmissibility of UV radiation, and protective water film around the microbial cells could be the reasons for a lower inactivation rate of *B. subtilis* (Butscher, Van Loon, et al., 2016; Muranyi et al., 2008; Ragni et al., 2010). The inactivation of oxidation-sensitive microorganisms such as *A. niger* is increased upon increasing the RH, while in the case of micro-organisms such as *B. subtilis*, where the UV radiation may be the main inactivation pathway, the inactivation rate was decreased by increasing RH (Muranyi et al., 2008).

- **Temperature and flow rate**

ACP treatments are generally carried out at relatively low temperatures (close to room temperature to 70 °C) and are regarded as “cold” due to the low temperatures of heavy particles in plasma. Hence, inactivation by thermal effect is often negligible (Geyter & Morent, 2012). Yadav et al.

(2019) reported a slight increase in the surface temperature of ham from 21.0 °C to 26.1 °C and 25.1 °C during and after ACP treatments, respectively. An increase in the airflow rate causes the gas temperature to decrease and reach room temperature (~23 °C) (Laroussi & Leipold, 2004). Furthermore, the relative concentration of atomic oxygen in the DBD decreases as the flow rate is increased. A correlation between flow-rate and antimicrobial inactivation is complicated to demonstrate as the concentration of O₃ and OH do not have a trend with flow rate (Laroussi & Leipold, 2004).

- **Material, thickness, and spacing of electrodes and barrier**

The type of DBD electrode material can influence the decontamination efficacy of ACP treatment. For instance, Ragni et al. (2016) investigated the decontamination efficacy of ACP treatments using four DBD electrode materials (i.e., stainless steel, brass, silver, and glass/brass) to inactivate *Listeria monocytogenes* and *E. coli* after 20, 40, and 60 min using air as the working gas. Significant differences were observed in the reduction of *L.monocytogenes* after 40 and 60 min of treatment, where higher reductions were achieved by the silver and brass electrodes (up to about 8 log CFU/ml) in comparison to stainless steel and glass/brass electrodes after 60 min of treatment. The molecules from silver and brass could have played a role in the higher antibacterial properties when long treatment times were used, while the difference in the decontamination may not have been related to pH, electric features of the discharge, amount of ozone produced, or nitrate and nitrite concentrations. It is worth noting that the authors did not observe any significant difference in decontamination efficacy when different electrodes were used for inactivating *E. coli* (Ragni et al., 2016). No study has assessed the impact of electrodes' and dielectrodes' material on DBD-ACP efficacy for fungi inactivation.

The dielectric material used in the DBD electrode also could influence the decontamination efficacy. Ozkan et al. (2016) used four dielectric materials (i.e., quartz, pyrex, mullite, alumina) for ACP generation. Alumina (ceramic) was chosen as the best among them as the number and lifetime of micro-discharges and the plasma charge were the highest, while quartz was observed as the second best dielectric material. Aging of the dielectric material due to UV degradation (Andrady et al., 1998) or plasma etching (Egitto et al., 1990) also could be the other factors affecting the decontamination efficacy of DBD treatment. Moreover, for a dielectric barrier with a larger thickness, the capacitance of the dielectric decreases while the electrical charge is constant; hence, the voltage increases over the dielectric barrier and a greater number of micro-discharges is generated (Ozkan et al., 2016), which might enhance the antimicrobial efficiency.

In general, a larger gap between the powered electrode and the substrate and a larger gap between electrodes can result in lower treatment efficacy (Hu & Guo, 2012; Liao, Xiang, et al., 2017; Miao & Yun, 2011) due to non-uniform production of plasma and by the recombination of active species before reaching the sample in larger gaps (Liao, Xiang, et al., 2017). However, in a simulation study by Iqbal and Turner (2015), the effect of gap spacing between 1 to 9 mm in DBD-ACP discharge was assessed, and the electrons' and ions' densities were the highest when a 3-mm gap between the electrodes was used. In general, it remains unclear whether gap and voltage should be considered in isolation for DBDs or considered as a single parameter, "electric field," for comparison. While the latter is physically more accurate, much of the literature pertinent to ACP applications in food science employ gap and voltage as two independent factors.

- **Treatment time and storage time**

Increasing treatment time can improve the inactivation efficacy of DBD-ACP treatment. Microorganisms at high concentrations exist in multiple layers; hence, longer ACP treatment times

are required to inactivate those residing in the inner layers. Extended ACP treatments generate higher concentrations of reactive species, a reduction in pH, and an increase in the mortality of pathogens, which explains the greater inactivation rates (Albertos et al., 2017; Berardinelli et al., 2016; Ghomi et al., 2009; Liao et al., 2018; Misra et al., 2012; Muranyi et al., 2008; Ragni et al., 2016; J. Wang et al., 2016; Xu et al., 2017; Zhang et al., 2017). Nevertheless, long treatment times could cause quality deterioration in the treated products (Berardinelli et al., 2012; Liao et al., 2018; Xu et al., 2017). However, J. Wang et al. (2018) reported that increasing treatment time from 3 to 9 min at 80 kV did not alter the antibacterial effect of in-package ACP treatment against the growth of natural microflora on raw chicken fillets that were packed in the air and stored under refrigeration. Treating the sample for more than 3 min did not increase the ozone concentration significantly. Ozone is a very reactive agent, and once its concentration reaches a certain level, it reacts with other reactive agents generated in the package due to ACP treatment to form other compounds. Treatment of more than 3 min resulted in changes in meat appearance by means of significant reductions in a^* and b^* values (J. Wang et al., 2018).

- **Headspace and volume ratio of product inside package and product rolling**

One of the advantages of DBD-ACP is its capability to be used for in-package treatment. Min et al. (2018) investigated the effect of the volume ratio of the headspace (the space between the surface of food and the underside of the lid) of grape tomatoes on the inactivation of *Salmonella*. A higher rate of inactivation was achieved when the headspace to tomato volume ratio was increased by either changing the container size or the number of tomatoes in the container. Moreover, incorporating rolling of the tomatoes to the treatment increased the inactivation rate impressively from 0.9 ± 0.1 log CFU/tomato to 3.3 ± 0.5 log CFU/tomato. This is possibly due to a better distribution of the reactive species throughout the package and an increase in the exposure

of individual tomatoes to the reactive species, hence facilitating the diffusion of ozone and consequent microbial inactivation (Min et al., 2018). In another study investigating the inactivation of *E. coli* on romaine lettuce packed in 1, 3, 5, or 7 layers, the microbial reduction was 0.5-0.8 log CFU/g lettuce for the 1-, 3-, and 5-layer configurations. On the other hand, a greater reduction of 0.9-1.1 log CFU/g was achieved on the top layer in the 7-layer configuration. The reductions in the middle and bottom layers of the 7-layer lettuce did not significantly differ from each other or from the reductions in the other configurations. The number of reactive species in the 7-layer configuration was the highest due to the narrowest headspace; hence, enhanced microbial inactivation by increasing the contact efficiency was attained at the top layer. More uniform microbial reductions in these cases could be obtained by shaking. Overall, ACP treatment will be more uniform if the package has sufficient headspace. Alternatively, ample physical movement of the packaged food should be ensured when the headspace is limited to facilitate the diffusion of the reactive species throughout the package (Min et al., 2017). No study was found regarding the effect of headspace on fungi inactivation via ACP treatment.

- **Direct and remote exposure**

One of the determining factors in ACP efficiency is whether the substrate is in direct contact with the plasma or located remotely from it. Uniform three-dimensional ACP exposure to all the sides of large-sized food products is difficult, owing to the small gap between the electrodes unless high voltages are used. Remote plasma exposure could be potentially used in this case. In remote exposure, the amount of transmitted heat to the sample is reduced, and the charged particles recombine before reaching the sample; hence, they do not play a significant role in microbial inactivation. Moreover, many of the short-lived neutral reactive species also do not reach the sample; therefore, direct plasma exposure is generally more effective for microbial inactivation

(Misra et al., 2011). In treating plasma-activated water, the pH decreased and conductivity increased more rapidly with direct treatment than indirect treatment, demonstrating a clear difference in the concentration and antimicrobial activities of reactive species (Suwal et al., 2019). The higher inactivation efficiency in direct DBD-ACP has been reported in other studies as well (Los et al., 2018; Xu et al., 2017; Zhang et al., 2017). After ACP treatment, alteration from a hydrophilic surface in untreated samples to a hydrophobic surface in treated samples due to damage of spore coat proteins was reported (Los et al., 2017).

2.4.2 Product factors

- **Product type and composition**

Several outbreaks and recalls have been frequently related to meat and meat products due to the presence of foodborne pathogens. Fruits and vegetables are commonly consumed as fresh and need decontamination prior to packaging and distribution. Washing of fruits, vegetables, fresh produce, and meat using chlorine and other chemical disinfectants has long been used for disinfection. However, limited decontamination efficiency and the formation of potentially carcinogenic chlorinated compounds in water are their main drawbacks (Oliveira et al., 2012). Other available decontamination methods include hydrogen peroxide, washing with organic acids (e.g., lactic acid, peracetic acid, etc.), and application of ozone. Low direct antimicrobial efficiency, pH dependence, and influence on quality factors have been reported as the disadvantages of these techniques (Ramos et al., 2013). Hence, alternative non-thermal methods such as ACP treatment may attract some interest from the food industry. In-package and open environment ACP has been used for decontaminating different food products including meat, fruits, vegetables, etc. The antimicrobial efficacy of ACP can be primarily dependent on the type, nature, and composition of

the tested food products. The nature of food constituents (e.g., fat, protein, carbohydrate content) is the other important factor influencing decontamination by ACP.

DBD-ACP treatment has been used for decontamination of plant-based products, such as fruit and fruit juices, with a significant decrease in natural microflora, pathogens, and polyphenol oxidase residual activity and browning without a noticeable change in quality parameters such as total soluble solids, reducing sugar, and total phenolics (Berardinelli et al., 2012; Pasquali et al., 2016; Tappi et al., 2014; Xiang et al., 2018). By using atmospheric DBD-ACP, mesophilic bacteria, yeasts, and molds were reported to decrease by 2.5 log CFU/fruit after 90 min of treatment without any significant adverse effect on quality traits immediately after the treatment. However, after 5 days of storage at 20 °C, the samples treated for 90 min had significant changes in the color and antioxidant capacity of the peel (Berardinelli et al., 2012). In radicchio leaves, decontamination without post-treatment antioxidant capacity change could be achieved using DBD-ACP. A significant change in terms of visual quality was observed after 1-day of storage in comparison to the control (Pasquali et al., 2016). The reduction in microbial content is often attributed to highly reactive chemical species and release of intracellular nucleic acids and proteins in response to alterations in cell membrane permeability (Mahnot et al., 2019; Xiang et al., 2018).

Jo et al. (2014) reported inactivation of *Gibberella fujikuroi*, a seed-borne pathogen, on rice seed surface by 50 %, 90 %, > 92 %, and > 99 %, after 9, 76, 120, and 180 s of ACP treatment, respectively. *Aspergillus flavus*, with an initial viable count of 1.2×10^5 CFU/sample on packaged pistachio, was completely removed after 18 min of ACP exposure (Sohbatzadeh et al., 2016).

- **Surface characteristics**

The substrate surface topology can influence the antimicrobial efficacy of the DBD-ACP treatment. For instance, considerable differences in *E. coli* inactivation efficacies were observed

on seeds with possibly different surface characteristics (Butscher, Van Loon, et al., 2016). The reduction of artificially inoculated *E. coli* on onion seeds was 1.4 log after 10 min of ACP treatment, while the identical treatment conditions resulted in a 3.4-log reduction on cress seeds. One of the main reasons for the observed difference is the different number of fissures, pits, and grooves on the surface of the seeds, which may protect the microorganisms from the plasma-generated species (Butscher, Van Loon, et al., 2016). On rough surfaces, bacteria may attach as multilayers, possibly making it difficult for plasma species to diffuse and inactivate. The antibacterial effect of ACP against bacterial endospores on polymeric model substrates was considerably more effective than on wheat grains (Butscher, Zimmermann, et al., 2016). This was attributed to the complex surface and the ventral furrow of wheat grains (Butscher, Zimmermann, et al., 2016; Los et al., 2018). In another study, better inactivation of bacteria inoculated on tomato surface was reported in comparison to strawberries (Ziuzina et al., 2014). This was due to the smooth surface of the tomato and lower concentration of ozone inside packages containing strawberries after ACP treatment. The presence of pores on strawberries exhibited more surface contact area; hence, the dissolution rate of ozone generated inside the packages containing strawberry increased, and subsequently, the antimicrobial efficacy reduced (Ziuzina et al., 2014).

- **Water content**

Microorganisms become more susceptible to inactivation at high water content with greater ROS (e.g., hydroxyl radicals) generation during ACP treatment in a liquid water phase (Butscher, Van Loon, et al., 2016; Oehmigen et al., 2010; Van Gils et al., 2013). In addition, high water content of substrates increases the relative humidity of the gas phase (Butscher, Van Loon, et al., 2016). High water content facilitates the uptake of ozone by the product surface since ozone is water-soluble. Hence, the contact between the substrate and ozone can be increased at elevated water

content. In the presence of water, ozonation could be catalyzed by free radicals (i.e., hydroxyl ions) (Alexandre et al., 2017). However, Amini and Ghoranneviss (2016) reported that the inactivation rate of *A. flavous* on dried walnuts was higher than that on fresh walnuts after ACP treatment. Food-intrinsic factors such as osmotic stress and suboptimal pH induce stress hardening, creating cells resistant towards the subsequent ACP treatment that influence the inactivation efficacy (Smet et al., 2016). Hence, an optimum water content for each product should be considered in ACP treatment. For instance, the reported optimum water content for inactivation of native microbiota on alfalfa seeds was 17 % (Butscher, Van Loon, et al., 2016). This is due to reactivation of bacteria from the dormant state in the presence of water, a result which makes the bacteria susceptible to ACP. Furthermore, higher amount of ROS could be triggered, which contribute to the inactivation of microorganisms (Reuter et al., 2015; Van Gils et al., 2013). However, high humidity in the discharge may reduce the electron energy and density, quench the excited molecules, and weaken the ACP (Nikiforov et al., 2011).

2.4.3 Microbiological factors

- **Pathogen type**

Bacterial type, strain, and mode of existence are the main microbiological factors relating to inactivation efficacy by DBD-ACP (Los et al., 2017). Yeasts and molds are more sensitive to treatments than mesophilic bacteria (Berardinelli et al., 2012). Applying DBD-ACP on tomatoes reduced both the mesophilic aerobic bacteria and the yeast and molds by 1.3 and 1.5 log CFU/tomato, respectively (Min et al., 2018). Berardinelli et al. (2012) also reported 1 log CFU/fruit reduction of yeast and molds by DBD-ACP in 10 min; however, no significant change was detected for the bacterial count within 30 min of treatment. In longer treatment times (60-90 min), the same decontamination level was observed for mesophile bacteria and for yeast and

molds. In another report, psychrotrophs, total bacteria, and yeast and molds were reduced by 2.1, 2.3 and 2.6 log CFU/cm² within 10 min of ACP treatment (Ulbin-Figlewicz et al., 2015). Morgan (2009) reported D-values of 7 and 4.7 min for *S. cerevisiae* and *M. frigida*, respectively, by argon DBD discharge that demonstrated the faster inactivation of *M. frigida* than *S. cerevisiae*. In that study, *M. frigida* was completely inactivated in 15 min, while *S. cerevisiae* was completely inactivated in 20 min. In a study on *Pseudomonas fluorescens* and *Micrococcus caseolyticus*, after 1.5 min of treatment, DBD-ACP treatment had more antimicrobial effects on gram-negative bacteria *P. fluorescens* than gram-positive bacteria *M. caseolyticus* (J. Wang et al., 2016). In another study, cascaded dielectric barrier discharge (CDBD) was used to inactivate strains like *Salmonella* serotype *Mons*, *Staphylococcus aureus*, and *E. coli* and spores of *Bacillus subtilis*, *Aspergillus niger*, and *Clostridium botulinum*. *Aspergillus niger* was the most resistant strain with an inactivation level of about 3, 4, and 5 log after 1, 3, and 5 s. The highest reduction was observed for the vegetative cells with at least 6.6 log CFU/foil within 1 s, except for *E. coli*. For *E. coli*, reduction of 5.6 log CFU/foil was seen in the first second, and it was reported that the inactivation of the pathogens takes place in the initial seconds of the treatment (Muranyi et al., 2007).

Generally, microbial spores exhibit high resistance against antimicrobial treatments. *Clostridium botulinum* endospores were reduced by 6.1 log CFU/foil within 1 s in comparison to 6.9 log CFU/foil reduction in *Staphylococcus aureus* count, and so, theoretically, the 12-D concept could be carried out after 2 s of CDBD plasma treatment (Muranyi et al., 2007). Important factors in spore resistance against numerous sterilizing agents, in particular in *B. subtilis*, are the relative impermeability of the inner membrane against chemicals, high quantity of dipicolinic acid, the protection of the DNA by small acid soluble proteins, and the low core water content (Setlow, 2006). In addition, bacterial spores contain detoxifying enzymes in their coat that play an important

role in detoxifying chemicals (Henriques & Moran, 2007; Setlow, 2006). The reactive species in ACP cause damage to membranes and enzymes and, as a result, affect the germination process of the spore (Patil et al., 2014). Patil et al. (2014) reported the importance of the water and O₃ presence for higher spore inactivation. High values of RH accelerate the spore swelling and generate more reactive species during ACP treatment that damage the spore structure.

By carefully reviewing the studies on antimicrobial efficacy of ACP treatment, it was observed that the sensitivity sequence of different microorganisms against ACP is yeast-mold-virus > bacteria > spores.

- **Initial count**

Surface microbial loading of the products is one of the microbiological factors that could influence the efficacy of DBD-ACP treatment. The negative correlation of the initial count of microorganisms with inactivation rate by ACP treatment was reported in several studies (Ahlfeld et al., 2015; Deng et al., 2005; Kamgang-Youbi et al., 2008; Perni et al., 2008; Yu et al., 2006). The study conducted by Fernandez et al. (2012) by a nitrogen plasma jet clearly proved that increasing the concentration of *S. typhimurium* from 5 to 8 log CFU/filter reduced the inactivation efficacy of ACP (Fernandez et al., 2012). It was assumed that microbial inactivation depends on cell density, in particular in high initial microbial counts, due to the protective effect of overlaying cells and agglomerates against ACP (Ghomi et al., 2009; Muranyi et al., 2007). In this circumstance, the inactivated top layers of microorganisms could form a physical barrier to shield the underlying microorganisms from ACP penetration (Deng et al., 2005).

- **Growth phase**

The *E. coli* cells at the logarithmic phase are more sensitive to ACP than those at stationary and declining phases (Deng et al., 2007). Similar results were documented for yeast cells exposed to high voltage electric pulses (Gášková et al., 1996; Jacob et al., 1981). In applying electric fields, it was assumed that in the logarithmic stage of yeasts, the amount of the cells in the state of budding was higher than that in the other phases. The budding area of the yeast was more sensitive to electric discharges, and so, they could be inactivated relatively easily (Jacob et al., 1981).

2.5 Antimicrobial mechanisms of DBD-ACP

Two main hypotheses for cell death caused by gas discharge are as follows: Firstly, the total electric force caused by the accumulation of surface charge could exceed the total tensile force on the membrane and cause electrostatic disruption. Secondly, energetic ions, radicals, and reactive species generated by gas discharge cause oxidation, which provokes damage to the cell membrane or cellular components. Scanning electron microscopy of *Saccharomyces* and *Candida* yeast before and after treatment showed rupture in the cell surface after treatment, which resulted in the inactivation of the yeast (Morgan, 2009). ROS from ACP alter the functions of biological membranes and cellular biomolecules via interaction with lipids, proteins, and DNA mostly by the oxidation process. The intense electric field of ACP ruptures the cell membrane and causes bacterial cell leakage and loss of cell functionality (Misra & Jo, 2017). In contrast to most opinions that there was no UV inactivation at atmospheric pressure and that chemically reactive species are entirely responsible for the observed inactivation, it was shown that spore inactivation could be achieved either under the sole action of the reactive species or under dominant UV radiation (Boudam et al., 2006). In Table 2.1, a summary of the inactivation mechanisms of microorganisms associated with ACP treatment is presented.

Table 2.1: Impact of ACP on bacterial cell structure

Bacterial cell structure	Impact by ACP		
Proteins and enzymes	Protein denaturation	Amino acid oxidation	Loss of enzyme activity
Lipids and fatty acids	Membrane lipid peroxidation		
Nucleic acids	Damage to DNA and RNA	Reduction in cell replication	
Cell membrane	Etching and perforation in membrane	Cell membrane damage by diffusion of reactive species	
Cell wall	Breaking of chemical bonds	Erosion due to reaction with radicals	Surface roughness increase
Cytoplasm	Deformation of the cytoplasm	Cell shrinkage	Cytoplasm leakage

*Adapted from (Misra and Jo, 2017)

2.6 Challenges

Production of hot streamers (regions of highly ionized matter) in the air is a feature of DBD-ACP. DBDs may be useful for treating hard solid foods such as nuts, but considering that these localized streamers may leave visible marks on the skins of fruits such as for mangoes and melons, the application of DBD-ACP would be limited due to its influence on appearance and color (Perni et al., 2008). Another factor that should be considered is the high oxidative action of ACP treatment that can affect the bioactive compounds and other food components such as lipids and proteins in food products (Tappi et al., 2014). Plasma exposure can induce the oxidation of sugars into organic acids, peroxidation of lipids, and the modification of amino acid residues in proteins (Cullen et al., 2018). For instance, Baier et al. (2014) used ACP to treat plant leaves and observed that the argon plasma jet was a gentle and suitable ACP source for the application on leafy greens. In contrast, a surface DBD and a remote exposure reactor, fed with plasma-treated air, had significant impacts on the leaf tissue. In ACP treatment, the presence of oxidizing agents could cause oxidation of lipids, thus limiting its potential for high-fat foods also.

During and after ACP treatment of in-packaged products, the generated ozone concentration could be reduced due to its interaction with the surface of the polymer bag. Furthermore, energetic Ar^+ ions in ACP can dissociate the carbon atoms from the polymer when argon gas is used. Ozone can interact with the dissociated carbon and produce carbon dioxide. Hence, the process should be switched off after the maximum ozone concentration is attained and before a significant amount of dissociated fragments form from the polymer surface of the package generated (Leipold et al., 2011). ACP decontamination of food products shares similarities with plasma medicine but also exhibits differences. The treated food products are sometimes more susceptible to plasma than human tissue, and the volume of the products is larger in the food industry (Brandenburg et al., 2019).

Different DBD systems have been designed in the past for a variety of applications in medical, electronics, and engineering fields. With the inherent complexity of ACP and the additional complexity of food products with different constituents, size, shape and surface characteristics, custom designed DBD systems should be developed for food product decontamination applications. Microbial survival during ACP treatment is greatly influenced by surface properties of the substrates used. On rough surfaces, microbial inactivation by ACP may be expected to be lower due to the shielding effect, although reactive species could diffuse on the surfaces. The ACP chemistry is greatly dependent on the electrode material, dielectric barrier and the substrate surfaces used. Hence, a great deal of work is required to understand the plasma chemistry when different food products are used in order to optimize ACP treatments for specific products. The effect of individual ACP components, mainly, ROS, RNS, UV, and electric field, on specific microorganisms is not clearly understood. Hence, additional research on microbial inactivation mechanisms by individual ACP components will help to identify the key components responsible

for microbial inactivation. Other than the aforementioned, several process related factors will influence the decontamination efficacy of ACP treatments, adding another layer of complexity. Application of ACP in the food industry is quite a new field, and it requires considerable research for a better understanding of reaction mechanisms, antimicrobial pathways, the impact of ACP on food quality and safety, and its probable side effects on consumer health. For defining standard ACP exposure conditions for treating the food products, focused research should be conducted on specific applications and the various factors described in this chapter. Hence, at the moment it is difficult to define standard exposure conditions for treating the food products.

2.7 Scale-up of atmospheric pressure DBD plasma technology

At present, the scaling-up of atmospheric pressure DBD plasma systems is limited by technological and economical challenges. Only a few attempts have been made to scale-up the DBD plasma technologies. A continuous atmospheric pressure, high voltage DBD plasma system was developed by researchers from the European Union and found to be successful in extending the shelf-life of cherry tomatoes and strawberries (Ziuzina et al., 2016; Ziuzina et al., 2020). Other attempts to scale-up include the surface DBD plasma technology developed by Anacail in the UK (Anacail, 2018) and a pilot-scale DBD developed and validated in Italy (Ragni et al., 2010).

Process and product parameters including treatment time, plasma density, power and current supply, gap between the sample and high voltage electrode, food properties, and cost of the system and the process should be considered for scaling-up an ACP based process without compromising the plasma uniformity. To keep the uniformity of the plasma in larger scales, much larger voltages (~130 kV) and customized dielectric materials are required (Cullen et al., 2018). For large volume treatments, a sustainable high voltage power source with sufficient lifetime is required. Process

validation is a critical step to assure the safety of food products. In conventional treatments such as heat treatment, process validation is performed through temperature profiling of the heated product. However, in ACP treatment, numerous factors (i.e. process, product and microbiological parameters as described in previous sections) that should be controlled, which is challenging. Yet another concern is controlling the amount and type of reactive species and tuning the plasma chemistry to ensure highest efficiency. The reactive species produced by ACP have a limited lifetime, and no active residue should be left when the food products are on the shelf for sale; however, more studies need to be conducted towards this aspect. The diversity of mechanisms and species involved in ACP treatment is an important challenge to scale-up this technology and define a plasma treatment dose, specific to each product. Some of the reactive species such as ozone, produced during ACP treatment, are stable over a period of time, and their exposure to workers and release from factories to the environment should be controlled. Regulatory approval may be required and toxicity studies in ACP treated foods need to be completed before the scale-up of ACP technology for various applications in food sector.

2.8 Deoxynivalenol (DON)

Cereal crops are infected by spoilage fungi in the field or during storage, and under optimum conditions, some of the fungal species can produce secondary metabolites named mycotoxins. Mycotoxins are toxic in low concentrations to humans and animals. Consumption of mycotoxin contaminated food can cause illnesses such as hepatic, gastrointestinal, and carcinogenic diseases (Fung & Clark, 2004). Trichothecenes are a group of sesquiterpene mycotoxins and DON is one of the most prevalent trichothecenes found on various cereal crops (Mishra et al., 2014). Trichothecenes have a 12,13-epoxytrichothec-9-ene ring as their basic structure. Type B trichothecenes share a keto substitution at C-8 such as DON (Bretz et al., 2006). DON is a common

contaminant of cereal grains with 57, 40, 68, 59, 49, and 27 % contamination rate in wheat, maize, oat, barley, rye, and rice, respectively (Joint FAO WHO Expert Committee on Food Additives, 2002). A recent review regarding the occurrence of DON in food commodities verified that in most of the assessed samples, DON concentration exceeded the permissible levels (Mishra et al., 2020).

DON produced by *Fusarium* spp. is a type B trichothecene. DON is the most predominant and economically important trichothecene, but its toxicity is less than other trichothecenes, i.e., nivalenol and T-2 toxin (Mayer et al., 2017). Studies on animal specimens showed that DON can bind to the ribosome and inhibit protein synthesis. It can cause anorexia and emesis, or exert an immunosuppressive or immunostimulatory effect. It is cytotoxic to fibroblasts and lymphocytes related to protein synthesis inhibition at the ribosomal level with an effective concentration of 0.1–2 µg/ml of DON. Following the ingestion of DON, animals have lower feed consumption and lower weight gain. In higher dietary concentrations of DON, vomiting also has been reported in animals. However, the severity of the effects can differ based on the animal species, age and sex of the animal, concentration of DON, and the source of contamination. A detailed description of the toxic effects of DON can be found in the studies by Rotter (1996), Mayer et al. (2017), Sobrova et al. (2010) and Pestka and Smolinski (2005).

2.9 Potential of atmospheric cold plasma for DON degradation

ACP is a novel non-thermal technology that has the potential for decontamination of microorganisms and mycotoxin. This system produces reactive species, ions, radicals, and UV light which are influenced by the process factors such as voltage, type of gas, relative humidity, treatment time, etc. (Chapter 2, section 2.4.1). Previous studies reported the effect of ACP on the degradation of DON, however, no study assessed the degradation products of DON during ACP

treatment. In Chapter 4, we performed ACP treatment (34 kV, 2 mm gap) for 6 min, which reduced the DON levels on spiked barley by 48.9%. The chemical reaction of reactive species produced during ACP with mycotoxin, decomposition of the mycotoxin after collision with electrons and ions, and UV light are considered as the factors that contribute to the cleavage of DON or other mycotoxins by ACP treatment (ten Bosch et al., 2017). This could explain the higher degradation rate of DON via ACP compared with ozone treatment, as numerous factors contribute to the degradation of the toxin in ACP. Among the reactive species produced during ACP treatment, reactive oxygen, and reactive nitrogen species (RONS) comprise the major part (N. Misra et al., 2019). Ozone, which is one of the ROS in ACP, probably plays a major role in the degradation of DON via ACP (Chapter 4).

The presence of water could contribute to the formation of RONS in ACP and improve the degradation rate of DON (Chapters 3 and 4). DON in solution (acetonitrile/water (20/80, v/v)) reached undetectable levels within 5 min of ACP treatment; however, in the dry state the degradation rate was 25.1%. In a solution, more ROS would be generated and the uptake of ozone which is soluble in water would increase, improving the degradation rate of DON (Chapter 3). Fourier-transform infrared spectroscopy results indicated the formation of carbonyl group or epoxy group in the degraded product after treating DON with ACP (Chapter 3). The effect of dielectric barrier discharge plasma (ten Bosch et al., 2017), gliding arc plasma (Kříž et al., 2015), low-pressure microwave plasma (Kříž et al., 2015), and microwave-induced argon plasma (Park et al., 2007) on DON degradation have been assessed previously. UV radiation and etching by plasma were mentioned as the probable reasons for the degradation of DON by plasma (Park et al., 2007). It was postulated that the presence of aromatic rings in the structure of a toxin may contribute to its lower plasma-induced degradation compared with another toxin with a different structure (ten

Bosch et al., 2017). Acytotoxicity assay showed the complete decrease of DON cytotoxicity after 5 s treatment by microwave-induced argon plasma system (Park et al., 2007).

Plasma activated water (PAW) is another method of degrading DON and other mycotoxins. There are multiple studies on the application of PAW on bacterial inactivation. These studies have mentioned one reason for the inactivation of bacteria which could be relevant in the degradation of mycotoxin as well. The synergistic action of a high positive oxidation-reduction potential (ORP) and low pH (pH~ 2–3) (Oehmigen et al., 2010; Tian et al., 2015b) are the main reasons for the inactivation of bacteria. H_2O_2 , $\cdot\text{OH}$, $\cdot\text{O}$, O_3 , and reactive nitrogen species (RNS) in PAW can increase the OPR. RNS also contributes to low pH (Rathore et al., 2021). A previous study reported that soaking the contaminated barley in PAW for 5, and 20 min, reduced the DON concentration by 22.5, and 25.8%, respectively (Chen et al., 2018). The degradation rate of DON was correlated to OPR and pH. In PAW, short-lived reactive species such as hydroxyl radical ($\cdot\text{OH}$), superoxide (O_2^-), and singlet oxygen (O or O^-) may not play any role in the degradation of DON; the major contribution for inactivation will be accomplished by long live reactive species such as O_3 , H_2O_2 , NO_3^- (Chen et al., 2018). It is important to state that during ACP treatments, the temperature of the sample does not rise to more than 60 °C, and hence no thermal degradation of the mycotoxin is expected (ten Bosch et al., 2017).

The concentration and type of the reactive species during ACP could vary according to the process factors such as relative humidity of the air, voltage and current of the system, treatment time, type of the carrier gas, type of electrodes and dielectric materials, the gap between the electrodes, direct or remote exposure of toxin to the ACP, and the water content of the sample (Chapter 2, section

2.4). This makes the identification of degradation products and degradation pathways of mycotoxins via ACP challenging.

2.10 Concluding remarks

The antimicrobial properties of ACP, primarily due to the radicals and reactive species, along with its lowest impact on food quality attributes, are the incentives for this technology to be applied in food processing. ACP can potentially be employed in the food production and processing lines for different products, including meat, fruit and vegetables, nuts, eggs, cereals, and packaged products, and scaled-up for surface decontamination of food products. However, ACP treatment may not be able to completely replace conventional sterilization processes used in the food industry due to the limitations of the technology (e.g., poor penetration of reactive species inside foods). Since food products vary in size, shape, and nature, ACP systems should be designed depending on the specific application and product type for future scale-up of this technology for food decontamination purposes. The antimicrobial properties of ACP depend on process factors including voltage, frequency, relative humidity, temperature, flow rate and gas, type of electrode, interelectrode spacing, treatment time, headspace, and exposure pattern type; product factors including water content, type of product, surface characteristics; and microbial factors including growth phase, initial count, and type of the pathogen. Optimization of process conditions (e.g., in-package ACP treatment) and custom-designed plasma systems for best outcomes require improved characterization and thorough knowledge about the important process, product, and microbiological factors.

There are limited studies focusing on evaluating the mycotoxin degradation efficacy when ACP is integrated with other decontamination approaches. This was addressed in Chapters 3, and 5 where

the degradation efficacy of ACP system was evaluated against two of the important mycotoxins prevalently found on grains in Canada. Moreover, further research is required to understand the influence of various product and process parameters and their interactions on the mycotoxin degradation efficacies of ACP which has been addressed in Chapters 3, 4, and 5. Chapter 6 addressed the research gap of understanding the degradation mechanism of DON, and also the possibility of using PAW in malting of barley for DON degradation. In Chapter 7, the antimicrobial efficacy of PAW bubbles was investigated against *F. graminearum* during malting of naturally infected barley.

Chapter 3: Degradation of deoxynivalenol by atmospheric-pressure cold plasma and sequential treatments with heat and UV light

3.1 Introduction

Mycotoxins are toxic secondary metabolites produced by fungi that can be present in animal feed and human food products. Each year, around 25 % of agricultural commodities are contaminated by mycotoxins (Chen et al., 2018), causing financial harm to the agricultural industry, product quality losses, and harmful effects on human and livestock health. Deoxynivalenol (DON, vomitoxin) (Figure 3.1), produced by *Fusarium graminearum* and *Fusarium culmorum*, is one of the prevalent mycotoxins that contaminate cereals and cereal-based products (Alizadeh et al., 2016). Consumption of DON-contaminated feed by animals can lead to vomiting, diarrhea, feed refusal, anorexia, hemorrhage, and weight loss (Brenn-Struckhoffova et al., 2007; Chen et al., 2018). The Canadian Food Inspection Agency (CFIA) has established maximum DON limits for different types of food products. Currently, the maximum permitted levels are: 2 ppm for uncleaned soft wheat for human consumption, 5 ppm in diets for cattle & poultry, and 1 ppm in diets for swine, young calves, & lactating dairy animals (Canadian Food Inspection Agency, 2022). Prevention strategies for mycotoxin contamination include preharvest methods (crop rotation, sowing date, and tillage), and crop processing methods (dehulling, sorting, milling), which are limited by low efficacy, and nutrient loss. Alternative strategies include fungicide applications and chemical and biological procedures applied before harvesting, but these strategies are limited by crop quality losses, strict national food safety regulations, detrimental effects on human health and the environment, and high cost (Akocak, 2016). Mycotoxins are resistant to the high temperatures encountered in food processing such as roasting, extrusion, baking, and even frying which can

only partially degrade them (Bullerman & Bianchini, 2007). Therefore, effective and practical methods for mycotoxin degradation need to be developed.

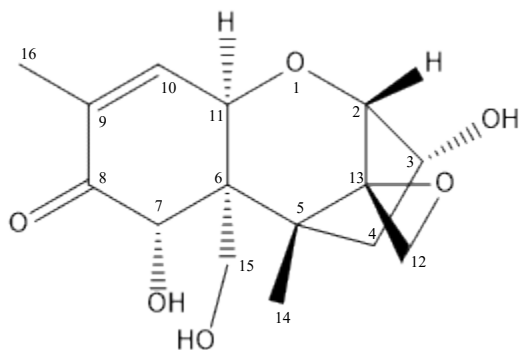


Figure 3.1: Chemical structure of DON

Atmospheric-pressure cold plasma (ACP) is a novel nonthermal technology with the potential to inactivate microorganisms such as fungi and degrade mycotoxins without affecting the quality of the treated products (Baier et al., 2014). ACP consists of neutral gases, ions, free electrons, atoms, and photons. The reactive chemical species, in particular, reactive oxygen species (ROS) and reactive nitrogen species (RNS) in ACP play a major role in mycotoxin degradation (Chapter 4). The reduction of mycotoxins by ACP treatment depends on processing factors (input power, treatment type, gas type, exposure mode, flow rate), environmental factors (food matrix and relative humidity), and mycotoxin properties (Chapter 4). ACP treatment has been reportedly used to degrade a number of mycotoxins (N. Misra et al., 2019). For instance, ten Bosch et al. (2017) evaluated the efficacy of ACP treatment to degrade pure DON, zearalenone, enniatins, fumonisin B1, and T2 toxin and reported almost complete degradation of these mycotoxins after 60 s ACP treatment. In Chapter 4, we reported the reduction in DON concentration by 48.9 % on barley grains with 10.8 % moisture content by 6 min ACP treatment. There is no information about the effect of ACP treatment on the structural changes in DON and the mechanisms by which it is degraded. Information on DON degradation mechanisms and the identification of the degradation

byproducts by ACP will help us to optimize treatment conditions and analyze the toxicity of degradation byproducts.

Heat and pulsed light treatments have been shown to inactivate mycotoxins in human food and animal feed products (Bretz et al., 2006; Moreau et al., 2013). However, no previous study has reported a synergistic effect of adding ACP to heat and light treatments. High temperatures (> 100 °C) are required to degrade mycotoxins (Bretz et al., 2006; Humpf & Voss, 2004), but high temperatures would have adverse effects on food quality. Mild heat (<100 °C) treatment along with ACP may provide a synergistic mycotoxin degradation effect, though no previous study has reported this possibility. The recent development of LEDs emitting high intensity monochromatic light pulses have opened new opportunities to use this technology in food processing including mycotoxin and microbial decontamination (Moreau et al., 2013; Subedi & Roopesh, 2020). A sequential treatment mode based on ACP, LED, and heat may have a synergistic effect on mycotoxin degradation; however, there is currently no record of this approach. The main objective of this study was to evaluate the ability of ACP alone and in combination with LED or mild heat treatment in sequential mode to reduce the concentration of DON in solution and dry forms. The structural changes in DON after ACP treatment were also investigated by selected analytical techniques.

3.2 Materials and methods

3.2.1 Mycotoxin standards

HPLC grade acetonitrile (ACN) and methanol (Fisher Chemical, Geel, Belgium), and standard solutions of DON (100 $\mu\text{g}/\text{ml}$ ACN, Sigma Aldrich, Mississauga, Canada) were used. To have 100 μl of DON solution with the concentration of 20 $\mu\text{g}/\text{ml}$ ACN/water (20/80, v/v), we diluted 20 μl of the initial DON solution (100 $\mu\text{g}/\text{ml}$ ACN) with 80 μl of water. ACN/water (20/80, v/v) was

used for the next dilutions of DON from 20 µg/ml ACN/water (20/80, v/v), to the desired experimental concentrations.

3.2.2 Sample preparation

A round cover-glass with a thickness of 150 µm and a diameter 18 mm was placed on microscopy slides and 100 µl deoxynivalenol (DON) solution (20 µg/ml ACN/water (20/80, v/v)) was applied centrally on the cover-glass. Air drying of the DON solution was performed at room temperature (~23 °C). After 75 min of air drying, the solution was completely evaporated on the coverglass, which was visually noticeable. After air-drying, 2 µg DON with 0 % water, and 0 % ACN content was treated by ACP, LED, or heat as described below. Then the cover-glass containing the DON was immersed in 1 ml methanol, shaken for 1 min with a vortex, and evaporated to dryness with a nitrogen stream. ACN/water (20/80 v/v), 1 ml, was then added and further analysis of the DON was performed by HPLC. To assess the degradation of DON as a solution (20 µg/ml ACN/water (20/80, v/v)), the 75 min drying step was skipped.

3.2.3 Atmospheric-pressure cold plasma treatment of DON

A dielectric barrier discharge (DBD) atmospheric-pressure cold plasma (ACP) system (PG 100-D, Advanced Plasma Solutions, Malvern, PA) was used to treat DON samples (Yadav et al., 2019) with the concentration of 20 µg/ml ACN/water (20/80, v/v) with 100 µl placed on a cover-glass which was on a microscopy slide, and the slide was positioned on a glass insulated cover (1 mm thickness) on top of a ground electrode of an ACP system. The gap between the high voltage electrode and the DON sample was 2 mm (Figure 3.2) during the experiments. The upper electrode was connected to the high voltage generator, which had a frequency of 3500 Hz and a 70 % duty cycle. The electrode produced a high pulsating voltage output of 0-30 kV with a 0-1 A current output and a 10 µs pulse width (Yadav et al., 2019). The DON samples with 0 % water, 0 % ACN

(dry sample, 2 μg) were subjected to ACP using air as the medium, with treatment times of 0.5, 1, 5, 15, 30, and 60 min while DON samples in solution were subjected to ACP treatments for 1, 2, 3, 4, and 5 min. Here, untreated samples were considered as control.

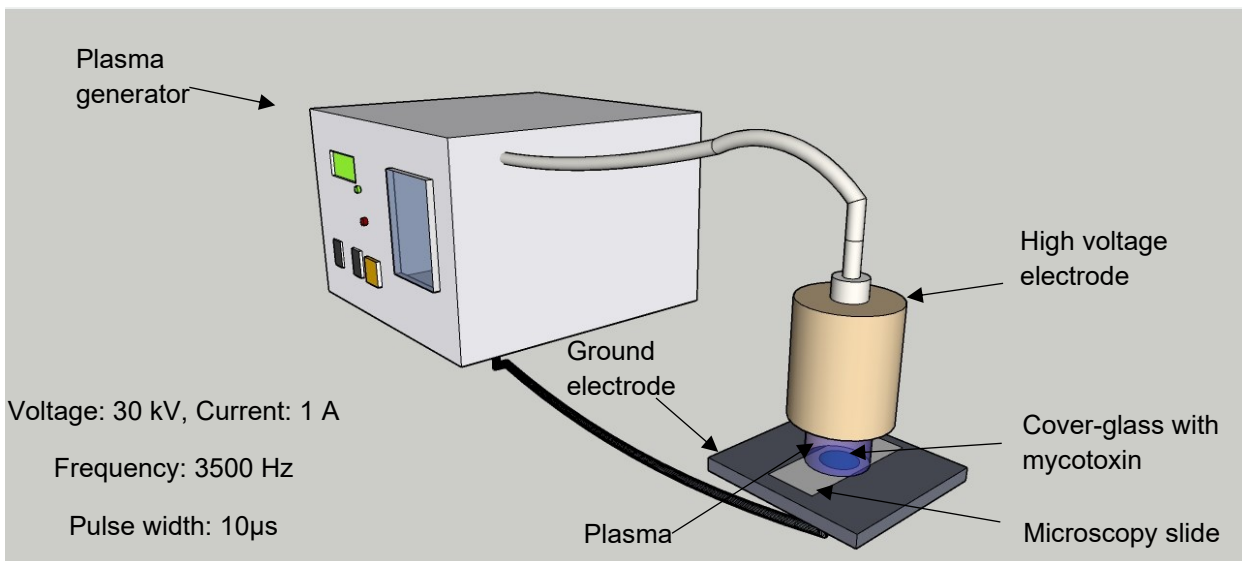


Figure 3.2: Schematic diagram of dielectric barrier discharge atmospheric cold plasma system used in this study

3.2.4 HPLC analysis

DON samples were stored at 4 °C for <24 h after treatments and before HPLC analysis. The concentration of DON was determined by high-performance liquid chromatography (HPLC) on a reversed-phase Agilent Zorbax SB-C18 250 mm \times 3 mm, 5 μm column with isocratic elution. The injection volume was 25 μl at a flow rate of 0.5 ml/min, using a mixture of water and ACN (85:15 v/v) as the mobile phase. DON concentrations were determined at a wavelength of 218 nm using a photo diode array (PDA) detector. The limit of quantification of DON by HPLC was 0.02 $\mu\text{g/ml}$.

3.2.5 TLC analysis

Thin-layer chromatography (TLC) has been used in other studies to analyze DON (Kim & Vujanovic, 2017; Rocha et al., 2017). TLC analysis was performed on aluminum plates coated with silica gel at room temperature. One milliliter of DON in solution mode (0.8 mg DON/ml

ACN/water (20/80, v/v)) was air-dried for 3.5 h and treated by ACP for 60 min. Then, control and ACP-treated DON were solubilized in 1 ml ACN and individually applied to a TLC plate. The TLC plates were developed in ACN: hexane (50:50), air-dried, then the spots were observed under UV light. For visual comparison, the plates were smeared in vanillin stain and heated with a heat gun. The relative mobility or retention factor (R_f) was calculated by the following equation.

$$R_f = \text{distance from start to the center of substance spot} / \text{distance from start to solvent front} \quad (1)$$

3.2.6 ATR-FTIR analysis

To assess the effect of ACP on the degradation of DON solution, 0.6 ml DON (0.8 mg DON/ml water, ACN (80:20 v/v)) was subjected to ACP (the gap between the electrodes was 5 mm) for 5 min before attenuated total reflectance Fourier transform infrared (ATR-FTIR) spectroscopy analysis. To assess the effect of ACP on the degradation of DON in a dry condition, 0.6 ml DON (0.8 mg DON/ml ACN/water (20/80, v/v)) was air-dried for 3.5 h to remove ACN and water from the stock solution, then treated with ACP for 60 min (the gap between the electrodes was 2 mm) before FTIR analysis. The control sample was air-dried DON solution without ACP treatment. The 5 and 60 min ACP treatment times were chosen as we observed the maximum degradation in DON concentration after these treatment times. A Bruker Alpha FTIR spectrophotometer (Bruker Optics, Esslingen, Germany) equipped with a single bounce diamond ATR (attenuated total reflectance) crystal was used to collect the spectrum at a resolution of 2 cm^{-1} over a range of $410\text{--}4000 \text{ cm}^{-1}$ (Peiris et al., 2012). All sample spectra were recorded with 64 scans and averaged using OPUS software (Bruker version 6.5). A background spectrum of the clean ATR crystal was collected before applying and collecting the sample spectrum. FTIR spectra were analyzed using Nicolet Omnic software (version 8).

3.2.7 Effects of initial DON concentration and ACN/water content on DON degradation by ACP

The DON stock solution (100 µg/ml acetonitrile) was diluted with ACN/water (20/80, v/v) to prepare samples with 4, 20, and 100 µg/ml ACN/water (20/80, v/v) concentrations. After air-drying at room temperature to remove water and ACN, samples were used to evaluate the effect of the initial concentration on the DON degradation efficacy of ACP. DON samples were treated with ACP for 15 min, then DON was quantified by HPLC analysis. The control samples were 4, 20, 100 µg/ml ACN/water (20/80, v/v) DON samples without ACP treatment.

Selected ACN/water contents of 0, 5, 20 and 100 % (wet basis) were used to estimate the effect of ACN/water content on DON degradation. For this analysis, 100 µl of the DON with the concentration of 20 µg/ml ACN/water (20/80, v/v) was air dried to reach the desired ACN/water content. The sample (20 µg/ml ACN/water (20/80, v/v)) was air dried to reduce the ACN/water content from 100 % to 20, 5, and 0 %, respectively. ACN/Water content of the samples were measured based on the weight reduction of the sample (20 µg/ml ACN/water (20/80, v/v)) during air drying. The sample was then treated with ACP and analyzed by HPLC.

3.2.8 Optical emission Spectroscopy of ACP discharge

Optical emission spectra (OES) were collected to identify the major reactive species in the excited state produced by the ACP discharge, using a spectrophotometer (Black Comet, C-25, S/N 17060712, StellarNet Inc., Tampa, FL) with a resolution of 0.5 nm in the wavelength region of 180 to 850 nm (Yadav et al., 2020). One end of the optical fiber (F600-UVVIS-SR, StellarNet, Inc., Tampa, FL) was connected to the spectrophotometer and the other end with the collimating lens and kept 30.4 mm away from the center of the plasma discharge to capture the emission intensity of plasma discharge. The obtained spectra were analyzed by SpectraWiz software

(StellarNet). The set integration time was 100 ms and the set values of the number of scans to average were 10 to capture uniform spectra. Three spectra were obtained and averaged for peak identification.

3.2.9 Pulsed light treatment using LEDs in combination with ACP

DON samples (20 µg/ml ACN/water (20/80, v/v)) air-dried, to obtain 0 % water and 0 % ACN, were treated by ACP, followed by pulsed light treatments using LEDs to assess the efficacy of DON degradation by LEDs. For this purpose, the effect of sequential treatment consisting of 30 min ACP + 30 min LED was evaluated. For pulsed light treatment, an LED head (JL3-395G2-6, Clearstone Technologies Inc., Minneapolis, MN) emitting light pulses with a wavelength of 395 nm (100 Hz at a 60 % power level) was connected to the power controller (CF3000, Clearstone Technologies Inc., Minneapolis, MN) during the experiments (Du et al., 2020; Prasad et al., 2019). During pulsed light treatments, the DON sample temperature reached a 50 °C maximum. The gap between the sample and the LED head was 2 cm. A fan (20 V, 0.284 A) was used during the pulsed light experiments to keep sample temperature at this maximum 50 °C. The power level of LED system was 60 %, and the frequency was 100 Hz. The height and positioning of the samples were uniform during all experiments. Control sample was air-dried DON sample without ACP treatment.

3.2.10 Heat treatments in combination with ACP

To investigate the synergistic effectiveness of sequential ACP and heat treatments on the degradation of air-dried DON samples (20 µg/ml ACN/water (20/80, v/v)), ACP-treated DON samples were heated to 80 °C on a digital hot plate (Fisher Scientific, Ottawa, ON, Canada) and held for 25 min. During heat treatments, sample temperature was monitored using an infrared

thermometer (Optris, Berlin, Germany). The time required for the samples to reach 80 °C was 4.5 min. The control sample was an untreated DON sample.

3.2.11 Statistical analysis

All parameters were evaluated in three replicates, and the results were expressed as mean value \pm standard deviations. Significant differences among the control and treated samples were determined by a one-way analysis of variance (ANOVA) followed by a Duncan's multiple range test at $p \leq 05$ (IBM SPSS v.21, Armonk, NY).

3.3 Results and Discussion

3.3.1 DON degradation and efficacy of ACP treatment

DON samples in solution (20 μg DON/ml (ACN/water (20/80, v/v)) reached undetectable levels within 5 min of treatment (Figure 3.3). However, the ability of ACP to degrade DON when completely dry, decreased significantly. For instance, five minutes of ACP treatment decreased the same amount of dried DON by only 25.1 %. Greater degradations were observed after longer ACP treatment; i.e., a 60 min ACP treatment of a dry sample reduced the DON concentration by 75.9 %. As ozone is water-soluble, the presence of water facilitates the sample uptake of the ozone produced during ACP treatment (Alexandre et al., 2017). Also, a higher amount of ROS could be generated during ACP treatment, when water is present in the system, which may have enhanced DON degradation. Ozone can oxidize organic compounds either directly or by radical intermediates such as $\cdot\text{OH}$ (Van Gils et al., 2013). The $\cdot\text{OH}$ radical is one of the main reactive species generated by photo-dissociation of water molecules due to the UV light originating from the ACP discharge. Production of $\cdot\text{OH}$ can lead to the formation of H_2O_2 , an oxidizing agent (Van Gils et al., 2013). It was proposed that the reaction between ozone and DON begins with the attack

of ozone at the 9, 10 double bond of DON and the net addition of two oxygen atoms (Figure 3.1) (Freitas-Silva & Venâncio, 2010). The oxidation state of the allylic carbon 8 position is an important factor in determining the reaction rate between ozone and DON, as determined by the number of moles of ozone required to affect oxidation (Freitas-Silva & Venâncio, 2010). Future research is required to understand the DON degradation mechanism, degradation byproducts, and their cytotoxicity after ACP treatment. Numerous factors are involved in the efficacy of the ACP system, i.e., process factors (voltage, frequency, current, type of gas, relative humidity, material, thickness, and spacing of electrodes and barrier, treatment time, etc.), and product factors (water content, surface characteristics, etc.) (See Chapter 2, Section 2.4). Any change in the aforementioned factors may impact the degradation mechanisms and hence the degradation byproducts, which makes it difficult to analyze the byproducts and their cytotoxicity.

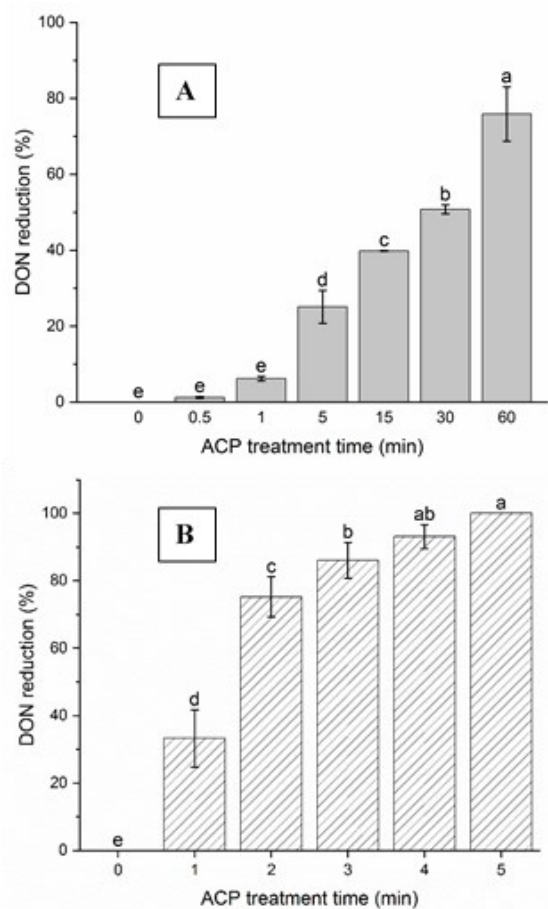


Figure 3.3: Effect of ACP treatment times at 30 kV and 2 mm gap on DON degradation (%) determined by HPLC. A) with 0 % water, 0 % ACN B) in ACN/water (20/80, v/v). Data are shown as least square means \pm standard deviations. Values with different letters are significantly different ($p < 0.05$, $n = 3$)

3.3.2 TLC analysis

TLC analysis was used to assess the number of byproducts generated after ACP treatment of dry DON samples. TLC analysis did not detect byproducts after ACP treatment of dry DON. Detection of a single spot in the treated sample in TLC plate might be due to the low ACP degradation of DON at high amounts (800 μg) and a dry condition. In addition, DON byproducts after ACP treatment could be masked by the undegraded DON if they share a similar polarity. A single spot aligned at an R_f of 0.66 was detected for the control and the treated samples. In retention factor

determination, the basic principle of solute retention is its distribution between the sorbent and the mobile phase (Zapala & Waksmundzka-Hajnos, 2004). The R_f value for the control and treated sample was 0.66. Kim and Vujanovic (2017) reported an R_f value of 0.63 for DON in a TLC mobile phase of 93 % dichloromethane and 7 % methanol.

3.3.3 ATR FTIR analysis

Infrared spectroscopy has widespread use in the structural characterization of chemical compounds because of its capability to identify different functional groups. It has good sensitivity, detection is rapid, and no previous expertise is required to use ATR FTIR (Astoreca et al., 2017). The position of absorption bands in the FTIR spectra of DON samples (Figure 3.4) obtained from ACP treated and control samples were analyzed for the 4000-500 cm^{-1} spectral region. The broad band from 3600-3100 cm^{-1} resulted from stretching vibrations of -OH groups attached to DON carbons at positions 3C, 7C, and 15C. Absorption bands in the region 3030-2800 cm^{-1} correspond to the stretching vibrations of -CH, -CH₂, and -CH₃ groups, including those attached to the C9-C10 double bond (Fu et al., 2014; Peiris et al., 2012) of DON. The peak intensity in the range of 1710-1600 cm^{-1} is due to alkene (C=C) and carbonyl group vibrations that are overlapped. The bands at 1450-1400 cm^{-1} can be assigned to CH₃-C=CH and bending vibrations of -CH₃, -CH₂ (Pretsch et al., 2000). Bending vibrations at 1350-1330 cm^{-1} can be attributed to methine protons of DON (Coates, 2000). The absorption bands at 1270-1200 cm^{-1} could represent C-O and C-O-C epoxy ring vibrations (Pretsch et al., 2000). Other bands that appear in the fingerprint region of the spectra represent: C-O stretch vibrations (1200-1100 cm^{-1}), C-OH (1100-1210 cm^{-1}), CH-O-CH vibrations (1170-1115 cm^{-1}), cyclohexane ring and C-O stretch vibrations (1055-1000 cm^{-1}), CH₂-OH (1075-1000 cm^{-1}), CH-OH (1100-1000 cm^{-1}), epoxy ring C-O antisymmetric stretch (947 cm^{-1}), C=CH (890 cm^{-1}), alkane stretching and bending vibrations (1150-800 cm^{-1}), C-H single bond bending

vibrations ($< 800 \text{ cm}^{-1}$) (Coates, 2000; Peiris et al., 2012; Pretsch et al., 2000). Peiris et al. (2012), studied the mid-infrared absorbance spectra of DON, and our FTIR spectra of the control sample were in complete agreement with the graph they obtained for DON. The FTIR spectrum of ACP treated DON in 0 % water did not show a significant difference from that of the control sample (Figure 3.4). On the other hand, the spectrum of DON treated with ACP in can/water (20/80, v/v) showed notable differences from the control sample, specifically at wavenumbers 1280, 1450-1400, 1730 cm^{-1} . The appearance of a new peak at 1730 cm^{-1} in the spectrum of the ACP treated DON in the presence of water can be attributed to the C=O group of either an aldehyde or a ketone formed during the treatment. An additional peak at 1280 cm^{-1} representing treated DON in the presence of 80 % water could be due to the formation of an epoxy ring or ether linkages (C-O-C) in the treated sample. Moreover, the disappearance of an absorption band at 1450-1400 cm^{-1} assigned to $\text{CH}_3\text{-C}=\text{C}$, $-\text{CH}_3$, and $-\text{CH}_2$ was observed in the treated sample. The absence of these -CH vibration bands could indicate the formation of additional carbonyl groups in the form of aldehyde or ketone functional groups or an epoxy ring. Reduction in DON concentration after ACP treatment, in the presence of 80 % water represents degradation of DON. FTIR analysis of DON does not provide sufficient information about the degradation byproducts after ACP treatment. Degradation product structures after ACP treatment of aflatoxin B₁ was proposed using HPLC-MS-MS analysis (Hu Shi et al., 2017). Due to the presence of possible multiple degradation products after ACP treatment, it is difficult to know the exact structure of each of the degradation byproducts. However, the results from FTIR could be helpful in drawing the structures

of the degradation products, with the help of other analytical techniques such as Nuclear Magnetic Resonance (NMR).

3.3.4 Effect of initial concentration on DON degradation by ACP

Experiments were conducted in this study to find out any possible effect of initial concentration of DON on the efficacy of ACP. The highest degradation rate of DON was achieved at the lowest initial DON concentration (Figure 3.5). However, no trend was observed between the initial concentration of DON and the degradation rate of DON by ACP. Vidal et al. (2015) studied the effect of baking at 200 °C on the degradation of DON. They observed that a DON concentration

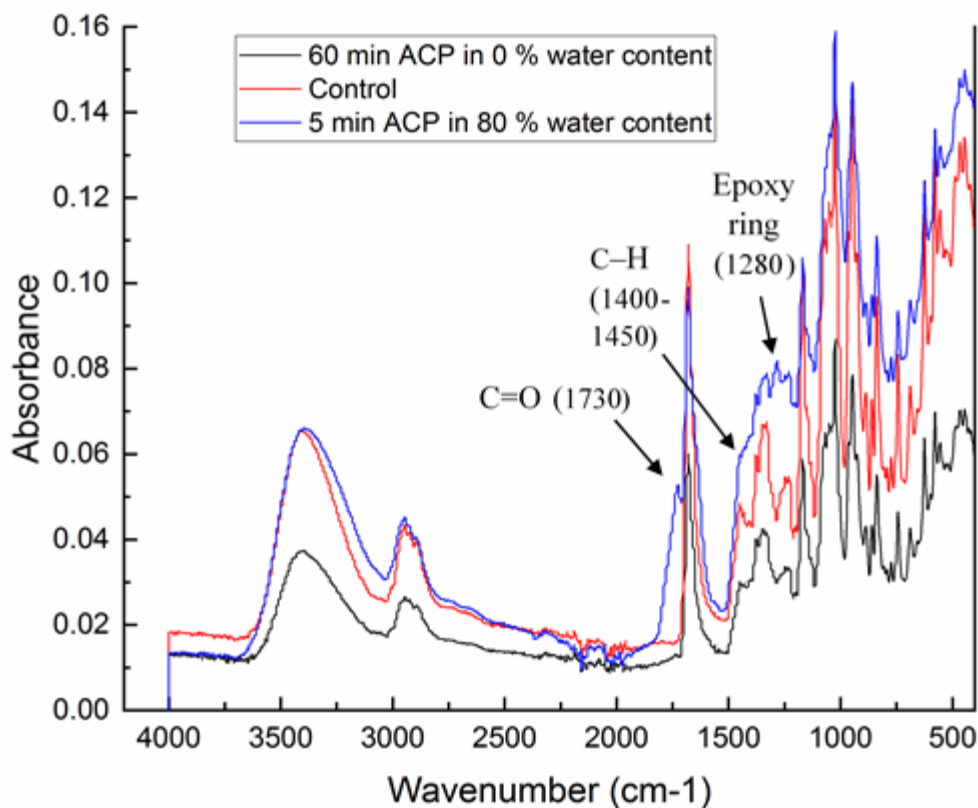


Figure 3.4: ATR-Fourier transform infrared spectrum of DON in solution (0.8 mg DON/ml ACN/water (20/80, v/v)) and dry mode (0 % water, 0 % ACN) after ACP treatment

of 1.04 µg/ml had a higher degradation rate than a DON concentration of 0.55 µg/ml. This observation could be due to the different degradation mechanisms of heat and ACP treatments. We

did not observe an increasing DON degradation trend with a DON concentration increase. The possible reason for higher DON degradation in a lower initial DON concentration could be due to no overlaying of toxin, and higher ratios of reactive oxygen species (ROS) and reactive nitrogen species (RNS) to the mycotoxin concentration. Another reason could be the ability of HPLC columns to differentiate between byproducts of different concentrations, as masking of the degraded and undegraded products in HPLC column can result in different detection limits. However, the above statements should be verified by careful investigations in the future.

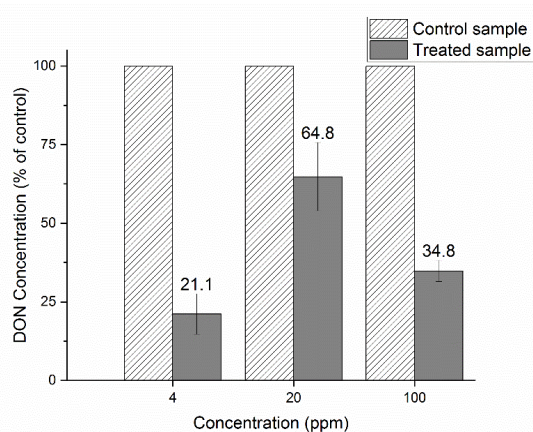


Figure 3.5: Effect of initial concentration of DON on degradation efficiency of 15 min ACP. Data are shown as least square means \pm standard deviations. Values with different letters are significantly different ($p < 0.05$, $n = 3$)

3.3.5 Effect of initial ACN/water content on DON degradation with ACP

To evaluate the influence of initial ACN/water content on DON degradation by ACP treatment, four initial ACN/water contents in DON samples were used (Table 3.1). The initial ACN/water content had a crucial effect on the DON degradation efficacy of ACP (Table 3.1) so that even 5 % of ACN/water significantly increased the degradation rate of DON. At the completely dry condition (0 % water content, 0 % ACN), only 14 % degradation of DON was observed. It is possible that a high water content in the sample would increase the relative humidity of the gas phase (Butscher, Van Loon, et al., 2016), and consequently would increase the generation of $\cdot\text{OH}$

radicals during ACP treatment, which eventually could lead to the oxidation of DON (Butscher, Van Loon, et al., 2016; Oehmigen et al., 2010; Van Gils et al., 2013). Furthermore, greater ROS generation could happen in a liquid water phase during ACP treatment (Butscher, Van Loon, et al., 2016; Oehmigen et al., 2010; Van Gils et al., 2013). Additionally, the presence of water could enable a higher uptake of ozone by DON (Alexandre et al., 2017).

Table 3.1: Effect of the initial ACN/water content on the reduction of DON concentration by ACP

Treatment method	Average concentration (µg/ml)	Average reduction (%)
Control sample 0 % ACN/water	20.2±0.1 ^a	0 ^d
Control sample 100 % ACN/water	20.1±0.2 ^a	0 ^d
sample with 0 % ACN/water, 2 min ACP	17.3±1.0 ^b	14.1±5.1 ^c
sample with 5 % ACN/water, 2 min ACP	0 ^d	100 ^a
sample with 20 % ACN/water, 2 min ACP	0 ^d	100 ^a
sample with 80 % ACN/water, 2 min ACP	3.0±1.8 ^c	84.8±9.1 ^b

Values with different letters in the same column are significantly different ($p < 0.05$, $n = 3$).

When the ACN/water content was 100 % (wet basis), we observed a lower reduction in the rate of DON degradation by ACP in comparison to 5 % and 20 % ACN/water contents. A high ACN/water content could have produced more vapor in the environment, which would reduce the number of micro-discharges in the ACP, as the adsorption of water would lower the surface resistance of the dielectric material by the adsorption of water molecules (Falkenstein, 1997; Falkenstein & Coogan, 1997). Moreover, the presence of high humidity in the plasma discharge might result in loss of electron energy in electron-molecule collisions, quenching the ACP effect (Bruggeman et al., 2009; Butscher, Van Loon, et al., 2016). Studies on the inactivation of microorganisms with ACP reported the decrease in the inactivation rate at higher relative humidities than the optimum. It was proposed that the reduced discharge homogeneity at high humidity, the poorer transmissibility of UV radiation, and a protective water film around the microbial cells could be

the reasons for lower ACP efficacy at high relative humidity (Maeda et al., 2003; Muranyi et al., 2008). The result of this experiment could be helpful for industries to reduce the concentration of DON in cereal grains such as barley. Water can be sprayed on the surface of the grains for increasing the degradation rate of DON by ACP, or ACP treatment can be applied where water is used in the processing of grains such as during malting process.

3.3.6 Optical emission spectroscopy of ACP discharge

Optical emission spectroscopy was used to investigate the major reactive species generated by ACP discharge in the wavelength range of 180 to 850 nm. As shown in Figure 3.6, the major peaks were observed in the UV range (200 to 400 nm) and a few minor peaks in the visible range. The emission intensities of ACP discharge were dominated by excited nitrogen second positive system at 316, 336.5, 357, 380, and 405 nm, and nitrogen first negative system at 391.5 nm (Zhou et al., 2018). The nitrogen second positive system and first negative system are mainly produced due to the electron impact excitation of the molecular ground state of nitrogen. The emission peaks in the range of 280 to 310 nm (Figure 3.6) were identified as OH radicals, which could be produced via electron impact dissociation of water vapor present in the atmospheric air (Chaplot et al., 2019; Zhou et al., 2018). The results of OES indicated that the ACP discharge used in this study is a significant source of RNS and ROS.

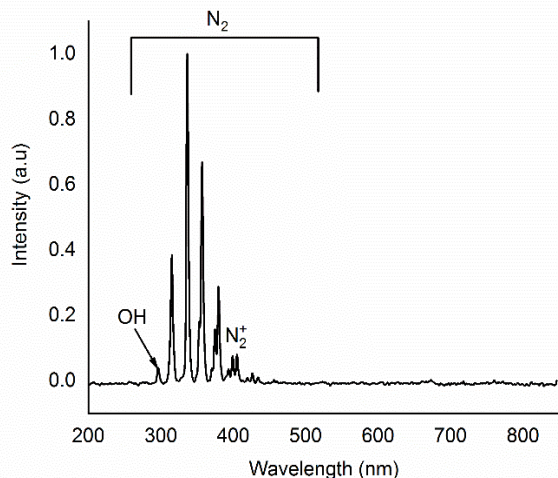


Figure 3.6: Optical emission spectra of atmospheric air DBD plasma generated at 34 kV

3.3.7 DON degradation with LED pulsed light treatment in combination with ACP

Treatments using 395 nm wavelength light pulses emitted from LEDs for 30 and 60 min in combination with ACP were performed to understand the synergistic DON degradation efficacy. In a previous study that treated aflatoxin with UV light, greater UV absorbance was observed at 362 nm than at lower wavelengths of 222 and 265 nm (Samarajeewa et al., 1990). LED treatment with 395 nm light pulses was not as effective as ACP treatments in degrading DON (Table 3.2). A 30 min treatment using 395 nm LED light pulses resulted in a 10.7 % reduction in DON concentration, and a 30 min ACP treatment resulted in a 59.1 % reduction in DON concentration. When 30 min of 395 nm light pulses was combined with a 30 min ACP treatment, the DON degradation was 68.8 %, which was more of an additive effect than a synergistic DON degradation effect of ACP and 395 nm LED treatment. In other words, a sequential technology consisting of ACP and pulsed light emitted from LEDs could not be effective to reduce the treatment intensities of ACP. The results suggest that the LED treatment is not as effective as ACP in reducing DON concentrations. This may also mean that the UV emission during the plasma discharge may not be

the principal factor for the degradation of DON, but other components present in ACP such as ROS and RNS could play the main role in DON degradation by ACP. This correlates with previous studies that mention the low impact of UV light on ACP inactivation of microorganisms (Estifae et al., 2019; Klämpfl et al., 2012; Yardimci & Setlow, 2010). Shanakhat et al. (2019) treated DON with 254 nm UV-C light for 2 h and no significant change was observed in the DON concentration. When aflatoxin1 (AFB₁) was degraded using UV irradiation, the primary degradation compounds contained residual toxicity, which needs to be degraded to non-toxin compounds (Samarajeewa et al., 1990). The toxicity of the degraded products after LED and ACP treatments of DON should be assessed.

Table 3.2: Effect of sequential treatments with atmospheric cold plasma (ACP) and light emitting diode (LED) on DON concentration and reduction

Treatment method	Average concentration (µg/ml)	Average reduction (%)
Control	16.5±0.9 ^a	0 ^d
30 min ACP	6.7±2.0 ^c	59.1±12.1 ^b
30 min LED	14.7±1.3 ^a	10.7±8.1 ^d
30 min ACP+30 min LED	5.2±0.9 ^{cd}	68.8±5.6 ^{ab}
60 min ACP	2.4±0.4 ^d	84.5±2.7 ^a
60 min LED	10.5±3.1 ^b	37.0±18.8 ^c

Values with different letters in the same column are significantly different (p<0.05, n =3).

3.3.8 DON degradation with heat treatment in combination with ACP

Heat treatment is a common method of killing bacteria in the food industry and it could have an effect on DON reduction. This study used moderate heating (80 °C) to increase the DON degradation efficacy of ACP. Heating DON at 80 °C for 25 min did not result in any reduction in DON concentration (Table 3.3). Vidal et al. (2015) observed no significant reduction in DON concentration after 35 min heat treatment at 140 °C. Using heat treatment as a hurdle technology with ACP did not increase DON degradation significantly in comparison with using ACP alone. In the next step, we used sequential ACP+ heat+ ACP treatments and we did not observe a higher

reduction in DON concentration in comparison with 30 min ACP treatment alone. Previous studies reported significant reduction in DON concentration at high temperatures ($\approx 140\text{ }^{\circ}\text{C}$) (Bretz et al., 2006; Shanakhat et al., 2019; Vidal et al., 2015), and there was a positive correlation reported between temperature and time of heat treatment on the degradation rate of DON (De Angelis et al., 2013; Vidal et al., 2015). However, the impact of temperature was reported to be higher than the impact of heat treatment time on the degradation of mycotoxins (Shanakhat et al., 2019). The high stability of DON to heat treatment may be related to the presence of a double bond between carbons in its structure (Vidal et al., 2015), as more energy is needed to break double bonds than to break single bonds. We observed an increase in DON concentration after heat treatment, possibly due to precursors of DON after heat treatment (Young et al., 1984), masking of mycotoxin by its reaction with other molecules before heating (Scudamore, 2008), or the failure of the analytical detection to document the masked form of mycotoxin (Nakagawa et al., 2011) before heating. In our study, the higher efficiency of DON dissolution by methanol from the cover-glass could be the reason for the higher concentration of DON after heat treatment in comparison with the control sample.

Table 3.3: Effect of sequential treatments with ACP and heat on DON concentration and reduction

Treatment method	Average concentration ($\mu\text{g/ml}$)	Average reduction (%)
Control	22.7 \pm 0.5 ^a	0 ^b
30 min ACP	8.5 \pm 0.8 ^b	63.0 \pm 3.9 ^a
30 min ACP+25 min heat (80 $^{\circ}\text{C}$)	8.0 \pm 0.4 ^b	64.6 \pm 1.7 ^a
25 min heat (80 $^{\circ}\text{C}$)	23.4 \pm 0.2 ^a	-2.7 \pm 0.75 ^b
15 min ACP +25 min heat (80 $^{\circ}\text{C}$) + 15 min ACP	7.8 \pm 1.5 ^b	65.9 \pm 6.5 ^a

Values with different letters in the same column are significantly different ($p < 0.05$, $n = 3$).

3.4 Conclusions

This study confirmed the ability of ACP to reduce DON concentrations significantly, however, the DON degradation efficacy of ACP was dependent on various process conditions. The presence of

water was important in determining the degradation efficacy of ACP. FTIR analysis showed three distinct bonds in the spectrum between untreated and ACP treated DON in the presence of water, which may be associated to the formation of a C=O group and epoxy ring in the treated sample that might have associated with CH₃-C=C in the control sample. TLC analysis did not differentiate the byproducts of DON degradation after ACP treatment at the treated concentration. The initial concentration of DON was important in determining the degradation efficacy of ACP. The results of the optical emission spectroscopy suggest that the atmospheric air DBD plasma produces a significant amount of ROS and RNS, which could be the reason for DON degradation. Heat treatment alone at 80 °C was not effective in degrading DON and heat at 80 °C in combination with ACP treatment did not exhibit synergistic DON degradation. DON was degraded by 395 nm LED light pulses, but no synergistic effect in the reduction of DON concentration was observed when LED light pulses were used along with ACP treatment. The results of this study will help to identify important process conditions to effectively degrade deoxynivalenol (DON) in human and animal food products by ACP technology in the future.

Chapter 4: Effects of atmospheric-pressure cold plasma treatment on deoxynivalenol degradation, quality parameters, and germination of barley grains

4.1 Introduction

Mycotoxins are poisonous compounds produced as secondary metabolites by some species of fungi, including *Fusarium*, *Aspergillus*, *Penicillium*, and *Alternaria* (N. Misra et al., 2019; Mousavi Khaneghah et al., 2019). Trichothecenes are a large group of mycotoxins sharing 9, 10 double bond and the 12, 13 epoxide group in their structures (Alizadeh et al., 2016). Deoxynivalenol (DON), mainly produced by *Fusarium graminearum* and *Fusarium culmorum*, is one of the major trichothecenes that contaminate cereals such as barley (Bianchini et al., 2015). DON can cause vomiting, anorexia, growth retardation, immune suppression, inflammation and the necrosis of various tissues, and diarrhea in animals (Bretz et al., 2006; Pestka, 2010). Barley is one of the major grains that is consumed as animal feed, used to produce cereal-based products and is widely used in brewery industries. DON in grains, especially in barley, reduces grain quality and financially impacts agricultural organizations. The economic loss associated with DON was estimated at \$655 million/year in the United States from 1993 to 1996 (Schmale III & Munkvold, 2020).

Many strategies have been suggested for suppressing fungal growth and reducing mycotoxin formation including pre-harvest methods (crop rotation, sowing date, tillage, use of fungicide), physical methods (i.e., dehulling, sorting, sieving, floatation, washing, steeping, milling, ultraviolet, gamma treatments, and thermal treatments), chemical methods (citric acid, acetic acid, lactic acid, NH₃, Ca(OH)₂, Na₂CO₃, oxidizing agents, and reducing agents), enzymatic methods

(amylases, glucanases, proteases), biological methods (fermentation, genetic engineering in plant genes for detoxification), and microbial decontamination method (prevention of ingestion by microorganism of gastrointestinal tract) (N. Misra et al., 2019). Despite the progress achieved by using these methods, they have several disadvantages, including low efficacy, requirement of expensive chemicals and sophisticated equipment. Furthermore, some of these methods may leave chemical residues that might cause a detrimental effect on the treated product, which may present health hazards to consumers. As a result, some of these methods are usually considered as impractical, costly, not completely effective, and time-consuming, especially for the large-scale treatment of food or feed products (N. Misra et al., 2019). Hence, there is a need to find an effective method to control DON contamination in food and feed products.

Atmospheric cold plasma (ACP) technology is a novel technology with the potential to reduce fungi and mycotoxins' concentration (N. Misra, O. Schlüter, & P. J. Cullen, 2016). The term plasma refers to an ionized state of a gas produced by increasing the internal energy of the gas. The ionization process leads to the formation of reactive species, radicals and UV light (Mandal et al., 2018; N. Misra, O. Schlüter, & P. J. Cullen, 2016). Reactive oxygen species (ROS) such as ozone (O_3), singlet oxygen (1O_2), superoxide (O_2^-), peroxide (O_2^{-2} or H_2O_2), hydroxyl radicals (OH), and reactive nitrogen species (RNS) such as excited molecules of N_2 and nitric oxide radical (NO) are the main effective species in ACP (Tappi et al., 2014). The degradation of mycotoxins by ACP could be related to their interaction with the reactive species, UV photons, and electrons. Mycotoxin degradation efficacy of ACP is greater than that of ozone or UV treatments, due to the possible contribution of reactive species, electron, and UV photon in the ACP treatment (N. Misra et al., 2019). The low temperature of ACP is an important aspect in preserving quality while improving the safety of the product. ACP may also improve the germination rate of grains and

length of seedlings (Park et al., 2018b). Previous research reported the effectiveness of ACP to reduce mycotoxins, including DON, aflatoxin and T-2 toxin (Kříž et al., 2015; N. Misra et al., 2019; ten Bosch et al., 2017). However, limited information is available on the efficacy of ACP to reduce DON on barley grains. Additionally, knowledge on the effect of ACP treatment on grain quality parameters and the germination capacity of barley is important for ACP treatment optimization.

This study aimed to evaluate the effectiveness of ACP treatment on the degradation level of DON. It also assessed the effect of ACP on barley germination and the important quality parameters of barley grains, including changes in protein and β -glucan content and water loss.

4.2 Material and Methods

4.2.1 Barley grains

Raw barley grains were provided by Canada Malting Co., Alberta, Canada. Barley grains were vacuum sealed in plastic bags and transported to the laboratory at the University of Alberta and stored at 4 °C until use. The initial wet basis moisture content (MC), water activity (a_w), density, and grain dimensions of barley grains were determined (Table 4.1).

Table 4.1: Physical specifications of barley grains

Crop Year	MC (g water/100 g Sample)	a_w	Grain Density (g/cm ³)	Grain Dimensions	
				Length (mm)	Width (mm)
2015	10.8 ± 1.7	0.450 ± 0.003	1.19 ± 0.09	9.32 ± 0.97	3.88 ± 0.02

Moisture content is a measurement of the total amount of water contained in the sample. Water activity provides information about the energy status of water in foods and indicates the available water for the growth of microorganisms and reactions in foods. Water activity is calculated as the ratio of the vapor pressure of water in a food sample to the vapor pressure of pure water. The MC of the barley grains was determined by the American Association for Clinical Chemistry (AACC)

Method (44-19.01, AACC International). The water activity (a_w) was determined using the a_w meter (Aqualab, Pullman, WA, USA). Grain density was determined by dividing the grain mass by the volume. The volume was measured by the liquid displacement method. Two grams of barley grain was added to a 15 ml Falcon tube (Fisher Scientific, Ottawa, ON, Canada) containing water. The rise in the level of the water in the tube was used to determine the volume (Chigbo, 2016).

4.2.2 Mycotoxin standards

HPLC grade acetonitrile (ACN) and methanol (Fisher Chemical, Geel, Belgium), and standard solutions of deoxynivalenol (1 mg/ml acetonitrile Sigma Aldrich, Mississauga, Canada) were used. ACN was used to dilute deoxynivalenol and produce 50 $\mu\text{g/ml}$ DON solution.

4.2.3 Sample preparation

Barley grains (11–12 grains, 0.495–0.505 g) were individually spiked using 200 μl of DON (50 $\mu\text{g/ml}$) in a plastic cup with a diameter of 3.89 cm and height of 1.14 cm. The samples were then dried at room temperature (~ 23 °C) for 10 min, to ensure that the ACN solution was evaporated completely.

4.2.4 ACP treatment

A dielectric barrier discharge (DBD) atmospheric cold plasma (ACP) system (PG 100-3D, Advanced Plasma Solutions, Malvern, USA) was used to treat the barley grains in an acrylic chamber (Figure 4.1). The airtight chamber ($8 \times 8 \times 10$ cm inner dimensions) had inlets and outlets for the transmission of humid air. Quartz glass on the side of the chamber was used to perform emission spectroscopy measurements. The upper electrode of the DBD unit was connected to an alternating high voltage (0–34 kV) plasma generator with 1 A current and approximately 300 W power. The high voltage electrode was made of solid copper (2.5 cm diameter) covered by a dielectric (1 cm thick) and with 1 mm thickness of quartz disk at the bottom. The mycotoxin spiked

barley grains (11–12 grains) inside the plastic cups were placed on the top of the ground electrode. The ground electrode was covered with a glass slide of 1 mm thickness. The gap between the electrodes was 5 mm and the gap between the surface of the barley grains and the high voltage electrode was ~2 mm. The selected ACP treatment times were 0, 2, 4, 6, 8, and 10 min. The standard output frequency of DBD system was 3500 Hz, duty cycle was 70%, and the output pulse width was 10 μ s.

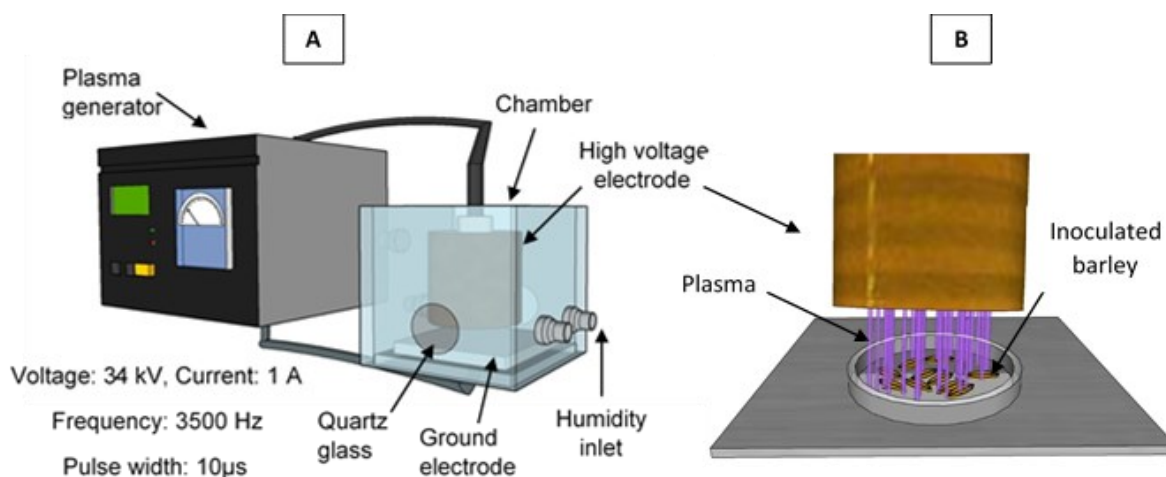


Figure 4.1: A: Schematic diagram of the experimental setup used for dielectric barrier discharge (DBD) atmospheric cold plasma (ACP) treatment. B: Close-up diagram presenting the treatment of barley grains inside the ACP chamber

4.2.5 Extraction and quantification of DON

DON extraction was based on the method described by (Lim et al., 2012) with modification. Treated barley grains (0.5 g) were transferred to 8 ml glass culture tubes and then 2 ml ACN-water in a proportion of 84:16 was added. The mixture was vortexed at 3000 rpm for 10 min. After thorough mixing of the samples with extraction solvent, 1 ml of the supernatant of the extract was passed through a 0.2- μ m PTFE syringe filter, and transferred into glass culture tubes and dried under a constant flow of N_2 gas. The residue was redissolved in 1 ml water, with acetonitrile (85:15 v/v) used as the mobile phase, vortexed for 1 min, and injected (25 μ l) into the HPLC for analysis.

The concentration of mycotoxin was determined by HPLC (Shimadzu Scientific Instruments, Inc. Maryland, USA). The chromatography was performed on a reverse phased Agilent Zorbax SB-C18 250 mm × 3 mm, 5 µm column in isocratic elution. The injection volume was 25 µl at the flow rate of 0.5 ml/min, using water and ACN (85:15 v/v) as the mobile phase. DON was determined at a wavelength of 218 nm, using a photodiode array (PDA) detector. The limit of HPLC detection of DON was 0.1 µg/ml. The recovery of the whole procedure was 76.6% and the precision was within +/- 5%.

4.2.6 Cold plasma diagnostics

The optical emission spectrum of ACP discharge in the treatment chamber was acquired using a spectrophotometer (Black comet C-25, StellarNet Inc., Tampa, USA), coupled to an optical fiber with a resolution of 0.5 nm, signal to noise ratio of 1000:1, in the wavelength range of 180 to 850 nm. The light emitted by excited plasma species between the electrodes was captured using optical fiber (F600-UVVIS-SR, StellarNet, Inc., Tampa, USA). One end of optical fiber was connected to the spectrophotometer and the other end with the collimating lens kept 25 mm away from the side quartz window incorporated to the center of the sidewall of the plasma chamber. The set integration time was 550 ms and the set values of the number of scans to average was 3 to obtain uniform spectra using SpectraWiz software (StellarNet Inc., Tampa, USA). The ACP system was operated for 1 min, then the spectra were acquired.

4.2.7 Measurements of ozone, nitrous gas, and hydrogen peroxide concentration

Concentrations of ozone (O₃), nitrous gas, and hydrogen peroxide (H₂O₂) inside the treatment chamber were measured at 60–80, 360–380, and 600–620 s during ACP treatment using Dräger short-term detector tubes (Dräger Safety AG & CO, Lubeck, Germany). The ozone 10/a Dräger tube (CH 21001), a nitrous fume 50/a Dräger tube (81 01 921) and a hydrogen peroxide 0.1/a

Dräger tube (81 01041) were used to measure the gas concentration with a Dräger accuro gas detector pump, following the manufacturer's instructions. Smaller volumes of gas were collected to ensure that ozone, and hydrogen peroxide content fell within the measurement range of Dräger detector tubes (i.e., 20 ml for ozone, and 20 ml for nitrous gases and hydrogen peroxide) were collected into the tubes.

4.2.8 Effect of moisture content of barley grains and environmental RH

The effects of wet basis moisture content (MC) of barley and relative humidity (RH) of air inside the chamber on DON degradation efficacy of ACP were determined. Barley grains were kept for 10 h and 17 h in a controlled humidity chamber (BTL-433, ESPEC North America Inc., Hudsonville, MI, USA), with 95% relative humidity (RH) at 25 °C, to increase the MC of barley from 9.5 g water/100 g sample to 15 and 16 g water/100 g sample, respectively. Then, DON was inoculated on the grains and air-dried for 10 min to allow the evaporation of ACN from inoculum and then treated by ACP. To understand the effect of environmental RH, a humidifier was connected to the chamber inside it, to increase the RH before ACP treatments.

4.2.9 Post-treatment storage of barley grains on DON degradation by ACP

Some of the reactive species in ACP have a long shelf life and are able to react with the sample for extended times. We stored the 6 min ACP-treated barley grains for 10 min inside the air-tight plasma chamber and also for 24 h inside sealed plastic cups outside the chamber at room temperature, to evaluate the effect of storage on further degradation of DON.

4.2.10 Effect of steeping of barley grains on DON degradation by ACP

Steeping is one of the crucial steps in producing malt from barley. The amount of moisture content of substrates is an important factor determining the efficacy of the ACP process. The effect of steeping on DON degradation by ACP was assessed to determine if in this process step we could

apply ACP, which is relevant to the brewing industry. For this purpose, the barley grains were steeped for 21 h before ACP treatment. The moisture content of the grains was increased from 9.5 to 43.9 (g water/100 g sample) after steeping. Previous reports noted the importance of the presence of water in increasing the antimicrobial efficacy of ACP treatment (Butscher, Van Loon, et al., 2016; Oehmigen et al., 2010; Van Gils et al., 2013). Moreover, to assess the effect of water on the surface of the steeped grain on DON degradation by ACP, two approaches were used. In the first, pure ACN was substituted with ACN/water with a ratio of 20:80 (v/v) to prepare the DON inoculum on steeped grain. In the second approach, samples with or without a drying step after inoculation were used for the ACP treatment of steeped grains. The drying step of inoculum was skipped to see the effect of water on DON degradation.

4.2.11 Quality parameters of barley grains after ACP

To assess the effect of ACP on quality parameters of barley, the moisture, protein, and β -glucan content were measured after ACP treatment of barley grains for a defined period of time. Moisture, protein, and β -glucan content are the important quality indicators of barley in the brewing industry. Protein content was determined by combustion nitrogen analysis (AACC 46-30.01). Protein content was calculated by multiplying the nitrogen content (% N) by 6.25 as the conversion factor. β -glucan content was determined using the megazyme mixed-linkage β -glucan assay procedure (AACC 32-23.01). The moisture content of the barley samples was determined by the oven method (44-19.01-AACC International).

4.2.12 Germination of barley grains after ACP

For assessing the effect of ACP on germination of barley grains, an ACP treatment was applied to the seeds for 0, 1, 6, 10 min. Each treatment contained three batches of grains, where ACP treatment was applied independently to each batch. Then, the individual grains were transferred to

germination pouches (17.8×16.5 cm, Mega International, Minneapolis, MN, United States) on light shelves containing 100 ml of deionized water. Five growth pouches, each containing two grains, were used for each treatment ($n = 10$) and every one of the batch. Altogether, there were 30 plants per each ACP treatment. Barley plants were grown at room temperature with supplemental lighting ($200 \mu\text{mol m}^{-2}\text{s}^{-1}$ at the top of the growth pouch, SunBlaster T5HO, 54W, 0900304), maintaining a photoperiod of 16 h/8 h light/dark cycles. After 1 week of germination, the shoot length and number of roots were measured manually. The roots were scanned using an optical scanner STD 4800 and analyzed for root length, surface area, average diameter, and volume, using WinRHIZO software (Regent Instruments Inc., Quebec City, QC, Canada).

4.2.13 Statistical analysis

All the experiments were performed in triplicate. Values from all experiments were expressed as the mean \pm standard deviation (SD). Significant differences ($p < 0.05$) were determined using one-way analysis of variance (ANOVA), followed by Duncan's multiple range test (IBM SPSS v.21, Armonk, NY, USA).

4.3 Results and discussion

4.3.1 Effect of ACP treatment on deoxynivalenol degradation on barley grains

A significant ($p < 0.05$) decline in the DON concentration of barley grains by ACP treatment was generally observed (Figure 4.2).

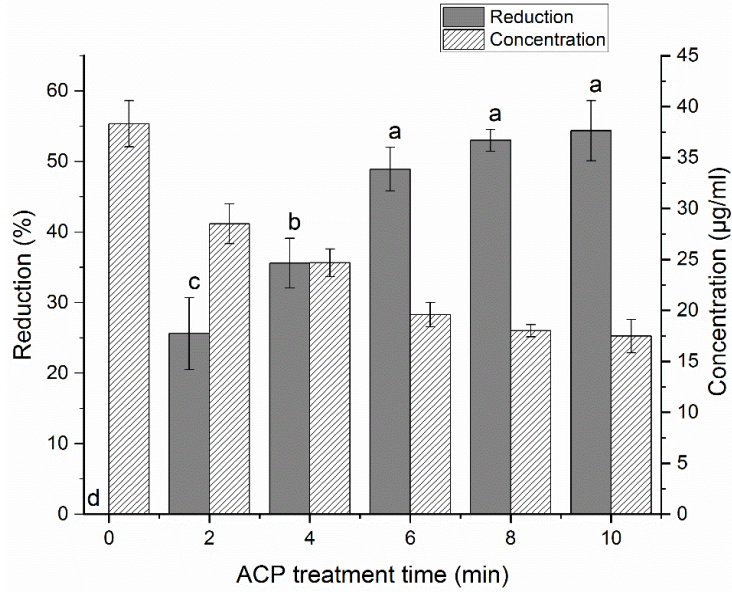
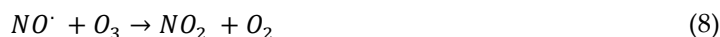


Figure 4.2: Effect of ACP treatment on (A) relative deoxynivalenol reduction % and (B) deoxynivalenol concentration ($\mu\text{g/ml}$) on barley. Data are shown as least square means \pm standard deviations. Values with different letters in each figure are significantly different ($p < 0.05$, $n=3$)

A significant decrease in DON concentration within 6 min ACP treatment was observed, but thereafter, the reduction rate was not significant ($p \geq 0.05$). The degradation rates after 6 and 10 min ACP treatments were 48.9% and 54.4%, respectively. The generated ozone in the plasma probably had a significant effect on DON degradation (Santos Alexandre et al., 2018; L. Wang et al., 2016). In general, for a long treatment time, with the production of more reactive species, an increase in the DON degradation rate should be observed. However, during extended treatment times, the generated ozone can be depleted by other reactive species by the following destruction cycles (Equations (1)–(9)) (Chang & Wu, 1997; Laroussi et al., 2005).





where the reactive species $HO_2\cdot$, $\cdot OH$, $\cdot H$, $\cdot O$, $\cdot N$, $NO\cdot$, $NO_2\cdot$ are the hydroperoxyl radical, hydroxyl radical, atomic hydrogen radical, atomic oxygen radical, atomic nitrogen radical, nitrogen oxide, and nitrogen dioxide radical, respectively. The constant concentration of ozone in the environment may be attributed to the simultaneous ozone generation and depletion, due to its reactions with other reactive species in longer treatment times. This could be the possible reason for small increases in degradation rates of DON after 6 min ACP treatment. The constant concentration of ozone under longer treatment times was observed in previous studies (Patil et al., 2014; Zhuang et al., 2019). Zhuang et al. (2019) reported no further increase in ozone concentration after 180 s of in-package cold plasma treatment, attributed to the quenching of ozone by reactions with N_2 , water, and/or new reactive species formed in plasma during long treatment times. It is worth mentioning that the ozone generation and depletion reactions are complicated and dependent on various factors, i.e., not only treatment time, but temperature, gas composition, voltage, etc (Chang & Wu, 1997).

Chen et al. (2018) reported 22.5 and 34.6% degradation in the DON level of raw and germinating barley, respectively, by using plasma-activated water (PAW), treated for 5 min. They did not observe a significant ($p \geq 0.05$) decline in DON concentration in the treated samples between 5 and 20 min using PAW. In Chapter 3, pure DON degradation on a cover-glass, formation of C = O group and epoxy ring in the ACP treated sample was observed, which could be due to the reaction between ROS with DON. We achieved a degradation level of 39.8% in pure DON after 15 min ACP on the cover-glass, in comparison with the 48.9% degradation of DON, applied on

barley after ACP treatment for 6 min. This highlights the importance of the type and nature of the substrate on DON degradation.

Abramson et al. (2005) applied 80 °C heat to DON on barley, and the concentration was reduced from 18.4 to 14.7 µg/g DON barley after 1 day of thermal treatment. DON concentration was reduced by 58%, 5 days after the treatment. L. Wang et al. (2016) reported the use of ozone treatment to wheat samples to reduce DON concentration. Treatment with 75 mg/L ozone for 90 min reduced DON concentration by 53.5% on wheat kernels. Santos Alexandre et al. (2018) reduced DON concentration by 32% after 240 min ozone treatment. It is assumed that a combination of different degrading mechanisms such as a chemical reaction with reactive species generated in ACP such as O₃, O, OH, NO_x, decomposition after collision with electrons and ions (ten Bosch et al., 2017), and UV light are responsible for cleavage of toxin molecule by ACP treatment. This combination could be the reason for obtaining a greater degradation rate by ACP in comparison with ozone treatment. In the current study, 54.4% reduction was achieved in 10 min of ACP treatment, which can be further increased by modifying the process factors in the ACP system (i.e., voltage and frequency, type of gas medium, RH of the air, hurdle treatment, etc.) However, further studies are necessary to evaluate the toxicity of the intermediate and final products formed during ACP processing of DON.

In Chapter 3, a thermal treatment at 80 °C for 25 min had no significant effect on DON degradation. As the temperature in our cold plasma system was less than 40 °C (Yadav et al., 2019), the increase in temperature during plasma treatment did not have any effect on DON degradation.

4.3.2 Cold plasma diagnostics

Optical emission spectroscopy (OES) is widely used for plasma diagnostics. OES enables an understanding of the degradation mechanisms and helps to optimize the decontamination process.

Excited states are produced mostly by collisions with energetic electrons, which can be measured by OES. The dominant plasma reactive species were detected by OES in the UV/VIS wavelength (180 to 850 nm) region (Figure 4.3). It was evident that the emission was in the near UV region (300–400 nm), which can explain the purple color of the ACP photons. In the spectrum, N₂ spectra were dominant, as the peaks in the wavelength region of 310–450 nm are the vibrational band of neutral and ionic emission of nitrogen molecule (Yadav et al., 2019). The peak in 296 nm corresponds to •OH as one of the reactive species (Machala et al., 2007). Some of the reactive oxygen species such as atomic O could not be identified, probably due to the particle collisions with N₂ and O₂, resulting in the quenching of O (³P) and O (⁵P) energy (Walsh et al., 2010) and production of ozone and nitrogen oxide species. The results demonstrate the fact that the major reactive species in ACP were ROS and RNS.

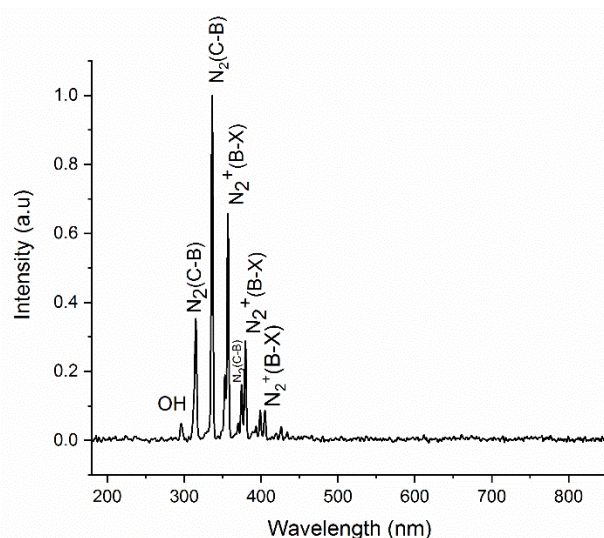


Figure 4.3: Optical emission spectra of DBD-ACP operating in air at 34 kV, 3.5 kHz, 5 mm gap

4.3.3 Ozone, nitrous gas, and hydrogen peroxide concentration in DBD-ACP

Concentrations of ozone, nitrous gases and hydrogen peroxide as the major reactive species in ACP were measured inside the plasma chamber over different time scales (Table 4.2).

Table 4.2: Ozone, nitrous oxides and hydrogen peroxide concentration during ACP treatment

ACP Treatment Time(s)	O ₃ (ppm)	H ₂ O ₂ (ppm)	NO _x (ppm)
60–80	600	100	400
360–380	675	150	470
600–620	675	200	480

In DBD-ACP, the electromagnetic field splits the O-O bond in the oxygen molecule and the resulting oxygen free radical reacts with another oxygen molecule to form ozone (Morgan, 2009). Hydrogen peroxide is derived from the reaction of plasma radicals ($\cdot\text{OH}$, O_2^-) with water molecules (H_2O) and molecular oxygen (O_2) (Lee et al., 2015). With an increase in ACP treatment time, the concentrations of all the reactive species would be increased. Ozone was the most prevalent reactive species with 600 ppm concentration after 1 min ACP. The concentrations of nitrous gases and H_2O_2 were increased in 6 and 10 min ACP treatments, in comparison with 1 min ACP. H_2O_2 had the lowest concentration compared with ozone and nitrous gases. The concentration of H_2O_2 was doubled and reached 200 ppm after 10 min, compared with after 1 min ACP treatment. This could be due to the generation of H_2O_2 by a number of reactions involving several reactive species, during plasma treatment. In the presence of water vapor present in the environment, H_2O_2 could be generated by several reactions (Equations (10)–(14)) (Locke & Shih, 2011; Machala et al., 2018).



It is believed that reactions (12) and (13) could be the major reactions involving hydrogen peroxide formation (Locke & Shih, 2011). Hydrogen peroxide could be primarily formed by recombination of hydroperoxyl radicals (Equation (13)) at high oxygen concentrations and low local OH radical

concentration (Locke & Shih, 2011). The generation of hydroperoxyl radicals from ozone depletion (Equation (2)) may also have indirectly contributed to H₂O₂ generation. The concentration of ozone was the same after 6 and 10 min treatments. Degradation rates of DON after 6 and 10 min ACP were not significantly different ($p \geq 0.05$). As discussed in Section 3.1, the ozone species possibly played a major role in the degradation of DON and hence, at the same concentration of ozone; after 6 and 10 min ACP treatments, the degradation rates of DON were similar. In previous studies, ozone was identified as the primary contributor for the degradation of mycotoxins (N.N. Misra et al., 2019; Hu Shi et al., 2017; L. Wang et al., 2016). Between 6 and 10 min ACP treatments, the concentration of ozone stayed the same, possibly due to the interaction of ozone with other reactive species present in ACP, to produce new compounds such as NO₂ and HO₂ (Locke & Shih, 2011). Further studies are required to achieve a better insight regarding the role of each of the reactive species in the degradation of each mycotoxin and their possible synergistic effects with ACP to degrade mycotoxins.

4.3.4 Effect of MC of barley grains and environmental RH on DON degradation by ACP

Environmental relative humidity and the moisture content of the substrate are important factors which can influence the decontamination by ACP (Chapter 2, section 2.4). The effects of RH of the air and MC of barley grains on the degradation of mycotoxin were evaluated (Table 4.3). Increasing the MC of the barley grains from 9.5 to 15.76 g water/100 g sample reduced the degradation level from 54.4% to 47.0% by ACP; however, this reduction was not significant ($p \geq 0.05$). Generally, the presence of water in the system increases the production of ROS (Butscher, Van Loon, et al., 2016), which can contribute to a greater degradation rate. However, due to the drying step after the inoculation of DON, the water content of the grains was similar to each other before ACP treatment. However, the reduction in DON degradation rate by increasing the water

content was not significant ($p \geq 0.05$), the possible changes in the surface of the grains due to the presence of higher water content could change the reaction rate of the reactive species with the toxin and affect the degradation rate. To know the optimum moisture content to achieve highest DON degradation, barley with different water content should be treated with ACP to draw a conclusion.

Table 4.3: Effect of moisture content (MC) of barley and relative humidity (RH) of the surrounding air on deoxynivalenol (DON) degradation by ACP

Plasma Time (min)	MC (g water/100 g sample)	DON Reduction (%)
0	9.5 ± 0.0	0 ^b
6	9.5 ± 0.3	54.4 ± 2.2 ^a
6	14.9 ± 0.3	49.8 ± 5.9 ^a
6	15.7 ± 0.2	47.0 ± 5.9 ^a
RH (%)		
0	12	0 ^b
6	12	62.9 ± 3.3 ^a
6	60	65.7 ± 3.0 ^a

Values with different letters in the same column are significantly different ($p < 0.05$, $n = 3$).

The effect of environmental RH on DON degradation by ACP was assessed. Increasing the RH from 12% to 60% increased the degradation rate of DON, but it was not significant ($p \geq 0.05$). A greater RH could be attributed to an increase in the concentration of OH radicals due to the presence of water molecules leading to greater oxidation (Berardinelli et al., 2012). On the other hand, high RH could reduce the surface resistance of the dielectric material, so it would reduce the number of micro-discharges (Falkenstein & Coogan, 1997). A high RH may weaken the plasma due to the loss of the electron energy in electron-molecule collisions. Poorer transmissibility of UV radiation, and protective water film around the mycotoxin, could be the other reason for reduced ACP efficiency (Butscher, Van Loon, et al., 2016). It is recommended that we assess the degradation of DON at different percentages of RH and determine an optimum RH under ACP to achieve the highest decontamination rate.

4.3.5 Effect of post-treatment storage of barley grains on DON degradation by ACP

Storage after ACP treatment affected the degradation of DON on barley (Table 4.4). An 8.1% reduction in DON was observed when the inoculated barley grains were stored for 24 h without ACP treatment. This could be due to the natural degradation of DON by oxidation, in contact with the air. DON degradation after 6 min ACP was 45%; when the 6 min ACP-treated DON was stored for 24 h at room temperature, the degradation rate was further increased to 53.6%. This increase in degradation was likely due to the degradation of DON during storage without much contribution from ACP. Degradation of DON increased when we stored the 6 min ACP treated grains for 10 min inside the air-tight treatment chamber after treatment, but the result was not significantly different ($p \geq 0.05$) from the reduction in DON after 6 min ACP treatment followed by 24 h storage. Some of the reactive species, such as ozone in ACP, have longer half-lives and they could have extended interactions with the substrate even when the ACP system was not functioning; however, this should be justified by comparing the result with 6 min ACP followed by 10 min storage outside the treatment chamber at room temperature. No previous study has reported the effect of post-treatment storage on mycotoxin stability. The effect of post-treatment storage on the inactivation of bacteria was evaluated by Yadav et al. (2019), and Klockow and Keener (2009), and a similar observation of higher reductions in the cell count of bacteria in post-treatment storage was reported.

Table 4.4: Effect of post-treatment storage on DON degradation on barley by ACP

Treatment	DON Degradation Rate (%)
No treatment, no storage	0 ^d
0 min ACP, 24 h storage	8.1 ± 2.7 ^c
6 min ACP, no storage	45.0 ± 0.9 ^b
6 min ACP, 24 h storage	53.6 ± 1.8 ^a

6 min ACP, 10 min storage inside treatment chamber

52.0 ± 1.6^a

Data are shown as least square means ± standard deviations. Values with different letters are significantly different ($p < 0.05$, $n = 3$).

4.3.6 Effect of steeping the barley grains on DON degradation by ACP

One of the major applications of barley is in the brewery industry. Steeping is one of the crucial steps to produce malt for the brewery. If barley is contaminated with DON, it can be present in the final product (Omurtag & Beyoğlu, 2007). On the other hand, the presence of moisture is a determining factor for the ACP treatment efficacy. Increasing the moisture content of the substrate was anticipated to increase the generation of ROS (e.g., hydroxyl radicals) (Butscher, Van Loon, et al., 2016; Oehmigen et al., 2010; Van Gils et al., 2013), which could then increase the DON degradation rate. An increase in hydroxyl radicals could further increase the generation of ozone, as ozonation is catalyzed by free radicals such as hydroxyl ion (Omurtag & Beyoğlu, 2007). The uptake of ozone by the product would then increase at higher moisture contents, since ozone is water-soluble (Alexandre et al., 2017). This could increase the contact between ozone and DON and consequently improve its degradation rate. However, the degradation of DON by 6 min ACP treatment on steeped and dried barley grains was 36.3% (Sample B) (Table 4.5). This DON degradation in steeped barley grains was lower compared with that in barley grains without steeping (48.9%), as reported in Section 3.1 (Figure 4.2). During the steeping process, water will be absorbed and the grains will swell, which can influence the surface properties and topology of the grain surfaces. The topology of the substrate surface can influence the efficiency of DON degradation by ACP treatment. The fissures and grooves on the rough surfaces of the grains could protect DON from plasma generated species (Butscher, Van Loon, et al., 2016). The effect of the surface characteristics of the substrate was determined in previous studies for the inactivation of bacteria by ACP (Butscher, Zimmermann, et al., 2016; Los et al., 2018; Ziuzina et al., 2014). The greater inactivation of bacteria via ACP treatment was observed on smooth surfaces. Moreover,

ACP treatment could modify surface topology and change surface properties. Park et al. (2018b) observed changes on the surface of plasma-treated barley grains compared with the untreated samples. The changes on the surface of the grains after ACP treatment could be due to the chemical reactions of the reactive species on surfaces or energy exposure by ACP.

Table 4.5: Effect of solvent type and treatment conditions (drying time and ACP treatment time) on degradation of DON on steeped barley grains by ACP

Treatment	Solvent (ACN:Water)	Treatment Description	Reduction (%)
A	100:0	10 min drying + 0 min ACP	0 ^c
B	100:0	10 min drying + 6 min ACP	36.3 ± 5.4 ^c
C	100:0	0 min drying + 6 min ACP	66.3 ± 2.3 ^a
D	20:80	10 min drying + 0 min ACP	15.7 ± 4.6 ^d
E	20:80	10 min drying + 6 min ACP	53.6 ± 1.0 ^b
F	20:80	0 min drying + 6 min ACP	65.6 ± 7.5 ^a

All the samples were steeped barley grains. Values with different letters in the same column are significantly different ($p < 0.05$, $n = 3$).

The drying step following mycotoxin inoculation on barley grains before ACP treatment had a significant impact ($p < 0.05$) on the degradation of DON. Since the drying step was used before ACP treatment, the effect of greater moisture on the surface of barley grains due to steeping on DON degradation during ACP treatment was negligible. Hence, we believe that the reduction in degradation rate in steeped barley compared with the unsteeped grains could be due to the changes in the surface properties of the steeped grains. In 10 min drying of the barley grains inoculated with DON in pure ACN, the solvent was completely evaporated. However, due to the higher boiling point of water compared to ACN, the water in ACN/Water (20:80 v/v) was not evaporated, but the ACN could be evaporated completely within 10 min. This means that the 10 min drying step would have allowed the ACN to evaporate, but some amount of water was still there. Consequently, we observed significantly ($p < 0.05$) higher degradation rates of DON in treatment E compared to B due to the presence of water. Comparison of treatment C (with a greater

percentage of ACN) with treatment F (with lesser ACN percentage) suggests the greater impact of ACN compared to water on the degradation of DON by ACP. The considerable effect of ACN on DON degradation under ACP could be observed by comparing treatments B and C. The degradation rate of DON increased from 36.3 to 66.3% by skipping the drying step and hence the presence of ACN. A greater degradation rate of DON in treatment F (no drying step) was observed in comparison to E (10 min drying), since the amounts of water and ACN were higher in treatment F, which contributed to the higher degradation of DON. Overall, the results of this experiment suggest the importance of drying step and hence the presence of water on the surface of the barley grains to increase the degradation rate by ACP; it seems that water contributes to the formation of greater amounts of ROS.

4.3.7 Effect of ACP treatment on quality parameters of barley grains

Moisture content, protein, and β -glucan content of barley were evaluated after 6 and 10 min ACP treatments (Table 4.6). ACP treatment could result in drying of the substrate (Bajgai et al., 2006); however, based on the process parameters, i.e., voltage, frequency, treatment time, the gap between the electrodes, etc., the drying effect could be negligible. ACP generates ionized molecules in a strong electric field. Water molecules orient themselves in the direction of the electric field and the evaporation of water molecules can occur, resulting in a drying effect of the product by ACP (Y. Wang et al., 2016). However, in our study, the moisture content of the grains was slightly reduced after ACP treatment, but this was not significant ($p \geq 0.05$). The protein and β -glucan were not affected significantly ($p \geq 0.05$) after ACP treatment. This could be due to the fact that although ACP treatment influenced the surface of the substrate, but it could not penetrate the inner parts of the grains, leaving them unaffected.

Table 4.6: Effect of ACP treatment on quality parameters of barley grains

Treatment	N ₂ (%)	Protein (%)	Carbon (%)	β-Glucan (%)	MC (g Water/100 g Sample)
Control	1.71 ± 0.02 ^a	10.68 ± 0.15 ^a	44.1 ± 0.2 ^a	3.96 ± 0.14 ^a	9.7 ± 0.1 ^a
6 min ACP	1.62 ± 0.05 ^a	10.39 ± 0.33 ^a	44.07 ± 0.21 ^a	3.98 ± 0.08 ^a	9.6 ± 0.0 ^a
10 min ACP	1.64 ± 0.05 ^a	10.26 ± 0.29 ^a	43.93 ± 0.55 ^a	4.23 ± 0.25 ^a	9.4 ± 0.2 ^a

Values with different letters in the same column are significantly different ($p < 0.05$, $n = 3$).

4.3.8 Effect of ACP treatment on the germination of barley grains

The effect of ACP on germination parameters of barley was time-dependent (Table 4.7). The grains treated for 6 min by ACP had the highest germination percentage (93.3%). ACP treatment for 1 and 10 min decreased some of the germination parameters such as root length and root surface area, shoot length, and the number of roots compared to the untreated control. However, the 6 min ACP treatment improved some of the germination parameters, but not significantly ($p \geq 0.05$) (i.e., the average root diameter, root volume, and the germination percentage) (Figure 4.4). Root growth parameters are important in exploiting the soil and uptake of the minerals, especially for less mobile nutrients. Root growth affects vigorous shoot growth and crop yield, especially in low nutrient soils (Y. Wang et al., 2016). ACP treatment can affect the root growth and, as a result, the ability of plants to explore soil and uptake water and nutrients will be changed (Pérez-Pizá et al., 2020). Previous research reported that ACP treatment impacted the germination rate and germination parameters of several grain crops (Kříž et al., 2015; Los et al., 2018; Park et al., 2018b). A number of theories reported that the changes in the germination rate of the ACP treated grains could be related to: (1) change in water absorption of the grains, (2) change in their surface characteristics as a result of chemical reaction of the reactive species with the seed surface, (3) or the physical energy deposition of plasma exposure on grains, (4) changes in the biological reactions of the grains, (5) change in the internal functional metabolites such as gamma-aminobutyric acid, and 1,1-diphenyl-2-picrylhydrazyl activity (Park et al., 2018b), (6) alterations

in protein structure, and (7) stimulation of the natural signal (i.e., stimulation of growth factor, opening the calcium channel) (Sera et al., 2010). The attack of oxygen radicals and bombardment by low energetic ions may induce seed coat erosion and contribute to a change in germination (Sera et al., 2010). Previous studies reported that the germination parameters were influenced based on the plasma treatment time and optimum plasma time should be considered for each plant species (Filatova et al., 2013; Jiayun et al., 2014; Sera et al., 2010). In this study, we determined that the ACP treatment for 6 min was able to reduce almost half of the DON on the barley grains and it did not show any significant ($p \geq 0.05$) adverse effects on germination parameters of barley. However, to fully understand the biological effects of ACP species on germination, the characteristics of each type of plasma, and the mechanisms between plasma species and each biomolecule should be studied. This could be quite challenging due to the inconstant state of ACP, diversity of target species in the plant, and the complexity of biomolecular response. A systematic approach for investigating the simple biomolecules and complex tissues to necessary to be able to realize the biological responses between plasma species and biomolecules. Overall, these results lay the foundation for future research that can optimize ACP treatment based on DON degradation, germination rate, and quality analysis.

Table 4.7: Comparison of germination parameters of barley grains as a function of ACP treatment time

Treatment	Average Root Length (cm)	Average Root Surface Area (cm ²)	Average Root Diameter (mm)	Root Volume (cm ³)	Shoot Length (cm)	Number of Roots	Germination Percentage (%)
Control	44.2 ± 17.8 ^a	6.37 ± 2.52 ^a	0.462 ± 0.037 ^a	0.073 ± 0.029 ^{ab}	6.76 ± 1.72 ^a	5.67 ± 0.64 ^a	80
1 min ACP	33.7 ± 19.4 ^{ab}	4.88 ± 2.50 ^b	0.495 ± 0.11 ^a	0.058 ± 0.026 ^b	6.40 ± 1.92 ^a	5.16 ± 1.49 ^a	83.3
6 min ACP	42.2 ± 15.7 ^{ab}	6.35 ± 2.23 ^a	0.489 ± 0.060 ^a	0.078 ± 0.029 ^a	7.36 ± 1.62 ^a	5.46 ± 0.84 ^a	93.3
10 min ACP	32.6 ± 20.0 ^b	4.84 ± 2.50 ^b	0.498 ± 0.066 ^a	0.058 ± 0.027 ^b	6.26 ± 2.07 ^a	5.15 ± 1.26 ^a	90

The values indicate the average of the germinated grains for each parameter. Values with different letters in the same column are significantly different ($p < 0.05$, $n = 3$).

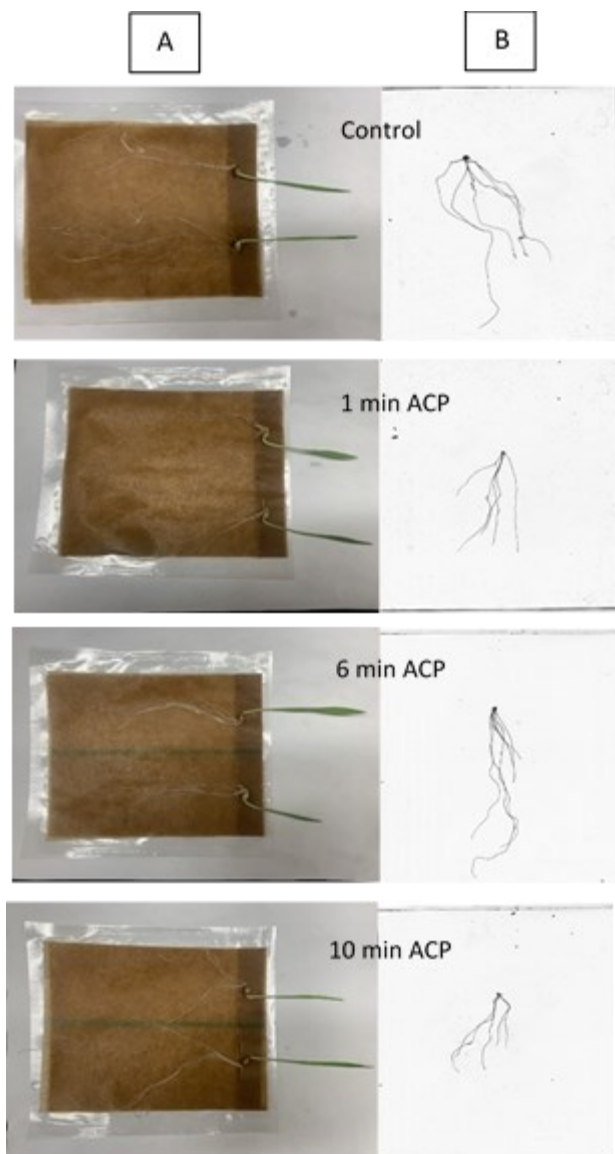


Figure 4.4: Effect of ACP treatment on seedling growth of barley after 7 days of germination. A: photo images. B: scanned root images using WinRHIZO software

4.4 Conclusions

In this study, the potential of ACP treatment for the degradation of DON on barley grains and the effects on selected grain quality parameters, germination, and seedling growth parameters were evaluated. ACP treatment was able to reduce DON concentration by 48.9% on barley grains in 6 min. The degradation rate was further increased by the addition of water to the surface by steeping

without subsequent drying of the grains before ACP treatment. ACP treatment produced ROS and RNS, however, ozone exhibited the highest concentration. The storage of barley grains after 6 min ACP treatment further increased the degradation rate of DON. Protein, β -glucan and moisture content of the barley grains were not significantly affected by ACP treatment. The effect of ACP on germination parameters of barley grains was time-dependent, and 6 min ACP treatment showed the best results. Overall, ACP treatment showed promising results on degrading DON, without significant adverse effects on the quality parameters of barley grains. Future research is needed to optimize and coordinate critical process factors required to achieve required DON degradation levels, while maintaining barley quality. Cost-efficiency and other practical challenges will also need to be addressed once this laboratory technique is validated, scaled-up and adapted for commercial applications.

Chapter 5: Degradation of zearalenone by atmospheric cold plasma: effect of selected process and product factors

5.1 Introduction

Zearalenone (ZEA) is a mycotoxin that is produced as a metabolite by *Fusarium* species such as *F. graminearum* (*Gibberella zeae*), *F. culmorum*, *F. crookwellense*, *F. semitectum* and *F. equiseti*. ZEA is a major problem for maize, barley, wheat, and rye. ZEA (C₁₈H₂₂O₅) is a 6-(10-hydroxy-6-oxo-trans-1-undecenyl) β-resorcylic acid lactone (Ropejko & Twarużek, 2021) and is structurally similar to endogenous estrogen; hence, it has mainly estrogenic effects which may cause reproductive disorders in women, by binding to estrogen receptors and influencing its transcription (Rai et al., 2019). ZEA can also cause hematological changes, and immunotoxic effects (Chain, 2011). Previous studies reported human and animal exposure to ZEA based on the presence of ZEA in raw food commodities (Chain et al., 2017; Guerre, 2016; Rai et al., 2019) and long-term exposure can cause major health risks (Rai et al., 2019). Permissible levels of ZEA in maize and other cereals vary from 50-1000 µg/kg based on the regulations enforced in different countries (FAO, 2003). The European Food Safety Authority established a tolerable daily intake of 0.25 µg/kg body weight for ZEA (Chain, 2011).

Many techniques have been assessed for the degradation of ZEA including ozone (Krstović et al., 2020; Santos Alexandre et al., 2018; Yang et al., 2020), electron beam (Yang et al., 2020), biological methods (Xu et al., 2020), alkali treatment (Zheng et al., 2020), and gamma irradiation (Sebaei et al., 2020). However, these methods have limitations such as low ZEA degradation efficacy, negative effects on product quality, high cost, and regulatory limits. ZEA is resistant to high temperature (up to 160 °C) treatments (Yumbe-Guevara et al., 2003). Hence, it is possible that ZEA would be stable during most food processing applications involving heat. Also, the use

of high-temperature treatments to degrade ZEA could negatively impact the quality of the product. Atmospheric cold plasma (ACP) is an emerging technology that has the potential to degrade mycotoxins without negatively affecting the quality attributes of the treated product (Chen et al., 2018). ACP consists of reactive species, UV light, and electrons and these components can contribute to the degradation of mycotoxins (N. Misra et al., 2019). Based on the voltage, gas medium, type of product substrate, relative humidity, and treatment time, a variety of reactive species could be generated in ACP, which could influence the efficacy of ACP treatment (Chapter 4, Chapter 2- section 2.4). Determining the influence of the main factors on the degradation of ZEA would be beneficial for optimizing the ACP treatment for an adequate reduction of ZEA in foods. The treatment using UV light pulses emitted from light-emitting-diodes (LED) is another recent method that could be effective against mycotoxins (Ferreira et al., 2021; Murata et al., 2008; Popović et al., 2018). At high UV light intensities, ZEA degradation could be enhanced; however, the quality of the product could be jeopardized. Combining ACP with thermal or UV light treatment could synergistically degrade mycotoxins, however, limited information is available about the potential of ACP-based combination treatments.

In this study, the degradation of ZEA was evaluated when ACP was generated with selected gas mixtures using DBD and jet plasma systems to determine the role of reactive species and UV light. To understand the influence of product substrate on the generation of reactive species and ZEA degradation, barley grains, canola grains (*Brassica napus*), and canola meal were selected for ACP treatment. Also, the synergistic effect of ACP with thermal and UV light treatments to degrade ZEA was evaluated.

5.2 Material and Methods

5.2.1 Mycotoxin standards

HPLC-grade methanol, acetonitrile (ACN) (Fisher 109 Chemical, Geel, Belgium), and a standard solution of ZEA (100 µg/ml ACN, Sigma-Aldrich, Mississauga, Canada) were used. To prepare 100 µl of ZEA solution with the concentration of 10 µg ZEA/ml ACN/water (10/90, v/v), 10 µl of the initial ZEA solution (100 µg ZEA/ml ACN) was diluted with 90 µl of deionized water. An ACN/water (10/90, v/v) solution was used to prepare the next dilutions of ZEA from 10 µg ZEA/ml ACN/ water (10/90, v/v) to the desired concentrations for standard samples.

5.2.2 Sample preparation

One hundred µl ZEA solution (10 µg ZEA/ml ACN/water (10/90, v/v)) was centrally applied on a cover-glass with a thickness of 150 µm and a diameter of 18 mm placed on microscopy slides. Then the ZEA solution was air-dried inside the biosafety chamber for 50 min before ACP, thermal, and LED treatment. After treatment, the cover-glass containing 1 µg ZEA was immersed in 1 ml methanol and shaken for 10 min at 200 RPM. The solution was evaporated using N₂ stream, then 1 ml ACN/water (10/90, v/v) was added and vortexed for 1 min before injection to HPLC for quantification. To assess the efficacy of ACP on ZEA degradation in solution, the air-drying step was skipped.

5.2.3 Atmospheric cold plasma treatment

A dielectric barrier discharge (DBD) ACP system (PG 100-3D, Advanced Plasma Solutions, Malvern, USA) was used to treat ZEA. The cover-glass containing 1 µg ZEA along with microscopy slide in the bottom were placed on top of the ground electrode (covered with 1 mm thickness glass). The high pulsating voltage electrode was connected to the generator with a pulse repetition frequency of 3500 Hz, a voltage of 0-30 kV, 70 % duty cycle, 10 µs pulse width, and 0-

1 A current. The gap between the ZEA sample and the high voltage electrode was 2 mm. One μg ZEA was treated for 0, 0.5, 1, 5, and 15 min. The ZEA in solution was treated for 0, 10, 20, 30, 40, and 50 s. For a schematic diagram of the DBD-ACP system, please refer to Chapter 3. The effect of DBD-ACP in direct and indirect modes on ZEA degradation was assessed. The ZEA sample was placed directly under the high voltage electrode in direct mode. The ZEA sample was placed 2.5 cm away from the center of the high voltage electrode (2.5-cm-diameter solid copper disk covered by 1-cm-thick quartz) in indirect mode.

5.2.4 HPLC analysis

ZEA samples were stored at 4 °C for <24 h before high-performance liquid chromatography (HPLC) analysis on a reversed-phase Agilent Zorbax SB-C18 250mm \times 3 mm, 5- μm column with isocratic elution. The injection volume was 10 μl at a flow rate of 0.5 ml/min, using a mixture of water and ACN (50:50 v/v) as the mobile phase. A photodiode array (PDA) detector at a wavelength of 238 nm was used to determine ZEA concentration. The limit of detection and the limit of quantification of HPLC for ZEA were 0.01, and 0.04 $\mu\text{g/ml}$, respectively. The recovery rate of ZEA was 80-88 % in different experiments.

5.2.5 Effect of product substrate on ZEA degradation

Barley grains, canola grains, and canola meal were used to assess the effect of product substrate on the generation of reactive species and ZEA degradation by DBD-ACP treatment. The grains were kept in Ziploc bags at 4 °C until use. The physicochemical characteristics of the grains before the experiments were determined (Table 5.1).

Table 5.1: Physicochemical specifications of substrates

Grain	Crop Year	Moisture content (g water/100 g Sample)	a_w	Grain density (g/cm ³)	Grain Dimensions	
					Length (mm)	Width (mm)
Barley	2015	10.7 ± 0.04	0.45 ± 0.003	1.058 ± 0.002	8.95 ± 1.57	3.71 ± 0.38
Canola meal	2019	11.1±0.1	0.58±0.000	1.31±0.04	<850 µm	<850 µm
Canola	2019	6.3±0.04	0.53±0.004	1.08±0.07	2.13±0.16	2.11±0.17

Values are expressed as the mean ± standard deviation (n=3).

The moisture content of the grains was measured by AACC Method (44-19.01-AACC International) using a convection oven. The water activity (a_w) meter (4TE, Aqualab, Pullman, WA, USA) was used to measure a_w . Grain density was measured by dividing the grains' mass by their volume. The volume of the grains was determined by the liquid displacement method (Chigbo, 2016) in which 2 g of grain were added to a 15 ml Falcon tube (Fisher Scientific, Ottawa, ON, Canada) and the rise in water level was used to measure the volume.

Barley grains, canola grains, and canola meal samples (0.5±0.05 g) were spiked using 200 µl of ZEA (10 µg/ml ACN) in which the concentration of ZEA on the grain was 4 µg/g. The samples were then air-dried in plastic cups with a diameter of 3.89 cm and a height of 1.14 cm at room temperature (~23 °C) for 20 min to evaporate ACN solution before ACP treatment. Barley seeds were individually spiked; canola meal samples were spiked by the ZEA solution followed by mixing after air-drying; canola seeds were placed inside 9 mm vials and mixed for 1 min by vortex at 3000 rpm with 200 µl ZEA solution. Then they were transferred to plastic cups for drying followed by ACP treatments. The reactive species concentrations were measured after 3 min of ACP treatment according to the procedure explained in the previous section.

The ZEA extraction of the samples was performed according to the method reported by Krstović et al. (2020) with some modifications. For ZEA extraction, 4 ml of ACN and water mixture (84:16,

v/v) was added to the treated and control samples followed by 10 min vortex at 3000 rpm. Two milliliter of the supernatant was filtered using a syringe filter and 20 μ l acetic acid was added to the filtered extract and cleaned up on Mycosep 112 column (Romer Labs. Inc., Union, MO, USA). The cleaned-up extract was evaporated under a nitrogen stream and the residue was dissolved in 1 ml of ACN/water 10:90 (v/v) and injected into HPLC for quantification. Control samples were spiked barley, canola, and canola meal without ACP treatments.

5.2.6 ZEA degradation by thermal and UV treatments in sequence with DBD-ACP

To assess the synergistic ZEA degradation effect, sequential thermal and DBD-ACP treatments were conducted. The thermal treatment of the ZEA samples in dry condition (1 μ g ZEA without solvent) was performed at 80 °C for 25 min. The cover-glass containing ZEA samples on a microscopy slide was heated on a digital hot plate (Fisher Scientific, assembled in China) and the sample temperature was monitored using an infrared thermometer (Optris, Berlin, Germany). The time for the sample on cover-glass to reach 80 °C was 4.5 min. After the sequential treatments, ZEA was extracted and quantified as described in the previous sections.

The efficacy of treatment using UV light pulses (395 nm wavelength, 100 Hz at a 60 % power level) emitted from LEDs (JL3-395G2-6, Clearstone Technologies Inc., Minneapolis, MN), connected to a power controller (CF3000, Clearstone Technologies Inc., Minneapolis, MN) in sequence with DBD-ACP on ZEA degradation was examined. As explained in Section 2.2, the ZEA sample (1 μ g without solvent) on cover-glass was prepared and treated with ACP for 30 s, followed by 30 min of UV treatment. The temperature of the cover glass reached a maximum of 45 °C during LED treatment. A fan (20 V, 0.284 A) was used during the UV treatment to prevent the further increase of sample temperature. The gap between the sample and the LED head was 2 cm, and the gap and positioning of the samples under the LED head were uniform in all the

treatments. To measure the irradiance and total energy dose on the sample during 395 nm LED treatment, a laser energy meter (7Z01580, Starbright, Ophir Photonics, USA) connected to a photodiode irradiance and dose sensor (PD300RM-8 W, Ophir Photonics, A Newport Corporation Brand, USA) was used. The irradiance of the UV light emitted from LEDs was measured as $0.62 \pm 0.01 \text{ W/cm}^2$. After the sequential treatments, ZEA was extracted and quantified as described in the previous sections.

5.2.7 Effect of different gas mixtures on ZEA degradation by DBD-ACP

To assess the effect of different gas mixtures on the efficacy of the ACP system to degrade ZEA, four different ratios of O₂ and N₂ were used. The gas mixtures used were: 100 % N₂, 90 % N₂+ 10 % O₂, 80 % N₂+ 20 % O₂, and air. These gas mixtures were delivered from gas cylinders to the DBD treatment chamber (inner dimensions: 8 × 8 × 10 cm) using mass flow controllers (Alicat Scientific, AZ, USA). The gases were supplied for 5 min at 5 SLPM (standard liter per minute) into the sealed ACP treatment chamber (specification of this chamber can be found at Chapter 4) with one outlet open to let the air inside the chamber to flow out. After 5 min, the outlet was closed, and no gas was flowing inside the chamber. Then, the ZEA samples were treated using ACP for 1 and 3 min inside the sealed chamber. The gap between the ZEA sample and the high voltage electrode was 2 mm.

Based on the results of the reactive species concentration and ZEA degradation by DBD-ACP with selected gas mixtures on selected product substrates, a jet-ACP system was used to improve understanding of the other factors influencing the ZEA degradation by ACP. A jet-ACP system connected to the power supply (Figure 5.1) was used to further evaluate the effect of reactive species and UV light on ZEA degradation.

The jet-ACP system was operated at a pulse repetition frequency of 1500 Hz, voltage of 0-22 kV, 70 % duty cycle, 10 μ s pulse width, and 0-0.25 A current using 75 % Ar+ 25 % N₂ at 5 SLPM. In indirect treatment, a diversion was designed (Figure 5.1) and mounted on the tip of the jet nozzle to prevent the UV light in the plasma from reaching the sample and to assess the effect of reactive species and high-energy electrons on ZEA degradation. Also, a direct pathway in jet-ACP system was built, which enabled the UV, reactive species, and high-energy electrons to reach the sample. The distance between the sample and the bottom of the nozzle was 2 mm. The traveling distances of reactive species in jet-ACP during direct and indirect treatments were equal. In another experiment, a transparent plastic shield was positioned between the sample (1 mm from sample) and jet-ACP (2 mm distance from tip of the jet nozzle) to prevent the reactive species and high energy electrons from reaching the sample, so that the effect of the UV light in jet-ACP on ZEA degradation could be evaluated. For this purpose, the coverglass containing ZEA was sealed inside a 50 mm Petri plate and positioned 1 mm under the lid of the Petri plate in which the distance between the plate and jet-ACP was 2 mm.

To evaluate the influence of reactive species and UV light on ZEA degradation, three different gas mixtures were used to generate jet-ACP. The process gas mixtures and other parameters used were 75 % Ar+ 25 % N₂ (frequency of 1500 Hz, a voltage of 0-18 kV, 70 % duty cycle, 10 μ s pulse width, and 0-0.25 A), 85 % Ar+ 15 % O₂ (frequency of 1500 Hz, a voltage of 0-22 kV, 70 % duty cycle, 10 μ s pulse width, and 0-0.25 A), and 100 % Ar (frequency of 3500 Hz, a voltage of 0-1 kV, 70 % duty cycle, 6 μ s pulse width, and 0-0.5 A) at 1 SLPM. The frequency, voltage, pulse width, and current could not be applied equally in all the selected gas mixtures due to the different excitation energy of the gases which were causing sparks or producing no plasma at the same ACP power. The UV intensity at the 240-310 nm range in jet-ACP was measured using an ILT 2400-

UVGI optical meter (International Light Technologies, Peabody, MA, USA). The detector was placed 2 mm away from the tip of the jet-ACP diversion nozzles to measure the irradiance intensity.

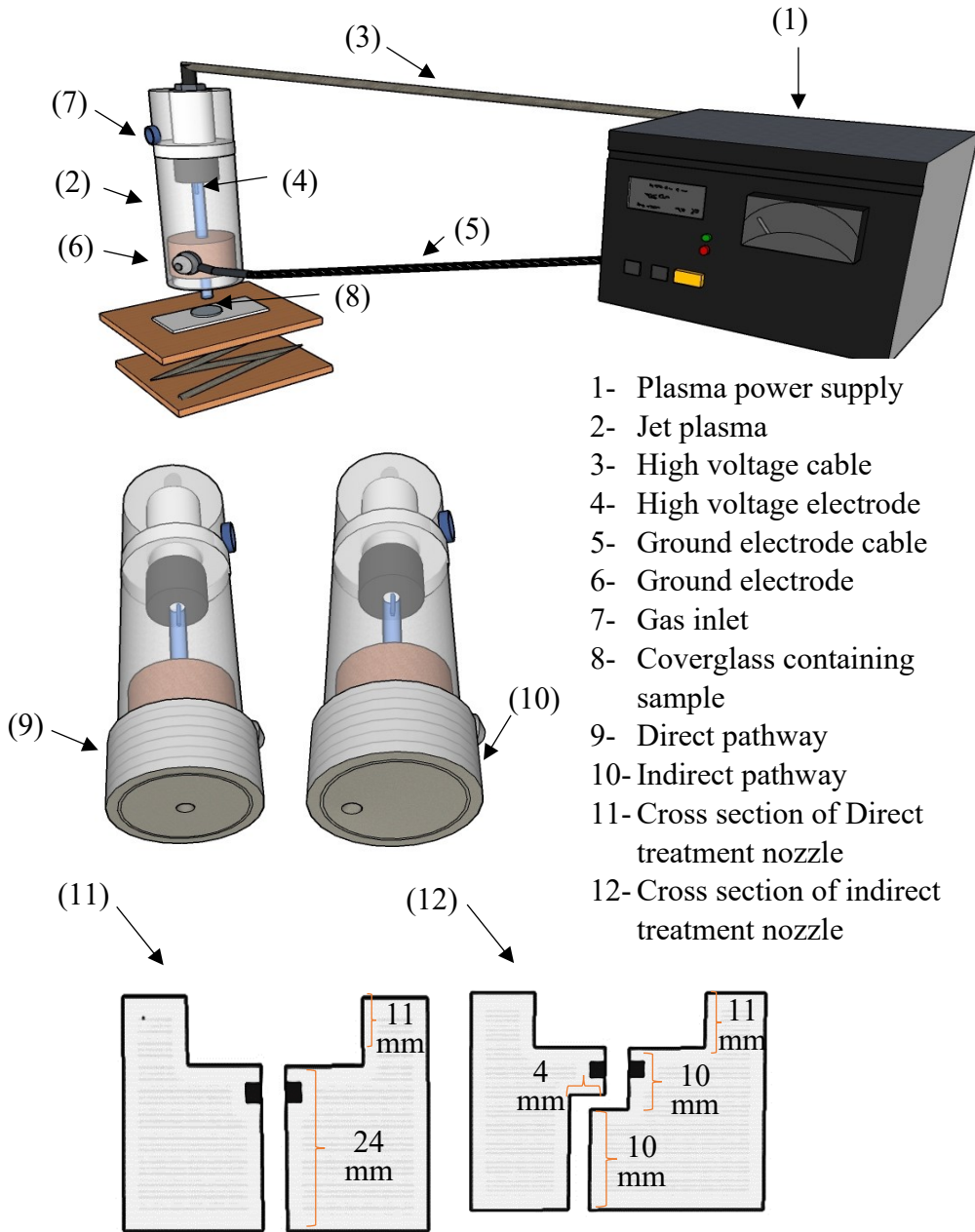


Figure 5.1: Schematic diagrams of the atmospheric cold plasma jet system

5.2.8 Cold plasma diagnostics

The optical emission spectra of DBD-ACP discharge inside the treatment chamber generated using different gas mixtures (100 N₂, 90 % N₂+ 10 % O₂, 80 % N₂+ 20 % O₂, and air) were acquired using a spectrophotometer (Black comet C-25, StellarNet Inc., Tampa, FL, USA), connected to an optical fiber (F600-UVVIS-SR, StellarNet, Inc., Tampa, FL, USA). The spectra were acquired in the wavelength range of 180 to 850 nm with a resolution of 0.5 nm, and a signal to noise ratio of 1000:1. The set integration time was 500 ms and the set values of the number of scans to average were 5 to obtain uniform spectra using SpectraWiz software (StellarNet Inc., Tampa, FL, USA). This experiment was conducted to capture the light emitted by excited plasma species between the electrodes. One end of the optical fiber was connected to the spectrophotometer and the other end to the collimating lens. The collimating lens was kept 15 mm away from the side of the quartz window incorporated to the center of the sidewall of the plasma chamber. The distance between the quartz window with the center of the electrode was 45 mm. The gas mixtures flowed inside the treatment chamber for 5 min at 5 SLPM, with one outlet open to let the air inside the chamber flow out. Then all the inlets and outlets were closed, the ACP system was turned on, and the spectra were acquired at 10 s, 1 min, and 3 min DBD-ACP treatment.

5.2.9 Measurements of ozone, nitrous gas, hydrogen peroxide, and humidity

Concentrations of ozone (O₃), nitrous gas (NO+NO₂+NO_x), hydrogen peroxide (H₂O₂), and relative humidity inside the DBD chamber during ACP treatments were determined when four different gas mixtures were used to generate ACP. The relative humidity was measured using Onset Hobo Temp/RH logger, MX1101 (Bourne, MA, USA). Dräger short-term detector tubes (Dräger Safety AG & CO, Lubeck, Germany) including an ozone 10/a Dräger tube (CH 21001), a nitrous fume 50/b Dräger tube (81 01 941), and a hydrogen peroxide 0.1/a Dräger tube (81 01041),

were used to measure the gas concentrations following the manufacturer's instructions. To measure the concentrations of H₂O₂ in all the gas combinations, and the concentrations of ozone, smaller volumes of gas was collected to ensure that the concentrations fell within the measurement range of Dräger detector tubes, i.e, 20 ml instead of 100 ml by Dräger accuro gas detector pump for ozone, and 20 ml instead of 2000 ml for H₂O₂.

To measure the approximate reactive species concentration in jet-ACP, the nozzle of the jet plasma was connected by a tube to the -airtight DBD-chamber to provide the type of reactive species and an approximate concentration of reactive species produced by jet-ACP. Using different gas mixtures, jet plasma was run for 3 min while one outlet of the DBD-chamber was left open. After 3 min, the outlet was closed, the plasma system was turned off and the reactive species concentration was measured instantly by the Dräger tubes inside the DBD-chamber.

5.2.10 Temperature measurement and plasma intensity

Temperature and plasma intensity were measured to understand any possible effect of different gas mixtures on the temperature and intensity of the DBD-ACP discharge and hence the degradation of ZEA. An imaging IR thermometer (FLIR TG165, systems Inc., Wilsonville, USA) was used to measure the surface temperature of the cover-glass positioned on the microscopy slide and treated by ACP for 3 min. The temperature of the cover-glass was measured in 12 s after 3 min ACP. The pictures of ACP discharge were captured using an iPhone XS camera in burst mode at 1 min ACP.

5.2.11 Statistical analysis

Statistical analysis of the experiments was performed by SPSS (IBM SPSS v.21, Armonk, NY). All the experiments were performed in triplicates and the values are expressed as the mean ±

standard deviation (SD). To determine the significant difference ($p < 0.05$) between the values, one-way analysis of variance (ANOVA) followed by Duncan's multiple range test was used.

5.3 Results and Discussion

5.3.1 ZEA degradation by DBD-ACP

ZEA concentration was reduced by 96.4% within 5 min ACP treatment with air as the medium and was undetectable after 15 min of ACP treatment (Figure 5.2). When ZEA was in solution, ZEA was undetectable after 30 s of ACP treatment, showing the effect of water on the ZEA degradation during ACP treatment.

Ozone is one of the major reactive species generated in air-ACP discharge and the degradation effect of ZEA was reported during ozone treatment (Krstović et al., 2020; Santos Alexandre et al., 2018; Yang et al., 2020). The degradation rate of mycotoxin by ACP is higher than using ozone, and UV light (N. Misra et al., 2019). The contributions of UV light, other reactive species such as reactive nitrogen species, and high energy electrons in ACP may help to achieve greater ZEA degradation compared to ozone treatment. The reactivity of ozone increases in the presence of water due to the high solubility of ozone in water, which increases the contact between the sample and ozone and probably contributes to the higher mycotoxin degradation (Ren et al., 2017). Also, through the reaction of ozone and water during ACP treatment, OH radicals with strong oxidizing properties are formed (H. Shi et al., 2017). In addition, to further understand the role of reactive species in ZEA degradation, indirect DBD-ACP treatment was carried out. Indirect treatment resulted in a significant reduction ($p < 0.05$) in ZEA concentration, indicating the crucial role of reactive species in ZEA degradation. However, the reductions were significantly lower ($p < 0.05$) compared with the ZEA reductions after direct treatments. For instance, the reduction of ZEA was

70.8 and 94.3 % after 1 and 3 min of direct treatment, respectively, while after indirect treatment, the reductions were 35.4 and 52.2 %, respectively.

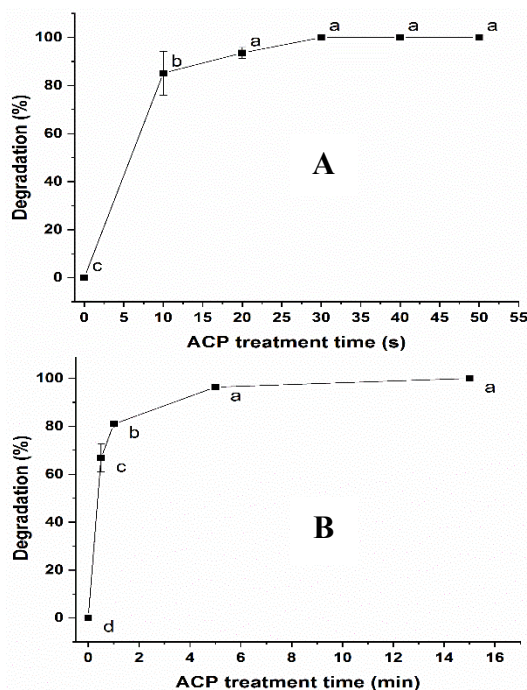


Figure 5.2: Effect of dielectric barrier discharge- atmospheric cold plasma treatment in A: solution B: dry condition on ZEA degradation. The error bars were determined based on the standard deviation of the replicates (n=3)

The characteristics of the substrate influenced the efficacy of DBD-ACP on ZEA degradation; however, the ZEA degradation rate did not correlate with size (dimensions) of the substrate, or the concentrations of reactive species produced when different substrates were used. The ZEA degradation rate was higher on canola grains and canola meal compared with barley grains after 1, and 3 min ACP treatment (Table 5.2). It is interesting to note that the concentrations of plasma reactive species produced were higher when barley and canola grains were treated compared to canola meal, suggesting the substrate effect in degrading ZEA by ACP. The compact structure of the canola meal might have produced ACP discharge with certain specific characteristics. However, in the case of canola and barley grains, the air space between the grains might have resulted in greater production of reactive species including ozone and H₂O₂. The substrates with

different number of fissures and grooves on their surface could protect the mycotoxins from ACP and reactive species. Roughness or smoothness of the substrate surfaces could change the contact area with the reactive species and consequently change the degradation rate of ZEA (Chapter 2, section 2.4). Other product characteristics such as a_w , water content, and product dimensions also could have contributed to the efficacy of ACP on ZEA degradation. For instance, a_w of canola meal was higher than those of canola and barley grains, while the moisture content of canola grains was lower than those of barley grains and canola meal (Table 5.1). The dimensions of the barley grains were larger than those of canola grains and canola meal, which also might have influenced the characteristics of the generated ACP discharge.

Table 5.2: Effect of product substrate on degradation of ZEA and production of reactive species by dielectric barrier discharge- atmospheric cold plasma

Product substrate	Treatment time (min)	Degradation (%)	O ₃ (ppm)	H ₂ O ₂ (ppm)	Nitrous fumes (NO _x , NO, NO ₂) (ppm)
Control	0	0 ^c	-	-	-
Barley grains	1	52.7±9.4 ^b	-	-	-
	3	64.8±9.5 ^b	175±25 ^a	7±1 ^a	<50 ^a
Canola meal	1	81.2±0.4 ^a	-	-	-
	3	83.2±6.7 ^a	45±5 ^b	3±1 ^b	<50 ^a
Canola grains	1	80.4±5.2 ^a	-	-	-
	3	91.6±4.2 ^a	183.3±14.4 ^a	7±1 ^a	<50 ^a

* Values are expressed as the mean ± standard deviation (n=3). Values with different letters in the same column are significantly different (p<0.05, n=3).

Sequential ACP and thermal treatment did not result in synergistic ZEA degradation, but an additive effect in ZEA degradation was observed (Table 5.3). The high stability of ZEA to thermal treatment was reported in previous studies (Chilaka et al., 2018; Jauković et al., 2014). The presence of double bonds in the ZEA structure (Figure 5.3) could be one of the reasons for their high stability to thermal treatment as the bond dissociation energy of double bonds is more than single bonds (Ouellette & Rawn, 2015). The decontamination mechanism of UV light pulses emitted from LEDs is due to the photolysis of the toxin (Stanley et al., 2020). No synergistic and/or

additive effect on degrading ZEA was observed when the sequential ACP and UV light pulses were used. As in the sequential treatment of ACP and UV light pulses in our experiment, 72.5 % of ZEA was already degraded by ACP, UV light pulses emitted from LED in sequential mode improved the degradation rate by only 2.1 %.

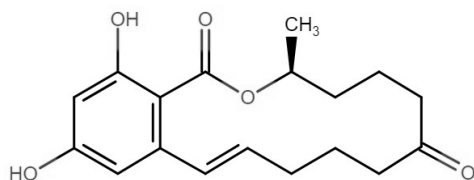


Figure 5.3: Chemical structure of zearalenone

Table 5.3: Effect of sequential dielectric barrier discharge- atmospheric cold plasma + thermal, and dielectric barrier discharge- atmospheric cold plasma + LED treatments on ZEA degradation

Treatment method	Concentration (µg/ml)	Degradation (%)
Control sample	8.1±0.04	0 ^c
30 s DBD-ACP	2.3±0.13	71.22±2.18 ^b
30 s DBD-ACP + 80 °C thermal treatment for 25 min	1.6±0.22	79.66±3.74 ^a
80 °C thermal treatment for 25 min	7.6±0.54	7.02±3.74 ^c
15 s DBD-ACP + 80 °C thermal treatment for 25 min+ 15 s DBD-ACP	2.7±0.45	67.14±7.54 ^b
Control sample	8±0.2	0 ^c
30 s DBD-ACP	2.2±0.28	72.52±5.02 ^a
30 min LED	4.22±0.07	47.20±0.86 ^b
30 s DBD-ACP + 30 min LED	2±0.17	74.58±3.1 ^a

* Values are expressed as the mean ± standard deviation. Values with different letters in the same column are significantly different and they are compared separately above and below the solid line in the table (p<0.05, n=3).

5.3.2 Effect of gas mixtures on ZEA degradation by DBD-ACP

ACP treatment of ZEA for 3 min using all the gas mixtures resulted in a 94.6 to 97 % reduction in its concentration, and the degradation rate of ZEA was not significantly (p > 0.05) influenced by the type of gas mixtures used, except for air plasma treatment for 1 min. ACP in air and 100 % N₂ generated the highest and lowest concentrations of reactive species (Table 5.4), respectively.

Hence the highest and lowest degradation rates of ZEA were expected to be in the air and 100 % N₂, respectively. However, there was no significant difference ($p > 0.05$) in the ZEA degradation levels when 100 % N₂ was used, compared with the other gas mixtures (Table 5.4). Other than the measured reactive species, the ZEA was degraded possibly by other contributing factors such as high energy electrons and UV light, and more studies are required to confirm this suggestion. The temperature of the ACP treated cover-glass with different gas mixtures was between 24.1- 24.5 °C (Figure 5.4). This proves the cold nature of the ACP treatment and the non-significant contribution of temperature to the degradation of ZEA. In a study by Siciliano et al. (2016), the degradation rate of aflatoxin by cold plasma at 100 % N₂ was higher than 21 % O₂+79 % N₂. In another study, plasma discharge using modified atmosphere (65 % O₂+ 30 % CO₂+ 5 % N₂) resulted in higher efficacy than plasma discharge using air to degrade aflatoxin, attributed to the higher concentration of reactive species such as ozone and NO_x in the modified gas (H. Shi et al., 2017). Also, using nitrogen plasma resulted in > 90 % degradation of aflatoxin in 15 min (Sakudo et al., 2017). These studies show the efficacy of N₂ in the degradation of mycotoxins.

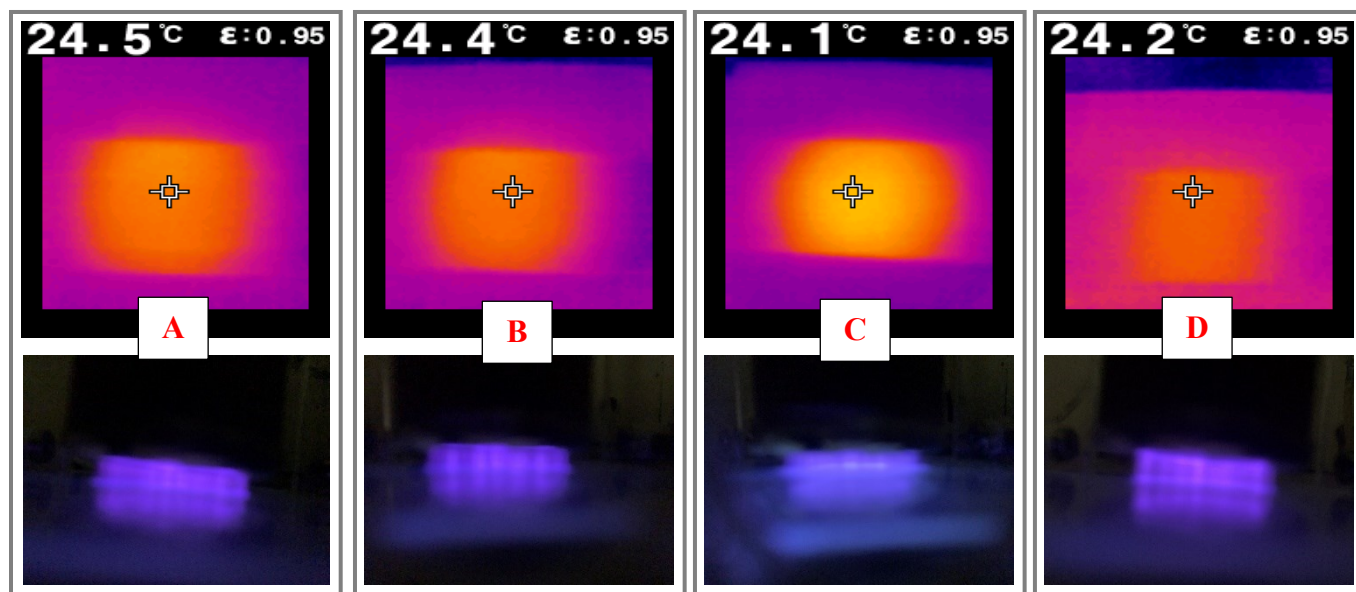


Figure 5.4: Surface temperature and intensity of plasma at different gas ratios after 3 min dielectric barrier discharge- atmospheric cold plasma treatment (A: 80 % N₂+ 20 % O₂- B: 90 % N₂+ 10 % O₂- C: 100 % N₂- D: Air)

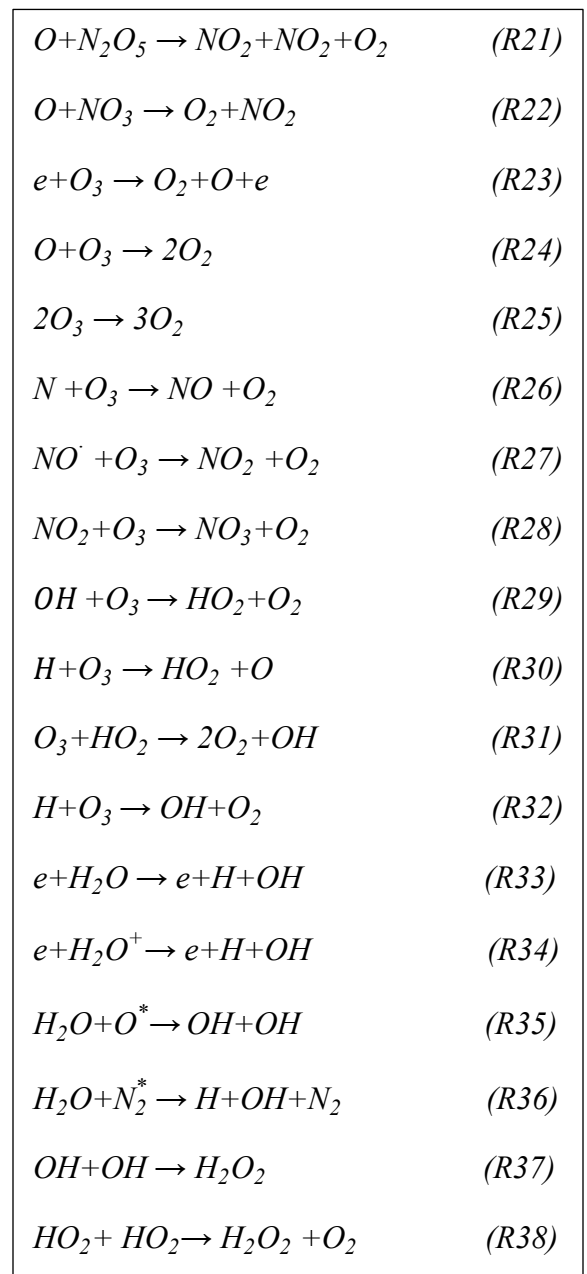
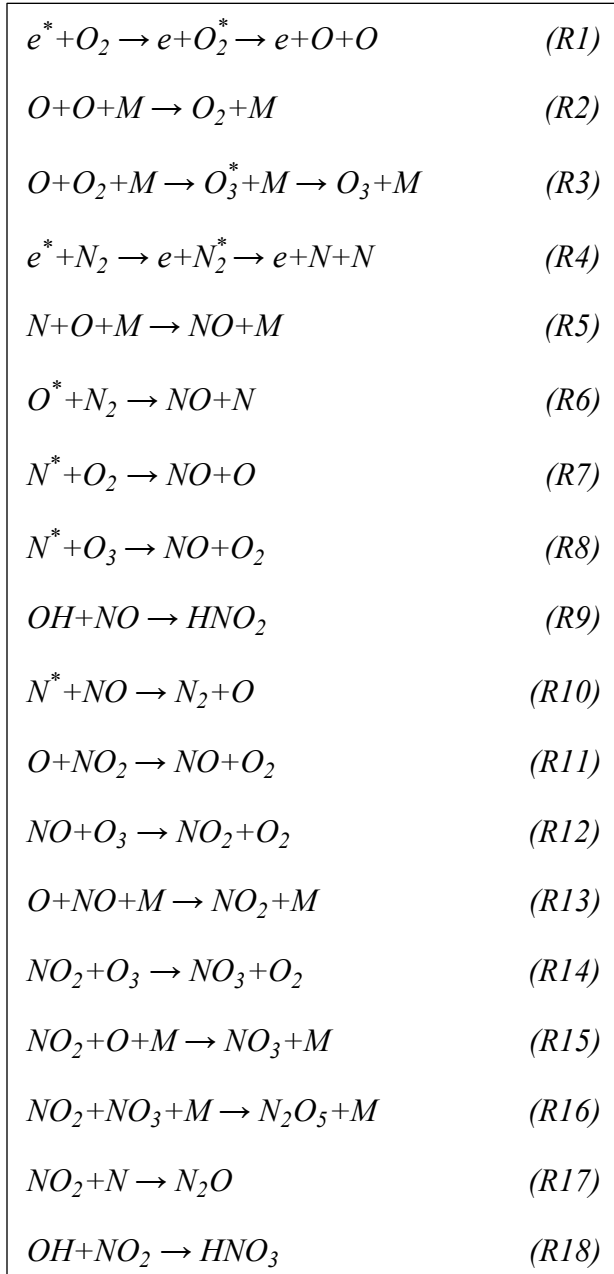
Table 5.4: Degradation of ZEA, and reactive species concentration by dielectric barrier discharge- atmospheric cold plasma treatment using selected gas mixtures

Gas mixtures	Treatment time (min)	ZEA Concentration ($\mu\text{g/ml}$)	Degradation (%)	O ₃ (ppm)	H ₂ O ₂ (ppm)	NO+NO ₂ +N O _x (ppm)	Humidity (%)
Control	0	8.3±0.4	0 ^d	<20 ^d	0 ^e	<50 ^c	37.2±1.8 ^a
100 % N ₂	1	0.8±0.2	89.8±3.1 ^{ab}	<20 ^d	2±0.5 ^{de}	<50 ^c	7.7±0.9 ^c
	3	0.3±0.1	96.1±1.4 ^a	<20 ^d	2.7±1.1 ^{de}	<50 ^c	12.2±1.7 ^b
90 % N ₂ , 10 % O ₂	1	1.1±0.5	86.0±7.2 ^b	93.33± 5.7 ^c	10±2 ^d	<50 ^c	5.2±0.2 ^{cd}
	3	0.2±0.06	97.0±0.8 ^a	126.7±20.8 ^c	9.3±1.1 ^d	<50 ^c	8.3±0.4 ^c
80 % N ₂ , 20 % O ₂	1	1.4±0.2	83.6±3.1 ^b	110±10 ^c	9.3±1.1 ^d	<50 ^c	3.8±0.4 ^d
	3	0.3±0.1	95.8±0.9 ^a	130±10 ^c	53.3±5.8 ^b	<50 ^c	6.9±0.4 ^{cd}
Air	1	2.2±0.6	73.5±8.6 ^c	300±50 ^b	40±10 ^c	116.7±5.8 ^b	37.2±2.2 ^a
	3	0.50±0.03	94.6±0.5 ^a	683.3±76.4 ^a	66.7±5.8 ^a	275±25 ^a	37.0±2.0 ^a

* Values are expressed as the mean ± standard deviation. Values with different letters in the same column are significantly different ($p < 0.05$, $n = 3$).

Based on the results, the presence of the H₂O₂ in 100 % N₂ could be due to the presence of humidity in the DBD chamber. Electrons produced in ACP excite and dissociate the oxygen and nitrogen molecules (reactions (R1), (R4)) (Pekárek, 2003). Higher concentrations of O₃ and H₂O₂ were observed when air was used to produce ACP compared to the other gas mixtures used (Table 5.4). Ozone is mainly generated in ACP by reactions (R1)- (R3) and decomposed by reactions (R23)- (R32) (Li et al., 2018; Pekárek, 2003). In a study by McClurkin-Moore et al. (2017), the higher concentration of O₂ resulted in a higher concentration of ozone. Similarly, in our study, the concentration of ozone increased with increasing the ACP treatment time and the O₂ ratio in the gas mixture due to the reactions (R1)- (R3). The H₂O₂ production rate was dependent on the O₂ concentration and humidity of the environment (Table 5.4). There was a high concentration of H₂O₂ in the air with high humidity as in the presence of water vapor, OH radicals can be formed that eventually lead to the production of H₂O₂ by the reactions (R37)- (R39). Air had a higher concentration of ozone than 80 % N₂+ 20 % O₂, probably due to the presence of high humidity in the air, which can produce OH radicals by reactions (R31)- (R36) (Whitehead, 2016). This is because a high concentration of NO_x (0.1 %<) can decompose ozone mainly by reaction (R27), however, in the presence of water vapor, OH radicals will be formed which can react with NO_x

and convert them to HNO_x (R9, R18) and so prevent the decomposition of ozone by NO_x . The same trend was observed by Han et al. (2016) in which ozone had a significantly ($p < 0.05$) higher concentration after ACP treatment for 15 s, 1 min, and 5 min in air compared to 90 % N_2 +10 % O_2 . NO and NO_2 are generated and decomposed by the reactions (R5)- (R13), and (R11)- (R22) respectively (Pekárek, 2003; Soler-Arango et al., 2018; Whitehead, 2016). Based on the concentration of nitrous gases, it is probable that the humidity of air played a major role in the generation of nitrous gases. N_2 molecules have stronger bonds than O_2 and hence higher electron energy is needed to dissociate N_2 compared to O_2 (Whitehead, 2016). The O atom may be dissociated from ozone (has a high concentration in air) by reaction (R23) and recombines with dissociated nitrogen molecules to generate NO_x . There was a positive correlation between ozone and NO_x concentration in this study and a study by H. Shi et al. (2017) in which for the high concentration of ozone, a high amount of atomic O could be produced leading to the formation of NO_x .



The asterisk denotes an excited state

Optical emission spectra (OES) is a non-destructive method, that can help to identify the excited reactive species generated due to collision with energetic electrons in the plasma (Figure 5.5). The emission spectrum of ACP in the air has been assessed by many researchers, previously. The emission peaks in all the gas mixtures at 315, 337, 353, 357, and 380 nm are due to the transition of N_2 species (H. Shi et al., 2017; Soler-Arango et al., 2018). The peak at 296 nm is related to the

excited ion, N_2^+ . Using 100 % N_2 as the medium gas of ACP exhibited two distinct peaks at 285 and 306-310 nm, in which their intensities were decreasing during ACP treatment and were not observed in the other gas mixtures. The peak at 285 nm is associated with NO (Cullen et al., 2014; Walsh et al., 2010). The presence of NO peak in 100 % N_2 could be due to the dissociation of low concentration O_2 (which has not been completely flushed out of the chamber) to atomic oxygen by plasma, which will then react with nitrogen species to generate NO. However, the concentration of O_2 was not enough to produce ozone or NO_2 instead of NO. The emission peaks at 306-310 and 306-322 were related to the OH radical (Cullen et al., 2014; H. Shi et al., 2017; Soler-Arango et al., 2018), which is generated when there is water vapor in the ACP discharge. This suggested the presence of water vapor in the treatment chamber which was later shown by measuring the relative humidity (Table 5.4). It is worth mentioning that 309 nm has been attributed as the main wavelength for OH radicals in different papers; however, 281.1 nm (Soler-Arango et al., 2018), 295-300 nm (Machala et al., 2007; Sarangapani et al., 2016), 306-312 nm (Yu et al., 2021), 305-317 nm (Machala et al., 2007), and 305-322 nm (Parigger et al., 2003) were also ascribed to different transitional system bands of OH radicals. The reduction in the intensity of NO emission peaks over time could be due to the reaction of OH with NO and NO_2 in the system and transform them into HNO_2 and HNO_3 (Soler-Arango et al., 2018) or via conversion of NO to NO_2 by reactions (R12), (R13). The excited states of atomic O at 777 ($O(^5P)$), and 845 nm ($O(^3P)$) (Walsh et al., 2010) were not observed due to collisions with N_2 and O_2 resulting in its quenching (Walsh et al., 2010). The ACP spectra at different times and gas ratios were not significantly different in the other wavelengths, as all the assessed gas mixtures contained N_2 and the spectra at 180-850 nm are mainly attributed to different states of N_2 molecule or N atoms (Yadav et al., 2019).

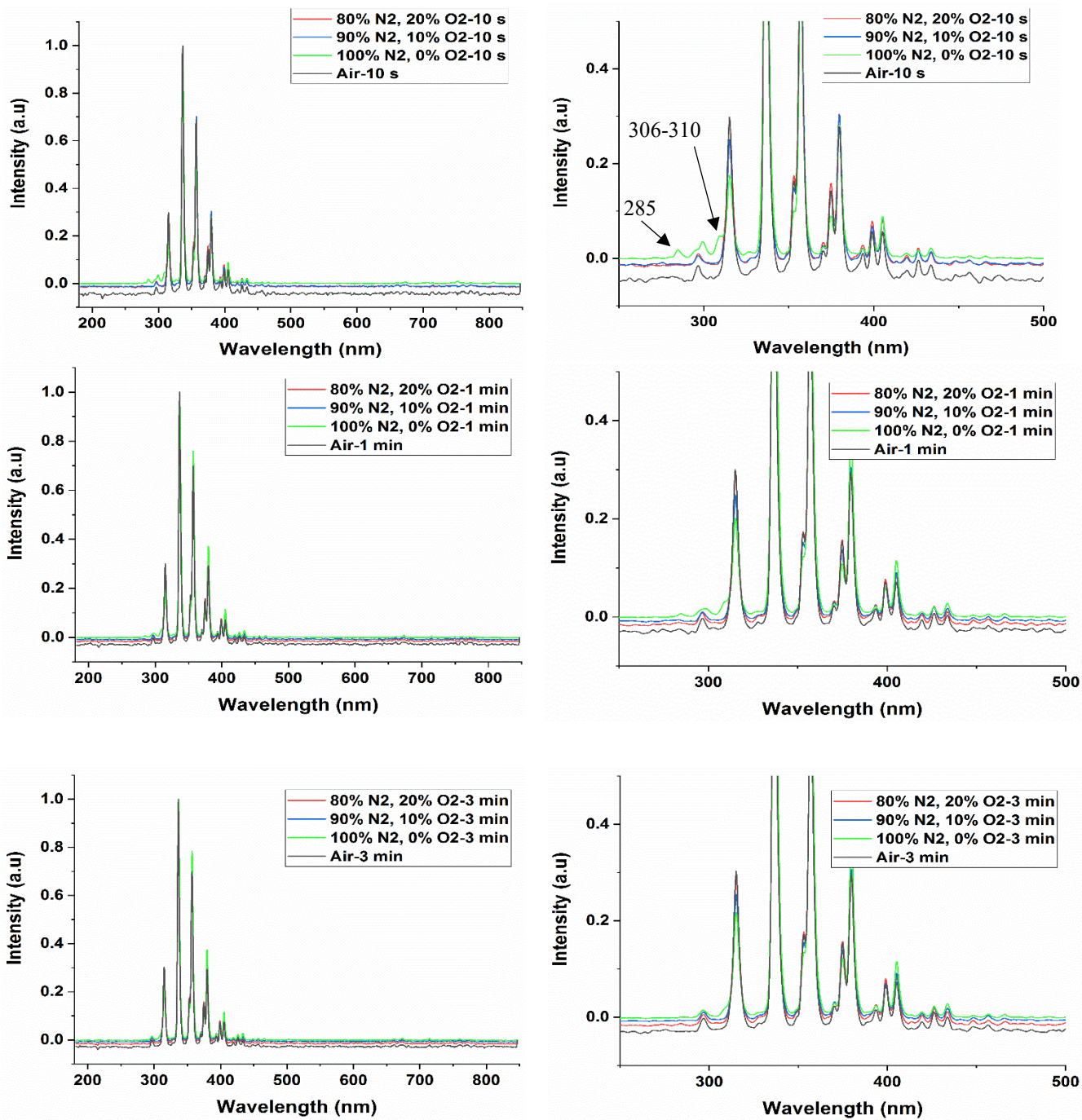


Figure 5.5: Optical emission spectra of dielectric barrier discharge- atmospheric cold plasma operating in different gas ratios (100 N₂, 90 % N₂+ 10 % O₂, 80 % N₂+ 20 % O₂, air) and different treatment times (10 s, 1 min, 3 min). Wavelength 285 nm is ascribed to NO; and 306-310 nm to OH radicals. The graphs on the right are the zoomed in versions of the graphs on the left.

5.3.3 Effect of ACP jet treatment on ZEA degradation

Results of the DBD-ACP experiments suggested the possible contribution of factors other than the observed reactive species on ZEA degradation. Hence, open atmosphere direct and indirect ACP jet treatments were performed to determine the effect of different gas mixtures, reactive species and UV intensity on ZEA degradation. The ZEA degradation after direct treatment was higher compared with the indirect treatment (Table 5.5, Table 5.6) although the distances between the high voltage electrode and tip of the jet nozzle during direct and indirect jet plasma treatments were equal. The concentrations of reactive species and the UV irradiation intensities in ACP after direct treatments were higher compared to indirect treatment, possibly contributing to the difference in ZEA degradation efficacies. To assess the contribution effect of UV light in ACP on ZEA degradation, a UV transparent shield was used, that possibly eliminated the contribution of reactive species and electrons in ACP on ZEA degradation. However, the UV light intensity by using a shield was lower compared to the direct treatment and so the contribution of UV light on ZEA degradation in direct treatment could be more than the 6.2 % that was observed by using the shield.

Table 5.5: Effect of atmospheric cold plasma jet in direct and indirect mode using different gas mixtures at 1 SLPM on degradation of ZEA

Gas mixtures	Treatment	Treat ment time (min)	ZEA degradation (open atmosphere, %)	ZEA degradation (inside the chamber, %)	O ₃ (ppm)	H ₂ O ₂ (ppm)	UV intensity (W/cm ²)
-	Control	0	0 ^f	0 ^c	0 ^b	0 ^b	0 ^d
		1	9.4±1.4 ^{cd}	-	-	-	-
75 % Ar + 25 % N ₂	Direct	3	14.5±2 ^d	-	0 ^b	0.8±0.7 _b	5.9×10 ⁻⁶ ±4.8×10 ^{-7 a}
		1	4.7±2.2 ^{ef}	-	-	-	0 ^d
	Indirect	3	2.5±1.6 ^f	-	-	-	0 ^d
		1	34.6±2.4 ^c	-	-	-	0 ^d
85 % Ar + 15 % O ₂	Direct	3	54.3±7.2 ^a	-	22.3±2.5 ^a	17.3±3.5 ^a	1.7×10 ⁻⁶ ±5×10 ^{-7 c}
		1	30±4.3 ^c	16.9±7.3 ^b	-	-	0 ^d
	Indirect	3	44.3±5.3 ^b	38.6±5.6 ^a	-	-	0 ^d
		1	30±4.3 ^c	16.9±7.3 ^b	-	-	0 ^d

100 % Ar	Direct	1	2.3±1.6 ^f	-	-	-	5.1×10 ⁻⁶
		3	10.5±4 ^{cd}	-	0 ^b	0 ^b	±4.7×10 ^{-7^b}

* Values are expressed as the mean ± standard deviation. Values with different letters in the same column are significantly different (p<0.05, n=3).

Table 5.6: Effect of atmospheric cold plasma jet using 75 % Ar+ 25 % N2 at 5 SLPM in direct and indirect modes on degradation of ZEA

Treatment	Treatment time (min)	ZEA Concentration (µg/ml)	Degradation (%)	UV intensity (W/cm ²)
Control	0	8.5±0.3	0 ^d	0 ^c
Direct	1	6.4±0.7	24.4±8 ^b	1.8×10 ⁻⁵ ± 9.1×10 ^{-7^a}
	3	5.4±0.8	36±9.9 ^a	
Indirect	1	7.4±0.3	13.3±3.1 ^c	4.8×10 ⁻⁶ ±1.1×10 ^{-7^b}
	3	6.0±0.3	29.1±4 ^{ab}	
Shield	1	8.2±0.02	3.3±0.2 ^d	4.4×10 ⁻⁶ ±8.6×10 ^{-8^b}
	3	8±0.2	6.2±2.3 ^{cd}	

* Values are expressed as the mean ± standard deviation. Values with different letters in the same column are significantly different (p<0.05, n=3).

Three different gas mixtures, 75 % Ar + 25 % N₂, 85 % Ar + 15 % O₂, and 100 % Ar were used in jet-ACP to determine the role of different reactive species in ZEA degradation (Table 5.5). The highest ZEA degradation rate was observed when 85 % Ar + 15 % O₂ was used, presenting the importance of O₂ to produce the reactive oxygen species and hence possibly contributing to ZEA degradation. Using argon as a medium gas could lead to the production of reactive oxygen and nitrogen species due to the interaction of ambient air with excited Ar species or high energy electrons (Jo et al., 2020). However, in our study, the concentration of oxidizing reactive species such as ozone or hydrogen peroxide using 100 % Ar was below the detection limit, hence the degradation of ZEA could be attributed to UV light, high energy electrons or any other reactive species produced but not measured. Further, the irradiation intensity of UV light at indirect treatment was zero and the traveling distances of reactive species in the direct and indirect treatment were equal, and hence the ZEA degradation in 75 % Ar + 25 % N₂ could be due to the presence of hydrogen peroxide (not measured in indirect treatment) or the high energy electrons (not measured).

5.4 Conclusions

ACP treatment was able to reduce ZEA concentration considerably in short treatments, showing the potential of this technology. The presence of water significantly ($p < 0.05$) affected the ZEA degradation rate during ACP treatment. Sequential treatment consisting of ACP followed by UV light pulses or thermal treatment did not show a synergistic effect on the degradation of ZEA. Use of different gas mixtures to generate DBD-ACP discharge resulted in different concentrations of reactive species; however, this did not influence the ZEA degradation levels after 3 min treatment. The type of product substrate affected the production of reactive species by ACP, although, there was no correlation between the reactive species concentration and the degradation rates of ZEA on different product substrates. The ZEA degradation rate was influenced by the type of gas mixture and treatment modes, i.e., direct or indirect, when jet-ACP was used. The results of this study suggest that the degradation mechanisms of ZEA under DBD-ACP and jet-ACP could be different and factors other than reactive oxygen and nitrogen species in ACP discharge, such as high energy electrons, and UV light also possibly contribute to ZEA degradation.

Chapter 6: Reduction of deoxynivalenol during barley steeping in malting using plasma activated water and the determination of major degradation products

6.1 Introduction

Barley is the most widely used cereal grain for malt production (Rani & Bhardwaj, 2021). Barley grains can be contaminated with fungal pathogens which can produce certain mycotoxins in the field or during storage. One of the most common mycotoxins in malt and beer is deoxynivalenol (DON)¹, which is mainly produced by *Fusarium graminearum* (Arrúa et al., 2019; Bertuzzi et al., 2011). DON has various toxic effects in humans and animals, causing acute temporary diarrhea, nausea, vomiting, headache, dizziness, fever, and abdominal pain. A detailed description of its toxic effects can be found in a study by Sobrova et al. (2010). In addition, contamination of grains by DON can lead to significant reduction in quality (Dohlman, 2003). There are strict guidelines regarding the presence of mycotoxins in food. The maximum permitted level of DON in unprocessed cereals other than durum wheat, oats and maize is 1250 µg/kg, and in cereals intended for direct human consumption, cereal flour, bran as end product for direct human consumption and germ the maximum permitted level of DON is 750 µg/kg (Commission, 2006). The common

¹ ACN (acetonitrile)
ACP (atmospheric cold plasma)
DBD (dielectric barrier discharge)
DBE (double-bond equivalent)
DON (deoxynivalenol)
DW (distilled water)
HPLC (high-performance liquid chromatography)
NIB (naturally infected barley)
ORP (oxidation reduction potential)
PAW (plasma activated water)
RNS (reactive nitrogen species)
ROS (reactive oxygen species)
RONS (reactive oxygen and nitrogen species)
SLPM (standard liter per minute)

postharvest methods for removing mycotoxins from food and feed are physical, chemical, enzymatic and microbial methods (Karlovsy et al., 2016). Malt and grain industries continue to seek better technologies to degrade mycotoxins in food and feed, since the current methods are time consuming, laborious, expensive, energy intensive, or may negatively impact the quality of the treated product (N. Misra et al., 2019).

Atmospheric cold plasma (ACP) is a promising new method, capable of degrading DON (Chapters 3, and 4). Plasma is the fourth state of matter, comprised of reactive species including atoms, and molecules in the ground or excited states, ions, free radicals, electrons, and ultraviolet radiation. Plasma can be produced by different gas discharge sources including corona discharge, glow discharge, plasma jet, and dielectric barrier discharge (N. Misra, O. Schlüter, & P. J. Cullen, 2016). ACP can be used to activate water to produce plasma activated water (PAW). There is a lack of research on assessing the efficacy of PAW on mycotoxin degradation. In a previous study, 20 min PAW treatment resulted in 25.8% DON reduction, which might be due to washing the DON off from barley and the degradation effect of reactive species (Chen et al., 2018). The long-lived reactive species such as ozone, hydrogen peroxide, and nitrates could play a role in DON degradation using PAW (Chen et al., 2018). The direct or indirect interaction of reactive species with water molecules, including reactive oxygen species (ROS) and reactive nitrogen species (RNS) in plasma can change the oxidation-reduction potential and pH of water (Rathore et al., 2021). The effect of ROS, including ozone (Young et al., 2006) and hydrogen peroxide (Fouler et al., 1994; Jalili et al., 2011) on mycotoxin degradation has been reported previously. The ROS and RNS, including nitrogen oxides such as nitric oxide and nitrogen dioxide in PAW can interact with DON and lead to its degradation (Machala et al., 2018). In addition to the mycotoxin reduction and antimicrobial effect of PAW, PAW treatment can also improve the germination rate of grains

(Sarinont et al., 2017; Sivachandiran & Khacef, 2017). Previously, PAW was used for microbial decontamination (Rathore et al., 2021), pesticide degradation (Chen et al., 2018), and germination improvement (Guragain et al., 2021). Malting process consists of steeping, germination, and kilning steps, in which PAW may be a suitable substitute for water in the steeping process of the grains for possible germination improvement and mycotoxin degradation. Also, to establish safe regulatory procedures using cold plasma or PAW treatment for DON reduction in food and feed in larger scales, it is important to determine the structure and toxicity of DON degradation products.

Previous literature reported the effect of ACP treatment on the degradation rate of DON (Feizollahi, Arshad, et al., 2020; Park et al., 2007; ten Bosch et al., 2017). However, there is a lack of knowledge regarding the degradation products of DON after ACP treatment. Also, limited information is available on the potential use of PAW for barley grain steeping and its effect on DON content as well as the improvement in germination and quality parameters. Hence, the aim of this research was to assess the potential of using PAW as a substitute for water during the steeping process in order to reduce the DON concentration in naturally infected barley (NIB) and to evaluate the effect of PAW on the germination and quality parameters of barley malt. Also, from consumer health and safety perspectives, this study focused on determining the major degradation products of DON after ACP treatment.

6.2 Material and methods

6.2.1 Barley grains and chemicals

Naturally infected barley grains (a 2-row malting variety named CDC Copeland) containing high concentrations of DON compared with the permitted levels on unprocessed cereals (1.25 ppm)

(Commission, 2006), with an initial moisture content of $10.27 \pm 0.04\%$ (wet basis) were obtained from the Brandon Research and Development Centre, Agriculture and Agri-Food Canada, Brandon, Manitoba, Canada. The grains were kept in Ziploc bags and stored at 4°C until used. The initial wet basis moisture content (MC), water activity (a_w), density, and grain dimensions of NIB grains were determined (Table 6.1). The MC of the barley grains was determined by AACC Method (44-19.01-AACC International). The water activity (a_w) was determined using an a_w meter (4TE, Aqualab, Pullman, WA, USA). The grain density was determined by dividing the grain mass by its volume. Liquid displacement method was used to measure the volume (Feizollahi, Iqdiem, et al., 2020). Analytical standard of DON (5 mg) was purchased from Milipore Sigma (Oakville, Ontario, Canada). HPLC-grade acetonitrile (ACN) was acquired from Fisher Scientific (Ottawa, Ontario, Canada).

Table 6.1: Physical specifications of naturally infected barley grains.

Crop year	MC (g water/100 g sample)	a_w	Grain density (g/cm^3)	Grain dimensions	
				Length (mm)	Width (mm)
2020	10.3 ± 0.04	0.48 ± 0.004	1.21 ± 0.08	9.18 ± 0.87	3.71 ± 0.12

6.2.2 PAW production and characterization

The ACP jet connected to a power supply (PG 100-D, Advanced Plasma Solutions, Malvern, PA, USA) was used to treat 30 ml of distilled water (DW) beneath the water surface for 30 min to generate PAW (Figure 6.1). Air was pumped at a flow rate of 0.5 standard liter per minute (SLPM) and the ACP jet was used at a frequency of 3500 Hz, 70% duty cycle, output voltage of 0-34 kV, current of 0-1 A, and a $10 \mu\text{s}$ pulse width in all the experiments. The characteristics of PAW such as pH, oxidation reduction potential (ORP), ozone, nitrate, and H_2O_2 concentrations were determined. The pH, and ORP were measured using a pH meter (Fisher Scientific, Accumet

AE150, Singapore) and ORP meter (Ohaus, ST20R, Parsippany, NJ, USA), respectively. CHEMets kits (Midland, VA, USA) were used to measure ozone (K-7404) based on the DPD (N,N-diethyl-p-phenylenediamine) method; nitrate (K-6904) based on the cadmium reduction method; and H₂O₂ (K-5510B) based on the ferric thiocyanate method.

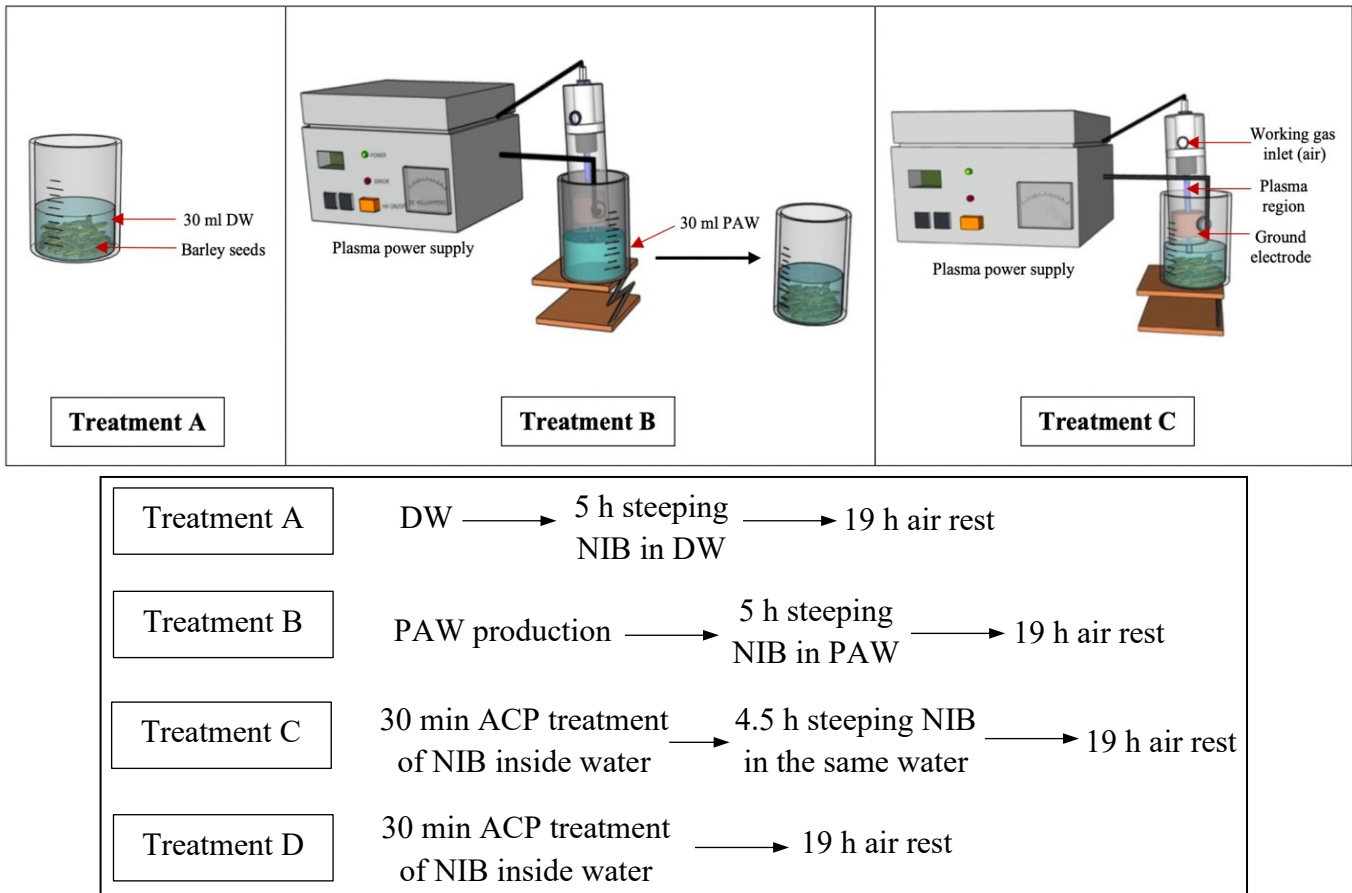


Figure 6.1: Schematic diagram and flow chart of PAW generation and treatment of NIB grains in ACP.

6.2.3 Determination of DON after PAW treatments

Ten grams of NIB grains were steeped in 30 ml PAW or DW (control) in a beaker for the following treatments (Figure 6.1). Treatment A: steeping NIB in DW for 5 h followed by 19 h air rest; Treatment B: Steeping NIB in PAW for 5 h followed by 19 h air rest; Treatment C: 30 min ACP

treatment of NIB inside DW followed by 4.5 h steeping, and 19 h air rest; Treatment D: 30 min ACP treatment of NIB inside DW without further steeping or air rest. The aforementioned treatments were performed in order to simulate the first day of steeping process in the industry to assess the potential of DW substitution with PAW for DON reduction. At the end of the steeping steps, the grains were drained for 5 min and then kept for 19 h air rest at $15\pm 0.3^{\circ}\text{C}$, $76\pm 4\%$ RH. After air rest, the barley grains were dried at room temperature for 2 days. Then the DON content was measured using Reveal® Q+ test kits (Neogen, Lansing, MI, USA) based on the single-step lateral flow immunochromatographic assay. The limit of detection for the kits was 0.3 ppm and their specificity for DON was 100%. The kits were validated by quantifying DON by HPLC on a reversed-phase Agilent Zorbax SB-C18 250 mm \times 3 mm, 5- μm column with isocratic elution. For HPLC analysis, DON was extracted based on the methodology described by (Krstović et al., 2020; Li et al., 2015) with modifications. Grains (12.00 ± 0.05 g) were ground in a laboratory mill (Hamilton Beach 80393 Grinder, China) with 0.5 mm mesh at 8000 rpm for 20 s. Ten grams were used to assess DON content using the Reveal® Q+ test kits and 1.5 g of the ground samples were used for HPLC analysis. A 1.5 g sample was blended with 6 ml of ACN and water mixture (84:16, v/v) and stirred for 30 min on an incubator shaker (ES-60, Hanchen, Canada) at 300 rpm followed centrifuging for 5 min at 6000 rpm. Three ml of the supernatant was cleaned up on MycoSep 113 Trich column (Romer Labs. Inc., Union, MO, USA). The cleaned-up extract was evaporated to dryness under a nitrogen stream and the residue was dissolved in 1 ml of water: ACN (85:15 v/v), vortexed for 1 min and injected (25 μl) into the HPLC for analysis. HPLC was run at a wavelength of 218 nm using a photodiode array (PDA) detector with an injection volume of 25 μL and flow rate of 0.5 ml/min, using a mixture of water/ACN/methanol (85:12:3 v/v) as the mobile phase. The

accuracy of the kits was >90 % which was calculated as follows: accuracy = (kits value/ HPLC value)×100.

6.2.4 Water uptake of barley treated by PAW

Barley samples (1.00±0.02 g) were immersed in PAW or DW (control) at 22°C. Samples were taken at 1, 5, 24, 48 h to measure water uptake. Before weighing the samples, the grains were drained and the excessive water from the grain surface was removed using a filter paper. The increase in sample weight was considered as the water uptake of the grain (Mayolle et al., 2012; Pater et al., 2020).

6.2.5 Effect of PAW on selected quality features of green malt

Barley malt was produced by 2 days steeping using the treatments A, B, and C (as described in section 2.3) at 15±0.3°C and 76±4% environmental humidity followed by 3 days germination at 15°C, 92±4% RH. After each steeping cycle, the grains were drained for 5 min before air rest. Also, over the 3 day germination process, the grains were washed with DW and drained followed by the addition of 3 ml DW to 10 g NIB each day.

The moisture content of the dry NIB grain and green malt was measured by the American Association for Clinical Chemistry (AACC) Method using air oven drying for 2 h at 135°C (44–19.01, AACC International). The α -amylase, β -amylase, and β -glucanase activities in dry NIB grain and green malt were determined using K-MALTA 07/20 malt amylase assay kit and S-ABG100 03/11 malt and bacterial β -glucanase assay kit (Megazyme, Bray, Wicklow, Ireland). Protein content of dry NIB grain and NIB grain before 3 day germination was determined by combustion using 6.25 as the nitrogen (%) to protein (%) conversion factor (AACC 46-30.01).

Also, forty barley seeds in triplicate (40×3) were used for each treatment to determine the percentage of germinated acrospires and rootlets. The grains with growing acrospires and rootlets were considered as the germinated seed.

6.2.6 Degradation products of DON after ACP treatment

The degradation products of DON were analyzed after ACP treatment using a dielectric barrier discharge (DBD) high voltage electrode connected to the ACP power supply. For the experiment, 5 mg of standard DON sample was dissolved in 3.1 ml ACN/water (20:80 v/v). For ACP treatment, DON sample inside plastic cups (3 cm diameter) was positioned on a glass insulated cover (1 mm thickness) on the top of a ground electrode with a 2 mm gap between the sample and the high voltage electrode. Three ml of the sample was treated with ACP for 30 min to quantify the DON degradation rate and assess the major degradation products using high-performance liquid chromatography ultraviolet mass spectroscopy (HPLC-UV-MS). One hundred milliliters of the sample was used as the control. Reverse phase HPLC-MS was performed using an Agilent 1200 SL HPLC System with a Phenomenex Luna 1.6 μm , 100Å, 50 x 2.1mm, C18 polar reverse-phase analytical column with guard (Phenomenex, Torrance, CA, USA), set to 50°C followed by mass spectrometric detection.

A 2 μl aliquot was loaded onto the column at a flow rate of 0.50 ml min⁻¹ and an initial buffer composition of 100% of 0.1% formic acid in water as mobile phase A and 0% of acetonitrile as mobile phase B. Elution of the analytes was achieved by using 100% mobile phase A for 0.5 min followed by a linear gradient from 0 % to 30% mobile phase B over a period of 5.5 min, 30% to 95% mobile phase B over a period of 1 min held at 95% mobile phase B for 2 min to remove all analytes from the column and 95% to 0% mobile phase B over a period of 1.0 min. Mass spectra

(total ion chromatogram) were acquired in the negative mode ionization using an Agilent 6220 Accurate-Mass HPLC/MS system (Agilent, Santa Clara, CA, USA) equipped with a dual sprayer electrospray ionization (ESI) source with the second sprayer providing a reference mass solution. Mass spectrometric conditions were: drying gas at 9 l/min at 325°C, nebulizer 20 psi, mass range 100-1100 Da, acquisition rate of ~1.03 spectra/sec, fragmentor 125 V, skimmer 65 V, capillary 3200 V, and instrument state 4 GHz high resolution. Mass correction was performed for every individual spectrum using peaks at m/z 112.98558 and 1033.988109 from the reference solution. Data acquisition was performed using the Mass Hunter software package (ver. B.04.00.) and the analysis of the HPLC-UV-MS data was performed. Definitions: the calculated mass or the theoretical mass was the exact mass of an ion whose elemental formula, isotopic composition and charge state are known. Accurate mass is the experimentally measured mass of an ion. Mass error is the difference between the accurate measured mass and the calculated exact mass (Brenton & Godfrey, 2010). DBE is the number of rings plus the number of double bonds to carbon atoms in the molecule (Bae et al., 2011). Based on the software, the scoring of the generated formulas was calculated based on three factors; 1) mass: how well the measured mass (or m/z) compared with the value predicted from the proposed formula, 2) abundance: how well the abundance pattern of the measured isotope cluster compared with values predicted from the proposed formula, and 3) spacing: how the m/z spacing between the lowest- m/z ion and the A^{+1} and A^{+2} ions compared with the values predicted from the proposed formula.

6.2.7 Statistical analysis

SPSS (IBM SPSS v.27, Armonk, NY) was used for determining the significant differences ($p < 0.05$) by one-way analysis of variance (ANOVA), followed by Duncan's multiple range test.

At least triplicate experiments were performed, and the data were expressed as the mean \pm standard deviation.

6.3 Results and Discussion

6.3.1 PAW characteristics

○ pH of PAW

After 30 min and 5 h storage of PAW, the pH was not changed (Table 6.2), which indicated the stability of the compounds causing the acidity of PAW during storage. Air was used as the working gas in this research to generate PAW. Acidic H_3O^+ ions could be formed by the reaction of hydrogen peroxide with water molecules (Chen et al., 2008), resulting in pH reduction. Also, nitrates and nitrites were produced in PAW, leading to the formation of nitrous and nitric acid and significant reduction in pH (Rathore et al., 2021; Tian et al., 2015a). . Brisset et al. (1990) reported that singlet oxygen plays a significant role in the acidification process. As singlet oxygen is involved in the production of nitrates, nitrites, and hydrogen peroxide, and the presence of either oxygen or humidity is required for singlet oxygen generation, it is possible that the reduction in pH may not occur if the gases without oxygen and humidity were used for plasma generation. Rathore et al. (2021) reported that the highest pH and lowest ORP were produced when nitrogen was used as the working gas.

Table 6.2: Characteristics of plasma activated water

	pH	ORP (mV)	H ₂ O ₂ (ppm)	Ozone (ppm)	Nitrate (ppm)
DW	8.4 \pm 0.17 ^a	194.4 \pm 51.3 ^b	<20	0 ^c	0 ^c
PAW 0 min storage	3.86 \pm 0.05 ^b	400 \pm 30.4 ^a	<20	0.53 \pm 0.06 ^a	11.95 \pm 2.16 ^a
PAW 30 min storage	3.88 \pm 0.04 ^b	392 \pm 28 ^a	<20	0.12 \pm 0.08 ^b	8.66 \pm 1.4 ^b
PAW 5 h storage	3.88 \pm 0.03 ^b	372.7 \pm 8.1 ^a	<20	0 ^c	8.65 \pm 1.4 ^b

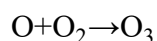
Values are expressed as the mean \pm standard deviation. Values with different letters in the same column are significantly different ($p < 0.05$, $n \geq 3$).

○ Oxidation reduction potential of PAW

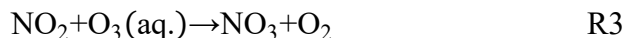
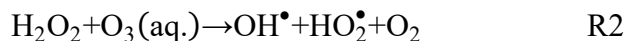
During the generation of PAW, the ORP of PAW increased from 194.4 to 400 mV after 30 min of ACP treatment of DW (Table 6.2), demonstrating the greater oxidizing potential and reactivity of PAW compared to DW. In an aqueous solution, ORP is the measure of the tendency of a solution to gain or lose electrons. A solution with a greater number of ORP has more tendency to gain electrons, i.e., to oxidize the other compounds compared to a solution with lower ORP. The reactive oxygen and nitrogen species (RONS) including hydrogen peroxide, ozone, nitrites, and nitrates are formed in the plasma phase above the surface of the water and diffused into the water, contributing to the overall ORP of PAW (Rathore et al., 2021). There are numerous reactions occurring at the same time in PAW, consisting of the formation and decomposition of reactive species. In R₁-R₃, the reactions for the formation of ozone, and nitrate, and decomposition of hydrogen peroxide are presented. The detailed reactions for the formation and decomposition of the above-mentioned reactive species are presented in Chapter 5.

- Hydrogen peroxide, ozone, nitrate concentration in PAW

The concentration of hydrogen peroxide was below the limit of the detection of the kits (LOD: 20 ppm) in DW and PAW (Table 6.2). Ozone is generated in the plasma phase above the surface of water by reaction R1 (Chapter 5) and then diffuses into the water. The concentration of ozone was 0.53 ppm in the PAW, and then the concentration decreased to 0.12 and 0 ppm after 30 min and 5 h storage, respectively due to the high reactivity of ozone (Table 6.2). The dissolved ozone reacted with nitrite ions and hydrogen peroxide, resulting in the formation of nitrate ions and hydroxyl radical (R 2-3) (Rathore et al., 2021). Nitrates could be formed in the plasma and liquid phases. The PAW contained 11.95 ppm of nitrates, which decreased in the first 30 min of storage and then remained the same during the 5 h storage period.



R1



Overall, the higher the concentration of the reactive species that can form nitrous and nitric acids, the lower would be the pH. Also, the higher the reactive species concentration, the higher would be the ORP. However, during storage, the concentration of reactive species could be reduced due to their reaction with each other, but the pH could be constant, as the acidifying agents such as nitrates are stable even in long storage periods.

6.3.2 Effect of PAW on DON reduction

Steeping is the first step in the malting procedure in which the water is added to the dry grain in order to increase the moisture content to 42-47% and initiate germination (Rani & Bhardwaj, 2021). We used PAW instead of DW to evaluate its potential to reduce DON besides increasing the moisture content of NIB. The initial DON content on NIB was 4.65 ppm, which is considered a heavily infected grain by fungal pathogen *Fusarium* spp. After the first wash and air rest during the steeping process using DW, the DON concentration was reduced by 33.3% (treatment A, Table 6.3). DON is soluble in water and could be washed out to the surrounding water during steeping process. Hence, removing the steeping water will also remove the dissolved DON from the grain. Using PAW, the reduction of DON was similar to that of DW after the first wash and air rest (treatment B). Immersing NIB in DW and treating them with ACP to produce PAW for 30 min without any further steeping and air rest resulted in a 21.1% reduction of DON (treatment D). During the steeping process, water absorption by grains causes an increase in moisture content. This process could lead to a changes in the surface properties of the grains and hence affects the permeability of reactive species into the layers of the grain. It was likely the reason for a lower

DON reduction after treatment D, where there was no steeping compared to treatments A and B (Table 6.3).

Table 6.3: Reduction of deoxynivalenol after steeping of naturally contaminated barley

	DON content (ppm)	Minimum (ppm)	Maximum (ppm)	Reduction (%)
Initial Don content on NIB	4.65±0.65 ^a	3.9	5.5	0 ^c
Treatment A	3.1±0.82 ^b	2.1	4.0	33.3±17.8 ^b
Treatment B	3.07±0.71 ^b	2.2	3.9	33.9±15.3 ^b
Treatment C	1.93±0.42 ^c	1.6	2.4	58.4±8.9 ^a
Treatment D	3.67±0.06 ^{ab}	3.6	3.7	21.1±1.2 ^b

Treatment A: Steeping NIB in DW for 5 h followed by 19 h air rest; Treatment B: Steeping NIB in PAW for 5 h followed by 19 h air rest; Treatment C: 30 min ACP treatment of NIB inside water followed by 4.5 h steeping, and 19 h air rest; Treatment D: 30 min ACP treatment of NIB inside water Values are expressed as the mean ± standard deviation. Values with different letters in the same column are significantly different ($p < 0.05$, $n \geq 4$).

The DON reduction in barley grains was the highest with a 58.4% reduction after treatment C, where NIB in water was treated with ACP for 30 min followed by steeping and air rest. This could be due to the interaction of short-lived reactive species such as hydroxyl radical (OH^\bullet), superoxide (O_2^-), and singlet oxygen ($^1\text{O}_2$) with the surface of the grains compared with treatments B. These changes in surface properties could possibly lead to an increase in the diffusion of long-lived reactive species such as hydrogen peroxide, ozone, and nitrate into the inner layers of grains during the treatment of NIB with PAW, thus reducing DON more than treatments B and D. In treatment B there was no contribution of short-lived reactive species, and the concentration of long-lived reactive species such as ozone, nitrate, and hydrogen peroxide were low. Probably, that was the reason for having a similar degradation rate for treatment B with treatment A. Previous studies reported surface changes in grains by ACP due to the direct energetic effects of plasma exposure and/or chemically by interacting with reactive species (Park et al., 2018a; Scholtz et al., 2019). It is likely that short-lived reactive species may directly interact with the seed coat and change the grain surface properties. Oxidation of the seed coat by RONS was reported previously (Waskow et al., 2021), in which the short-lived reactive species could play a major role. Also, the hydroxyl

radicals were reported to be responsible for cell wall loosening, enhancing the penetration of long-lived reactive species into the grain (Müller et al., 2009). The results of treatments A and C, suggest that 33% of DON reduction was due to washing of the DON in the steeping water and 25% could be due the effect of ACP treatment in a direct treatment mode.

Another factor influencing the degradation of DON could be the pH of PAW. At acidic pH (especially at a pH range of 1-3) DON was reported to be unstable and form an unknown degraded product (Mishra et al., 2014). At pH 4, the degradation rate of DON was 11% (Mishra et al., 2014). The average pH of PAW in our study was 3.87, which probably played a role in DON degradation. The DON content was not completely reduced since it was likely residing in the inner layers of the grains, where the RONS could not diffuse to the inner layers. Previously, a 66% reduction in DON content was observed after a 15 s pearling process (gradual removal of grain layers by abrasive action starting from the outer layers of grain), irrespective of the initial level of contamination. This highlights that DON is mainly present in the outer layer of the grain. After 120 s pearling, which reduced the grain mass by 47.7%, there was 7.9% DON left in the grain indicating how deep the DON could reside in the grains (House et al., 2003). Overall, the malting industry may benefit from using treatment C, as it results in greater DON degradation rate. However, optimizing the PAW properties is needed to achieve greater reduction rates of DON.

6.3.3 Effect of PAW on water uptake, germination, enzymatic activity, and protein content of barley

○ Water uptake

The barley malting process includes three main steps: steeping, germination, and kilning. The water uptake and increase in water content initiates the germination of grains. In this study, there were no significant differences between the water uptake and moisture content values of barley

grains after the first day of steeping, when using PAW or DW for all the steeping times (Table 6.4). Published research focusing on water uptake of the barley grains treated by PAW is scarce. The majority of the previous literature used the direct exposure of the grain to the ACP discharge, followed by assessing the water uptake levels. In a study on the direct treatment of barley seeds by DBD-ACP, cracks in the outer layer of grains were observed, which was associated with greater water absorption (Mazandarani et al., 2020). Similarly, the water uptake capacity of the barley grains increased from 18.3 to 21.5% in the samples submerged in PAW (produced by glow plasma) for 5 h (Pater et al., 2020). However, determining the reasons for increased water uptake can be challenging because the grain size, variety, temperature of water, and the characteristics of PAW are different and all can influence the outcome. ACP affects the surface characteristics of the outer layers of grains (Waskow et al., 2021). The change in the surface of the seeds during plasma treatment of the dry grains could be due to the energy deposition of plasma, or to the chemical reaction of plasma reactive species with the grain surface. The water uptake values for treatment A and B with the lowest and highest germination rates, respectively were not significantly different. As the germination rate of treatment C was between treatment A and B, hence its water uptake values were not measured. The moisture content of the NIB increased after the 2nd day of steeping (Table 6.4). The moisture content of barley malt steeped in PAW (Treatment B) was significantly ($p < 0.05$) greater than that steeped in DW (Treatment A) after the second day of steeping. However, the moisture content of steeped barley grains treated by PAW (Treatment B) compared to direct ACP treatment (Treatment C) after the 1st and 2nd days of steeping was not significantly different ($p \geq 0.05$).

Table 6.4: Effect of plasma-activated-water on the selected malting qualities

Treatment A	Treatment B	Treatment C	Dry grain
-------------	-------------	-------------	-----------

Water uptake after 1 h (g water absorbed / 100g)	18.2±0.6 ^d	18.2±0.4 ^d	-	-
Water uptake after 5 h (g water absorbed / 100g)	36.1±1.9 ^c	36.9±2.2 ^c	-	-
Water uptake after 24 h (g water absorbed / 100g)	67.4±2.6 ^b	67.3±1.7 ^b	-	-
Water uptake after 48 h (g water absorbed / 100g)	86.4±2.8 ^a	89.8±2.9 ^a	-	-
MC 1 st day steeping (g water/100 g sample)	34.2±1.6 ^a	35±0.2 ^a	33.7±0.7 ^a	-
MC 2 nd day steeping (g water/100 g sample)	41±1.8 ^b	45.3±2.5 ^a	43.5±1.7 ^{ab}	-
Germinated acrospire (%)	13.5±4.8 ^b	44.1±1.7 ^a	11.7±1.9 ^b	-
Germinated rootlets (%)	81.2±9.6 ^a	91.2±5.6 ^a	87.3±4.1 ^a	-
α-amylase (units/g dry basis)	28.9±6.4 ^a	37.4±11.7 ^a	29.7±3.6 ^a	5.1±2.7 ^b
β-amylase (units/g dry basis)	23.9±3.7 ^b	27.6±1.2 ^a	28.4±1.6 ^a	22.6±4.1 ^b
β-glucanase (units/g dry basis)	198.2±35.2 ^a	216.7±67.2 ^a	207.3±34.5 ^a	109.1±29.2 ^b
Protein content (%)	14±0.7 ^a	13.6±0.2 ^a	14.2±0.5 ^a	13.5±0.2 ^a

Two days steeping using treatments A, B, C. Treatment A: Steeping NIB in DW for 5 h followed by 19 h air rest; Treatment B: Steeping NIB in PAW for 5 h followed by 19 h air rest; Treatment C: 30 min ACP treatment of NIB inside water followed by 4.5 h steeping, and 19 h air rest. For measuring the germination, treatments A, B, and C were followed by 3 day germination. Values are expressed as the mean ± standard deviation. Values with different letters in the same row are significantly different ($p < 0.05$, $n \geq 4$).

○ Germination

Germination is one of the important steps in malting, which is marked by embryo development, modification of endosperm, and the growth of rootlets and acrospires. The main visual change in the appearance of the grain during germination is the growth of rootlets and acrospire. At the end of the germination process, maltsters prefer to have a germinated grain in which the acrospire length is approximately 75% of the kernel length (Schwarz & Li, 2011). At the end of the germination period, the number of germinated seeds based on their acrospire using treatment B was greater compared with treatment C and the control sample. However, there was no significant difference in the germination of the seeds based on their rootlets among all the treatments. A greater germination rate and changes in the surface of the plasma-treated barley grain were reported by Park et al. (2018a). Also, for treating seeds with ACP, the working gas and the

exposure time to ACP are the two important factors. Petřková et al. (2021) reported a greater germination rate of barley seeds under short treatment times; however, the germination decreased during longer exposures to ACP. In a direct DBD-ACP treatment of barley seeds, crack formation on the grain surface was observed, resulting in more water uptake, water penetration, and a greater germination rate in the ACP treated seeds compared to the control samples (Mazandarani et al., 2020).

- Enzymatic activity

During germination, different enzymes are produced among which three of the important ones are α -amylase, β -amylase, and β -glucanase (Rani & Bhardwaj, 2021). Lower levels of β -glucanase and higher levels of β -glucan (major constituent of barley endosperm cell wall) negatively affect the wort viscosity and beer filtration rate in the breweries (Fox et al., 2003). The α -amylase and β -glucanase activity values of NIB grain after treatments A, B and C were not significantly different, while β -amylase activity increased after treatments B and C compared to treatment A. The α - and β -amylases are the principal enzymes for hydrolyzing starch into fermentable sugars during beer production. As expected, a higher enzymatic activity was observed in green malt compared with the non-malted grains in the previous studies (Mayolle et al., 2012; Toffoli et al., 2003). Enzymatic activity and the germination rate of the seeds treated by PAW can also be negatively affected due to oxidative stress if the characteristics of the PAW are not adjusted appropriately (Kostoláni et al., 2021).

ACP can alter the enzymatic activity as it can affect the primary and secondary metabolites of plants and enhance their content (Song et al., 2020). ROS and RNS were reported to promote seed dormancy release and subsequent germination in numerous plants (Arc et al., 2013). Also, nitric oxide, which is also generated in ACP, is an endogenous regulator of barley seed dormancy and

increases germination (Bethke et al., 2004). Abscisic acid and gibberellic acid are the most important hormones regulating seed dormancy and germination (Bahin et al., 2011). In barley, hydrogen peroxide, generated during ACP treatment, can activate gibberellic acid synthesis which results in the germination of the seed (Bahin et al., 2011). All the aforementioned reactive species are generated via ACP and are present in PAW. Hence, it is more likely that they contribute to a greater germination rate of barley steeped in PAW. Depending on plasma treatment time and the working gas, our results concur with other studies which have reported increases in germination rates in ACP treated grains. These increases are likely due to the synthesis of more lytic enzymes (Petřková et al., 2021; Švubová et al., 2020; Švubová et al., 2021).

- Protein content

The protein content of the NIB grains in our study was not significantly affected by PAW treatment. The protein content is important during the malting process, as strong protein-starch binding can limit the access of hydrolytic enzymes to starch and lead to a poor malt extract (Brennan et al., 1996). However, a too low protein content can impair the brewing performance through poor yeast amino acid nutrition. Also, protein negatively increases haze formation in beer, but it is important for enhancing foam stability (Fox et al., 2003).

6.3.4 Degradation products of ACP treated DON

To determine the possible degradation products of DON after ACP treatment, a relatively large concentration of DON in ACN/ water (20:80 v/v) solution was treated by ACP (Table 6.5). Based on the results of the HPLC-MS-MS chromatogram, 388 compounds were detected in the treated solution, which prevented us from determining the elemental composition of each one of these compounds. This large number and diversity of compounds could be due to the presence of a

several reactive species generated in ACP that reacted with DON and formed many different compounds. Due to the large number of these compounds, we only focused on the detection of the major degradation products. The total ion chromatogram of the major detected compounds is shown in Figure 6.2A. The retention time, possible molecular formula, calculated mass, observed mass, and double-bond equivalent (DBE) of the 13 major peaks were determined by Agilent Mass Hunter Qualitative Analysis software (ver. B.07.00) (Figure 6.2A and Table 6.5). The mass errors were all below 6.15 ppm, suggesting an accurate assessment of the proposed compounds.

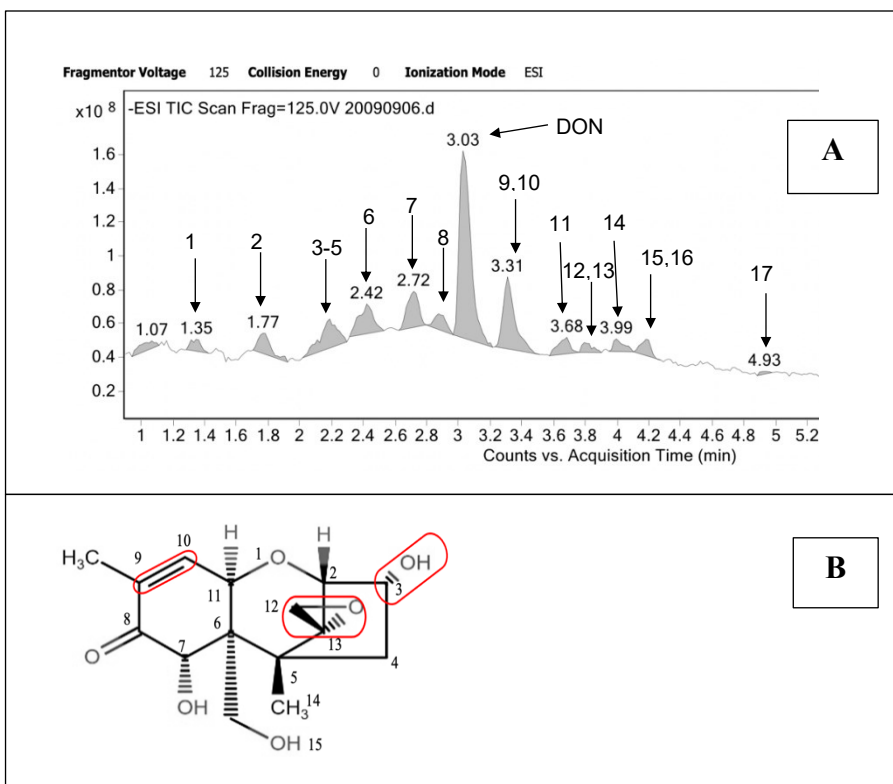


Figure 6.2: Total Ion Chromatogram (TIC) of DON degradation products via PAW in negative ESI mode and the associated DON degradation products from table 5; B: DON structure and the Key toxicity functional groups of DON. Red ellipses are the key toxic

The key toxicity related functional groups of DON are the unsaturated bond at C₉₋₁₀, the 12,13-epoxy ring, and hydroxyl group at C₃ (Figure 6.2B) (Feizollahi & Roopesh, 2021; He et al., 2010). Any change in these functional groups can significantly reduce the toxicity of DON. ACP consists of reactive species, UV light, and high energy electrons that can contribute to DON degradation. One of the major reactive species generated in ACP is ozone, which is a strong oxidant and can react with DON. Li et al. (2019) reported 6 key ozonation products of DON and C₁₅H₁₈O₇, C₁₅H₁₈O₈, C₁₅H₁₈O₉ (Figure 6.3C) were among the detected ozonation products of DON. These compounds were also detected in our study, indicating the possible contribution of ozone in the oxidation and degradation of DON. Sun et al. (2020) used aqueous ozone to degrade DON, and

$C_{15}H_{20}O_7$ (Figure 6.3C) and $C_{15}H_{16}O_8$ were determined as the two ozone degradation products, in which $C_{15}H_{20}O_7$ was the compound also detected in our study. The ozonolysis pathway of DON in acetonitrile solution was also explored and the $C_{15}H_{18}O_7$ detected in our study was the product of DON ozonolysis. It was proposed that $C_{15}H_{18}O_7$ was further ozonolyzed to $C_{13}H_{14}O_{10}$, $C_{13}H_{14}O_{11}$, and $C_{13}H_{14}O_{12}$ (Ren et al., 2020). The Criegee mechanism is believed as the main reaction that occurs between ozone and DON, which cleaves the double bond at C_{9-10} (Figure 6.3A) (Ren et al., 2020). For detoxification by biological treatment, DON can be metabolized via oxidative biotransformation to 3-keto-DON ($C_{15}H_{18}O_6$) (He et al., 2010). Also, it is possible that during ACP treatment, 3-OH groups could be oxidized in a same way as the ketone group, resulting in reduced toxicity of DON (Figure 6.3B). In another study, the effect of DBD-ACP treatment on DON degradation was assessed and $C_{15}H_{22}O_7$, $C_{15}H_{20}O_5$, $C_{14}H_{16}O_4$, $C_{15}H_{21}NO_9$ were detected as the degradation products of DON (Chen et al., 2022). In their study, the structure of key toxicity functional groups in the degraded products were affected by ACP and hence the toxicity was reported to be reduced. It is possible that ACP had the same effect on the toxicity of the degradation products in our study. However, due to differences in the treatment conditions of the studies (i.e., solid vs solution form of DON, concentration of DON, voltage, frequency, treatment time, gap between electrodes, type and concentration of generated plasma reactive species), an absolute comparison of the DON degradation products is not be possible. Overall, based on the chemical formula of the DON degradation products and their proposed structure from the literature, the 3 toxicity functional groups of DON including C_{9-10} double bond, the 12,13-epoxy ring, and hydroxyl group at C_3 could be changed during ACP treatment and resulted in reduced toxicity of DON.

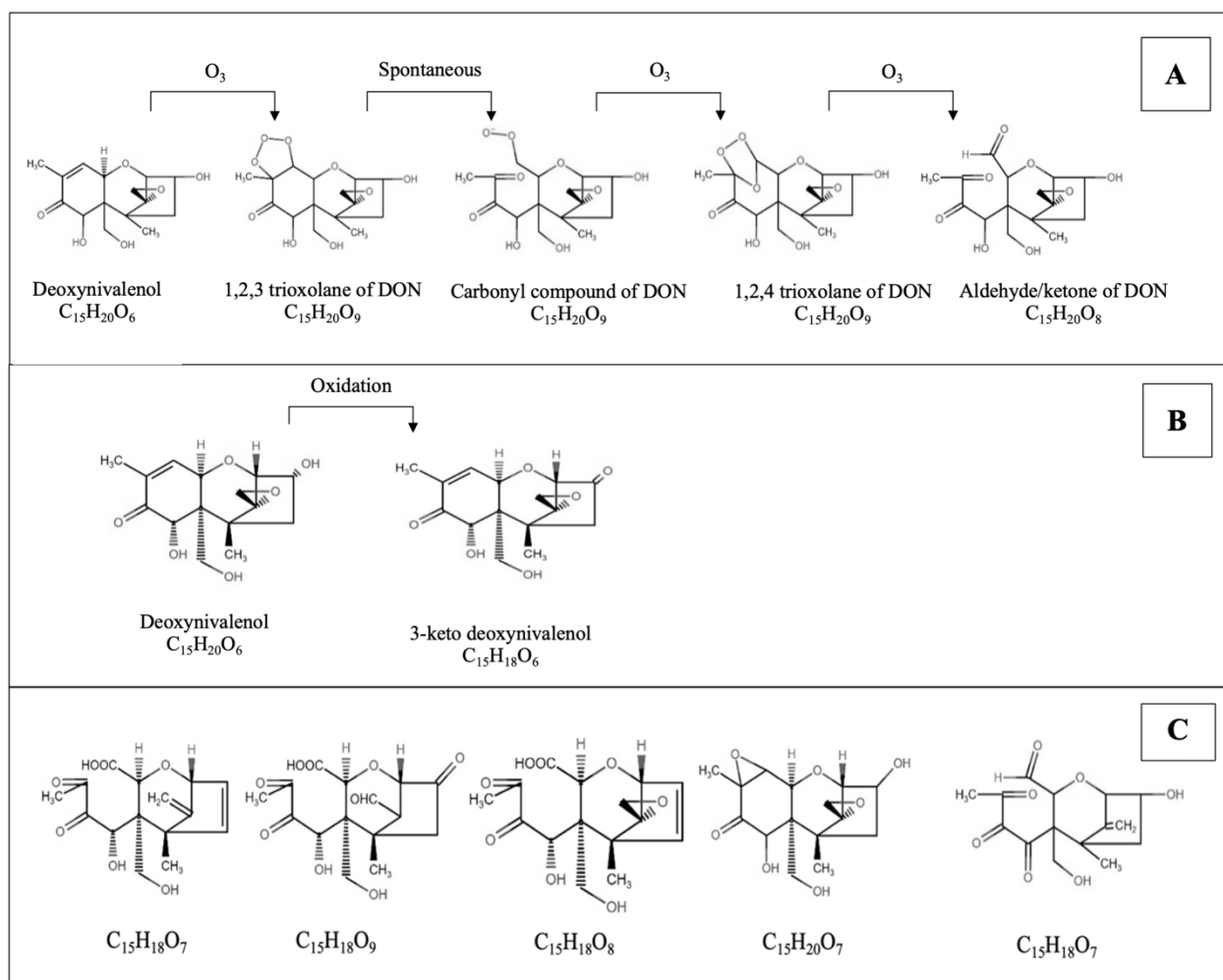


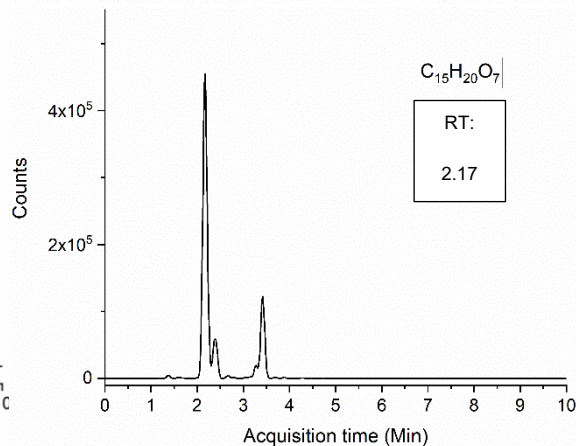
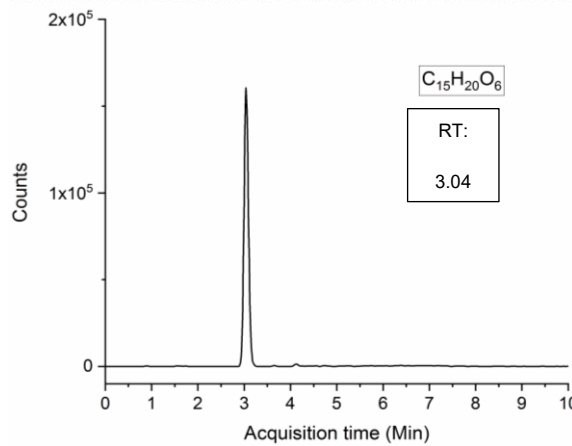
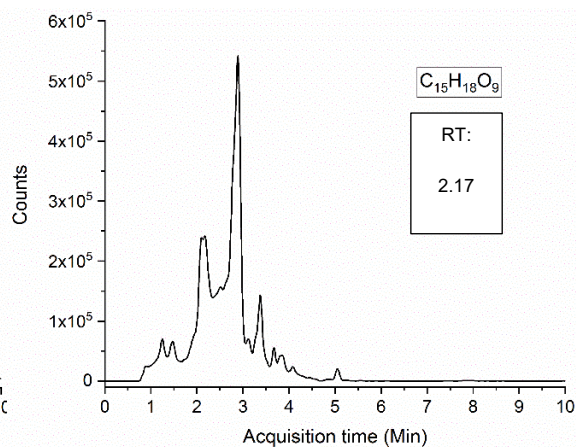
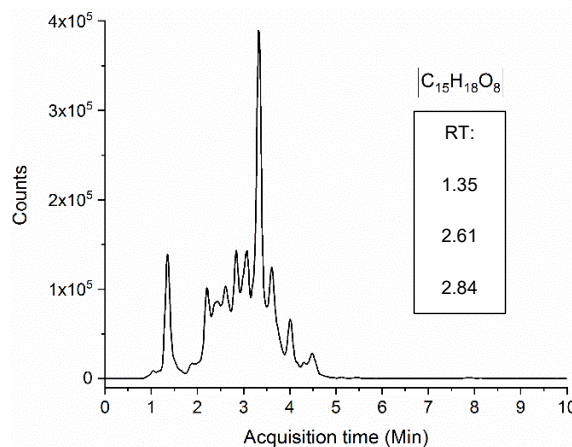
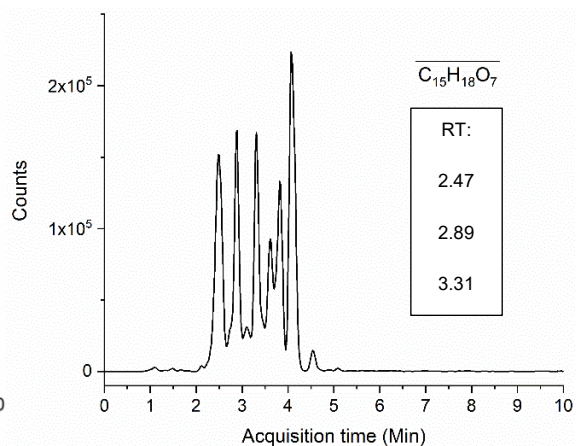
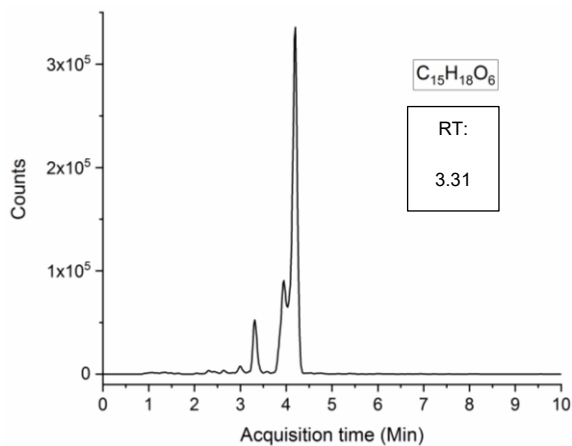
Figure 6.3: Proposed Criegee mechanism for degradation of DON. Adapted from (Ren et al., 2020). **B**: Proposed oxidation of DON to 3-keto-DON (Wang et al., 2019); **C**: Proposed structure of the DON ozonolysis products from the literature. Adapted from (Li et al., 2019; Ren et al., 2020; Sun et al., 2020).

Table 6.5: Major degradation compounds of deoxynivalenol after ACP treatment

Compound	Retention time (min)	Formula	Mass	Calculated mass	Error (ppm)	DBE	Score
A	1.35	$C_{15}H_{22}O_8$	330.13	330.1315	2.12	5	96.12
B	1.77	$C_{15}H_{20}O_8$	328.11	328.1158	3.63	6	93.06
C	2.03-2.28	$C_{15}H_{20}O_8$	328.11	328.1158	6.15	6	68.87
D	2.03-2.28	$C_{15}H_{20}O_7$	312.11	312.1209	3.28	6	89.08
E	2.03-2.28	$C_{15}H_{18}O_9$	342.09	342.0951	4.27	7	75.85
F	2.33-2.51	$C_{15}H_{20}O_8$	328.11	328.1158	3.69	6	81.72

G	2.72	C ₁₅ H ₂₀ O ₈	328.11	328.1158	2.05	6	97.56
H	2.84-2.94	C ₁₅ H ₁₈ O ₉	342.09	342.0951	2.71	7	75.86
DON	3.03	C ₁₅ H ₂₀ O ₆	296.12	296.126	2.9	6	95.51
I	3.26-3.45	C ₁₅ H ₂₁ NO ₁₀	375.11	375.1165	2.79	6	96.22
G	3.26-3.45	C ₁₅ H ₁₈ O ₈	326.09	326.1002	3.19	7	94.80
K	3.68	C ₁₅ H ₁₉ NO ₁₁	389.09	389.0958	1.9	7	98.16
L	3.78-3.89	C ₁₅ H ₁₉ NO ₉	357.10	357.106	3.29	7	94.80
M	3.78-3.89	C ₁₅ H ₁₈ O ₇	310.10	310.1053	2.77	7	76.36
N	3.99	C ₁₅ H ₁₉ NO ₁₁	389.09	389.0958	2.43	7	97.17
O	4.13-4.23	C ₁₅ H ₁₈ O ₆	294.10	294.1103	3.45	7	93.41
P	4.13-4.23	C ₁₅ H ₁₉ NO ₉	357.10	357.106	3.05	7	92.95
Q	4.93	C ₁₅ H ₁₇ NO ₁₀	371.08	371.0852	1.94	8	80.52

Based on the chemical formula of the DON degradation products (Table 6.5), the main degradation mechanism of DON by ACP could be via oxidation of the mycotoxin compound. Some of the detected compounds in the chromatogram have nitrogen in their chemical structure, indicating the importance of the presence of RNS produced in ACP. The extracted ion chromatograms were generated for the 13 peaks that were detected by LC-MS (Figure 6.4). The results show that the DON degradation products are eluting at different retention times, most likely due to the same elemental composition but different structure, i.e., isomers (Figure 6.4). More studies are required using analytical techniques such as preparative HPLC followed by nuclear magnetic resonance (NMR) to confirm the results of this study and determine the exact structure of the DON degradation products. Also, it should be noted that the degradation behavior and degradation products could be different on barley and other real matrices compared with the model condition used in this study.



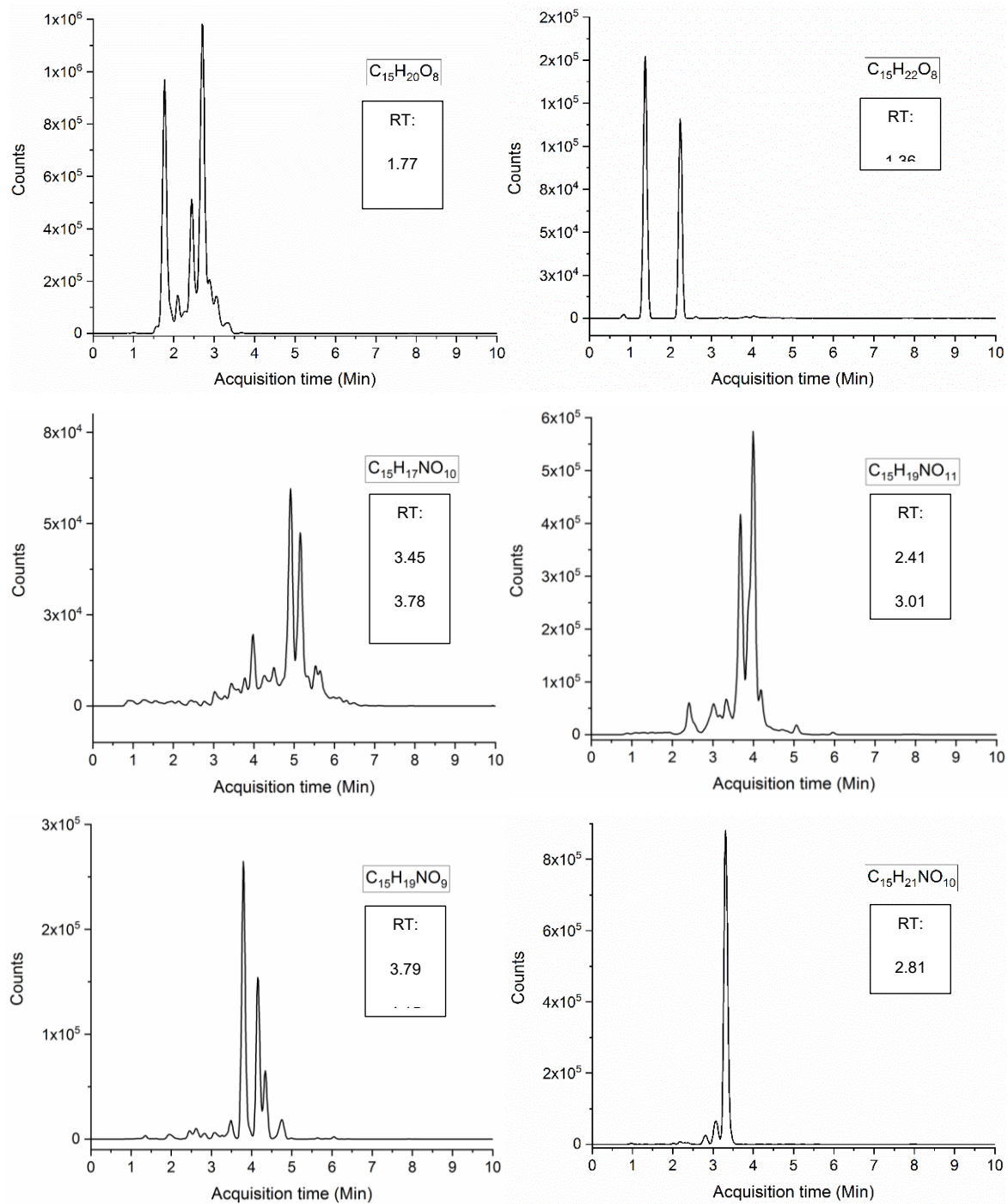


Figure 6.4: Extracted ion chromatograms of the possible DON degradation products. Retention times (RTs) of the compounds are presented in the figure

6.4 Conclusions

This study aimed to assess the potential of using PAW as a substitute for water during barley steeping in the malting process and to determine the major degradation products of DON. Use of PAW for steeping in treatment C resulted in the highest DON reduction with 58.4%, which suggested the significant role of short-lived reactive species in DON reduction. The increase in enzymatic activity, germination improvement, and DON reduction in PAW treated grains suggested that the malting industry may benefit using PAW for steeping in order to improve grain germination and degradation of DON. Results of the DON degradation products after plasma treatment indicated the formation of several DON degradation products, in which methods such as NMR should be applied for confirming the structure of the DON degradation products. Based on the structure of the similar degradation compounds in other studies, ACP may have substantially reduced the toxicity of DON. The structure of the major degradation products of DON suggested that oxidation could be the main degradation mechanism of DON by plasma treatment however, further research is required to confirm the underlying DON degradation mechanisms. More understanding on the role of different plasma reactive species associated with DON degradation will allow the optimization of the PAW parameters for steeping to obtain maximum DON reduction with probable improvement in barley malt germination. It is possible to implement an ACP or PAW process for barley malting by using PAW, which is already generated outside the steeping tank for barley steeping. Also, it may be feasible to treat the grains during steeping by producing plasma bubbles in steeping water. More research is required to optimize such processes to achieve maximum DON reduction with possible improvement in germination of barley grains during steeping.

Chapter 7: Effect of plasma activated water bubbles on *Fusarium graminearum*, deoxynivalenol, and germination of naturally infected barley during steeping

7.1 Introduction

The contamination of agricultural products with fungi and their secondary metabolites (mycotoxins) creates major challenges to the food industry. *Fusarium graminearum* is an ascomycete fungus that causes fusarium head blight in wheat and barley (Guo, Wang, et al., 2021). *F. graminearum* produces deoxynivalenol (DON), a type B trichothecene mycotoxin (Feizollahi & Roopesh, 2021), and the consumption of foods contaminated with DON can affect animal and human health, causing nausea, vomiting, headaches, diarrhea, dizziness, fever and other acute or chronic toxicities (Sobrova et al., 2010). Atmospheric cold plasma (ACP) is one of the most explored novel antimicrobial interventions with mycotoxin degradation potential (N. Misra et al., 2019). Plasma is the fourth state of matter and is comprised of UV light and reactive species including positive and negative ions, free radicals, atoms and molecules in the ground or excited states. In cold plasma, the temperature of ions and uncharged molecules is close to room temperature, while electrons have much higher temperatures (N. Misra, O. Schlüter, & P. Cullen, 2016). Cold plasma can be used to treat water to generate plasma activated water (PAW), which alters the physicochemical properties of water such as the oxidation reduction potential (ORP), pH, reactive species type, and concentration (Rathore et al., 2021). The physicochemical properties of PAW are largely affected by the plasma power supply and production system, configuration of electrodes, treatment time, type of working gas, process parameters such as voltage and frequency, gas flow rate, etc. (Rathore & Nema, 2021).

Barley (*Hordeum vulgare*) is extensively used in the malting and brewing industries. Steeping of the barley grains in water is one of the crucial steps for making a barley malt. If *F. graminearum* is present in the grain, it can potentially grow during the steeping process and cause quality issues in barley malt. Furthermore, if DON is present in the barley grains, it may end up in the final products, if the barley malting unit operations cannot degrade this mycotoxin. The antifungal properties of PAW have been previously reported (Guo, Wang, et al., 2021; Wu et al., 2019). In a recent study by Guo, Wang, et al. (2021), microbial activity of *F. graminearum* spores, including mycelial growth, conidial germination, and disease development, were significantly inhibited by PAW treatment of spiked wheat samples. In addition, PAW improved the germination of the seeds (Grainge et al., 2022; Jirešová et al., 2022), which was attributed to its physicochemical properties. There are no reports, however, regarding the effect of PAW treatment on *F. graminearum* in naturally infected barley (NIB) and DON. Previous studies have focused on pure culture or artificially spiked grains, but no study has yet used naturally infected grain, which represents the samples treated at an industrial scale. Trichothecenes are produced by different genera including *Fusarium*, *Myrothecium*, *Spicellum*, *Stachybotrys*, *Cephalosporium*, *Trichoderma*, and *Trichothecium* (McCormick et al., 2011). DON as a type B trichothecene is produced by *Fusarium* spp., (Feizollahi & Roopesh, 2021). Biosynthesis of trichothecenes in *Fusarium* spp. begins with the cyclization of farnesyl pyrophosphate, and is catalyzed by terpene cyclase trichodiene synthase (*Tri5*) that is encoded by the (*Tri5*) gene (McCormick et al., 2011). The *Tri6* gene is one of the genes regulating the expression of other *Tri* genes for the biosynthesis of trichothecenes (Faltusová et al., 2019). *EFIA* is involved in the protein translation machinery of eukaryotic cells and has been shown to be a powerful tool for distinguishing related *Fusarium* species (Boutigny et al., 2019). Actin is the most abundant protein in most of eukaryotic cells (Dominguez & Holmes,

2011) and is encoded by the housekeeping actin gene that can be used for *F. graminearum* identification. The aforementioned genes can be used for *F. graminearum* detection and relative quantification based on Quantitative PCR (qPCR).

In this study, we assessed the potential for the use of PAW in steeping of barley for DON degradation, *F. graminearum* inactivation, and improving germination of NIB grain. We investigated the characteristics of PAW bubbles produced using a bubble spark discharge (BSD) reactor and a continuous jet (CJ) ACP. We also fabricated a process unit with a Venturi tube and plasma jet for continuously producing PAW bubbles for improving the diffusion of plasma reactive species into water. The PAW bubbles produced by these units were characterized by measuring the pH, ORP, and reactive species concentration. Then, the effects of PAW bubbles on DON degradation and germination improvement of NIB were measured. Finally, the antifungal effect of PAW bubbles on NIB was assessed by use of fungal culture and qPCR techniques.

7.2 Material and methods

7.2.1 Barley grains

Naturally infected barley grains (2-row malting variety, ‘CDC Copeland’) with high concentrations of DON (4.6-5.8 ppm) were procured from Agriculture and Agri-Food Canada, Brandon Research and Development Centre, Brandon, Manitoba. The grains were kept in Ziploc bags and stored at 4°C until used. The initial moisture content of the grains before use was $8.6 \pm 0.2\%$ (wet basis).

7.2.2 PAW bubble production

Plasma activated water (PAW) bubbles were produced by three methods. First, a bubble spark discharge (BSD) reactor (Figure 7.1A) was connected to a high voltage micropulse generator

Leap100 (PlasmaLeap Technologies), with a voltage pulse of 150 V, a repetitive pulse frequency of 1000 Hz, and a duty cycle of 66 μ s. The BSD reactor consisted of a stainless-steel high voltage electrode rod (4 mm outside diameter (OD)) inserted coaxially along the length of a 175-mm-length quartz tube (10 mm OD, and 1.5 mm wall thickness) with one end sealed. At 5 mm above the sealed end, eight holes were positioned radially to allow the formation of bubbles in the water. The generated bubbles with certain flow rate created agitation and distribution of plasma species in to the water. A PTFE tee fitting was connected to the open end of the quartz tube to supply the airflow into the tubes and to support the electrode in its place. Another stainless-steel electrode rod was used as the ground electrode during the treatments. Air was pumped at a flow rate of 1 standard liter per minute (SLPM) via mass flow controller (MC-Series, Alicat scientific, Tucson, USA) to the reactor and 80 ml water was used, producing PAW bubbles for all the experiments using the BSD reactor. Here plasma was generated continuously for selected times and carried by the underwater bubbles. The agitation and movement of bubbles containing plasma species allowed further interaction of these species with water due to large water surface areas. In the 20 (Treatment A) and 30 min (Treatment B) direct BSD treatments, ice cubes were placed around the treatment beaker to prevent a temperature increase during PAW bubble generation.

In another set of experiments, a continuous jet (CJ) ACP unit (Figure 7.1B) consisting of a Venturi tube mounted on the tip of the jet system's nozzle, a water pump (Micro Diaphragm Pump, Riuty) and a quartz chamber (9 \times 9 \times 9 cm) was used for PAW bubbles production. The pump was connected to a digital control DC power supply (kd3005d, Korad technology, Dongguan, China), providing 1.8 V with 0.55- 0.66 Hz frequency to the pump. The jet system was connected to a power supply (PG 100-D, Advanced Plasma Solutions, Malvern, PA, USA), providing a frequency of 3500 Hz, 70% duty cycle, output voltage of 0-34 kV, power of 300 W, and a 10 μ s pulse width.

Air was pumped at a flow rate of 0.5 SLPM and 180 ml water was used for all the experiments using CJ ACP. Plasma was injected into the Venturi tube using the plasma jet, with water passing through the Venturi, producing plasma activated water bubbles. The interaction of plasma reactive species from plasma jet with water at the Venturi created bubbles with plasma reactive species and they were carried to the treatment chamber. Also, pumping of water through the Venturi resulted in hydrodynamic cavitation and bubble formation, leading to better interaction of plasma reactive species with water. Both the BSD and CJ ACP designs support continuous treatment of grains with plasma activated water bubbles and the scaling of the plasma reactor for industrial applications.

For the next set of experiments, the above jet unit was used for batch treatments. The batch jet (BJ) ACP was used to produce PAW bubbles and assess its effect on the pathogens and *F. graminearum* inactivation. The PAW bubbles from the BJ ACP unit could be more effective than CJ ACP due to a greater concentration of RONS in a smaller amount of PAW. Water (30 ml) was treated using the BJ ACP unit inside a beaker and the treatment parameters were similar to the CJ ACP treatment. The characteristics of the PAW bubbles produced using the BJ ACP unit is presented in Chapter 6.

In treatment C (indirect 30 min BSD), PAW bubbles were generated by ACP and then added to the NIB grains for steeping. However, in the direct treatments, i.e., treatment A (direct 20 min BSD (surrounded by ice), treatment B (direct 30 min BSD (surrounded by ice), treatment D (30 min direct CJ), and treatment E (1 h direct CJ), NIB grains were in contact with PAW inside the container during PAW generation. The various treatments are summarized Table 7.1.

Table 7.1: Nomenclature of different treatments included in this study

Name	Treatment name
------	----------------

Treatment A	Direct 20 min BSD (surrounded by ice)
Treatment B	Direct 30 min BSD (surrounded by ice)
Treatment C	Indirect 30 min BSD
Control D	Control 30 min CJ
Treatment D	Direct 30 min CJ
Control E	Control 1h CJ
Treatment E	Direct 1 h CJ
Treatment F	Direct 30 min BJ

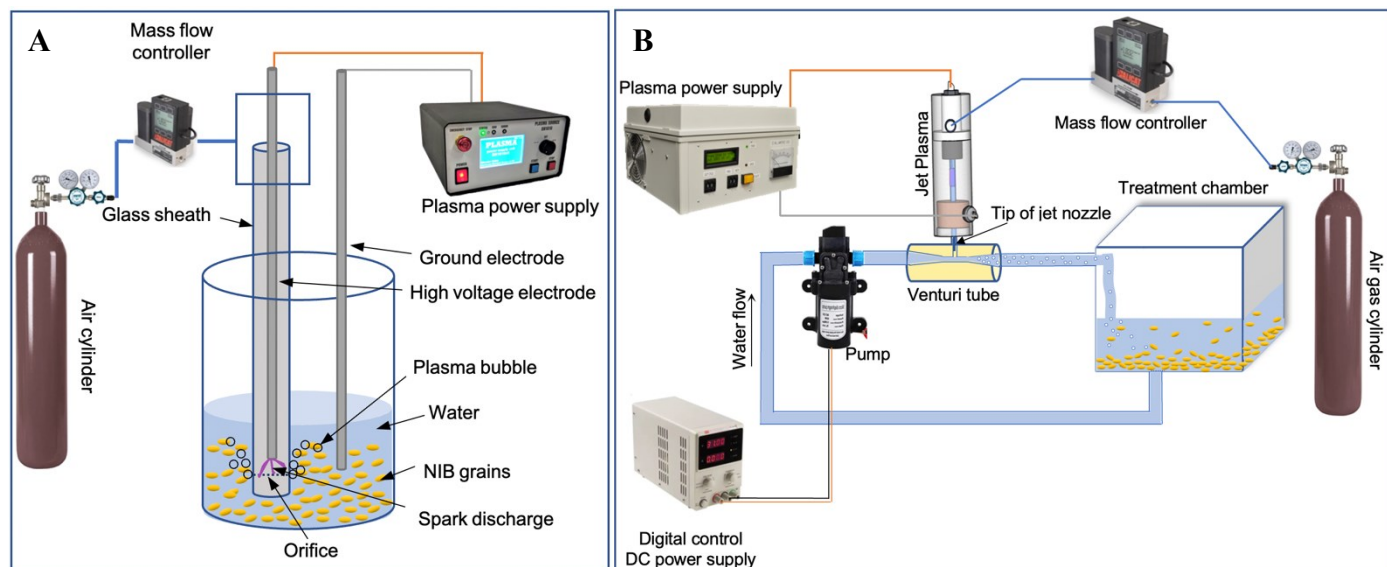


Figure 7.1: Schematic diagram of plasma activated water (PAW) bubble treatment of naturally infected barley (NIB) grains using: A, bubble spark discharge atmospheric cold plasma (ACP); and B, continuous jet ACP

7.2.3 PAW bubble characterization

PAW bubbles were produced by treating 80 ml water using the BSD ACP, 80 ml water using the CJ ACP and 30 ml water using the BJ ACP units for different treatment times. The characteristics of PAW were measured indirectly after ACP treatments, where the PAW was generated first and then used for measuring its physicochemical properties of PAW. The pH and ORP values were determined using a pH meter (Fisher Scientific, Accumet AE150, Singapore) and an ORP meter (Ohaus, ST20R, Parsippany, NJ, USA), respectively. CHEMetrics kits (Midland, VA, USA) were

used to determine hydrogen peroxide (K-5543) based on the ferric thiocyanate method; nitrate (K-6933) based on cadmium reduction method; nitrite (K-7003) based on azo dye formation method; and ozone (K-7423) based on DPD (N,N-diethyl-p-phenylenediamine) oxidation method in PAW bubbles. The color change in the kits was measured with a V-2000 photometer (CHEMetrics, Midland, VA, USA). Deionized water at room temperature was used for all the treatments. The temperatures of PAW bubbles generated by treatment A and B using ice cubes surrounding the treatment chamber were 9.8 ± 0.7 °C, and 12.3 ± 0.6 °C, respectively. The temperature of the PAW bubbles generated after treatment B without any ice surrounding the treatment chamber was 51.9 ± 1.2 °C.

7.2.4 EPR spectroscopy

Electron spin resonance or Electron paramagnetic resonance (ESR/EPR) spectroscopy is a measurement technique that can detect unpaired electrons. In this study, the commonly used spin trap DMPO (5,5-dimethyl-1-pyrroline-N-oxide) (Dojindo Molecular Technologies, Inc., Rockville, MD, USA) was used to trap hydroxyl and superoxide radicals to be identified by EPR spectroscopy. Five milliliters of deionized water was mixed with 28 μ l DMPO (8.97 M, undiluted and used without further purification) to make a 50 mM final concentration of DMPO. The solution was then treated with BSD ACP at different treatment times, using ice surrounding the treatment chamber. For free radical measurement, 50 μ l of the sample was drawn into a 50 μ l capillary tube (BRAND® disposable BLAUBRAND® micropipettes, Sigma Aldrich Canada Co., Item code: BR708733) and sealed at the end with Hemato-Seal™ Tube Sealing Compound (Item: 02-678, Fisherbrand®, Fisher Scientific Co., Ottawa, ON). The microcapillary tube was then placed in a 5 mm thin wall quartz EPR tube (Wilmad Labglass, USA) in an EPR resonator (Elexsys E-500

Spectrometer, Bruker, Billerica, MA) for analysis. The EPR spectroscopy settings: center field = 3504 G, sweep width = 80 G, modulation amplitude = 1 G, scans = 5, microwave frequency = 9.8 GHz, microwave power = 20 mW, receiver gain of 60 dB. The acquired EPR spectra were plotted with OriginLab 2022 (OriginLab Corporation, Northampton, USA).

7.2.5 DON quantification after PAW bubble treatments

First, 80 ml deionized water was added to 10 g of NIB grains in a beaker and treated directly by BSD ACP for 20 or 30 min to generate PAW bubbles. Ice cubes were placed around the treatment beaker to avoid temperature increase during the direct BSD ACP treatment (treatments A, B). In the indirect treatment (treatment C), 80 ml deionized water was treated with BSD ACP for 30 min and the generated PAW bubbles were used for steeping the NIB grains. To evaluate DON degradation during the malting process, the grains were steeped in PAW bubbles for 5 h, drained for 5 min, and air rested (19 h) at $15 \pm 0.3^\circ\text{C}$, $78 \pm 3\%$ RH after the treatments. The grains were dried at room temperature for 2 days and DON content was determined using Reveal® Q+ test kits (Neogen, Lansing, MI, USA) based on the single-step lateral flow immunochromatographic assay. The limit of detection and the specificity of the kits for DON were 0.3 ppm, and 100 %, respectively. The kits were validated previously by HPLC, and their accuracy confirmed to be >90 %. For measuring DON content after direct CJ ACP treatment, 180 ml water was added to 10 g NIB grains inside the treatment chamber (Figure 7.1B), and the grains were treated for 30 min and 1 h to produce PAW bubbles followed by steeping (5 h overall), draining (5 min), and air rest (19 h) at $15 \pm 0.3^\circ\text{C}$, $77 \pm 4\%$ RH. The grains then were dried, and DON content was determined using Reveal® Q+ test kits as above.

7.2.6 Grain germination and enzymatic activity after PAW bubble treatments

Following a 2-day steeping in PAW bubbles and air-rest, the NIB grains were allowed to germinate over a 3-day period inside a glass beaker. After/during BSD ACP, or CJ ACP treatments, the grains were steeped for 5 h in PAW bubbles followed by 5 min draining and 19 h air rest. The following day, the grains were treated using BSD ACP and CJ treatments again to produce PAW bubbles and steeped for 5 h, then 5 min draining, and 19 h air rest at $15 \pm 0.3^\circ\text{C}$ and $77 \pm 4\%$ RH. Finally, the grains were washed with DW and drained, followed by the addition of 3 ml DW to 10 g NIB each day for 3 days during the germination period. The moisture content of the grains after the 1st and 2nd day of steeping was determined as per the American Association for Clinical Chemistry (AACC) method by drying in an air oven for 2 h at 135°C (44-19.01-AACC International). The α -amylase, β -amylase, and β -glucanase activities were determined in the green malt before germination using K-MALTA 07/20 malt amylase assay kit and S-ABG100 03/11 malt and bacterial β -glucanase assay kit (Megazyme, Bray, Wicklow, Ireland). Moreover, 5 g of germinated seeds (containing 110-130 seeds) were used to determine the percentage of germinated acrospires and rootlets separately. Grains with visible acrospires and rootlets with a length >3 mm were considered to be germinated.

7.3 Analysis of microbial contamination and in vitro germination

Treated and untreated NIB grains were placed in Petri dishes (100×15 mm for PDA, 100×25 mm for WA) filled with potato dextrose agar (PDA) or water agar (WA) (Fisher Scientific, Canada) for mycological and germination analyses, respectively. Ten seeds were spread evenly in each Petri dish and three dishes were used for each replicate of the treatment. The seeds were not surface-sterilized in order to evaluate the effect of ACP treatment on the naturally occurring microflora on the seeds. Fungal colony diameter and the proportion of seeds from which *F.*

graminearum could be recovered was evaluated by incubating the seeds on PDA medium for 3 days at room temperature. Isolates of *F. graminearum* were identified based on their cultural and morphological characteristics (Leslie & Summerell, 2008). Percentage germinated grains, shoot height, and number of *F. graminearum* colonies were recorded on the WA plates after 5 days incubation at room temperature.

7.3.1 DNA extraction

For DNA extraction, 1-2 g of the treated and untreated NIB grains were ground to a powder in liquid nitrogen in a mortar with a pestle. Approximately 100 mg of the ground sample was used to extract total DNA using a DNeasy Plant Pro Kit (QIAGEN, Maryland, USA). The quality of the extracted DNA was assessed with a NanoDrop1000 spectrophotometer (ThermoFisher Scientific) and diluted to a final concentration of 25 µg/ml.

7.3.2 Quantitative PCR

The fungal biomass of *F. graminearum* was estimated by quantitative PCR analysis. Four *F. graminearum*-specific genes were targeted. The full sequence of the genes, including Trichothecene biosynthesis transcription regulator (*Tri6*, GenBank: AB017495.1), Terpene cyclase trichodiene synthase (*Tri5*; GenBank: KJ677974.1) (Kimura et al., 2007), Elongation factor 1-alpha (*EF1 A*; GenBank: KX084040.1) (Hafez et al., 2020), and Actin (NCBI Reference Sequence: XM_011328784.1) (Tang et al., 2020) were retrieved from the NCBI sequence database. Gene-specific primers (Table 7.2) were designed using Primer Express 3.0.1 (Applied Biosystems, Canada). The primers were diluted to 20 µM in nuclease free water.

Table 7.2: The primers for *F. graminearum* genes

	Forward Primer (5'-3')	T _m (°C)	Reverse Primer	Product size (bp)	T _m (°C)
Tri6	GCGGCATTACCGACAACACT	60	CGCACTGTTGGTTTGTGCTT	1247	58
EF1A	AAATTTGCGGCTTTGTCGTA	58	GGCTTCCTATTGACAGGTGGTT	629	58

Actin	CGTCGCCCTTGA	59	CCAAGGACAGAAGGCTGGAA	1544	59
Tri5	AGGAGCGCATCGAGAATTTG	59	TTGCCAGCTGTATACAACCAT	1062	58

Quantitative PCR was performed on a QuantStudio 6 Flex system (Applied Biosystems, Canada). Each amplification reaction (10 µl volume) contained diluted DNA (2 µl), Fast SYBR Green Master Mix (5 µl; ThermoFisher Scientific) and 1 µl each of the forward and reverse primers in a Micro Amp Fast Optical well plate. Each reaction was performed in triplicate. A no template control, containing only nuclease-free water with master mix, was also included in the analysis. The qPCR was carried out using the following program: 95 °C for 20 s, followed by 40 cycles of 95°C for 1 s and 60°C 20 s. A melting curve (95°C for 1 s, 60°C for 20 s and 95°C for 1 s) was generated to ensure the specificity of the amplification for each product. Relative quantification of *F. graminearum* genes was carried out using the $2^{(-\Delta\Delta Ct)}$ method (Livak & Schmittgen, 2001) with β -Actin as internal reference gene and dry grain sample as a calibrator.

7.3.3 Statistical analysis

SPSS (IBM SPSS v.27, Armonk, NY) was used to determine significant differences ($p < 0.05$) by analysis of variance (ANOVA), followed by Duncan's multiple range test. At least triplicate experiments were performed for all of the experiments, and the data are expressed as the mean \pm standard deviation.

7.4 Results and Discussion

7.4.1 Characteristics of PAW bubbles

The physicochemical properties of PAW bubbles were affected by the formation of RONS (Table 7.3). The reactions for the formation of hydrogen peroxide (H₂O₂), nitrate (NO₃⁻), nitrite (NO₂⁻), and ozone (O₃) are reported in Chapter 5. As the ACP treatment time increased, we observed a significant ($p < 0.05$) increase in the ORP and a significant ($p < 0.05$) decrease in the pH (increase

in H^+ ion concentration) of the treated water (Table 7.3). The greatest ORP was obtained in PAW bubbles produced using 30 min BSD treatment (treatment B), which had a positive correlation with the concentration of other reactive species, i.e., H_2O_2 , NO_3^- , NO_2^- , and O_3 . In addition, DW had the least ORP and the highest pH. Also, treatment D had higher pH and lower ORP compared to other treatments which was due to weaker plasma in treatment D, and also higher amount of water used in this treatment. The increase in ORP was likely due to an increase in the concentration of active ions and oxidizing species such as H_2O_2 , HNO_3 , HNO_2^- , and O_3 in PAW bubbles (Rathore & Nema, 2021). It should be noted that pH affects the ORP; in acidic pH, hydrogen ions (H^+) increase the ORP, while in alkaline pH, hydroxide ions (OH^-) decrease the ORP value (Wu et al., 2019).

Since PAW was used to steep the grains for 5 h, we also measured the RONS concentration after 5 h storage of PAW to determine its physicochemical properties. For the PAW bubbles produced by 20 min BSD treatment (treatment A), the concentrations of all the RONS decreased significantly ($p < 0.05$) after 5 h storage, except for NO_3^- . After 5 h, the concentrations of all the RONS in the PAW bubbles produced by treatment B decreased significantly ($p < 0.05$) (Table 7.3). In the case of treatment D (PAW bubbles produced by 30 min CJ ACP), the % reduction in the concentrations of H_2O_2 (6.67%) were smaller after 5 h storage compared to those for treatments A (37.3%) and B (55.8%) after storage. However, higher % reduction in the concentration of O_3 (62.5%) was observed in PAW bubbles produced by treatment D after 5 h storage compared to treatments A (60.6%) and B (58.8%) after 5 h storage. The treatment D (CJ ACP) produced a considerably lower concentrations of RONS in the PAW bubbles compared to BSD ACP treatment. It is possible to have low reaction rates of RONS with each other, as their concentration was too low in the PAW bubbles produced by CJ ACP. However, this assumption may not be

accurate as highest ozone reduction during storage happened for PAW bubbles produced by CJ ACP. During treatment D, bubble formation happens in the Venturi, and hence RONS could be captured inside the bubbles. The reduction in O_3 concentration during storage in the PAW bubbles could be due to the reaction of O_3 with H_2O_2 , and NO_2^- (equation 1-2). H_2O_2 was formed mainly from water decomposition and subsequent recombination of $\cdot OH$ radicals (reaction 7) (Julák et al., 2018). Due to reactions 1 and 3, the concentration of H_2O_2 was also reduced during storage (Rathore & Nema, 2021). Reactions 2 and 3 could also be the reason for the reduction in NO_2^- during storage. Moreover, NO_3^- had the greatest concentration in PAW compared with other RONS due to its formation via reactions 2 and 3 in addition to formation via ACP. It is also possible that NO_2 and NO , which are formed via ACP, react with water and form stable RONS (NO_3^- , NO_2^-) via reactions 4-5. The ozone concentration was very high in the PAW bubbles treated with BSD (treatments A, B). The stability of ozone was the greatest at pH 2-6 (Egorova et al., 2015), and this could be the reason for having a large concentration of ozone even after 5 h of storage.

The ORP and pH of the water remained stable after 5 h of storage (treatments A, B, D), suggesting the presence of oxidizing and acidic agents in the solution. Nitrous and nitric acid, as well as H_2O_2 , cause the PAW acidification, in which nitrous and nitric acid are formed from nitrate and nitrite ions in the solution following reactions 4-5 (Park & Lee, 1988; Rathore et al., 2021). Julák et al. (2018) reported that HNO_2 had a negligible effect on the acidity of the PAW and the overall acidity is assigned to HNO_3 . This is because HNO_2 could be decomposed following reaction 6 within a few minutes (Julák et al., 2018). With the reaction of H_2O_2 with water, acidic H_3O^+ ions will be formed and this can also decrease the pH (Chen et al., 2008). Wu et al. (2019) used oxygen as the carrier gas for jet plasma to produce PAW and the pH of the PAW was not significantly different from the untreated water. This suggests the importance of the presence of nitrogen atoms in the

carrier gas for acidifying the PAW via HNO₃ generation. Similar to our study, the pH of PAW did not change in the previous studies, even after 1 year of storage at 4°C (Julák et al., 2018).

The PAW bubbles produced by treatment B were formed at room temperature (~23 °C) and by surrounding the treatment container with ice cubes. During treatment, the temperature of PAW bubbles increased from room temperature to 51.9±1.2 °C after treatment B. However, the final temperature was 12.3±0.6 °C when the ice cubes were placed around the treatment container. The results show that at high water temperature, the concentrations of reactive species were considerably lower. This could be due to the higher reaction rates at higher temperatures, which resulted in faster decomposition of the major reactive species (H₂O₂, NO₃⁻, NO₂⁻, and O₃) in PAW bubbles.

The characteristics of PAW bubbles depends upon several factors, including the ACP generation method, quantity of water, working gas, operating parameters of the ACP, and treatment time. As the plasma generated by CJ was significantly (p < 0.05) weaker than BSD, and due to the larger quantity of water used, lower concentrations of RONS in PAW bubbles prepared by CJ ACP were observed.

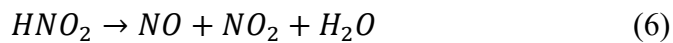
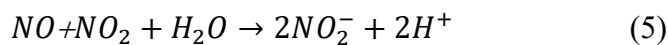
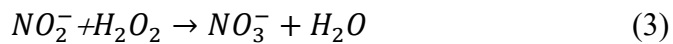
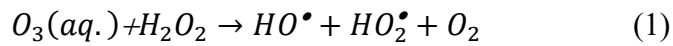


Table 7.3: Characteristics of PAW bubbles produced by different treatments used in this study. The characteristics of PAW were measured indirectly after ACP treatments, i.e., the generated PAW after plasma treatments was used for measuring the physicochemical properties of PAW

	pH	ORP (mV)	H ₂ O ₂ (ppm)	NO ₃ ⁻ (ppm)	NO ₂ ⁻ (ppm)	O ₃ (ppm)
DW	8.1±0.2 ^a	208±33.2 ^c	-	-	-	-
Treatment A	2.7±0.06 ^d	599±1 ^a	87.3±11.9 ^b	277.47±19.6 ^b	22.6±2.2 ^b	79.6±8.2 ^b
Treatment A + 5h storage	2.64±0.06 ^d	594.3±0.6 ^a	54.7±3.8 ^c	299.6±5.7 ^b	16±0.7 ^c	34.1±3.4 ^{cd}
Treatment B without ice	2.5±0.04 ^d	606.7±4.2 ^a	15.6±0.9 ^d	238.6±5.6 ^c	6.3±0.1 ^d	22.7±2.5 ^d
Treatment B	2.5±0.07 ^d	608.7±3.2 ^a	133.5±14.9 ^a	465.2±24.3 ^a	33.7±2.5 ^a	103.8±20 ^a
Treatment B + 5h storage	2.5±0.04 ^d	600±1 ^a	59±6.2 ^c	267.7±40.1 ^{bc}	16.9±2.1 ^c	42.8±5.5 ^c
Treatment D	5.99±0.15 ^b	236.3±13.8 ^c	0.3±0.06 ^e	4.24±0.3 ^d	0.057±0.004 ^e	0.08±0.02 ^e
Treatment D+ 5h storage	6.04±0.14 ^b	210.7±10 ^c	0.28±0.06 ^e	4.14±0.4 ^d	0.037±0.006 ^e	0.03±0.006 ^e
Treatment E	5.07±0.2 ^c	336±31.4 ^b	0.23±0.04 ^e	4.22±0.69 ^d	0.043±0.003 ^e	0.06±0.01 ^e

Treatment A: Direct 20 min BSD (surrounded by ice); Treatment B: Direct 30 min BSD (surrounded by ice); Treatment D: Direct 30 min CJ; Treatment E: Direct 1 h CJ. Values are expressed as the mean ± standard deviation. Values with different letters in the same column are significantly different (p<0.05, n=3).

7.4.2 EPR spectroscopy

Hydroxyl radical ($\bullet\text{OH}$) is one of the most important reactive oxygen species that can be formed in PAW through reaction of O₃ with H₂O₂ (reaction 1), and also through the dissociation of water molecules during ACP treatment (Rathore et al., 2021). DMPO was used to spin trap the $\bullet\text{OH}$. The reaction of DMPO with short-lived $\bullet\text{OH}$ forms a long-lived spin adduct, DMPO-OH (2-hydroxy-5,5-dimethyl-1-pyrrolidinyloxy) (Figure 7.2), which has a unique ESR spectrum with a peak intensity ratio of 1:2:2:1 (Liu et al., 2016). However, the EPR results showed a dominant 7-peak spectrum rather than the characteristic 4-peak spectrum of DMPO-OH. This spectrum is ascribed to DMPOX (5,5-dimethyl-2-pyrrolidone-N-oxyl) based on the literature (Chen et al., 2017; Floyd & Soong, 1977). Similar results were reported by Liu et al. (2016), Chen et al. (2017) and Gao et al. (2022), where DMPO was oxidized to DMPOX after plasma treatment. We observed that the species formed initially regardless of the conditions, and we simulated the spectrum (Figure 7.2, Simulation of 10 sec) based on the 10 sec PAW treatment, which is similar to previous report on

the simulation of this species (Barr and Mason, 1995. JBC. 270:12709-12716). Conditions that exceeded the 10 sec PAW treatment continued to produce a dominant DMPOX spectrum, but another DMPO oxidation product most likely related to DMPOX was observed with 5 and 10 min treatments. As oxidation occurred at 10 min treatment time, the input voltage was reduced from 150 V to 100 V in which the weakest plasma was generated at this voltage and no plasma was generated at voltages below 100 V. The spectrum indicated that the DMPO was oxidized again; however, the intensity of the peaks was lower. Furthermore, the results show that increasing the treatment time allows the spin adducts to accumulate and intensifies the peaks' height. As longer treatment times oxidized the DMPO, the BSD ACP treatment for one second was applied to the water. Interestingly, the DMPO was oxidized to DMPOX again, which indicates the presence of oxidizing agents even after a very short ACP treatment. We also added 5% dimethyl sulfoxide (DMSO), a potent $\bullet\text{OH}$ scavenger, however, DMPO was oxidized and an asymmetric 7-peak spectrum was observed (not shown in the Figure 7.2). This demonstrated that the oxidation of DMPO was not due to $\bullet\text{OH}$. In a previous study, sodium azide (scavenger of $^1\text{O}_2$) was used along with DMPO. The presence of 10 mM of sodium azide resulted in a complete reduction of DMPOX concentration, which suggested the possibility of oxidation of DMPO via $^1\text{O}_2$ (Chen et al., 2017). Overall, the spectrum of DMPO-OH was not observed, as the potential of DMPO oxidation was greater than its potential for trapping the $\bullet\text{OH}$ radicals in PAW.

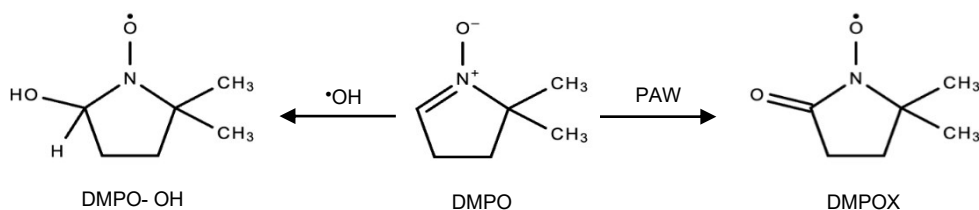
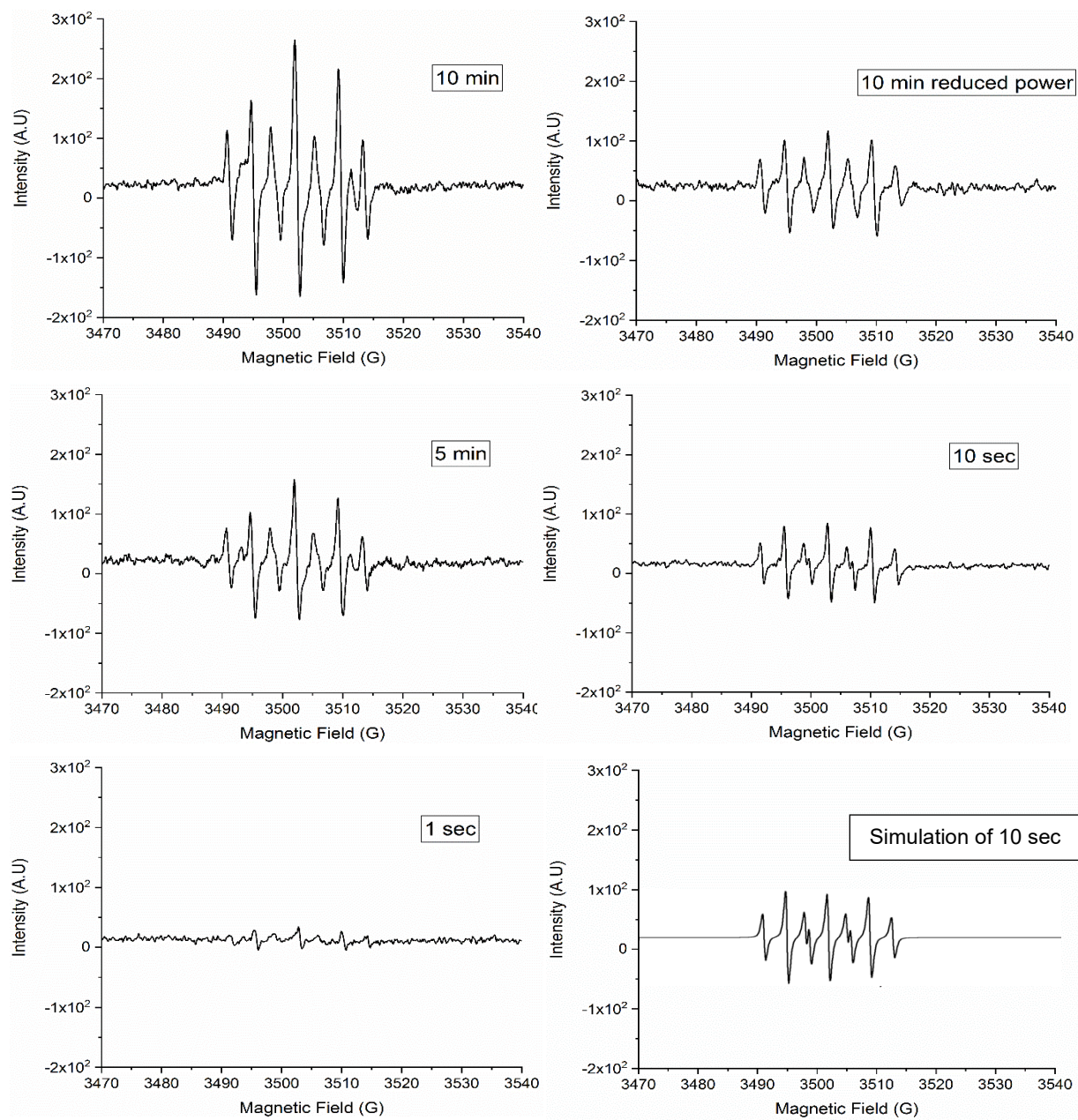


Figure 7.2: Electron paramagnetic resonance spectra of 5 ml deionized water+50 mM DMPO treated with BSD ACP at different times and power, and the chemical structure of DMPO, DMPO-OH, and DMPOX (adapted from Chen et al. (2017)). The simulated spectrum had hyperfine splitting constants of $a^{\text{N}} = 7.26$ G, $a^{\text{H}(2)} = 4.02$ G, and a correlation parameter of $r = 0.98$. The EPR spectrum was simulated using WinSim2002 (NIEHS/NIH).

7.4.3 DON reduction after PAW bubble treatments

As shown in Table 7.4, different PAW bubble treatments did not have a significant ($p > 0.05$) impact on DON reduction compared with the control sample. This was due to a high standard deviation in the naturally contaminated samples. However, comparison of the minimum and maximum amount of DON within the treated samples shows the impact of the PAW bubble treatments on DON degradation. Among the different treatments, direct PAW production for 30 min using BSD at low temperature (surrounded by ice) (treatment B) resulted in the highest reduction of DON compared with the other treatments. Treating NIB grains by treatment B (direct treatment) resulted in higher DON degradation, with 57.3% reduction relative to treatment C (indirect treatment) with 31.2% reduction. Treatment B also had the highest concentration of long-lived RONS, i.e., H_2O_2 , NO_3^- , NO_2^- , and O_3 . Among these, H_2O_2 , and O_3 could play a role in DON degradation; however, NO_3^- , and NO_2^- have no significant ($p > 0.05$) impact on DON degradation (Qiu et al., 2022). In the direct treatment, there are short lived free radicals such as ($\cdot\text{OH}$), superoxide (O_2^-), singlet oxygen, and high energy electrons aside from the RONS, which could be the main reason for greater degradation of DON in the direct vs. indirect treatment. Singlet oxygen is very unstable and reacts with electron-rich double bonds. DON has an olefinic double bond at the C9–10 position, which is one of the most reactive sites for O_3 and singlet oxygen (Fang et al., 2022). The results from treatments A and B demonstrate the higher efficacy of longer treatment time. Higher RONS concentration after treatment B might play a role in the higher DON degradation efficacy. In addition, under longer treatment times, a larger amount of short-lived reactive species could react with the grain surface and DON molecules, resulting in higher DON degradation efficacy. Another factor is the pH of the solution, which may influence the degradation of DON. The degradation of DON was reported as 30 and 60% at pH 3 and 2, respectively (Mishra

et al., 2014). However, in our experiments, the pH of treatments A and B was similar, but the DON degradation rates were different. Hence, factors other than pH play a more important role in DON degradation in naturally infected grain.

During the barley steeping process, DON can possibly be washed away, resulting in the reduction of DON even in the control NIB samples (Table 7.4). After steeping the barley in PAW bubbles produced directly by CJ reactor for 30 min (treatment D), there was a 7% increase in DON reduction compared with the control (Table 7.4). However, 1 h of direct PAW bubble (treatment E) steeping treatment did not increase the DON reduction. This could be due to the larger quantity of water used and the lower concentrations of RONS (Table 7.3), which seems insufficient for the DON degradation.

In a previous study on using PAW produced by plasma jet at 4.4 kV for DON degradation, there was no significant ($p > 0.05$) reduction in DON in the PAW-treated barley samples (Chen et al., 2018). Lower degradation of mycotoxins in artificially infected grains compared with the pure form of the mycotoxin was reported in previous studies (Chen et al., 2022; Siciliano et al., 2016). Severely *Fusarium*-infected grains have deeper infections (Edwards et al., 2011) and DON can be present in the inner layers of the grain. This could be the main reason for the lower efficiency of PAW bubbles in NIB grains compared with artificially infected grains, as RONS and other active species in plasma cannot penetrate to the deeper layers of the grains.

Table 7.4: Effect of different PAW bubble treatments on DON reduction in NIB

	DON content (ppm)	Minimum (ppm)	Maximum (ppm)	Reduction (%)
Dry grain	5.2±0.6 ^a	4.6	5.9	0 ^b
Control (5h steeping) + 19 h air rest	3.3±1 ^b	2.6	4.4	36.9±18.4 ^a
Treatment A +4h 40 min steeping+ 19h air rest	3.3±0.9 ^b	2.4	4.1	37.6±16.2 ^a

Treatment B +4.5h steeping+ 19h air rest	2.2±0.7 ^b	1.5	3	57.3±14.3 ^a
Treatment C +5 h steeping+ 19 h air rest	3.6±0.5 ^b	3.2	4.1	31.2±8.8 ^a
Control D +4.5 h steeping+ 19 h air rest	3.3±1.1 ^b	2	4.9	37.7±20.1 ^a
Treatment D +4.5 h steeping+ 19 h air rest	2.9±0.5 ^b	2.6	3.5	44.6±9.9 ^a
Control E +4.5 h steeping+ 19 h air rest	3±0.6 ^b	2.5	3.7	43.3±12.3 ^a
Treatment E +4 h steeping+ 19 h air rest	3.1±0.3 ^b	2.9	3.5	40.1±6.1 ^a

Treatment A: Direct 20 min BSD (surrounded by ice); Treatment B: Direct 30 min BSD (surrounded by ice); Treatment C: Indirect 30 min BSD; Treatment D: Direct 30 min CJ; Treatment E: Direct 1 h CJ. Values are expressed as the mean ± standard deviation. Values with different letters in the same column are significantly different ($p < 0.05$, $n \geq 4$).

7.4.4 Germination of NIB grains after PAW bubble treatments

To determine the potential of utility of PAW bubble treatment in the steeping process of barley malting, the germination of the NIB grains was assessed. The greatest germination of the barley rootlets was after 30 min indirect PAW bubble treatment (treatment C) using the BSD reactor (Table 7.5). The direct 30 min BSD treatment at low temperature (surrounded by ice) (treatment B) had a significantly ($p < 0.05$) negative impact on the germination of the rootlets and acrospires. The direct PAW bubble treatment using BSD (treatments A, B) negatively affected the acrospire germination; however, rootlet germination could be negatively/positively affected based on the treatment time (i.e., long lived, and short lived RONS concentration). Comparing treatment B with treatment C demonstrates the importance of the short lived RONS and free radicals on the germination efficacy of the ACP system in the direct treatment, as in treatment B there is a constant production of the short lived RONS and free radicals, which negatively affected the germination of the grain. However, in the 20 min direct PAW bubble treatment using the BSD reactor (surrounded by ice) (treatment A), the germination of the rootlets was slightly reduced while acrospire germination declined significantly ($p < 0.05$) compared with treatment C. The results show that the long-lived RONS had improved the germination parameters, while short-lived RONS, or free radicals decreased the germination of the NIB seeds.

Similarly, in a previous study by Chen et al. (2018), the germination of barley grains decreased with increasing the PAW treatment time. It should be noted that the state of the seeds used in different studies is important to consider when comparing the results of these studies, as the efficacy of PAW is different for fresh mature seeds compared with ripened seeds (Grainge et al., 2022). The 30 min direct PAW bubble treatment using the CJ reactor (treatment D) increased the germinated rootlets by 5% however, it was not significant ($p>0.05$) compared with its respective control. This is because the concentration of RONS was insufficient to cause any change in the germination of the grain.

In response to environmental cues, seeds produce H_2O_2 , NO_3^- , $\bullet OH$, and NO to release physiological dormancy by activating molecular signaling pathways (Grainge et al., 2022). It was demonstrated that PAW could trigger many of these pathways, such as abscisic acid degradation and gibberellin synthesis and signaling, which might result in dormancy release of the seed (Grainge et al., 2022). In a study by , Than et al. (2022) the optimum germination of lettuce seeds was obtained after 15 min PAW treatment, while longer treatment times resulted in lower germination rates. In another study, longer treatment times of the barley seeds using microwave discharge resulted in lower shoot and root lengths in the seedlings. It was determined that using the gas mixtures with high NO content in a microwave discharge treatment inhibited barley germination (Szóke et al., 2018).

Plants produce different ROS such as H_2O_2 , superoxide ($O_2^{\bullet -}$), $\bullet OH$, and singlet oxygen ($^1O^{\bullet 2}$) in response to environmental stresses. Overproduction of these ROS can cause oxidative damage to plant macromolecules and cell structures, which will lead to inhibition of plant growth and development or death (Hossain et al., 2015). In contrast, at moderate amounts, ROS like H_2O_2 may be beneficial for plant germination (Barba-Espin et al., 2010). In a study by Jirešová et al. (2022),

the effect of PAW on wheat germination was compared with artificial PAW prepared from H₂O₂ and nitric acid. There were no significant ($p > 0.05$) differences between the efficacy of both PAW treatments on percentage germination, root and shoot length, or fresh/dry weights of the roots and shoots. This suggested that the major RONS of PAW involved in the germination are H₂O₂, NO₃⁻, and NO₂⁻. Moreover, the RONS generated by ACP can impact the expression of germination-related genes, the activity of growth hormones, antioxidants and enzymes, changes in sugar, chlorophyll, amino acids, and water absorption (Attri et al., 2021).

The activity of the α -amylase, β -amylase, and β -glucanase enzymes was also assessed, as these enzymes are involved in the germination of barley grain. The percentage germination of rootlets and acrospire in Control D and treatment C samples were not significantly different from treatment D, hence their enzymatic activity was not measured. The activity of α -amylase, and β -glucanase increased after malting of the NIB grains. There were no significant ($p > 0.05$) differences in α -amylase activity between the DW and PAW bubble-treated samples. Treatment A had the highest α - and β -amylase activities, which correlated well with its rootlet germination rate. The β -glucanase increased significantly ($p < 0.05$) in all of the PAW bubble treated samples, except for treatment B, which also had the lowest germination based on the rootlets and acrospire germination. The results from the enzymatic activity measurement suggests that in longer ACP treatment time, β -glucanase activity is negatively affected, which influenced the germination of the grain. As discussed in this section, there are numerous parameters involved in the germination of a seed and RONS from plasma can differently impact any of these, thereby changing the percentage germination. More study is needed in this regard to comprehend fully the mechanism(s) of long-lived and short-lived reactive species on regulating the germination of a plant.

Table 7.5: Effect of different PAW bubble treatments on germination of NIB

	MC 1 st day steeping (g water/100 g sample)	MC 2 nd day steeping (g water/100 g sample)	Germinated acrospire (%)	Germinated rootlets (%)	α -amylase (units/g dry basis)	β -amylase (units/g dry basis)	β -glucanase (units/g dry basis)
Dry grain	-	-	-	-	12.6±1.6 ^b	31.6±2.1 ^{ab}	22.3±3.7 ^d
DW+5h steeping+ 19 h air rest	30.9±0.6 ^a	41.2±0.8 ^a	47.3±7 ^a	58.2±2.7 ^a	41.9±0.7 ^a	31.8±1 ^{ab}	33.3±2.9 ^{bc}
Treatment A+4h 40 min steeping+ 19h air rest	31.7±1.4 ^a	42.7±0.9 ^a	15.1±0.7 ^b	70.1±7 ^a	45.1±6.5 ^a	33.4±1 ^a	39.9±4.6 ^b
Treatment B+ 4h 30 min steeping+ 19h air rest	32.9±1.9 ^a	42.6±1.5 ^a	3.6±6.2 ^c	18.5±16.9 ^b	39.5±7.4 ^a	30.9±0.5 ^{ab}	26.7±2.8 ^{cd}
Treatment C+ 5h steeping+ 19 h air rest	31.5±1.7 ^a	41.7±3 ^a	38.1±4.8 ^a	75.08±7.3 ^a	-	-	-
Control D+4h 30 min steeping+ 19h air rest	33.36±0.7 ^a	42.5±0.8 ^a	41.1±10.4 ^a	63.7±8.1 ^a	-	-	-
Treatment D+4h 30 min steeping+ 19h air rest	33.46±0.5 ^a	43.6±0.7 ^a	44.1±4.7 ^a	68.5±11 ^a	39.2±1.6 ^a	30.2±1.3 ^b	51.6±7.3 ^a

Treatment A: Direct 20 min BSD (ice surrounding); Treatment B: Direct 30 min BSD (ice surrounding); Treatment C: Indirect 30 min BSD; Treatment D: Direct 30 min CJ. Values are expressed as the mean \pm standard deviation. Values with different letters in the same column are significantly different ($p < 0.05$, $n=3$).

7.4.5 Effect of PAW bubble treatments on microflora and *F. graminearum* in NIB grains

To determine the antimicrobial activity of PAW bubbles, the treated and untreated NIB grains were plated on PDA agar, which confirmed the presence of other microflora in addition to *F. graminearum* (Figure 7.3). The average diameter of microbial colonies recovered from NIB following the various treatments is summarized in Table 7.6. While the PAW bubble treatments did not have a significant ($p > 0.05$) effect on colony diameter (Figure 7.3), there was a reduction in the colony diameter of the steeped vs. dry grain (grain without steeping in water) samples. There was no significant ($p > 0.05$) difference in the proportion of *F. graminearum*-infected grains, as assessed on PDA, between the treated and untreated samples. Similarly, the colonies of *F. graminearum* (confirmed by its morphology under microscope) recovered seemed to be of similar size based on visual inspection of the treated and untreated samples. Nonetheless, the sample size

used in this work was small, and further testing may be required to confirm the absence of an effect of PAW bubble treatment on the microbiota associated with NIB.

The NIB grains were also incubated on WA plates to assess their germination. As expected, dry grain had significantly ($p < 0.05$) lower shoot length compared with other samples. However, percentage germination and shoot length were not significantly ($p > 0.05$) different between the treated and control grains. This was probably due to favorable conditions on the WA plates such as the presence of water and nutrients for germination of the grains, which overcame any differences in the relative viability of the seeds. In addition, as was observed on the PDA plates, the number of *F. graminearum*-infected grains was not significantly ($p > 0.05$) different between the treated and untreated samples incubated on WA medium (Table 7.6, Figure 7.3). In a previous study, the growth of *F. graminearum* was significantly inhibited following PAW treatment of *F. graminearum* in culture (Guo, Wang, et al., 2021). Moreover, the growth rate of *F. graminearum* was significantly ($p < 0.05$) reduced after treating the fungus with gliding arc plasma (Kaur et al., 2022). There are other studies on the reduction of the growth of *Aspergillus parasiticus* and *Aspergillus flavus* on inoculated groundnuts (Devi et al., 2017), *Penicillium italicum* on inoculated kumquat (Guo, Qin, et al., 2021), *Aspergillus parasiticus* and *Aspergillus flavus* on inoculated hazelnuts (Sen et al., 2019) after ACP/PAW treatment. These studies assessed the effect of ACP/PAW treatment in fungal cultures or grains artificially inoculated with the fungi. In our study, naturally infected barley grains were used, in which *F. graminearum* and other microflora could reside in the inner layers of the grain, especially in severely infected grains. This would reduce the capacity of RONS from PAW to react with the fungi and could be the main reason for the apparent inefficacy of the PAW treatment on reducing infection of NIB grains.

In a study by Xu et al. (2016), 5 and 10 min PAW treatments of naturally contaminated button mushrooms reduced fungal content by approximately 1 log value. However, a 15 min PAW treatment did not affect fungal content significantly. In another study, 10 min air plasma treatment resulted in a 4% decrease in *Fusarium* in naturally contaminated field pea, and a 15 min air plasma treatment resulted in a 9% decrease of *Fusarium* in naturally contaminated blue lupin seeds (Filatova et al., 2012). Similar to our study, the efficacy of cold plasma on naturally infected grains seems to be considerably lower relative to inoculated seeds. Nonetheless, more studies are required to improve understanding of the effect of PAW bubble treatments and RONS on microflora and *F. graminearum* on or in NIB grains.

The RONS and radicals from PAW can react with the cell walls of fungi and result in the oxidation of the cell wall components such as glucose, (N-acetyl)-glucosamine, glycoproteins and glucan, and peroxidation of the lipids in the plasma membrane. This will result in the damage and perforation of the cell wall and membrane, and subsequent exposure of the intracellular components to RONS (Guo, Wang, et al., 2021). Different parameters in PAW, such as type and concentration of RONS and pH of PAW, can influence the growth of microflora. In previous studies, *F. graminearum* germination and mycelium growth were higher at pH 4 vs. pH 8 (Thompson et al., 1993) and the mycelial growth of *F. graminearum* at different pH was pH 5 > 6 > 7 > 8 (Panwar et al., 2016). This shows that the pH of PAW produced from BJ in the ACP treatment (treatment F) (pH=3.86) may favor the growth of *F. graminearum*. However, a previous study on *Colletotrichum gloeosporioides* inactivation by PAW determined that long-lived RONS (ozone, nitrate, and nitrite) made the greatest contributions to fungal growth inhibition, while acidic pH had a minor effect on fungal inactivation (Wu et al., 2019). In addition, NO₂ showed higher antifungal activity relative to NO₃ (Wu et al., 2019). The fungal biomass of *F. graminearum*

is positively correlated with DON content on grains (Demeke et al., 2010). The factors that promote fungal growth including environmental factors, growth stage, chemotype of pathogen isolate, lodging, tillage, cultivar resistance, and fungicide application (Wegulo, 2012) can affect DON accumulation on grains. Hence controlling and optimizing the aforementioned factors could be beneficial for *F. graminearum* reduction as PAW treatment did not exhibit antifungal properties.

Table 7.6: Effect of PAW bubble treatment on *F. graminearum* and grain germination¹

	Average colony diameter on PDA (cm) ²	Number of <i>F. graminearum</i> colonies on PDA	Number of <i>F. graminearum</i> colonies on WA	Plant shoot length on WA (cm)	Germination % on WA
Dry grain	2.12±0.06 ^a	1.2±0.8 ^a	1.2±1 ^a	3.66±0.06 ^b	85.6±1.9 ^a
Control 5 h steeping+ 19 h air rest	1.99±0.07 ^b	2.1±1.4 ^a	0.7±0.5 ^a	4.51±0.69 ^a	86.7±3.3 ^a
Treatment A +4h 40 min steeping+ 19 h air rest	1.99±0.08 ^b	1.4±1.4 ^a	1.4±1.1 ^a	4.29±0.36 ^{ab}	87.8±5.1 ^a
Treatment C +5h steeping+19 h air rest	1.89±0.04 ^b	2.3±2.1 ^a	1.4±1.2 ^a	4.38±0.47 ^{ab}	84.4±5.1 ^a
Treatment F +4.5 h steeping+ 19 h air rest	1.99±0.05 ^b	1.3±0.9 ^a	1.1±1.1 ^a	4.89±0.34 ^a	81.1±1.9 ^a

1: All the values in the table are the average number per Petri dish with 10 NIB seeds. 2: average colony diameter of all microflora, except *F. graminearum*, recovered from NIB seeds. Treatment A: Direct 20 min BSD (surrounded by ice); Treatment C: Indirect 30 min BSD; Treatment F: Direct 30 min BJ. PDA: potato dextrose agar; WA: water agar. Germination expressed as percentage of seeds that had shoot length more than 3 mm. Values are expressed as the mean ± standard deviation. Values with different letters in the same column are significantly different (p<0.05, n=3).

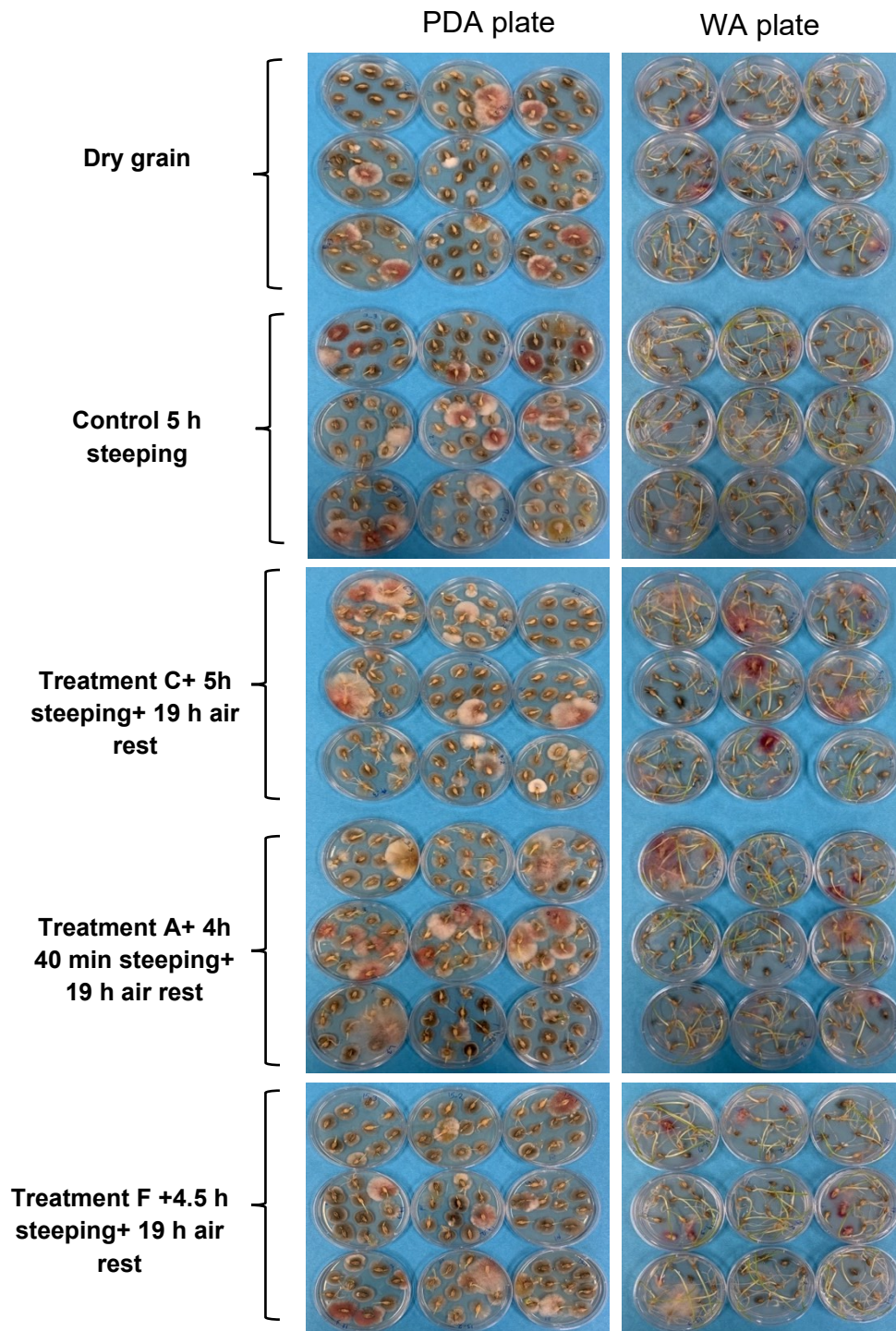


Figure 7.3: Effect of PAW bubble treatments on natural microflora, *F. graminearum* and germination of naturally infected barley grains. Treatment A: Direct 20 min BSD (ice surrounding); Treatment C: Indirect 30 min BSD; Treatment F: Direct 30 min BJ. Seeds were plated on potato dextrose agar medium (PDA) and water agar (WA)

7.5 Effect of bubble ACP treatment on fungal biomass of *F. graminearum*

Tri5, *Tri6*, *EF1-A* and β -*Actin* genes were used for *F. graminearum* detection and relative quantification based on qPCR (Hafez et al., 2020; Kimura et al., 2007; Livak & Schmittgen, 2001; Tang et al., 2020), in order to confirm the results obtained with the plating technique, which indicated that the PAW bubble treatment did not have any effect on *F. graminearum* infection or growth. DON biosynthesis is governed by fifteen genes that are present over three chromosomes (Khaneghah et al., 2018) and an acidic pH of environment encourages DON biosynthesis. Also, DON biosynthesis is induced in response to plants defense mechanism to fungi infection (Kamle et al., 2022).

RONS from ACP can damage the structure of the fungal cell walls and reach intracellular components, such as nucleic acids, and degrade them (Veerana et al., 2022). The fold-changes in relative abundance of the three target genes *Tri5*, *Tri6* and *EF1-A* (with β -*Actin* used as an endogenous control) following PAW bubble treatments are presented in Figure 7.4. Relative to the dry grain sample, the abundance of *Tri5* and *Tri6* was reduced in all treatments, with the strongest reduction observed in treatment C (Figure 7.4). In contrast, the abundance of *EF1-A* was not altered relative to the dry grain sample. There was a large standard deviation in the Ct values of the samples for each gene, likely because some grains were highly contaminated, while others were not infected. The presence of a few contaminated or infected seeds in one sample relative to others can result in a large standard deviation. This variability, combined with an apparent lack of reduction of *EF1-A*, suggests that reductions in fungal biomass because of the PAW treatments were not consistent or particularly pronounced.

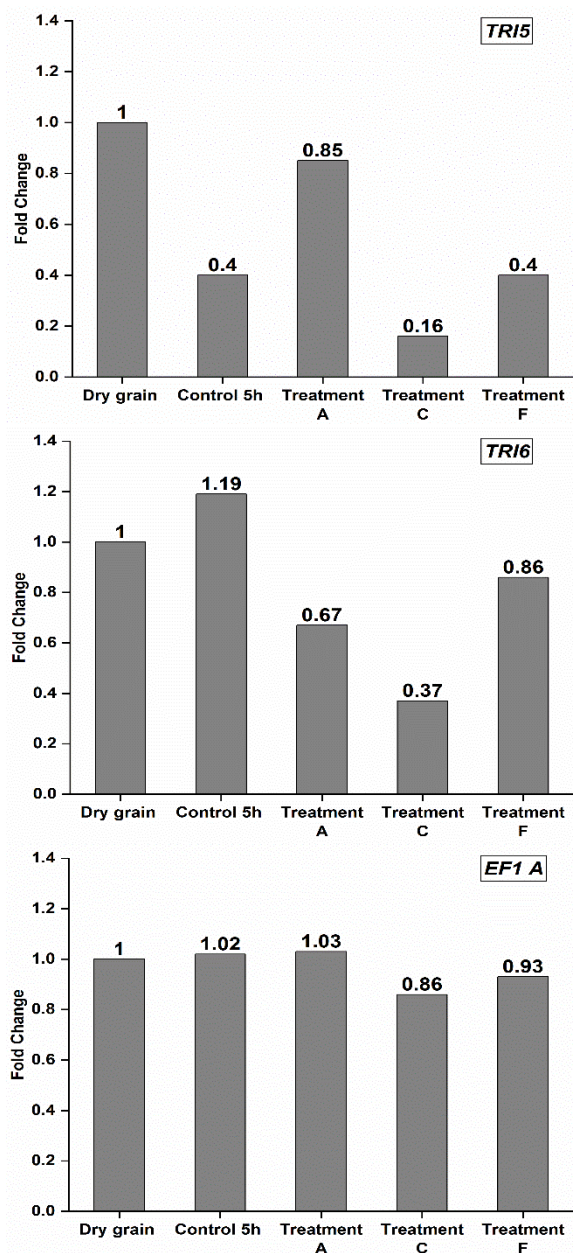


Figure 7.4: Effect of PAW bubble treatments on the relative abundance of three target genes (Tri5, Tri6 and EF1-A) of *F. graminearum* with β -Actin as an endogenous reference gene, based on quantitative PCR analysis. Values are reported based on fold-change values. The fold-change was calculated using $\text{Fold-change} = 2^{-\Delta\Delta C_t}$ where, $\Delta C_t = C_t(\text{target gene}) - C_t(\text{reference gene})$, and $\Delta\Delta C_t = \Delta C_t(\text{treatment}) - \Delta C_t(\text{control})$. Treatment A: Direct 20 min BSD (ice surrounding); Treatment C: Indirect 30 min BSD; Treatment F: Direct 30 min BJ. Control and treatments A, C, and F were followed by steeping and air rest step before qPCR test

7.6 Conclusions

Contamination of barley grains by mycotoxins and pathogenic fungi is one of the major issues facing the malting industry. Deoxynivalenol (DON) and *F. graminearum* are the main mycotoxin and pathogenic fungus, respectively, affecting barley seed. In this study, the potential of plasma activated water (PAW) bubbles produced from different atmospheric cold plasma (ACP) units was assessed for DON degradation and *F. graminearum* inactivation during the steeping of barley grains. There was a positive correlation between the concentration of RONS in PAW and DON reduction. Further research is required for determining the main reactive specie responsible for DON degradation in PAW. Previous research determined the efficacy of ACP/PAW treatment on inactivation of fungi and DON spiked on grains (Devi et al., 2017; Guo, Qin, et al., 2021; Sen et al., 2019). In this study we used naturally infected barley (NIB). The PAW bubble treatments used in this study were not able to inactivate *F. graminearum* on NIB grains probably due to the presence of fungi in the inner layers of the NIB grains and/or growth promotion of fungi in acidic pH. As using ACP in gaseous state has etching effect and pH does not play a role in promoting the fungal growth, its efficacy against *F. graminearum* on naturally contaminated grains should be investigated. Our results determined that to reduce both the DON concentration and improve germination, PAW bubbles produced by the continuous ACP jet treatment (treatment D) performed better compared to the other tested ACP treatments. Collectively, the use of an optimized PAW bubble treatment can improve germination and reduce DON content in barley grains.

Chapter 8: Conclusions and recommendations

8.1 Overall conclusions

In this research, application of atmospheric cold plasma (ACP) technology for the degradation of two of the important mycotoxins prevalent in Canada, DON and ZEA, was assessed. The effects of process parameters such as the type of gas, relative humidity, treatment time, treatment mode, type of ACP system, and the sequential treatments consisting of ACP+ heat, and ACP+LED on the degradation of DON and ZEA were determined. The degradation of DON spiked on barley, quality changes, and germination by ACP treatment were studied. Different ACP units including jet-ACP and a bubble spark discharge ACP unit were used to generate PAW. The application of PAW in the steeping process of barley malting for DON reduction, germination improvement and *F. graminearum* inactivation was evaluated. Furthermore, the main RONS produced via ACP in gaseous or liquid state were determined and quantified, and the DON degradation mechanisms via ACP treatment was studied.

In Chapter 3, the efficacies of DBD-ACP and sequential treatments on DON degradation were determined. The results of this study confirmed the ability of ACP for significant reduction of DON. The presence of water increased DON degradation significantly. To determine the changes in the structure of the treated DON and know the number of the degradation products of DON, FTIR and TLC experiments were performed. Three distinct bonds were detected in the ACP-treated samples compared to the control sample by FTIR analysis, which was probably associated to the formation of C=O group and epoxy ring in the treated DON's structure. In TLC analysis, the degradation by-products of DON were not differentiated, which could be due to the similar polarity of the degraded products. The optical emission spectroscopy analysis proved the presence of a significant amount of RONS in ACP, which contributed to the DON degradation. Heat

treatment at 80 °C and LED treatment using 395 nm light pulses did not show synergistic effect with ACP treatment on DON degradation.

The efficacy of DBD-ACP on the degradation of DON spiked on barley grains was assessed in Chapter 4. The DON was degraded by 48.9 % after 6 min DBD-ACP treatment. The quantification of RONS showed that ozone had the highest concentration with 600 ppm after 1 min ACP treatment. The assessed quality parameters of barley, including protein, β -glucan and moisture content, were not significantly affected by DBD-ACP treatment. The 6 min DBD-ACP treatment improved the germination parameters of the treated barley grains compared with the control.

Chapter 5 focused on the effect of process and product parameters on ZEA degradation using DBD-ACP and jet-ACP systems. Similar to DON, ZEA degradation was improved considerably in the presence of water, and the heat and LED treatments did not show a synergistic effect with DBD-ACP on ZEA degradation. However, ZEA was considerably more sensitive to ACP treatment compared to DON. The ZEA was spiked on selected matrices and the highest degradation was obtained on canola grains, followed by canola meal and barley grains by ACP treatment. The concentrations of RONS while treating canola and barley grains were significantly higher than canola meal, which could be due to the presence of air space between the grains in canola and barley grains that resulted in greater production of RONS. Also, better scavenging of RONS could be possible by canola meal with larger surface area and surface characteristics compared to grain surfaces. Use of different gases, i.e., 100% N₂, 90% N₂+ 10% O₂, 80% N₂+ 20% O₂, and air, in a closed chamber, did not show a significant difference on ZEA degradation after 3 min DBD-ACP treatment, while the concentration of RONS were the highest in air which suggests that factors other than the assessed RONS in ACP discharge such as high-energy electrons, UV light, and/or free radicals possibly contribute to ZEA degradation. In jet ACP, 85%

Ar+15% O₂ resulted in a considerably higher ZEA degradation compared to 75% Ar+25% N₂ and 100% Ar, which suggested the importance of the presence of oxygen in the carrier gas for achieving the highest degradation rate of ZEA.

Due to satisfactory results from using ACP for DON degradation, naturally contaminated grains were tested in Chapter 6. This chapter focused on producing PAW bubbles via jet-ACP and assessed its potential for using in steeping of NIB during malting. The degradation mechanisms of DON during DBD-ACP treatment were also investigated. The highest reduction of DON was 58.4% compared to 33.3% in the control sample. Ozone and nitrates were detected in the PAW and the ORP of the PAW was considerably higher than the control sample, suggesting the presence of oxidizing species in PAW. Water uptake and the germinated rootlets % of the PAW treated NIB grains were not significantly different compared to the control, while the germinated rootlets % were significantly increased. The chemical formula of the 12 major degradation products of DON were determined and the possible structures of the degraded products suggested possibly reduced toxicity of DON. Also, comparing DON and the degraded products' structure suggested oxidation as the main degradation mechanism of DON during ACP treatment.

In Chapter 7, a continuous treatment system to produce PAW bubbles using jet-ACP was built. The potential of this continuous system and a BSD-ACP system on PAW bubble production was assessed for treating NIB grains for *F. graminearum* inactivation and DON degradation during steeping. The 30 min BSD-ACP treatment at generated the highest concentration of RONS in PAW compared to other treatments. The PAW generated at a high temperature had considerably lower amount of RONS compared with PAW generated at a low temperature (using an ice jacket). The EPR spectroscopy analysis showed that the DMPO that was used for quantification of OH radicals, was oxidized to DMPOX during BSD-ACP treatments. A direct 30 min BSD-ACP treatment

reduced DON content by 57.3% compared to 36.9% in the control sample, however, the same treatment negatively affected the germination parameters of NIB grains. Indirect 30 min BSD-ACP, and/or direct 20 min BSD-ACP increased the germinated rootlets percentage compared to the control. The plating and qPCR results showed the inefficacy of BSD-ACP and CJ-ACP treatment on the inactivation of natural pathogens and *F. graminearum* on NIB grains, however, more studies are required to confirm this result and achieve a conclusive understanding on fungal inactivation by ACP in NIB grains.

Overall, the results from this thesis suggest that ACP treatment can degrade mycotoxins in pure form, however, in naturally contaminated barley grain, the degradation efficacy of ACP is reduced considerably. This is probably due to the inability of RONS to react with the mycotoxin (DON in our study), which may be residing in the inner layers of the grain. Also, there may be significant scavenging of RONS by the grain surfaces. This technology can be used for simultaneous improvement of germination and DON reduction during malting of barley, however, optimization in PAW generation and treatment is required. The efficacy of ACP is affected by the process factors such as voltage, frequency, RH, treatment time, mode of treatment, type of carrier gas, gas flow rate, type of ACP system. The product factors such as moisture content, size, shape, and surface characteristics, and the microbial/chemical factors such as type of pathogen/chemical and initial count, can influence the ACP efficacy. The type and concentration of RONS generated by ACP are affected by the aforementioned factors. These RONS react with each other so their concentrations are different at every moment during treatment, which makes ACP an inherently complex treatment method. Hence, a great deal of work is needed for defining a standard ACP treatment condition for a specific product at an industrial scale for commercial use. However, the

results of this work laid the foundation for applying ACP treatment in the malting industry for mycotoxin degradation and germination improvement of the barley grain.

8.2 Recommendations

This research demonstrated the DON and ZEA degradation efficacy of ACP with specific focus on its application during barley malting with possible germination improvement. This study presented the effect of certain product and process parameters on mycotoxin degradation efficacy of ACP and investigated the DON degradation mechanisms. The effects of ACP treatment on barley quality parameters and *F. graminearum* inactivation were also studied. The following suggestions can be further explored for the application of ACP treatment:

- Application of ACP in gaseous form (Chapter 4) or in PAW form (Chapters 6-7) can reduce DON content and affect barley germination. As the efficacy of ACP is based on the RONS concentration, more studies are needed to identify the major RONS involved in DON degradation and germination improvement. Also, the mechanisms of RONS on DON degradation and germination improvement needs further research for applying ACP and PAW in a most optimized form.
- Addition of specific chemicals (e.g., H₂O₂, ozone, nitrogen compounds etc.) to water at a defined concentration to prepare solutions and comparison of their efficacy with PAW may help in identifying the major RONS of PAW, which are affecting the mycotoxin degradation or germination parameters of the grains.
- The chemical formula of the major degradation products of DON were determined in this research, however, more studies for elucidating the chemical structure of the degradation products using NMR are needed for identifying the degradation pathway of DON.

- The results of Chapter 5 suggested that factors other than the assessed RONS are involved in ZEA degradation. In ACP, long-lived and short-lived RONS, high energetic electrons, and UV light exist together. The effect of each of these parameters especially free radicals and high energetic electrons, on mycotoxin degradation and grain quality needs to be investigated separately for elucidating the ZEA degradation mechanism of ACP.
- As there are numerous RONS in PAW, which makes it difficult to determine the role of each of these species in DON degradation and barley germination improvement. Using scavengers of specific RONS can help in defining the role of the individual RONS in PAW for different applications such as germination improvement.
- The estimated relative abundance of the *F. graminearum* genes obtained in this study could be correlated with the fungal biomass using plating techniques.
- As the degree of polymerization (DP) of beta glucan is important for the malting industry, hence the effect of ACP treatment on DP of beta glucan could be investigated.
- The results from Chapter 7 suggested the significant role of short-lived RONS on reducing the germination of barley. More studies are needed on the effect of short-lived RONS on germination of grains.
- In Chapter 7, PAW bubbles were produced and their efficacy on DON degradation and germination of barley was explored. As the nanobubbles are stable for several days, hence the efficacy of PAW nanobubbles on the aforementioned factors could be studied.
- Finally, the cost efficiency and practical challenges in applying an ACP system in industry, such as PAW waste disposal, integration of PAW treatment unit to barley steeping, large scale continuous production of PAW and any safety issues associated with ozone production in gaseous ACP or in PAW, should be investigated.

Bibliography

- 44-19.01-AACC International. *AACC Approved Methods of Analysis. 11th Ed. Method 44-19.01. Moisture—Air-Oven Method, Drying at 135°C. November 3, 1999. Cereals & Grains Association, St. Paul, MN, U.S.A.* <http://dx.doi.org/10.1094/AACCIntMethod-44-19.01>
- AACC 32-23.01. *AACC Approved Methods of Analysis. 11th Ed. Method 32-23.01. β -Glucan Content of Barley and Oats—Rapid Enzymatic Procedure. November 3, 1999. Cereals & Grains Association, St. Paul, MN, U.S.A.* <http://dx.doi.org/10.1094/AACCIntMethod-32-23.01>
- AACC 46-30.01. *AACC Approved Methods of Analysis. 11th Ed. Method 46-30.01. Crude Protein—Combustion Method. November 3, 1999. Cereals & Grains Association, St. Paul, MN, U.S.A.* <http://dx.doi.org/10.1094/AACCIntMethod-46-30.01>
- Abramson, D., House, J. D., & Nyachoti, C. M. (2005, 2005/11/01). Reduction of Deoxynivalenol in Barley by Treatment with Aqueous Sodium Carbonate and Heat. *Mycopathologia*, 160(4), 297-301. <https://doi.org/10.1007/s11046-005-0087-1>
- Ahlfeld, B., Li, Y., Boulaaba, A., Binder, A., Schotte, U., Zimmermann, J. L., Morfill, G., & Klein, G. (2015). Inactivation of a foodborne norovirus outbreak strain with nonthermal atmospheric pressure plasma. *MBio*, 6(1), e02300-02314.
- Akocak, P. B. (2016). Current Progress in Advanced Research into Fungal and Mycotoxin Inactivation by Cold Plasma Sterilization. *Gas Plasma Sterilization in Microbiology*, 59.
- Albertos, I., Martín-Diana, A., Cullen, P., Tiwari, B., Ojha, S., Bourke, P., Álvarez, C., & Rico, D. (2017). Effects of dielectric barrier discharge (DBD) generated plasma on microbial reduction and quality parameters of fresh mackerel (*Scomber scombrus*) fillets. *Innovative Food Science & Emerging Technologies*, 44, 117-122.
- Alexandre, A. P. S., Castanha, N., Calori-Domingues, M. A., & Augusto, P. E. D. (2017). Ozonation of whole wheat flour and wet milling effluent: Degradation of deoxynivalenol (DON) and rheological properties [Article]. *Journal of Environmental Science and Health - Part B Pesticides, Food Contaminants, and Agricultural Wastes*, 52(7), 516-524. <https://doi.org/10.1080/03601234.2017.1303325>
- Alizadeh, A., Braber, S., Akbari, P., Kraneveld, A., Garssen, J., & Fink-Gremmels, J. (2016, Nov). Deoxynivalenol and Its Modified Forms: Are There Major Differences? [Article]. *Toxins*, 8(11), 16, Article 334. <https://doi.org/10.3390/toxins8110334>

- Amini, M., & Ghoranneviss, M. (2016, 2016/11/01/). Effects of cold plasma treatment on antioxidants activity, phenolic contents and shelf life of fresh and dried walnut (*Juglans regia* L.) cultivars during storage. *LWT*, 73, 178-184.
<https://doi.org/https://doi.org/10.1016/j.lwt.2016.06.014>
- Anacail. (2018). *Sterilization inside a sealed package using ozone*. Anacail Limited. Retrieved 27 March from <http://www.anacail.com/>
- Andrady, A. L., Hamid, S., Hu, X., & Torikai, A. (1998). Effects of increased solar ultraviolet radiation on materials. *Journal of Photochemistry and Photobiology B: Biology*, 46(1-3), 96-103.
- Arc, E., Galland, M., Godin, B., Cueff, G., & Rajjou, L. (2013, 2013-September-19). Nitric oxide implication in the control of seed dormancy and germination [Review]. *Frontiers in plant science*, 4(346). <https://doi.org/10.3389/fpls.2013.00346>
- Arrúa, A. A., Mendes, J. M., Arrúa, P., Ferreira, F. P., Caballero, G., Casal, C., Kohli, M. M., Peralta, I., Ulke, G., & Fernández Ríos, D. (2019). Occurrence of Deoxynivalenol and Ochratoxin A in Beers and Wines Commercialized in Paraguay. *Toxins*, 11(6), 308.
<https://doi.org/10.3390/toxins11060308>
- Astoreca, A., Ortega, L., Fígoli, C., Cardós, M., Cavaglieri, L., Bosch, A., & Alconada, T. (2017). Analytical techniques for deoxynivalenol detection and quantification in wheat destined for the manufacture of commercial products [Article]. *World Mycotoxin Journal*, 10(2), 111-120. <https://doi.org/10.3920/WMJ2016.2121>
- Attri, P., Koga, K., Okumura, T., & Shiratani, M. (2021, 2021/03/23). Impact of atmospheric pressure plasma treated seeds on germination, morphology, gene expression and biochemical responses. *Japanese Journal of Applied Physics*, 60(4), 040502.
<https://doi.org/10.35848/1347-4065/abe47d>
- Bae, E., Yeo, I. J., Jeong, B., Shin, Y., Shin, K. H., & Kim, S. (2011, Jun 1). Study of double bond equivalents and the numbers of carbon and oxygen atom distribution of dissolved organic matter with negative-mode FT-ICR MS. *Analytical Chemistry*, 83(11), 4193-4199. <https://doi.org/10.1021/ac200464q>
- Bafoil, M., Jemmat, A., Martinez, Y., Merbahi, N., Eichwald, O., Dunand, C., & Yousfi, M. (2018). Effects of low temperature plasmas and plasma activated waters on *Arabidopsis thaliana* germination and growth. *PLoS ONE*, 13(4), e0195512.
- Bahin, E., Bailly, C., Sotta, B., Kranner, I., Corbineau, F., & Leymarie, J. (2011). Crosstalk between reactive oxygen species and hormonal signalling pathways regulates grain

- dormancy in barley. *Plant, Cell & Environment*, 34(6), 980-993. <https://doi.org/https://doi.org/10.1111/j.1365-3040.2011.02298.x>
- Baier, M., Görgen, M., Ehlbeck, J., Knorr, D., Herppich, W. B., & Schlüter, O. (2014). Non-thermal atmospheric pressure plasma: screening for gentle process conditions and antibacterial efficiency on perishable fresh produce. *Innovative Food Science & Emerging Technologies*, 22, 147-157.
- Bajgai, T. R., Raghavan, G. V., Hashinaga, F., & Ngadi, M. O. (2006). Electrohydrodynamic drying—A concise overview. *Drying Technology*, 24(7), 905-910.
- Barba-Espin, G., Diaz-Vivancos, P., Clemente-Moreno, M. J., Albacete, A., Faize, L., Faize, M., Pérez-Alfocea, F., & Hernández, J. A. (2010). Interaction between hydrogen peroxide and plant hormones during germination and the early growth of pea seedlings. *Plant, Cell & Environment*, 33(6), 981-994. <https://doi.org/https://doi.org/10.1111/j.1365-3040.2010.02120.x>
- Becker, K. H., Kogelschatz, U., Schoenbach, K., & Barker, R. (2004). *Non-equilibrium air plasmas at atmospheric pressure*. CRC press.
- Berardinelli, A., Pasquali, F., Cevoli, C., Trevisani, M., Ragni, L., Mancusi, R., & Manfreda, G. (2016). Sanitisation of fresh-cut celery and radicchio by gas plasma treatments in water medium. *Postharvest Biology and Technology*, 111, 297-304.
- Berardinelli, A., Vannini, L., Ragni, L., & Guerzoni, M. E. (2012). Impact of atmospheric plasma generated by a DBD device on quality-related attributes of “Abate Fetel” pear fruit. In *Plasma for bio-decontamination, medicine and food security* (pp. 457-467). Springer.
- Bertuzzi, T., Rastelli, S., Mulazzi, A., Donadini, G., & Pietri, A. (2011, 2011/12/01/). Mycotoxin occurrence in beer produced in several European countries. *Food Control*, 22(12), 2059-2064. <https://doi.org/https://doi.org/10.1016/j.foodcont.2011.06.002>
- Bethke, P. C., Gubler, F., Jacobsen, J. V., & Jones, R. L. (2004, 2004/09/01). Dormancy of Arabidopsis seeds and barley grains can be broken by nitric oxide. *Planta*, 219(5), 847-855. <https://doi.org/10.1007/s00425-004-1282-x>
- Bianchini, A., Horsley, R., Jack, M. M., Kobiush, B., Ryu, D., Tittlemier, S., Wilson, W. W., Abbas, H. K., Abel, S., & Harrison, G. (2015). DON occurrence in grains: a North American perspective. *Cereal Foods World*, 60(1), 32-56.

- Bogaerts, A., Neyts, E., Gijbels, R., & van der Mullen, J. (2002). Gas discharge plasmas and their applications. *Spectrochimica Acta Part B: Atomic Spectroscopy*, 57(4), 609-658. [https://doi.org/10.1016/s0584-8547\(01\)00406-2](https://doi.org/10.1016/s0584-8547(01)00406-2)
- Boudam, M., Moisan, M., Saoudi, B., Popovici, C., Gherardi, N., & Massines, F. (2006). Bacterial spore inactivation by atmospheric-pressure plasmas in the presence or absence of UV photons as obtained with the same gas mixture. *Journal of Physics D: Applied Physics*, 39(16), 3494.
- Boutigny, A. L., Gautier, A., Basler, R., Dauthieux, F., Leite, S., Valade, R., Aguayo, J., Ioos, R., & Laval, V. (2019). Metabarcoding targeting the EF1 alpha region to assess Fusarium diversity on cereals. *PLoS ONE*, 14(1), e0207988. <https://doi.org/10.1371/journal.pone.0207988>
- Brandenburg, R. (2017). Dielectric barrier discharges: progress on plasma sources and on the understanding of regimes and single filaments. *Plasma Sources Science and Technology*, 26(5), 053001.
- Brandenburg, R., Bogaerts, A., Bongers, W., Fridman, A., Fridman, G., Locke, B. R., Miller, V., Reuter, S., Schiorlin, M., Verreycken, T., & Ostrikov, K. (2019). White paper on the future of plasma science in environment, for gas conversion and agriculture. *Plasma Processes and Polymers*, 16(1), 1700238. <https://doi.org/10.1002/ppap.201700238>
- Brenn-Struckhova, Z., Cichna-Markl, M., Böhm, C., & Razzazi-Fazeli, E. (2007, 2007/01/01). Selective Sample Cleanup by Reusable Sol-Gel Immunoaffinity Columns for Determination of Deoxynivalenol in Food and Feed Samples. *Analytical Chemistry*, 79(2), 710-717. <https://doi.org/10.1021/ac061672w>
- Brennan, C. S., Harris, N., Smith, D., & Shewry, P. R. (1996, 1996/09/01/). Structural Differences in the Mature Endosperms of Good and Poor Malting Barley Cultivars. *Journal of Cereal Science*, 24(2), 171-177. <https://doi.org/https://doi.org/10.1006/jcrs.1996.0050>
- Brenton, A. G., & Godfrey, A. R. (2010, 2010/11/01/). Accurate Mass Measurement: Terminology and Treatment of Data. *Journal of the American Society for Mass Spectrometry*, 21(11), 1821-1835. <https://doi.org/https://doi.org/10.1016/j.jasms.2010.06.006>
- Bretz, M., Beyer, M., Cramer, B., Knecht, A., & Humpf, H. U. (2006). Thermal degradation of the Fusarium mycotoxin deoxynivalenol [Article]. *Journal of Agricultural and Food Chemistry*, 54(17), 6445-6451. <https://doi.org/10.1021/jf061008g>

- Brisset, J., Lelievre, J., Doubla, A., & Amouroux, J. (1990). Interactions with aqueous solutions of the air corona products. *Revue de physique appliquée*, 25(6), 535-543.
- Brisset, J.-L., & Pawlat, J. (2016). Chemical effects of air plasma species on aqueous solutes in direct and delayed exposure modes: discharge, post-discharge and plasma activated water. *Plasma Chemistry and Plasma Processing*, 36(2), 355-381.
- Bruggeman, P., Iza, F., Guns, P., Lauwers, D., Kong, M. G., Gonzalvo, Y. A., Leys, C., & Schram, D. C. (2009). Electronic quenching of OH (A) by water in atmospheric pressure plasmas and its influence on the gas temperature determination by OH (A–X) emission. *Plasma Sources Science and Technology*, 19(1), 015016.
- Bullerman, L. B., & Bianchini, A. (2007, 2007/10/20/). Stability of mycotoxins during food processing. *International Journal of Food Microbiology*, 119(1), 140-146. <https://doi.org/https://doi.org/10.1016/j.ijfoodmicro.2007.07.035>
- Butscher, D., Van Loon, H., Waskow, A., von Rohr, P. R., & Schuppler, M. (2016). Plasma inactivation of microorganisms on sprout seeds in a dielectric barrier discharge. *International Journal of Food Microbiology*, 238, 222-232.
- Butscher, D., Zimmermann, D., Schuppler, M., & von Rohr, P. R. (2016). Plasma inactivation of bacterial endospores on wheat grains and polymeric model substrates in a dielectric barrier discharge. *Food Control*, 60, 636-645.
- Canadian Food Inspection Agency. (2022). *Section 1: Mycotoxins in Livestock Feed*. Retrieved April 26 from <https://inspection.canada.ca/animal-health/livestock-feeds/regulatory-guidance/rg-8/eng/1347383943203/1347384015909?chap=1>
- Chain, E. P. o. C. i. t. F. (2011). Scientific Opinion on the risks for public health related to the presence of zearalenone in food. *EFSA Journal*, 9(6), 2197.
- Chain, E. Panel o. C. i. t. F., Knutsen, H.-K., Alexander, J., Barregård, L., Bignami, M., Brüschweiler, B., Ceccatelli, S., Cottrill, B., Dinovi, M., Edler, L., Grasl-Kraupp, B., Hogstrand, C., Hoogenboom, L., Nebbia, C. S., Petersen, A., Rose, M., Roudot, A.-C., Schwerdtle, T., Vleminckx, C., Vollmer, G., Wallace, H., Dall'Asta, C., Dänicke, S., Eriksen, G.-S., Altieri, A., Roldán-Torres, R., & Oswald, I. P. (2017, 2017/07/01). Risks for animal health related to the presence of zearalenone and its modified forms in feed. *EFSA Journal*, 15(7), e04851. <https://doi.org/10.2903/j.efsa.2017.4851>
- Chang, J.-S., Lawless, P. A., & Yamamoto, T. (1991). Corona discharge processes. *IEEE Transactions on plasma science*, 19(6), 1152-1166.

- Chang, M. B., & Wu, S.-J. (1997, 1997/01/01). Experimental Study on Ozone Synthesis via Dielectric Barrier Discharges. *Ozone: Science & Engineering*, 19(3), 241-254. <https://doi.org/10.1080/01919519708547304>
- Chaplot, S., Yadav, B., Jeon, B., & Roopesh, M. S. (2019). Atmospheric cold plasma and peracetic acid-based hurdle intervention to reduce Salmonella on raw poultry meat [Article]. *Journal of Food Protection*, 82(5), 878-888. <https://doi.org/10.4315/0362-028X.JFP-18-377>
- Chauvin, J., Judee, F., Merbahi, N., & Vicendo, P. (2018). Effects of plasma activated medium on head and neck FaDu cancerous cells: Comparison of 3D and 2D response. *Anti-Cancer Agents in Medicinal Chemistry (Formerly Current Medicinal Chemistry-Anti-Cancer Agents)*, 18(6), 776-783.
- Chen, B.-M., Wang, Z.-H., Li, S.-X., Wang, G.-X., Song, H.-X., & Wang, X.-N. (2004, 2004/09/01/). Effects of nitrate supply on plant growth, nitrate accumulation, metabolic nitrate concentration and nitrate reductase activity in three leafy vegetables. *Plant Science*, 167(3), 635-643. <https://doi.org/https://doi.org/10.1016/j.plantsci.2004.05.015>
- Chen, C., Li, F., Chen, H.-L., & Kong, M. G. (2017). Interaction between air plasma-produced aqueous IO₂ and the spin trap DMPO in electron spin resonance. *Physics of Plasmas*, 24(10), 103501.
- Chen, C. W., Lee, H.-M., & Chang, M. B. (2008). Inactivation of aquatic microorganisms by low-frequency AC discharges. *IEEE Transactions on Plasma Science*, 36(1), 215-219.
- Chen, D., Chen, P., Cheng, Y., Peng, P., Liu, J., Ma, Y., Liu, Y., & Ruan, R. (2018). Deoxynivalenol Decontamination in Raw and Germinating Barley Treated by Plasma-Activated Water and Intense Pulsed Light [Article in Press]. *Food and Bioprocess Technology*. <https://doi.org/10.1007/s11947-018-2206-2>
- Chen, X., Qiu, Y., Zhang, J., Guo, Y., Ding, Y., & Lyu, F. (2022, 2022/06/01/). Degradation efficiency and products of deoxynivalenol treated by cold plasma and its application in wheat. *Food Control*, 136, 108874. <https://doi.org/https://doi.org/10.1016/j.foodcont.2022.108874>
- Chigbo, E. O. J. (2016). Selected Physical Properties of Soybean In Relation To Storage Design. *International Journal of Engineering Research and Applications*, 6, 71-75.
- Chilaka, C. A., De Boevre, M., Atanda, O. O., & De Saeger, S. (2018, 2018/11/01). Stability of fumonisin B1, deoxynivalenol, zearalenone, and T-2 toxin during processing of traditional Nigerian beer and spices. *Mycotoxin Research*, 34(4), 229-239. <https://doi.org/10.1007/s12550-018-0318-1>

- Chiper, A. S., Chen, W., Mejlholm, O., Dalgaard, P., & Stamate, E. (2011, 2011/02/28). Atmospheric pressure plasma produced inside a closed package by a dielectric barrier discharge in Ar/CO₂ for bacterial inactivation of biological samples. *Plasma Sources Science and Technology*, 20(2), 025008. <https://doi.org/10.1088/0963-0252/20/2/025008>
- Coates, J. (2000). Interpretation of Infrared Spectra, A Practical Approach. In *Encyclopedia of Analytical Chemistry*. <https://doi.org/10.1002/9780470027318.a5606>
- Setting maximum levels for certain contaminants in foodstuffs, 20 L 364/5 (2006). <https://eur-lex.europa.eu/LexUriServ/LexUriServ.do?uri=OJ:L:2006:364:0005:0024:EN:PDF>
- Conrads, H., & Schmidt, M. (2000). Plasma generation and plasma sources. *Plasma Sources Science and Technology*, 9(4), 441.
- Cullen, P. J., Lalor, J., Scally, L., Boehm, D., Milosavljević, V., Bourke, P., & Keener, K. (2018). Translation of plasma technology from the lab to the food industry [Review]. *Plasma Processes and Polymers*, 15(2), Article 1700085. <https://doi.org/10.1002/ppap.201700085>
- Cullen, P. J., Misra, N., Han, L., Bourke, P., Keener, K., O'Donnell, C., Moiseev, T., Mosnier, J. P., & Milosavljević, V. (2014). Inducing a dielectric barrier discharge plasma within a package. *IEEE Transactions on Plasma Science*, 42(10), 2368-2369.
- De Angelis, E., Monaci, L., Pascale, M., & Visconti, A. (2013). Fate of deoxynivalenol, T-2 and HT-2 toxins and their glucoside conjugates from flour to bread: an investigation by high-performance liquid chromatography high-resolution mass spectrometry. *Food Additives & Contaminants: Part A*, 30(2), 345-355.
- Demeke, T., Gräfenhan, T., Clear, R. M., Phan, A., Ratnayaka, I., Chapados, J., Patrick, S. K., Gaba, D., Lévesque, C. A., & Seifert, K. A. (2010, Jun 30). Development of a specific TaqMan real-time PCR assay for quantification of *Fusarium graminearum* clade 7 and comparison of fungal biomass determined by PCR with deoxynivalenol content in wheat and barley. *International Journal of Food Microbiology*, 141(1-2), 45-50. <https://doi.org/10.1016/j.ijfoodmicro.2010.04.020>
- Deng, S., Ruan, R., Mok, C. K., Huang, G., Lin, X., & Chen, P. (2007). Inactivation of *Escherichia coli* on almonds using nonthermal plasma. *Journal of Food Science*, 72(2), M62-M66.
- Deng, X. T., Shi, J. J., Shama, G., & Kong, M. G. (2005). Effects of microbial loading and sporulation temperature on atmospheric plasma inactivation of *Bacillus subtilis* spores. *Applied Physics Letters*, 87(15), 153901. <https://doi.org/10.1063/1.2103394>

- Devi, Y., Thirumdas, R., Sarangapani, C., Deshmukh, R. R., & Annapure, U. S. (2017, 2017/07/01/). Influence of cold plasma on fungal growth and aflatoxins production on groundnuts. *Food Control*, 77, 187-191.
<https://doi.org/https://doi.org/10.1016/j.foodcont.2017.02.019>
- Di, L., Zhang, J., & Zhang, X. (2018). A review on the recent progress, challenges, and perspectives of atmospheric-pressure cold plasma for preparation of supported metal catalysts. *Plasma Processes and Polymers*, 15(5), 1700234.
- Dohlman, E. (2003). Mycotoxin hazards and regulations. *International Trade and Food Safety*, 97.
- Dominguez, R., & Holmes, K. C. (2011). Actin structure and function. *Annu Rev Biophys*, 40, 169-186. <https://doi.org/10.1146/annurev-biophys-042910-155359>
- Du, L., Jaya Prasad, A., Gänzle, M., & Roopesh, M. S. (2020, 2020/01/01/). Inactivation of Salmonella spp. in wheat flour by 395 nm pulsed light emitting diode (LED) treatment and the related functional and structural changes of gluten. *Food Research International*, 127, 108716. <https://doi.org/https://doi.org/10.1016/j.foodres.2019.108716>
- Edwards, S. G., Dickin, E. T., MacDonald, S., Buttler, D., Hazel, C. M., Patel, S., & Scudamore, K. A. (2011, 2011/12/01). Distribution of Fusarium mycotoxins in UK wheat mill fractions. *Food Additives & Contaminants: Part A*, 28(12), 1694-1704.
<https://doi.org/10.1080/19440049.2011.605770>
- Egitto, F. D., Vukanovic, V., & Taylor, G. N. (1990). 5 - Plasma Etching of Organic Polymers. In R. d'Agostino (Ed.), *Plasma Deposition, Treatment, and Etching of Polymers* (pp. 321-422). Academic Press. <https://doi.org/https://doi.org/10.1016/B978-0-12-200430-8.50011-7>
- Egorova, G., Voblikova, V., Sabitova, L., Tkachenko, I., Tkachenko, S., & Lunin, V. (2015). Ozone solubility in water. *Moscow University Chemistry Bulletin*, 70(5), 207-210.
- Ercan, U. K., Smith, J., Ji, H.-F., Brooks, A. D., & Joshi, S. G. (2016). Chemical changes in nonthermal plasma-treated N-Acetylcysteine (NAC) solution and their contribution to bacterial inactivation. *Scientific Reports*, 6, 20365.
- Ercan, U. K., Wang, H., Ji, H., Fridman, G., Brooks, A. D., & Joshi, S. G. (2013). Nonequilibrium Plasma-Activated Antimicrobial Solutions are Broad-Spectrum and Retain their Efficacies for Extended Period of Time. *Plasma processes and polymers*, 10(6), 544-555.

- Estifae, P., Su, X., Yannam, S. K., Rogers, S., & Thagard, S. M. (2019, 2019/02/20). Mechanism of *E. coli* Inactivation by Direct-in-liquid Electrical Discharge Plasma in Low Conductivity Solutions. *Scientific Reports*, *9*(1), 2326. <https://doi.org/10.1038/s41598-019-38838-7>
- Falkenstein, Z. (1997). The influence of ultraviolet illumination on OH formation in dielectric barrier discharges of Ar/O₂/H₂O: The Joshi effect. *Journal of Applied Physics*, *81*(11), 7158-7162.
- Falkenstein, Z., & Coogan, J. J. (1997). Microdischarge behaviour in the silent discharge of nitrogen-oxygen and water-air mixtures. *Journal of Physics D: Applied Physics*, *30*(5), 817.
- Faltusová, Z., Vaculová, K., Pavel, J., Svobodová, I., Hajšlová, J., & Ovesná, J. (2019). Fusarium culmorum Tri genes and barley HvugT13248 gene transcription in infected barley cultivars. *Plant Protection Science*, *55*(3), 172-180.
- Fang, H., Zhang, C., Sun, A., Man, C., Zhang, Q., Kuang, Y., Wang, K., Liu, A., & Shao, T. (2022, 2022/03/18). Effect of Reactive Chemical Species on the Degradation of Deoxynivalenol, 3-Acetyldeoxynivalenol, and 15-Acetyldeoxynivalenol in Low-Temperature Plasmas. *ACS Food Science & Technology*, *2*(3), 558-567. <https://doi.org/10.1021/acsfoodscitech.1c00445>
- FAO. (2003). *Mycotoxin regulations in 2003 and current developments*. Retrieved April 27, 2021 from <http://www.fao.org/3/y5499e/y5499e07.htm>
- Feizollahi, E., Arshad, M., Yadav, B., Ullah, A., & Roopesh, M. S. (2020, 2020/08/07). Degradation of Deoxynivalenol by Atmospheric-Pressure Cold Plasma and Sequential Treatments with Heat and UV Light. *food engineering reviews*. <https://doi.org/10.1007/s12393-020-09241-0>
- Feizollahi, E., Iqdam, B., Vasanthan, T., Thilakarathna, M. S., & Roopesh, M. (2020). Effects of atmospheric-pressure cold plasma treatment on deoxynivalenol degradation, quality parameters, and germination of barley grains. *Applied Sciences*, *10*(10), 3530. <https://doi.org/10.3390/app10103530>
- Feizollahi, E., & Roopesh, M. S. (2021). Mechanisms of deoxynivalenol (DON) degradation during different treatments: a review. *Critical Reviews in Food Science and Nutrition*, 1-22. <https://doi.org/10.1080/10408398.2021.1895056>

- Fernandez, A., Shearer, N., Wilson, D., & Thompson, A. (2012). Effect of microbial loading on the efficiency of cold atmospheric gas plasma inactivation of *Salmonella enterica* serovar Typhimurium. *International Journal of Food Microbiology*, 152(3), 175-180.
- Ferreira, C. D., Lang, G. H., Lindemann, I. d. S., Timm, N. d. S., Hoffmann, J. F., Ziegler, V., & de Oliveira, M. (2021, 2021/03/01/). Postharvest UV-C irradiation for fungal control and reduction of mycotoxins in brown, black, and red rice during long-term storage. *Food Chemistry*, 339, 127810. <https://doi.org/https://doi.org/10.1016/j.foodchem.2020.127810>
- Filatova, I., Azharonok, V., Lushkevich, V., Zhukovsky, A., Gadzhieva, G., Spasic, K., Zivkovic, S., Puac, N., Lazovic, S., & Malovic, G. (2013). Plasma seeds treatment as a promising technique for seed germination improvement. 31st international conference on phenomena in ionized gases, Granada, Spain,
- Filatova, I., Azharonok, V., Shik, A., Antoniuk, A., & Terletskaia, N. (2012). Fungicidal effects of plasma and radio-wave pre-treatments on seeds of grain crops and legumes. In *Plasma for bio-decontamination, medicine and food security* (pp. 469-479). Springer.
- Floyd, R. A., & Soong, L. M. (1977, 1977/01/10/). Spin trapping in biological systems. Oxidation of the spin trap 5,5-dimethyl-1-pyrroline-1-oxide by a hydroperoxide-hematin system. *Biochemical and Biophysical Research Communications*, 74(1), 79-84. [https://doi.org/https://doi.org/10.1016/0006-291X\(77\)91377-8](https://doi.org/https://doi.org/10.1016/0006-291X(77)91377-8)
- Fouler, S. G., Trivedi, A. B., & Kitabatake, N. (1994). Detoxification of citrinin and ochratoxin A by hydrogen peroxide. *Journal of AOAC International*, 77(3), 631-637.
- Fox, G. P., Panozzo, J. F., Li, C. D., Lance, R. C. M., Inkerman, P. A., & Henry, R. J. (2003). Molecular basis of barley quality. *Australian Journal of Agricultural Research*, 54(12), 1081-1101. <https://doi.org/https://doi.org/10.1071/AR02237>
- Freitas-Silva, O., & Venâncio, A. (2010). Ozone applications to prevent and degrade mycotoxins: a review. *Drug Metabolism Reviews*, 42(4), 612-620.
- Fridman, A. (2008). *Plasma chemistry*. Cambridge university press.
- Fu, Y., Toyoda, K., & Ihara, I. (2014). Application of ATR-FTIR spectroscopy and principal component analysis in characterization of 15-acetyldeoxynivalenol in corn oil [Article]. *Engineering in Agriculture, Environment and Food*, 7(4), 163-168. <https://doi.org/10.1016/j.eaef.2014.07.001>
- Fung, F., & Clark, R. F. (2004). Health effects of mycotoxins: a toxicological overview. *Journal of Toxicology: Clinical Toxicology*, 42(2), 217-234.

- Gadkari, S., & Gu, S. (2017). Numerical investigation of co-axial DBD: Influence of relative permittivity of the dielectric barrier, applied voltage amplitude, and frequency. *Physics of Plasmas*, 24(5), 053517. <https://doi.org/10.1063/1.4982657>
- Gao, Y., Li, M., Sun, C., & Zhang, X. (2022, 2022/10/15/). Microbubble-enhanced water activation by cold plasma. *Chemical Engineering Journal*, 446, 137318. <https://doi.org/https://doi.org/10.1016/j.cej.2022.137318>
- Garamoon, A., Elakshar, F., Nossair, A., & Kotp, E. (2002). Experimental study of ozone synthesis. *Plasma Sources Science and Technology*, 11(3), 254.
- Gášková, D., Sigler, K., Janderová, B., & Plášek, J. (1996, 1996/03/01/). Effect of high-voltage electric pulses on yeast cells: factors influencing the killing efficiency. *Bioelectrochemistry and Bioenergetics*, 39(2), 195-202. [https://doi.org/https://doi.org/10.1016/0302-4598\(95\)01892-1](https://doi.org/https://doi.org/10.1016/0302-4598(95)01892-1)
- Geyter, N. D., & Morent, R. (2012). Nonthermal Plasma Sterilization of Living and Nonliving Surfaces. *Annual Review of Biomedical Engineering*, 14(1), 255-274. <https://doi.org/10.1146/annurev-bioeng-071811-150110>
- Ghomi, H., Safa, N. N., Ramezani, K., & Karimi, M. (2009, 26-31 July). Bacterial inactivation by DBD plasma in atmospheric pressure. Ispc conference, paper (<http://www.ispc-conference.org/ispcproc/papers/169.pdf>), Bochum, Germany.
- Grainge, G., Nakabayashi, K., Steinbrecher, T., Kennedy, S., Ren, J., Iza, F., & Leubner-Metzger, G. (2022). Molecular mechanisms of seed dormancy release by gas plasma-activated water technology. *Journal of Experimental Botany*, 73(12), 4065-4078. <https://doi.org/10.1093/jxb/erac150>
- Guerre, P. (2016). Worldwide Mycotoxins Exposure in Pig and Poultry Feed Formulations. *Toxins*, 8(12), 350. <https://doi.org/10.3390/toxins8120350>
- Guo, J., Qin, D., Li, W., Wu, F., Li, L., & Liu, X. (2021). Inactivation of *Penicillium italicum* on kumquat via plasma-activated water and its effects on quality attributes. *International Journal of Food Microbiology*, 343, 109090.
- Guo, J., Wang, J., Xie, H., Jiang, J., Li, C., Li, W., Li, L., Liu, X., & Lin, F. (2021). Inactivation effects of plasma-activated water on *Fusarium graminearum*. *Food Control*, 108683.
- Guragain, R. P., Pradhan, S. P., Baniya, H. B., Pandey, B. P., Basnet, N., Sedhai, B., Dhungana, S., Chhetri, G. K., Joshi, U. M., & Subedi, D. P. (2021, 2021/12/29). Impact of Plasma-

- Activated Water (PAW) on Seed Germination of Soybean. *Journal of Chemistry*, 2021, 7517052. <https://doi.org/10.1155/2021/7517052>
- Guzel-Seydim, Z. B., Greene, A. K., & Seydim, A. (2004). Use of ozone in the food industry. *LWT-Food Science and Technology*, 37(4), 453-460.
- Hafez, M., Abdelmagid, A., Adam, L. R., & Daayf, F. (2020, Apr). Specific Detection and Identification of *Fusarium graminearum* Sensus Stricto Using a PCR-RFLP Tool and Specific Primers Targeting the Translational Elongation Factor 1 α Gene. *Plant Disease*, 104(4), 1076-1086. <https://doi.org/10.1094/pdis-03-19-0572-re>
- Han, L., Boehm, D., Amias, E., Milosavljević, V., Cullen, P. J., & Bourke, P. (2016, 2016/12/01/). Atmospheric cold plasma interactions with modified atmosphere packaging inducer gases for safe food preservation. *Innovative Food Science & Emerging Technologies*, 38, 384-392. <https://doi.org/https://doi.org/10.1016/j.ifset.2016.09.026>
- He, J., Zhou, T., Young, J. C., Boland, G. J., & Scott, P. M. (2010). Chemical and biological transformations for detoxification of trichothecene mycotoxins in human and animal food chains: a review. *Trends in Food Science & Technology*, 21(2), 67-76.
- Henriques, A. O., & Moran, C. P., Jr. (2007). Structure, assembly, and function of the spore surface layers. *Annual Review of Microbiology*, 61, 555-588. <https://doi.org/10.1146/annurev.micro.61.080706.093224>
- Hossain, M. A., Bhattacharjee, S., Armin, S.-M., Qian, P., Xin, W., Li, H.-Y., Burritt, D. J., Fujita, M., & Tran, L.-S. P. (2015, 2015-June-16). Hydrogen peroxide priming modulates abiotic oxidative stress tolerance: insights from ROS detoxification and scavenging [Review]. *Frontiers in plant science*, 6. <https://doi.org/10.3389/fpls.2015.00420>
- House, J. D., Nyachoti, C. M., & Abramson, D. (2003, 2003/08/01). Deoxynivalenol Removal from Barley Intended as Swine Feed through the Use of an Abrasive Pearling Procedure. *Journal of Agricultural and Food Chemistry*, 51(17), 5172-5175. <https://doi.org/10.1021/jf034244p>
- Hu, M., & Guo, Y. (2012, 2012/08). The Effect of Air Plasma on Sterilization of *Escherichia coli* in Dielectric Barrier Discharge. *Plasma Science and Technology*, 14(8), 735-740. <https://doi.org/10.1088/1009-0630/14/8/10>
- Humpf, H. U., & Voss, K. A. (2004). Effects of thermal food processing on the chemical structure and toxicity of fumonisin mycotoxins [Review]. *Molecular Nutrition and Food Research*, 48(4), 255-269. <https://doi.org/10.1002/mnfr.200400033>

- Hygreeva, D., Pandey, M., & Radhakrishna, K. (2014). Potential applications of plant based derivatives as fat replacers, antioxidants and antimicrobials in fresh and processed meat products. *Meat Science*, 98(1), 47-57.
- Iqbal, M., & Turner, M. (2015). Influence of gap spacing between dielectric barriers in atmospheric pressure discharges. *Contributions to Plasma Physics*, 55(6), 444-458.
- Jacob, H. E., Förster, W., & Berg, H. (1981). Microbiological implications of electric field effects II. Inactivation of yeast cells and repair of their cell envelope. *Zeitschrift für Allgemeine Mikrobiologie*, 21(3), 225-233.
- Jalili, M., Jinap, S., & Son, R. (2011, 2011/04/01). The effect of chemical treatment on reduction of aflatoxins and ochratoxin A in black and white pepper during washing. *Food Additives & Contaminants: Part A*, 28(4), 485-493. <https://doi.org/10.1080/19440049.2010.551300>
- Jauković, M., Stanišić, N., Nikodijević, B., & Krnjaja, V. (2014). Effects of temperature and time on deoxynivalenol (DON) and zearalenone (ZON) content in corn. *Zbornik Matice srpske za prirodne nauke*(126), 25-34.
- Jiayun, T., Rui, H., Xiaoli, Z., Ruoting, Z., Weiwen, C., & Size, Y. (2014). Effects of atmospheric pressure air plasma pretreatment on the seed germination and early growth of *Andrographis paniculata*. *Plasma Science and Technology*, 16(3), 260.
- Jirešová, J., Scholtz, V., Julák, J., & Šerá, B. (2022). Comparison of the Effect of Plasma-Activated Water and Artificially Prepared Plasma-Activated Water on Wheat Grain Properties. *Plants*, 11(11), 1471.
- Jo, A., Joh, H. M., Chung, J., & Chung, T. (2020). Cell viability and measurement of reactive species in gas-and liquid-phase exposed by a microwave-excited atmospheric pressure argon plasma jet. *Current Applied Physics*, 20(4), 562-571.
- Jo, Y.-K., Cho, J., Tsai, T.-C., Staack, D., Kang, M.-H., Roh, J.-H., Shin, D.-B., Cromwell, W., & Gross, D. (2014). A Non-thermal plasma seed treatment method for management of a seedborne fungal pathogen on rice seed. *Crop Science*, 54(2), 796-803.
- Joint FAO WHO Expert Committee on Food Additives. (2002). *Safety evaluation of certain mycotoxins in food: fifty-sixth report of the Joint FAO/WHO Expert Committee on Food Additives*. World Health Organization.
- Judée, F., Simon, S., Bailly, C., & Dufour, T. (2018, 2018/04/15/). Plasma-activation of tap water using DBD for agronomy applications: Identification and quantification of long

- lifetime chemical species and production/consumption mechanisms. *Water Research*, 133, 47-59. <https://doi.org/https://doi.org/10.1016/j.watres.2017.12.035>
- Julák, J., Hujacová, A., Scholtz, V., Khun, J., & Holada, K. (2018). Contribution to the chemistry of plasma-activated water. *Plasma Physics Reports*, 44(1), 125-136.
- Kamgang-Youbi, G., Herry, J.-M., Brisset, J.-L., Bellon-Fontaine, M.-N., Doubla, A., & Naïtali, M. (2008). Impact on disinfection efficiency of cell load and of planktonic/adherent/detached state: case of *Hafnia alvei* inactivation by plasma activated water. *Applied Microbiology and Biotechnology*, 81(3), 449-457.
- Kamle, M., Mahato, D. K., Gupta, A., Pandhi, S., Sharma, B., Dhawan, K., Vasundhara, Mishra, S., Kumar, M., Tripathi, A. D., Rasane, P., Selvakumar, R., Kumar, A., Gamlath, S., & Kumar, P. (2022). Deoxynivalenol: An Overview on Occurrence, Chemistry, Biosynthesis, Health Effects and Its Detection, Management, and Control Strategies in Food and Feed. *Microbiology Research*, 13(2), 292-314. <https://www.mdpi.com/2036-7481/13/2/23>
- Karlovsky, P., Suman, M., Berthiller, F., De Meester, J., Eisenbrand, G., Perrin, I., Oswald, I. P., Speijers, G., Chiodini, A., Recker, T., & Dussort, P. (2016, 2016/11/01). Impact of food processing and detoxification treatments on mycotoxin contamination. *Mycotoxin Research*, 32(4), 179-205. <https://doi.org/10.1007/s12550-016-0257-7>
- Kaur, M., Huberli, D., & Bayliss, K. (2022). A protocol for the use of cold plasma treatment to inhibit in vitro growth of *Fusarium graminearum*. *bioRxiv*.
- Kaushik, N. K., Ghimire, B., Li, Y., Adhikari, M., Veerana, M., Kaushik, N., Jha, N., Adhikari, B., Lee, S.-J., & Masur, K. (2018). Biological and medical application of plasma-activated media, water and solutions. *Biological Chemistry*.
- Khaneghah, A. M., Martins, L. M., von Hertwig, A. M., Bertoldo, R., & Sant'Ana, A. S. (2018, 2018/01/01/). Deoxynivalenol and its masked forms: Characteristics, incidence, control and fate during wheat and wheat based products processing - A review. *Trends in Food Science & Technology*, 71, 13-24. <https://doi.org/https://doi.org/10.1016/j.tifs.2017.10.012>
- Kim, J.-S., Lee, E.-J., & Kim, Y.-J. (2014). Inactivation of *Campylobacter jejuni* with dielectric barrier discharge plasma using air and nitrogen gases. *Foodborne Pathogens and Disease*, 11(8), 645-651.
- Kim, S. H., & Vujanovic, V. (2017). Biodegradation and biodetoxification of Fusarium mycotoxins by *Sphaerodes mycoparasitica* [Article]. *AMB Express*, 7(1), Article 145. <https://doi.org/10.1186/s13568-017-0446-6>

- Kimura, M., Tokai, T., Takahashi-Ando, N., Ohsato, S., & Fujimura, M. (2007). Molecular and genetic studies of *Fusarium trichothecene* biosynthesis: pathways, genes, and evolution. *Bioscience, biotechnology, and biochemistry*, 0707310525-0707310525.
- Klämpfl, T. G., Isbary, G., Shimizu, T., Li, Y.-F., Zimmermann, J. L., Stolz, W., Schlegel, J., Morfill, G. E., & Schmidt, H.-U. (2012). Cold Atmospheric Air Plasma Sterilization against Spores and Other Microorganisms of Clinical Interest. *Applied and Environmental Microbiology*, 78(15), 5077-5082. <https://doi.org/10.1128/aem.00583-12>
- Klockow, P. A., & Keener, K. M. (2009). Safety and quality assessment of packaged spinach treated with a novel ozone-generation system. *LWT-Food Science and Technology*, 42(6), 1047-1053.
- Kogelschatz, U. (2003). Dielectric-barrier discharges: their history, discharge physics, and industrial applications. *Plasma Chemistry and Plasma Processing*, 23(1), 1-46.
- Kong, M. G., Kroesen, G., Morfill, G., Nosenko, T., Shimizu, T., Van Dijk, J., & Zimmermann, J. (2009). Plasma medicine: an introductory review. *new Journal of Physics*, 11(11), 115012.
- Kostoláni, D., Ndiffo Yemeli, G. B., Švubová, R., Kyzek, S., & Machala, Z. (2021). Physiological responses of young pea and barley seedlings to plasma-activated water. *Plants*, 10(8), 1750.
- Kostov, K. G., Honda, R. Y., Alves, L. M. S., & Kayama, M. E. (2009). Characteristics of dielectric barrier discharge reactor for material treatment. *Brazilian Journal of Physics*, 39, 322-325. http://www.scielo.br/scielo.php?script=sci_arttext&pid=S0103-97332009000300015&nrm=iso
- Kříž, P., Bartoš, P., Havelka, Z., Kadlec, J., Olšan, O., Špatenka, P., & Dienstbier, M. (2015). Influence of plasma treatment in open air on mycotoxin content and grain nutrients [Article]. *Plasma Medicine*, 5(2-4), 145-158. <https://doi.org/10.1615/PlasmaMed.2016015752>
- Krstović, S., Krulj, J., Jakšić, S., Bočarov-Stančić, A., & Jajić, I. (2020). Ozone as decontaminating agent for ground corn containing deoxynivalenol, zearalenone, and ochratoxin A [Article]. *Cereal Chemistry*. <https://doi.org/10.1002/cche.10289>
- Laroussi, M., & Leipold, F. (2004). Evaluation of the roles of reactive species, heat, and UV radiation in the inactivation of bacterial cells by air plasmas at atmospheric pressure. *International Journal of Mass Spectrometry*, 233(1-3), 81-86.

- Laroussi, M., Schoenbach, K., Kogelschatz, U., Vidmar, R., Kuo, S., Schmidt, M., Behnke, J., Yukimura, K., & Stoffels, E. (2005). Current applications of atmospheric pressure air plasmas. In *Non-Equilibrium Air Plasmas at Atmospheric Pressure, Series in Plasma Physics* (pp. 537-672). Institute of Physics Publishing.
- Laurita, R., Barbieri, D., Gherardi, M., Colombo, V., & Lukes, P. (2015). Chemical analysis of reactive species and antimicrobial activity of water treated by nanosecond pulsed DBD air plasma. *Clinical Plasma Medicine*, 3(2), 53-61.
- Lee, G. J., Sim, G. B., Choi, E. H., Kwon, Y.-W., Kim, J. Y., Jang, S., & Kim, S. H. (2015). Optical and structural properties of plasma-treated *Cordyceps bassiana* spores as studied by circular dichroism, absorption, and fluorescence spectroscopy. *Journal of Applied Physics*, 117(2), 023303.
- Leipold, F., Schultz-Jensen, N., Kusano, Y., Bindslev, H., & Jacobsen, T. (2011). Decontamination of objects in a sealed container by means of atmospheric pressure plasmas. *Food Control*, 22(8), 1296-1301.
- Leslie, J. F., & Summerell, B. A. (2008). *The Fusarium laboratory manual*. Blackwell Publishing Ltd.
- Li, M., Guan, E., & Bian, K. (2015). Effect of ozone treatment on deoxynivalenol and quality evaluation of ozonised wheat. *Food Additives & Contaminants: Part A*, 32(4), 544-553.
- Li, M., Guan, E., & Bian, K. (2019). Structure elucidation and toxicity analysis of the degradation products of deoxynivalenol by gaseous ozone [Article]. *Toxins*, 11(8), Article 474. <https://doi.org/10.3390/toxins11080474>
- Li, M., Yan, Y., Jin, Q., Liu, M., Zhu, B., Wang, L., Li, T., Tang, X.-J., & Zhu, Y.-M. (2018). Experimental study on ozone generation from oxygen in double surface dielectric barrier discharge. *Vacuum*, 157, 249-258.
- Li, X., Li, W., Cai, Y., Shi, Y., Xu, H., Gu, L., & Pu, X. (2016). Comparative analysis on characteristics in non-thermal plasma reactor with oxygen and air. *Transactions of the Chinese Society of Agricultural Engineering*, 32(11), 103-108.
- Liao, X., Li, J., Muhammad, A. I., Suo, Y., Chen, S., Ye, X., Liu, D., & Ding, T. (2018). Application of a Dielectric Barrier Discharge Atmospheric Cold Plasma (Dbd-Acp) for *Eshcherichia Coli* Inactivation in Apple Juice. *Journal of Food Science*, 83(2), 401-408.

- Liao, X., Liu, D., Xiang, Q., Ahn, J., Chen, S., Ye, X., & Ding, T. (2017). Inactivation mechanisms of non-thermal plasma on microbes: a review. *Food Control*, 75, 83-91.
- Liao, X., Xiang, Q., Liu, D., Chen, S., Ye, X., & Ding, T. (2017). Lethal and sublethal effect of a dielectric barrier discharge atmospheric cold plasma on *Staphylococcus aureus*. *Journal of Food Protection*, 80(6), 928-932.
- Lim, C. W., Tai, S. H., Lee, L. M., & Chan, S. H. (2012, July 01). Analytical method for the accurate determination of tricothecenes in grains using LC-MS/MS: a comparison between MRM transition and MS3 quantitation [journal article]. *Analytical and Bioanalytical Chemistry*, 403(10), 2801-2806. <https://doi.org/10.1007/s00216-011-5558-2>
- Liu, D. X., Liu, Z. C., Chen, C., Yang, A. J., Li, D., Rong, M. Z., Chen, H. L., & Kong, M. G. (2016, 2016/04/01). Aqueous reactive species induced by a surface air discharge: Heterogeneous mass transfer and liquid chemistry pathways. *Scientific Reports*, 6(1), 23737. <https://doi.org/10.1038/srep23737>
- Livak, K. J., & Schmittgen, T. D. (2001). Analysis of relative gene expression data using real-time quantitative PCR and the $2^{-\Delta\Delta CT}$ method. *Methods*, 25(4), 402-408.
- Locke, B. R., & Shih, K.-Y. (2011). Review of the methods to form hydrogen peroxide in electrical discharge plasma with liquid water. *Plasma Sources Science and Technology*, 20(3), 034006.
- Los, A., Ziuzina, D., Akkermans, S., Boehm, D., Cullen, P. J., Van Impe, J., & Bourke, P. (2018). Improving microbiological safety and quality characteristics of wheat and barley by high voltage atmospheric cold plasma closed processing [Article]. *Food Research International*, 106, 509-521. <https://doi.org/10.1016/j.foodres.2018.01.009>
- Los, A., Ziuzina, D., Boehm, D., Cullen, P. J., & Bourke, P. (2017). The potential of atmospheric air cold plasma for control of bacterial contaminants relevant to cereal grain production. *Innovative Food Science & Emerging Technologies*, 44, 36-45.
- Lu, P., Cullen, P. J., & Ostrikov, K. (2016). Chapter 4 - Atmospheric Pressure Nonthermal Plasma Sources. In N. N. Misra, O. Schlüter, & P. J. Cullen (Eds.), *Cold Plasma in Food and Agriculture* (pp. 83-116). Academic Press. <https://doi.org/https://doi.org/10.1016/B978-0-12-801365-6.00004-4>
- Lukes, P., Brisset, J.-L., & Locke, B. R. (2012). Biological effects of electrical discharge plasma in water and in gas-liquid environments. *Plasma chemistry and catalysis in gases and liquids*, 11(8), 309-352.

- Ma, R., Wang, G., Tian, Y., Wang, K., Zhang, J., & Fang, J. (2015). Non-thermal plasma-activated water inactivation of food-borne pathogen on fresh produce. *Journal of Hazardous Materials*, 300, 643-651.
- Machala, Z., Janda, M., Hensel, K., Jedlovský, I., Leštinská, L., Foltin, V., Martišovits, V., & Morvova, M. (2007). Emission spectroscopy of atmospheric pressure plasmas for bio-medical and environmental applications. *Journal of Molecular Spectroscopy*, 243(2), 194-201.
- Machala, Z., Tarabová, B., Sersenová, D., Janda, M., & Hensel, K. (2018, 2018/11/09). Chemical and antibacterial effects of plasma activated water: correlation with gaseous and aqueous reactive oxygen and nitrogen species, plasma sources and air flow conditions. *Journal of Physics D: Applied Physics*, 52(3), 034002. <https://doi.org/10.1088/1361-6463/aae807>
- Maeda, Y., Igura, N., Shimoda, M., & Hayakawa, I. (2003). Inactivation of *Escherichia coli* K12 using atmospheric gas plasma produced from humidified working gas. *Acta Biotechnologica*, 23(4), 389-395.
- Mahnot, N. K., Mahanta, C. L., Keener, K. M., & Misra, N. (2019). Strategy to achieve a 5-log Salmonella inactivation in tender coconut water using high voltage atmospheric cold plasma (HVACP). *Food Chemistry*, 284, 303-311.
- Mandal, R., Singh, A., & Singh, A. P. (2018, 2018/07/26/). Recent developments in cold plasma decontamination technology in the food industry. *Trends in Food Science & Technology*, 80, 93-103. <https://doi.org/https://doi.org/10.1016/j.tifs.2018.07.014>
- Mayer, E., Novak, B., Springler, A., Schwartz-Zimmermann, H. E., Nagl, V., Reisinger, N., Hessenberger, S., & Schatzmayr, G. (2017). Effects of deoxynivalenol (DON) and its microbial biotransformation product deepoxy-deoxynivalenol (DOM-1) on a trout, pig, mouse, and human cell line. *Mycotoxin Research*, 33(4), 297-308. <https://doi.org/10.1007/s12550-017-0289-7>
- Mayolle, J. E., Lullien-Pellerin, V., Corbineau, F., Boivin, P., & Guillard, V. (2012, 2012/04/01/). Water diffusion and enzyme activities during malting of barley grains: A relationship assessment. *Journal of Food Engineering*, 109(3), 358-365. <https://doi.org/https://doi.org/10.1016/j.jfoodeng.2011.11.021>
- Mazandarani, A., Goudarzi, S., Ghafoorifard, H., & Eskandari, A. (2020). Evaluation of DBD Plasma Effects on Barley Seed Germination and Seedling Growth. *IEEE Transactions on Plasma Science*, 48(9), 3115-3121. <https://doi.org/10.1109/TPS.2020.3012909>

- McClurkin-Moore, J. D., Ileleji, K. E., & Keener, K. M. (2017). The Effect of High-Voltage Atmospheric Cold Plasma Treatment on the Shelf-Life of Distillers Wet Grains [Article]. *Food and Bioprocess Technology*, 10(8), 1431-1440. <https://doi.org/10.1007/s11947-017-1903-6>
- McCormick, S. P., Stanley, A. M., Stover, N. A., & Alexander, N. J. (2011). Trichothecenes: from simple to complex mycotoxins. *Toxins*, 3(7), 802-814.
- Miao, C., Liu, F., Wang, Q., Cai, M., & Fang, Z. (2018). Investigation on the influence of electrode geometry on characteristics of coaxial dielectric barrier discharge reactor driven by an oscillating microsecond pulsed power supply. *The European Physical Journal D*, 72(3), 57.
- Miao, H., & Yun, G. (2011). The sterilization of *Escherichia coli* by dielectric-barrier discharge plasma at atmospheric pressure. *Applied Surface Science*, 257(16), 7065-7070.
- Min, S. C., Roh, S. H., Niemira, B. A., Boyd, G., Sites, J. E., Fan, X., Sokorai, K., & Jin, T. Z. (2018). In-package atmospheric cold plasma treatment of bulk grape tomatoes for microbiological safety and preservation [Article]. *Food Research International*, 108, 378-386. <https://doi.org/10.1016/j.foodres.2018.03.033>
- Min, S. C., Roh, S. H., Niemira, B. A., Boyd, G., Sites, J. E., Uknalis, J., & Fan, X. (2017). In-package inhibition of *E. coli* O157: H7 on bulk Romaine lettuce using cold plasma. *Food Microbiology*, 65, 1-6.
- Mishra, S., Dixit, S., Dwivedi, P. D., Pandey, H. P., & Das, M. (2014). Influence of temperature and pH on the degradation of deoxynivalenol (DON) in aqueous medium: comparative cytotoxicity of DON and degraded product. *Food Additives & Contaminants: Part A*, 31(1), 121-131.
- Mishra, S., Srivastava, S., Dewangan, J., Divakar, A., & Kumar Rath, S. (2020, 2020/04/27). Global occurrence of deoxynivalenol in food commodities and exposure risk assessment in humans in the last decade: a survey. *Critical Reviews in Food Science and Nutrition*, 60(8), 1346-1374. <https://doi.org/10.1080/10408398.2019.1571479>
- Misra, N., Moiseev, T., Patil, S., Pankaj, S., Bourke, P., Mosnier, J., Keener, K., & Cullen, P. (2014). Cold plasma in modified atmospheres for post-harvest treatment of strawberries. *Food and Bioprocess Technology*, 7(10), 3045-3054.
- Misra, N., Schlüter, O., & Cullen, P. (2016). Plasma in food and agriculture. In *Cold plasma in food and agriculture* (pp. 1-16). Elsevier.

- Misra, N., Schlüter, O., & Cullen, P. J. (2016). *Cold plasma in food and agriculture: fundamentals and applications*. Academic Press.
- Misra, N., Tiwari, B., Raghavarao, K., & Cullen, P. (2011). Nonthermal plasma inactivation of food-borne pathogens. *food engineering reviews*, 3(3-4), 159-170.
- Misra, N., Yadav, B., Roopesh, M., & Jo, C. (2019). Cold Plasma for Effective Fungal and Mycotoxin Control in Foods: Mechanisms, Inactivation Effects, and Applications. *Comprehensive Reviews in Food Science and Food Safety*, 18(1), 106-120. <https://doi.org/10.1111/1541-4337.12398>
- Misra, N., Ziuzina, D. D., Cullen, P. J., & Keener, K. M. (2012). Characterization of a novel cold atmospheric air plasma system for treatment of packaged liquid food products. 2012 Dallas, Texas, July 29-August 1, 2012,
- Misra, N. N., & Jo, C. (2017, 2017/06/01/). Applications of cold plasma technology for microbiological safety in meat industry. *Trends in Food Science & Technology*, 64, 74-86. <https://doi.org/https://doi.org/10.1016/j.tifs.2017.04.005>
- Misra, N. N., Schlüter, O., & Cullen, P. J. (2016). Chapter 1 - Plasma in Food and Agriculture. In N. N. Misra, O. Schlüter, & P. J. Cullen (Eds.), *Cold Plasma in Food and Agriculture* (pp. 1-16). Academic Press. <https://doi.org/https://doi.org/10.1016/B978-0-12-801365-6.00001-9>
- Misra, N. N., Yadav, B., Roopesh, M. S., & Jo, C. (2019). Cold Plasma for Effective Fungal and Mycotoxin Control in Foods: Mechanisms, Inactivation Effects, and Applications. *Comprehensive Reviews in Food Science and Food Safety*, 18(1), 106-120. <https://doi.org/10.1111/1541-4337.12398>
- Misra, N. N., Yopez, X., Xu, L., & Keener, K. (2019, 2019/03/01/). In-package cold plasma technologies. *Journal of Food Engineering*, 244, 21-31. <https://doi.org/https://doi.org/10.1016/j.jfoodeng.2018.09.019>
- Moreau, M., Lescure, G., Agoulon, A., Svinareff, P., Orange, N., & Feuilleley, M. (2013). Application of the pulsed light technology to mycotoxin degradation and inactivation [Article]. *Journal of Applied Toxicology*, 33(5), 357-363. <https://doi.org/10.1002/jat.1749>
- Morfill, G., Kong, M. G., & Zimmermann, J. (2009). Focus on plasma medicine. *New Journal of Physics*, 11(11), 115011.
- Morgan, N. (2009). Atmospheric pressure dielectric barrier discharge chemical and biological applications. *International Journal of Physical Sciences*, 4(13), 885-892.

- Morgan, N., Elsabbagh, M., Desoky, S., & Garamoon, A. (2009). Deactivation of yeast by dielectric barrier discharge. *The European Physical Journal-Applied Physics*, *46*(3), Article 31001.
- Mousavi Khaneghah, A., Fakhri, Y., Gahrui, H. H., Niakousari, M., & Sant'Ana, A. S. (2019, 2019/09/01/). Mycotoxins in cereal-based products during 24 years (1983–2017): A global systematic review. *Trends in Food Science & Technology*, *91*, 95-105. <https://doi.org/https://doi.org/10.1016/j.tifs.2019.06.007>
- Müller, K., Linkies, A., Vreeburg, R. A. M., Fry, S. C., Krieger-Liszkay, A., & Leubner-Metzger, G. (2009). In vivo Cell Wall Loosening by Hydroxyl Radicals during Cress Seed Germination and Elongation Growth. *Plant Physiology*, *150*(4), 1855-1865. <http://www.jstor.org/login.ezproxy.library.ualberta.ca/stable/40537901>
- Muranyi, P., Wunderlich, J., & Heise, M. (2007). Sterilization efficiency of a cascaded dielectric barrier discharge. *Journal of Applied Microbiology*, *103*(5), 1535-1544.
- Muranyi, P., Wunderlich, J., & Heise, M. (2008). Influence of relative gas humidity on the inactivation efficiency of a low temperature gas plasma. *Journal of Applied Microbiology*, *104*(6), 1659-1666.
- Murata, H., Mitsumatsu, M., & Shimada, N. (2008, 2008/09/01). Reduction of feed-contaminating mycotoxins by ultraviolet irradiation: an in vitro study. *Food Additives & Contaminants: Part A*, *25*(9), 1107-1110. <https://doi.org/10.1080/02652030802057343>
- Nakagawa, H., Ohmichi, K., Sakamoto, S., Sago, Y., Kushiro, M., Nagashima, H., Yoshida, M., & Nakajima, T. (2011). Detection of a new Fusarium masked mycotoxin in wheat grain by high-resolution LC–Orbitrap™ MS. *Food Additives & Contaminants: Part A*, *28*(10), 1447-1456.
- Nikiforov, A. Y., Sarani, A., & Leys, C. (2011). The influence of water vapor content on electrical and spectral properties of an atmospheric pressure plasma jet. *Plasma Sources Science and Technology*, *20*(1), 015014.
- Oehmigen, K., Hähnel, M., Brandenburg, R., Wilke, C., Weltmann, K. D., & Von Woedtke, T. (2010). The role of acidification for antimicrobial activity of atmospheric pressure plasma in liquids. *Plasma Processes and Polymers*, *7*(3-4), 250-257.
- Oehmigen, K., Winter, J., Hähnel, M., Wilke, C., Brandenburg, R., Weltmann, K. D., & von Woedtke, T. (2011). Estimation of possible mechanisms of Escherichia coli inactivation by plasma treated sodium chloride solution. *Plasma Processes and Polymers*, *8*(10), 904-913.

- Olaimat, A. N., & Holley, R. A. (2012). Factors influencing the microbial safety of fresh produce: a review. *Food Microbiology*, 32(1), 1-19.
- Oliveira, M., Viñas, I., Anguera, M., & Abadias, M. (2012). Fate of *Listeria monocytogenes* and *Escherichia coli* O157: H7 in the presence of natural background microbiota on conventional and organic lettuce. *Food Control*, 25(2), 678-683.
- Omurtag, G. Z., & Beyoğlu, D. (2007). Occurrence of deoxynivalenol (vomitoxin) in beer in Turkey detected by HPLC. *Food Control*, 18(2), 163-166.
- Ouellette, R. J., & Rawn, J. D. (2015). 3 - Introduction to Organic Reaction Mechanisms. In R. J. Ouellette & J. D. Rawn (Eds.), *Organic Chemistry Study Guide* (pp. 31-46). Elsevier. <https://doi.org/https://doi.org/10.1016/B978-0-12-801889-7.00003-0>
- Ozkan, A., Dufour, T., Bogaerts, A., & Reniers, F. (2016, 2016/06/30). How do the barrier thickness and dielectric material influence the filamentary mode and CO₂ conversion in a flowing DBD? *Plasma Sources Science and Technology*, 25(4), 045016. <https://doi.org/10.1088/0963-0252/25/4/045016>
- Panwar, V., Aggarwal, A., Paul, S., Singh, V., Singh, P. K., Sharma, D., & Shaharan, M. (2016). Effect of temperature and pH on the growth of *Fusarium* spp. causing Fusarium head blight (FHB) in wheat. *South Asian J. Exp. Biol*, 6, 186-193.
- Parigger, C. G., Guan, G., & Hornkohl, J. O. (2003). Measurement and analysis of OH emission spectra following laser-induced optical breakdown in air. *Applied Optics*, 42(30), 5986-5991.
- Park, B. J., Takatori, K., Sugita-Konishi, Y., Kim, I. H., Lee, M. H., Han, D. W., Chung, K. H., Hyun, S. O., & Park, J. C. (2007). Degradation of mycotoxins using microwave-induced argon plasma at atmospheric pressure [Article]. *Surface and Coatings Technology*, 201(9-11 SPEC. ISS.), 5733-5737. <https://doi.org/10.1016/j.surfcoat.2006.07.092>
- Park, J. Y., & Lee, Y. N. (1988). Solubility and decomposition kinetics of nitrous acid in aqueous solution. *The Journal of Physical Chemistry*, 92(22), 6294-6302.
- Park, Y., Oh, K. S., Oh, J., Seok, D. C., Kim, S. B., Yoo, S. J., & Lee, M.-J. (2018a). The biological effects of surface dielectric barrier discharge on seed germination and plant growth with barley. *Plasma Processes and Polymers*, 15(2), 1600056. <https://doi.org/https://doi.org/10.1002/ppap.201600056>

- Park, Y., Oh, K. S., Oh, J., Seok, D. C., Kim, S. B., Yoo, S. J., & Lee, M. J. (2018b). The biological effects of surface dielectric barrier discharge on seed germination and plant growth with barley. *Plasma Processes and Polymers*, *15*(2), 1600056.
- Pasquali, F., Stratakos, A. C., Koidis, A., Berardinelli, A., Cevoli, C., Ragni, L., Mancusi, R., Manfreda, G., & Trevisani, M. (2016). Atmospheric cold plasma process for vegetable leaf decontamination: A feasibility study on radicchio (red chicory, *Cichorium intybus* L.). *Food Control*, *60*, 552-559.
- Pater, A., Zdaniewicz, M., Satora, P., Khachatryan, G., & Oszczęda, Z. (2020). Application of water treated with low-temperature low-pressure glow plasma for quality improvement of barley and malt. *Biomolecules*, *10*(2), 267.
- Patil, S., Moiseev, T., Misra, N. N., Cullen, P. J., Mosnier, J. P., Keener, K. M., & Bourke, P. (2014, 2014/11/01/). Influence of high voltage atmospheric cold plasma process parameters and role of relative humidity on inactivation of *Bacillus atrophaeus* spores inside a sealed package. *Journal of Hospital Infection*, *88*(3), 162-169. <https://doi.org/https://doi.org/10.1016/j.jhin.2014.08.009>
- Peiris, K. H. S., Bockus, W. W., & Dowell, F. E. (2012). Infrared spectral properties of germ, pericarp, and endosperm sections of sound wheat kernels and those damaged by fusarium graminearum [Article]. *Applied Spectroscopy*, *66*(9), 1053-1060. <https://doi.org/10.1366/11-06683>
- Pekárek, S. (2003). Non-thermal plasma ozone generation. *Acta Polytechnica*, *43*(6).
- Pérez-Pizá, M. C., Cejas, E., Zilli, C., Prevosto, L., Mancinelli, B., Santa-Cruz, D., Yannarelli, G., & Balestrasse, K. (2020). enhancement of soybean nodulation by seed treatment with non-thermal plasmas. *Scientific Reports*, *10*(1), 1-12.
- Perni, S., Liu, D. W., Shama, G., & Kong, M. G. (2008). Cold atmospheric plasma decontamination of the pericarps of fruit. *Journal of food protection*, *71*(2), 302-308.
- Pestka, J. (2010). Toxicological mechanisms and potential health effects of deoxynivalenol and nivalenol. *World Mycotoxin Journal*, *3*(4), 323-347.
- Pestka, J. J., & Smolinski, A. T. (2005, Jan-Feb). Deoxynivalenol: toxicology and potential effects on humans. *Journal of Toxicology and Environmental Health. Part B, Critical Reviews*, *8*(1), 39-69. <https://doi.org/10.1080/10937400590889458>
- Petřková, M., Švubová, R., Kyzek, S., Medvecká, V., Slováková, Ľ., Ševčovičová, A., & Gálová, E. (2021). The Effects of Cold Atmospheric Pressure Plasma on Germination Parameters,

- Enzyme Activities and Induction of DNA Damage in Barley. *International Journal of Molecular Sciences*, 22(6), 2833. <https://doi.org/10.3390/ijms22062833>
- Popović, V., Fairbanks, N., Pierscianowski, J., Biancaniello, M., Zhou, T., & Koutchma, T. (2018, 2018/08/01). Feasibility of 3D UV-C treatment to reduce fungal growth and mycotoxin loads on maize and wheat kernels. *Mycotoxin Research*, 34(3), 211-221. <https://doi.org/10.1007/s12550-018-0316-3>
- Prasad, A., Gänzle, M., & Roopesh, M. (2019). Inactivation of Escherichia Coli and Salmonella Using 365 and 395 nm High Intensity Pulsed Light Emitting Diodes. *Foods*, 8(12), 679.
- Pretsch, E., Buehlmann, P., Affolter, C., Pretsch, E., Bhuhlmann, P., & Affolter, C. (2000). *Structure determination of organic compounds*. Springer.
- Qiu, Y., Chen, X., Zhang, J., Ding, Y., & Lyu, F. (2022, 2022/10/20/). Effects of tempering with plasma activated water on the degradation of deoxynivalenol and quality properties of wheat. *Food Research International*, 112070. <https://doi.org/https://doi.org/10.1016/j.foodres.2022.112070>
- Ragni, L., Berardinelli, A., Iaccheri, E., Gozzi, G., Cevoli, C., & Vannini, L. (2016). Influence of the electrode material on the decontamination efficacy of dielectric barrier discharge gas plasma treatments towards *Listeria monocytogenes* and *Escherichia coli*. *Innovative Food Science & Emerging Technologies*, 37, 170-176.
- Ragni, L., Berardinelli, A., Vannini, L., Montanari, C., Sirri, F., Guerzoni, M. E., & Guarnieri, A. (2010). Non-thermal atmospheric gas plasma device for surface decontamination of shell eggs. *Journal of Food Engineering*, 100(1), 125-132.
- Rai, A., Das, M., & Tripathi, A. (2019). Occurrence and toxicity of a fusarium mycotoxin, zearalenone. *Critical Reviews in Food Science and Nutrition*, 1-20. <https://doi.org/10.1080/10408398.2019.1655388>
- Ramos, B., Miller, F., Brandão, T. R., Teixeira, P., & Silva, C. L. (2013). Fresh fruits and vegetables—an overview on applied methodologies to improve its quality and safety. *Innovative Food Science & Emerging Technologies*, 20, 1-15.
- Rani, H., & Bhardwaj, R. D. (2021). Quality attributes for barley malt: “The backbone of beer”. *Journal of Food Science*, 86(8), 3322-3340. <https://doi.org/https://doi.org/10.1111/1750-3841.15858>

- Rathore, V., & Nema, S. K. (2021). Optimization of process parameters to generate plasma activated water and study of physicochemical properties of plasma activated solutions at optimum condition. *Journal of Applied Physics*, 129(8), 084901.
- Rathore, V., Patel, D., Butani, S., & Nema, S. K. (2021). Investigation of physicochemical properties of plasma activated water and its bactericidal efficacy. *Plasma Chemistry and Plasma Processing*, 41(3), 871-902.
- Raybaudi-Massilia, R. M., Mosqueda-Melgar, J., Soliva-Fortuny, R., & Martín-Belloso, O. (2009). Control of pathogenic and spoilage microorganisms in fresh-cut fruits and fruit juices by traditional and alternative natural antimicrobials. *Comprehensive Reviews in Food Science and Food Safety*, 8(3), 157-180.
- Ren, C., Xiao, J., Wang, S., Jiang, W., Zhang, Y., & Liu, Z. (2017). Effect of Peanut Components on the Degradation of Aflatoxin B₁ Treated by Atmospheric Pressure Plasma. *Sci. Technol. Cereal. Oils Foods*, 2, 7.
- Ren, D., Diao, E., Hou, H., & Dong, H. (2020, 2020/01/30/). Degradation and ozonolysis pathway elucidation of deoxynivalenol. *Toxicon*, 174, 13-18.
<https://doi.org/https://doi.org/10.1016/j.toxicon.2019.11.015>
- Reuter, S., Winter, J., Iséni, S., Schmidt-Bleker, A., Dünnbier, M., Masur, K., Wende, K., & Weltmann, K.-D. (2015). The influence of feed gas humidity versus ambient humidity on atmospheric pressure plasma jet-effluent chemistry and skin cell viability. *IEEE Transactions on Plasma Science*, 43(9), 3185-3192.
- Rocha, D. F. D. L., Oliveira, M. D. S., Furlong, E. B., Junges, A., Paroul, N., Valduga, E., Backes, G. T., Zeni, J., & Cansian, R. L. (2017). Evaluation of the TLC quantification method and occurrence of deoxynivalenol in wheat flour of southern Brazil [Article]. *Food Additives and Contaminants - Part A Chemistry, Analysis, Control, Exposure and Risk Assessment*, 34(12), 2220-2229. <https://doi.org/10.1080/19440049.2017.1364872>
- Ropejko, K., & Twarużek, M. (2021, Jan 6). Zearalenone and Its Metabolites-General Overview, Occurrence, and Toxicity. *Toxins (Basel)*, 13(1). <https://doi.org/10.3390/toxins13010035>
- Rotter, B. A. (1996). Invited review: Toxicology of deoxynivalenol (vomitoxin). *Journal of Toxicology and Environmental Health Part A*, 48(1), 1-34.
- Rybkin, V., & Shutov, D. (2017). Atmospheric-pressure electric discharge as an instrument of chemical activation of water solutions. *Plasma Physics Reports*, 43(11), 1089-1113.

- Sakudo, A., Toyokawa, Y., Misawa, T., & Imanishi, Y. (2017). Degradation and detoxification of aflatoxin B1 using nitrogen gas plasma generated by a static induction thyristor as a pulsed power supply. *Food Control*, 73, 619-626.
- Samarajeewa, U., Sen, A., Cohen, M., & Wei, C. (1990). Detoxification of aflatoxins in foods and feeds by physical and chemical methods. *Journal of Food Protection*, 53(6), 489-501.
- Samoilovich, V., Gibalov, V., & Kozlov, K. (1997). Physical Chemistry of the Barrier Discharge (in Russian), Moscow State University (1989), English translation: JPF Conrads, F. *DVS-Verlag GmbH, Düsseldorf*.
- Santos Alexandre, A. P., Vela-Paredes, R. S., Santos, A. S., Costa, N. S., Canniatti-Brazaca, S. G., Calori-Domingues, M. A., & Augusto, P. E. D. (2018). Ozone treatment to reduce deoxynivalenol (DON) and zearalenone (ZEN) contamination in wheat bran and its impact on nutritional quality [Article]. *Food Additives and Contaminants - Part A Chemistry, Analysis, Control, Exposure and Risk Assessment*, 35(6), 1189-1199. <https://doi.org/10.1080/19440049.2018.1432899>
- Sarangapani, C., Misra, N., Milosavljevic, V., Bourke, P., O'Regan, F., & Cullen, P. (2016). Pesticide degradation in water using atmospheric air cold plasma. *Journal of Water Process Engineering*, 9, 225-232.
- Sarinont, T., Katayama, R., Wada, Y., Koga, K., & Shiratani, M. (2017). Plant growth enhancement of seeds immersed in plasma activated water. *MRS Advances*, 2(18), 995-1000.
- Sartori, A. V., de Moraes, M. H. P., dos Santos, R. P., Souza, Y. P., & da Nóbrega, A. W. (2017, 2017/12/01). Determination of Mycotoxins in Cereal-Based Porridge Destined for Infant Consumption by Ultra-High Performance Liquid Chromatography-Tandem Mass Spectrometry. *Food analytical methods*, 10(12), 4049-4061. <https://doi.org/10.1007/s12161-017-0965-4>
- Schmale III, D. G., & Munkvold, G. P. (2020). *Mycotoxins in Crops: A Threat to Human and Domestic Animal Health*. The American Phytopathological Society (APS). Retrieved 31/3/2020 from <https://www.apsnet.org/edcenter/disimpactmngmnt/topc/Mycotoxins/Pages/EconomicImpact.aspx>
- Scholtz, V., Šerá, B., Khun, J., Šerý, M., & Julák, J. (2019). Effects of nonthermal plasma on wheat grains and products. *Journal of Food Quality*, 2019.

- Schwarz, P., & Li, Y. (2011). Malting and brewing uses of barley. *Barley: Production, improvement, and uses*, 478-521.
- Scudamore, K. (2008). Fate of Fusarium mycotoxins in the cereal industry: Recent UK studies. *World Mycotoxin Journal*, 1(3), 315-323.
- Sebaei, A. S., Sobhy, H. M., Fouzy, A. S. M., & Hussain, O. A. (2020). Occurrence of zearalenone in grains and its reduction by gamma radiation [Article]. *International Journal of Environmental Analytical Chemistry*.
<https://doi.org/10.1080/03067319.2020.1756282>
- Sen, Y., Onal-Ulusoy, B., & Mutlu, M. (2019). Aspergillus decontamination in hazelnuts: Evaluation of atmospheric and low-pressure plasma technology [Article]. *Innovative Food Science and Emerging Technologies*, 54, 235-242.
<https://doi.org/10.1016/j.ifset.2019.04.014>
- Sera, B., Spatenka, P., Sery, M., Vrchotova, N., & Hruskova, I. (2010). Influence of plasma treatment on wheat and oat germination and early growth. *IEEE Transactions on Plasma Science*, 38(10), 2963-2968.
- Setlow, P. (2006). Spores of *Bacillus subtilis*: their resistance to and killing by radiation, heat and chemicals. *Journal of Applied Microbiology*, 101(3), 514-525.
- Shanakhat, H., Sorrentino, A., Raiola, A., Reverberi, M., Salustri, M., Masi, P., & Cavella, S. (2019). Technological properties of durum wheat semolina treated by heating and UV irradiation for reduction of mycotoxin content [Article]. *Journal of Food Process Engineering*, 42(3), Article e13006. <https://doi.org/10.1111/jfpe.13006>
- Shen, J., Tian, Y., Li, Y., Ma, R., Zhang, Q., Zhang, J., & Fang, J. (2016). Bactericidal Effects against *S. aureus* and Physicochemical Properties of Plasma Activated Water stored at different temperatures. *Scientific Reports*, 6, 28505.
- Shi, H., Cooper, B., Stroshine, R. L., Ileleji, K. E., & Keener, K. M. (2017, 2017/08/02). Structures of Degradation Products and Degradation Pathways of Aflatoxin B1 by High-Voltage Atmospheric Cold Plasma (HVACP) Treatment. *Journal of Agricultural and Food Chemistry*, 65(30), 6222-6230. <https://doi.org/10.1021/acs.jafc.7b01604>
- Shi, H., Ileleji, K., Stroshine, R. L., Keener, K., & Jensen, J. L. (2017). Reduction of Aflatoxin in Corn by High Voltage Atmospheric Cold Plasma [Article]. *Food and Bioprocess Technology*, 10(6), 1042-1052. <https://doi.org/10.1007/s11947-017-1873-8>

- Shintani, H., Sakudo, A., Burke, P., & McDonnell, G. (2010). Gas plasma sterilization of microorganisms and mechanisms of action. *Experimental and therapeutic medicine*, 1(5), 731-738.
- Siciliano, I., Spadaro, D., Prella, A., Vallauri, D., Cavallero, M. C., Garibaldi, A., & Gullino, M. L. (2016). Use of cold atmospheric plasma to detoxify hazelnuts from aflatoxins [Article]. *Toxins*, 8(5), Article 125. <https://doi.org/10.3390/toxins8050125>
- Sivachandiran, L., & Khacef, A. (2017). Enhanced seed germination and plant growth by atmospheric pressure cold air plasma: combined effect of seed and water treatment. *RSC advances*, 7(4), 1822-1832.
- Smet, C., Noriega, E., Rosier, F., Walsh, J., Valdramidis, V., & Van Impe, J. (2016). Influence of food intrinsic factors on the inactivation efficacy of cold atmospheric plasma: Impact of osmotic stress, suboptimal pH and food structure. *Innovative Food Science & Emerging Technologies*, 38, 393-406.
- Sobrova, P., Adam, V., Vasatkova, A., Beklova, M., Zeman, L., & Kizek, R. (2010). Deoxynivalenol and its toxicity. *Interdisciplinary toxicology*, 3(3), 94-99. <https://doi.org/10.2478/v10102-010-0019-x>
- Sohbatzadeh, F., Mirzanejad, S., Shokri, H., & Nikpour, M. (2016, 2016/06/01). Inactivation of *Aspergillus flavus* spores in a sealed package by cold plasma streamers. *Journal of Theoretical and Applied Physics*, 10(2), 99-106. <https://doi.org/10.1007/s40094-016-0206-z>
- Soler-Arango, J., Brelles-Mariño, G., Rodero, A., & Garcia, M. C. (2018, 2018/05/01). Characterization of an Air-Based Coaxial Dielectric Barrier Discharge Plasma Source for Biofilm Eradication. *Plasma Chemistry and Plasma Processing*, 38(3), 535-556. <https://doi.org/10.1007/s11090-018-9877-3>
- Song, J.-S., Lee, M. J., Ra, J. E., Lee, K. S., Eom, S., Ham, H. M., Kim, H. Y., Kim, S. B., & Lim, J. (2020, 2020/06/01). Growth and bioactive phytochemicals in barley (*Hordeum vulgare* L.) sprouts affected by atmospheric pressure plasma during seed germination. *Journal of Physics D: Applied Physics*, 53(31), 314002. <https://doi.org/10.1088/1361-6463/ab810d>
- Stanley, J., Patras, A., Pendyala, B., Vergne, M. J., & Bansode, R. R. (2020, 2020/08/10). Performance of a UV-A LED system for degradation of aflatoxins B1 and M1 in pure water: kinetics and cytotoxicity study. *Scientific Reports*, 10(1), 13473. <https://doi.org/10.1038/s41598-020-70370-x>

- Subedi, D. (2010). An investigation of the effect of electrode geometry and frequency of power supply in the homogeneity of dielectric barrier discharge in air. *Kathmandu University Journal of Science, Engineering and Technology*, 6(1), 96-101.
- Subedi, S., & Roopesh, M. (2020). Simultaneous drying of pet food pellets and Salmonella inactivation by 395 nm light pulses in an LED reactor. *Journal of Food Engineering*, 110110.
- Sun, X., Ji, J., Gao, Y., Zhang, Y., Zhao, G., & Sun, C. (2020, 2020/11/01/). Fate of deoxynivalenol and degradation products degraded by aqueous ozone in contaminated wheat. *Food Research International*, 137, 109357.
<https://doi.org/https://doi.org/10.1016/j.foodres.2020.109357>
- Suwal, S., Coronel-Aguilera, C. P., Auer, J., Applegate, B., Garner, A. L., & Huang, J.-Y. (2019, 2019/05/01/). Mechanism characterization of bacterial inactivation of atmospheric air plasma gas and activated water using bioluminescence technology. *Innovative Food Science & Emerging Technologies*, 53, 18-25.
<https://doi.org/https://doi.org/10.1016/j.ifset.2018.01.007>
- Švubová, R., Kyzek, S., Medvecká, V., Slováková, L., Gálová, E., & Zahoranová, A. (2020). Novel insight at the effect of cold atmospheric pressure plasma on the activity of enzymes essential for the germination of pea (*Pisum sativum* L. cv. Prophet) seeds. *Plasma Chemistry and Plasma Processing*, 40, 1221-1240.
- Švubová, R., Slováková, L., Holubová, L., Rovňanová, D., Gálová, E., & Tomeková, J. (2021). Evaluation of the Impact of Cold Atmospheric Pressure Plasma on Soybean Seed Germination. *Plants*, 10(1), 177. <https://www.mdpi.com/2223-7747/10/1/177>
- Szóke, C., Nagy, Z., Gierczik, K., Székely, A., Spitzkól, T., Zsuboril, Z. T., Galiba, G., Marton, C. L., & Kutasi, K. (2018). Effect of the afterglows of low pressure Ar/N₂-O₂ surface-wave microwave discharges on barley and maize seeds. *Plasma Processes and Polymers*, 15(2), 1700138. <https://doi.org/https://doi.org/10.1002/ppap.201700138>
- Tang, F., Chen, J., Wang, X., Zhang, S., & Zhang, X. (2015). Development of dielectric-barrier-discharge ionization. *Analytical and Bioanalytical Chemistry*, 407(9), 2345-2364.
- Tang, G., Chen, A., Dawood, D. H., Liang, J., Chen, Y., & Ma, Z. (2020, Feb). Capping proteins regulate fungal development, DON-toxisome formation and virulence in *Fusarium graminearum*. *Molecular Plant Pathology*, 21(2), 173-187.
<https://doi.org/10.1111/mpp.12887>

- Tappi, S., Berardinelli, A., Ragni, L., Dalla Rosa, M., Guarnieri, A., & Rocculi, P. (2014). Atmospheric gas plasma treatment of fresh-cut apples. *Innovative Food Science & Emerging Technologies*, 21, 114-122.
- ten Bosch, L., Pfohl, K., Avramidis, G., Wieneke, S., Viöl, W., & Karlovsky, P. (2017). Plasma-based degradation of mycotoxins produced by *Fusarium*, *Aspergillus* and *Alternaria* species [Article]. *Toxins*, 9(3), Article 97. <https://doi.org/10.3390/toxins9030097>
- Than, H. A. Q., Pham, T. H., Nguyen, D. K. V., Pham, T. H., & Khacef, A. (2022, 2022/01/01). Non-thermal Plasma Activated Water for Increasing Germination and Plant Growth of *Lactuca sativa* L. *Plasma Chemistry and Plasma Processing*, 42(1), 73-89. <https://doi.org/10.1007/s11090-021-10210-6>
- Thompson, D. P., Metevia, L., & Vessel, T. (1993, Feb). Influence of pH Alone and in Combination with Phenolic Antioxidants on Growth and Germination of Mycotoxigenic Species of *Fusarium* and *Penicillium*. *Journal of Food Protection*, 56(2), 134-138. <https://doi.org/10.4315/0362-028x-56.2.134>
- Tian, Y., Ma, R., Zhang, Q., Feng, H., Liang, Y., Zhang, J., & Fang, J. (2015a). Assessment of the Physicochemical Properties and Biological Effects of Water Activated by Non-thermal Plasma Above and Beneath the Water Surface. *Plasma Processes and Polymers*, 12(5), 439-449. <https://doi.org/https://doi.org/10.1002/ppap.201400082>
- Tian, Y., Ma, R., Zhang, Q., Feng, H., Liang, Y., Zhang, J., & Fang, J. (2015b). Assessment of the physicochemical properties and biological effects of water activated by non-thermal plasma above and beneath the water surface. *Plasma processes and polymers*, 12(5), 439-449.
- Toffoli, F., Gianinetti, A., Cavallero, A., Finocchiaro, F., & Stanca, A. (2003). Effects of pulses of higher temperature on the development of enzyme activity during malting. *Journal of the Institute of Brewing*, 109(4), 337-341.
- Traylor, M. J., Pavlovich, M. J., Karim, S., Hait, P., Sakiyama, Y., Clark, D. S., & Graves, D. B. (2011). Long-term antibacterial efficacy of air plasma-activated water. *Journal of Physics D: Applied Physics*, 44(47), 472001.
- Ulbin-Figlewicz, N., Brychcy, E., & Jarmoluk, A. (2015, Feb). Effect of low-pressure cold plasma on surface microflora of meat and quality attributes [Article]. *Journal of Food Science and Technology-Mysore*, 52(2), 1228-1232. <https://doi.org/10.1007/s13197-013-1108-6>

- Van Gils, C., Hofmann, S., Boekema, B., Brandenburg, R., & Bruggeman, P. (2013). Mechanisms of bacterial inactivation in the liquid phase induced by a remote RF cold atmospheric pressure plasma jet. *Journal of Physics D: Applied Physics*, *46*(17), 175203.
- Veerana, M., Yu, N., Ketya, W., & Park, G. (2022, Jan 21). Application of Non-Thermal Plasma to Fungal Resources. *J Fungi (Basel)*, *8*(2). <https://doi.org/10.3390/jof8020102>
- Vidal, A., Marín, S., Ramos, A. J., Cano-Sancho, G., & Sanchis, V. (2013, Mar). Determination of aflatoxins, deoxynivalenol, ochratoxin A and zearalenone in wheat and oat based bran supplements sold in the Spanish market. *Food and Chemical Toxicology*, *53*, 133-138. <https://doi.org/10.1016/j.fct.2012.11.020>
- Vidal, A., Sanchis, V., Ramos, A. J., & Marín, S. (2015). Thermal stability and kinetics of degradation of deoxynivalenol, deoxynivalenol conjugates and ochratoxin A during baking of wheat bakery products [Article]. *Food Chemistry*, *178*, 276-286. <https://doi.org/10.1016/j.foodchem.2015.01.098>
- Walsh, J. L., Liu, D.-X., Iza, F., Rong, M.-Z., & Kong, M. G. (2010). Contrasting characteristics of sub-microsecond pulsed atmospheric air and atmospheric pressure helium–oxygen glow discharges. *Journal of Physics D: Applied Physics*, *43*(3), 032001.
- Wang, G., Wang, Y. X., Ji, F., Xu, L. M., Yu, M. Z., Shi, J. R., & Xu, J. H. (2019, Mar). Biodegradation of deoxynivalenol and its derivatives by *Devosia insulae* A16 [Article]. *Food Chemistry*, *276*, 436-442. <https://doi.org/10.1016/j.foodchem.2018.10.011>
- Wang, J., Zhuang, H., Lawrence, K., & Zhang, J. (2018). Disinfection of chicken fillets in packages with atmospheric cold plasma: effects of treatment voltage and time. *Journal of Applied Microbiology*, *124*(5), 1212-1219.
- Wang, J., Zhuang, H., & Zhang, J. (2016). Inactivation of spoilage bacteria in package by dielectric barrier discharge atmospheric cold plasma—Treatment time effects. *Food and Bioprocess Technology*, *9*(10), 1648-1652.
- Wang, L., Shao, H., Luo, X., Wang, R., Li, Y., Li, Y., Luo, Y., & Chen, Z. (2016). Effect of Ozone Treatment on Deoxynivalenol and Wheat Quality. *PLoS ONE*, *11*(1), e0147613-e0147613. <https://doi.org/10.1371/journal.pone.0147613>
- Wang, Q., Liu, F., Miao, C., Yan, B., & Fang, Z. (2018, 2018/02/01). Investigation on discharge characteristics of a coaxial dielectric barrier discharge reactor driven by AC and ns power sources. *Plasma Science and Technology*, *20*(3), 035404. <https://doi.org/10.1088/2058-6272/aaa357>

- Wang, S.-Q., Huang, G.-Q., Li, Y.-P., Xiao, J.-X., Zhang, Y., & Jiang, W.-L. (2015, July 01). Degradation of aflatoxin B1 by low-temperature radio frequency plasma and degradation product elucidation [journal article]. *European Food Research and Technology*, 241(1), 103-113. <https://doi.org/10.1007/s00217-015-2439-5>
- Wang, Y., Thorup-Kristensen, K., Jensen, L. S., & Magid, J. (2016). Vigorous root growth is a better indicator of early nutrient uptake than root hair traits in spring wheat grown under low fertility. *Frontiers in plant science*, 7, 865.
- Warning, A., & Datta, A. K. (2013). Interdisciplinary engineering approaches to study how pathogenic bacteria interact with fresh produce. *Journal of Food Engineering*, 114(4), 426-448.
- Waskow, A., Howling, A., & Furno, I. (2021, 2021-April-14). Mechanisms of Plasma-Seed Treatments as a Potential Seed Processing Technology [Review]. *Frontiers in Physics*, 9(174). <https://doi.org/10.3389/fphy.2021.617345>
- Wegulo, S. N. (2012, Nov 6). Factors influencing deoxynivalenol accumulation in small grain cereals. *Toxins (Basel)*, 4(11), 1157-1180. <https://doi.org/10.3390/toxins4111157>
- Whitehead, J. C. (2016). Chapter 3 - The Chemistry of Cold Plasma. In N. N. Misra, O. Schlüter, & P. J. Cullen (Eds.), *Cold Plasma in Food and Agriculture* (pp. 53-81). Academic Press. <https://doi.org/https://doi.org/10.1016/B978-0-12-801365-6.00003-2>
- Winter, J., Brandenburg, R., & Weltmann, K. D. (2015, 2015/10/08). Atmospheric pressure plasma jets: an overview of devices and new directions. *Plasma Sources Science and Technology*, 24(6), 064001. <https://doi.org/10.1088/0963-0252/24/6/064001>
- Wu, M. C., Liu, C. T., Chiang, C. Y., Lin, Y. J., Lin, Y. H., Chang, Y. W., & Wu, J. S. (2019). Inactivation Effect of Colletotrichum Gloeosporioides by Long-Lived Chemical Species Using Atmospheric-Pressure Corona Plasma-Activated Water. *IEEE Transactions on Plasma Science*, 47(2), 1100-1104. <https://doi.org/10.1109/TPS.2018.2871856>
- Xiang, Q., Liu, X., Li, J., Liu, S., Zhang, H., & Bai, Y. (2018). Effects of dielectric barrier discharge plasma on the inactivation of *Zygosaccharomyces rouxii* and quality of apple juice. *Food Chemistry*, 254, 201-207.
- Xu, L., Garner, A. L., Tao, B., & Keener, K. M. (2017). Microbial inactivation and quality changes in orange juice treated by high voltage atmospheric cold plasma. *Food and Bioprocess Technology*, 10(10), 1778-1791.

- Xu, L., Sun, X., Wan, X., Li, H., Yan, F., Han, R., Li, H., Li, Z., Tian, Y., Liu, X., Kang, X., & Wang, Y. (2020). Identification of a *Bacillus amyloliquefaciens* H6 Thioesterase Involved in Zearalenone Detoxification by Transcriptomic Analysis [Article]. *Journal of agricultural and food chemistry*, 68(37), 10071-10080. <https://doi.org/10.1021/acs.jafc.0c03954>
- Xu, Y., Tian, Y., Ma, R., Liu, Q., & Zhang, J. (2016, 2016/04/15/). Effect of plasma activated water on the postharvest quality of button mushrooms, *Agaricus bisporus*. *Food Chemistry*, 197, 436-444. <https://doi.org/https://doi.org/10.1016/j.foodchem.2015.10.144>
- Yadav, B., Spinelli, A. C., Govindan, B. N., Tsui, Y. Y., McMullen, L. M., & Roopesh, M. S. (2019, 2019/09/01/). Cold plasma treatment of ready-to-eat ham: Influence of process conditions and storage on inactivation of *Listeria innocua*. *Food Research International*, 123, 276-285. <https://doi.org/https://doi.org/10.1016/j.foodres.2019.04.065>
- Yadav, B., Spinelli, A. C., Misra, N., Tsui, Y. Y., McMullen, L. M., & Roopesh, M. (2020). Effect of in-package atmospheric cold plasma discharge on microbial safety and quality of ready-to-eat ham in modified atmospheric packaging during storage. *Journal of Food Science*.
- Yang, K., Li, K., Pan, L., Luo, X., Xing, J., Wang, J., Wang, L., Wang, R., Zhai, Y., & Chen, Z. (2020). Effect of Ozone and Electron Beam Irradiation on Degradation of Zearalenone and Ochratoxin A. *Toxins*, 12(2), 138.
- Yardimci, O., & Setlow, P. (2010). Plasma sterilization: opportunities and microbial assessment strategies in medical device manufacturing. *IEEE Transactions on Plasma Science*, 38(4), 973-981.
- Young, J. C., Fulcher, R. G., Hayhoe, J. H., Scott, P. M., & Dexter, J. E. (1984). Effect of milling and baking on deoxynivalenol (vomitoxin) content of eastern Canadian wheats. *Journal of agricultural and food chemistry*, 32(3), 659-664.
- Young, J. C., Zhu, H., & Zhou, T. (2006). Degradation of trichothecene mycotoxins by aqueous ozone [Article]. *Food and Chemical Toxicology*, 44(3), 417-424. <https://doi.org/10.1016/j.fct.2005.08.015>
- Yu, H., Perni, S., Shi, J., Wang, D., Kong, M., & Shama, G. (2006). Effects of cell surface loading and phase of growth in cold atmospheric gas plasma inactivation of *Escherichia coli* K12. *Journal of Applied Microbiology*, 101(6), 1323-1330.
- Yu, J., Zhang, W., Wu, X., Wu, L., Tao, J., & Huang, K. (2021). The influence of gas humidity on the discharge properties of a microwave atmospheric-pressure coaxial plasma jet. *AIP Advances*, 11(2), 025131.

- Yumbe-Guevara, B. E., Imoto, T., & Yoshizawa, T. (2003, 2003/12/01). Effects of heating procedures on deoxynivalenol, nivalenol and zearalenone levels in naturally contaminated barley and wheat. *Food Additives & Contaminants*, 20(12), 1132-1140. <https://doi.org/10.1080/02652030310001620432>
- Zapala, W., & Waksmundzka-Hajnos, M. (2004, Aug). Retention process in normal-phase TLC systems [Article]. *Journal of Liquid Chromatography & Related Technologies*, 27(14), 2127-2141. <https://doi.org/10.1081/jlc-200025680>
- Zhang, Z., Xu, Z., Cheng, C., Wei, J., Lan, Y., Ni, G., Sun, Q., Qian, S., Zhang, H., Xia, W., Shen, J., Meng, Y., & Chu, P. K. (2017). Bactericidal Effects of Plasma Induced Reactive Species in Dielectric Barrier Gas–Liquid Discharge. *Plasma Chemistry and Plasma Processing*, 37(2), 415-431. <https://doi.org/10.1007/s11090-017-9784-z>
- Zheng, T., Liu, Y., Wang, J., & Pei, Y. (2020). Degradation of Mycotoxins in Corn Germ and Crude Corn Oil by Steaming Corn Germ with Dilute Alkali [Article]. *Shipin Kexue/Food Science*, 41(13), 8-13. <https://doi.org/10.7506/spkx1002-6630-20190605-049>
- Zhou, R., Zhou, R., Prasad, K., Fang, Z., Speight, R., Bazaka, K., & Ostrikov, K. K. (2018). Cold atmospheric plasma activated water as a prospective disinfectant: the crucial role of peroxyxynitrite. *Green Chemistry*, 20(23), 5276-5284.
- Zhuang, H., Rothrock, M. J., Jr., Hiatt, K. L., Lawrence, K. C., Gamble, G. R., Bowker, B. C., Keener, K. M., & Šerá, B. (2019). In-Package Air Cold Plasma Treatment of Chicken Breast Meat: Treatment Time Effect [Article]. *Journal of Food Quality*, 2019, Article 1837351. <https://doi.org/10.1155/2019/1837351>
- Ziuzina, D., & Misra, N. N. (2016). Chapter 9 - Cold Plasma for Food Safety. In N. N. Misra, O. Schlüter, & P. J. Cullen (Eds.), *Cold Plasma in Food and Agriculture* (pp. 223-252). Academic Press. <https://doi.org/https://doi.org/10.1016/B978-0-12-801365-6.00009-3>
- Ziuzina, D., Misra, N. N., Cullen, P. J., Keener, K., Mosnier, J. P., Vilaró, I., Gaston, E., & Bourke, P. (2016). Demonstrating the Potential of Industrial Scale In-Package Atmospheric Cold Plasma for Decontamination of Cherry Tomatoes. *Plasma Medicine*, 6(3-4), 397-412. <https://doi.org/10.1615/PlasmaMed.2017019498>
- Ziuzina, D., Misra, N. N., Han, L., Cullen, P. J., Moiseev, T., Mosnier, J. P., Keener, K., Gaston, E., Vilaró, I., & Bourke, P. (2020). Investigation of a large gap cold plasma reactor for continuous in-package decontamination of fresh strawberries and spinach. *Innovative Food Science & Emerging Technologies*, 59, 102229. <https://doi.org/10.1016/j.ifset.2019.102229>

Ziuzina, D., Patil, S., Cullen, P. J., Keener, K., & Bourke, P. (2014). Atmospheric cold plasma inactivation of *Escherichia coli*, *Salmonella enterica* serovar Typhimurium and *Listeria monocytogenes* inoculated on fresh produce. *Food microbiology*, *42*, 109-116.